



A Robust directly Solvable Inverter-based Energy Management Model to Investigate the effects of Electric Vehicle Employment on Distribution System

By

Mehrdad Aghamohamadi

Thesis

*Submitted to Flinders University
for the degree of Doctor of Philosophy, Ph.D.*

Ph.D. in Electrical Engineering

College of Science and Engineering

30 March 2022

Certificate of Original Authorship

I certify that the work in this thesis has not previously been submitted for a degree, nor has it been submitted as part of requirements for a degree. I also certify that the thesis has been written by me. Any help that I have received in my research work, and the preparation of the thesis itself has been acknowledged.

In addition, I certify that all information sources and literature used are indicated in the thesis.

I certify that this thesis:

does not incorporate without acknowledgment any material previously submitted for a degree or diploma in any university and the research within will not be submitted for any other future degree or diploma without the permission of Flinders University; and to the best of my knowledge and belief, does not contain any material previously published or written by another person except where due reference is made in the text.

Signature of Student:

A handwritten signature in black ink, appearing to be 'M.A.' with a large, stylized flourish above it.

Mehrdad Aghamohamadi

Date: 10/01/2022

Acknowledgments

I would like to express my deep gratitude and appreciation to my supervisors, Dr. Amin Mahmoudi, Dr. Mohammed Haque, and Dr. John Ward for their guidance, encouragement, and belief in my abilities. Their constructive comments contributed significantly to the quality of this research.

I would like to thank the financial supporters of my study including Australian Government for providing the Research Training Program Scholarship (AGRTPS) as well as the Commonwealth Scientific and Industrial Research Organization (CSIRO) for their financial support through a Post-Graduate Top-up Scholarship.

Finally, none of this was possible without the endless love and unconditional support of my mum and dad, Mahnaz and Abbas, who I love the most in this world.

Abstract

Restructuring of power systems, along with the integration of renewable energy resources in electricity networks, have transformed traditional power electricity distribution systems (EDSs) into new active distribution systems (ADSs). In addition, the rapid advancement of technology has enabled the bulk utilization of renewable generation units and battery energy storage (BES) systems in EDSs. The next step in this trend is the employment of electric vehicles (EV) and the coordinated integration of these vehicles into EDS which is investigated in this thesis.

Following contributions are presented in this thesis to achieve the objectives in section 1.2:

Contribution 1: A novel directly solvable set of power flow equations

A new directly solvable power flow problem has been proposed for EDS, introducing a connectivity matrix in line with a new indexing of load flow equations. The new power flow model is developed generally and is capable to be added to any EDS study as the constraints of the model. This means, the power flow calculation does not need to be conducted separately. Therefore, the need of load flow calculation methodologies, such as Newton–Raphson method (NR) and forward backward sweep-based method (FBS), as well as optimization approaches, such as Genetic Algorithm (GA) and Particle Swarm Optimization (PSO), is eliminated as the proposed model characterizes both load flow and energy management constraints in a single and unified model. This provides users the opportunity of solving the problem with commercial optimization packages, i.e., CPLEX, GAMS, etc., in a single shot with no need to develop further optimization approaches involving iterative procedures and load flow calculations. Note that, the employed modified load flow equations in line with the connectivity matrix can be used in any

other EDS study, concerning load flow calculation, as the constraints of the model.

Contribution 2: A general multi-objective energy management model for inverter-based integration of RES, and BES system

The proposed directly solvable power flow problem is used to build up a multi-objective energy management model for RES-BES-equipped distribution systems. The first objective of the model minimizes total EDS power losses, and the second objective minimizes the voltage deviations of each bus over time. These objective functions are optimized being subject to load flow constraints, RES/BES optimal operation, and voltage/current tolerance of EDS. The proposed energy management model enables both active and reactive power controllability of RES and BES systems. New continuous variables are defined for RES and BES representing active and reactive power share of these systems during the operation. Accordingly, BES can absorb active or reactive power in each time slot and inject it back to the network as active or reactive power in another time slot.

Contribution 3: Integration of EV loading into the energy management model and investigating the effects of EV charging on EDS voltage and power loss

Electric vehicle activity is modelled by probability distribution functions. The EV's dynamic energy balance is modelled based on EV connections and the model is merged into the energy management model.

Contribution 4: The new robust optimization model to characterize uncertainties of RESs employing block coordinate decent method

An adaptive robust optimization (ARO) approach is implemented to deal with the uncertainties of load in operating EDS through the proposed energy management model. Uncertain parameters are characterized by bounded intervals in polyhedral uncertainty sets. The

ARO model is a tri-level min-max-min problem which is not directly solvable. Therefore, a decomposition methodology is employed to recast the min-max-min ARO problem into two problems including a master problem and a sub-problem. A column-and-constraints (C&C) generation methodology is used to iteratively solve the decomposed problem through primal cutting planes. Two main decisions are made in ARO, namely "here-and-now" decisions, which are obtained before any uncertainty realizations, and "wait-and-see" decisions, which are obtained after the realization of uncertain parameters. Several binary variables such as BES charging/discharging status must be obtained after uncertainty realizations in the sub-problem to be able to compensate the effects of uncertain load/price as recourse decisions. However, this is not possible by conventional dual-based robust models as considering these binary variables results in a mixed-integer sub-problem and the dual of a mixed-integer model is generally weak, non-tractable and complicated. Therefore, instead of using duality theory in solving the sub-problem, Block Coordinate Descent (BCD) method is used in the proposed model.

In terms of solution methodology, BCD method is used in the robust approach to iteratively solve the inner bi-level max-min sub-problem by means of Taylor series instead of transforming it into a single-level max problem by duality theory in conventional ARO models. BCD technique was originally devised to deal with single-level problems. By extending the application of the BCD technique to solve the two-level max-min sub-problem (resulted from the C&C generation technique), it is possible to avoid duality theory in solving the sub-problem.

Therefore, the associated limitation in considering binary variables in the sub-problem is eliminated. In fact, mixed-integer models (even non-linear models) can be solved in the sub-problem through the proposed BCD robust model. As a result, uncertainty-dependent binary variables such as BES charging/discharging statuses can be obtained after uncertainty realization

in the sub-problem as recourse decisions, resulting in more system flexibility in compensating the uncertainty effects of load. Moreover, the linearization of the dualized inner problem is avoided as the Lagrange multipliers are eliminated in this methodology. Thus, the case-sensitivity of the proposed model reduces as it does not reflect dual variables.

The structure of the thesis is given below:

After presenting an introduction to the objectives and scope of the research in the first chapter, the second chapter aims to present a review of recent advancements in both operation and planning of electric vehicle charging stations (EVCSs) in EDSs. In this respect, the conducted review provides supportive insights on the state-of-the-art operation and planning of electric vehicle charging stations in EDSs by introducing the recent trends, methodologies, and novelties in this field of study. The literature has been presented considering both qualitative and quantitative aspects. Since, the focus of this thesis is on the operation of EVCSs, after presenting the literature on operation and planning aspects of these systems, a more detailed operation-based review is conducted on the employment of CSs in electricity distribution system to highlight their associated effects on EDSs.

In the third chapter, a new directly solvable and non-iterative load flow model is proposed to assist with EDS operation at the presence of EV loading, renewable energy sources (RESs) and BES. In particular, a connectivity matrix is introduced to characterize the configuration of EDS and provide a feasible general representation of load flow equations. This enables the proposed modified load flow equations to be mergeable in any type of EDS study as constraints. This way, the power flow model in Chapter 3 is employed and accordingly merged into the proposed energy management model which is presented and discussed in Chapter 4. In chapter 3, first he IEEE 33-bus electricity distribution system is employed to evaluate the effectiveness of the

proposed general power flow model. Results are also compared to other power flow solutions such as forward backward Sweep-based method.

The energy management model in Chapter 4 first integrates the employment of inverter-based RES and BES in the operation of power electricity distribution system. The energy management model is evaluated through the same system incorporating BES and RES to illustrate the effectiveness of the proposed energy management model in Chapter 4.

Then, EV loading patterns are added to the model in Chapter 5 to investigate the effects of EV charging patterns on the operation of active EDSs at the presence of RES and BES systems. To do so, the EV load, formed by EV charging patterns, is modelled by probability density functions.

The uncertainty of RES in distribution system is modelled through robust optimization (RO) in Chapter 6. The uncertainties are modelled by polyhedral uncertainty sets. Moreover, the conventional dual-based RO model is replaced with a new proposed RO model which employs block coordinate descent (BCD) technique instead of duality in solving the RO model. As a result, the obtained solutions are more realistic and robust as binary wait-and-see variables can be obtained as recourse decisions after uncertainty realizations which was not applicable in previous dual-based RO models. Moreover, linearization of the dualized inner problem is also avoided as Lagrange multipliers are eliminated. The effects of EV charging patterns, however, are investigated on a relatively smaller, but real-world, system which is the distribution system of a suburb in Adelaide, Australia. The results for operation of EVs are given in this chapter and different comparisons are conducted. Note that, the BCD robust model is also conducted on the last case study to characterize the uncertainties of RES generation in the model.

Finally, Chapter 7 presents a summary of the conducted research in this thesis along with

future research plans.

Further studies and application conducted by the proposed robust and BCD robust optimization models in this thesis are presented in Chapter 8 for interested readers. In chapter 8, two studies are presented. These studies are among the published studies.

Keywords:

Adaptive robust, block coordinate decent method, Connectivity matrix, directly solvable load flow, electricity distribution system, non-linear programming, plug-in electric vehicles, Power loss minimization, robust optimization, storage system, uncertainty, voltage stability, voltage deviation.

Publications

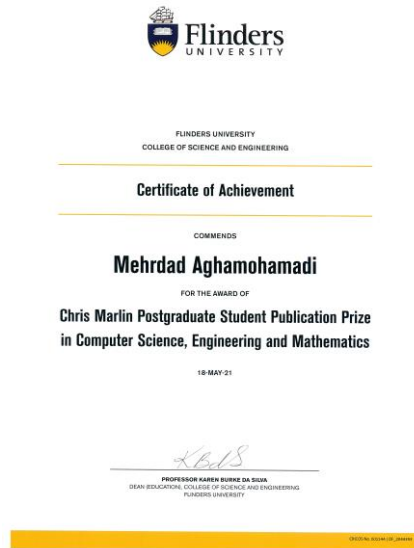
Following Studies have been published during the PhD study at Flinders University:

- [1] M. Aghamohamadi, A. Mahmoudi and M. H. Haque, "Adaptive Robust Recourse-Based Bidding Strategy and Capacity Allocation of PV-WT-BES Owning Prosumers Under Uncertainties," in **IEEE Transactions on Industry Applications**, vol. 57, no. 4, pp. 4170-4186, July-Aug. 2021, doi: 10.1109/TIA.2021.3072603.
- [2] M. Aghamohamadi, A. Mahmoudi and M. H. Haque, "Two-Stage Robust Sizing and Operation Co-Optimization for Residential PV–Battery Systems Considering the Uncertainty of PV Generation and Load," in **IEEE Transactions on Industrial Informatics**, vol. 17, no. 2, pp. 1005-1017, Feb. 2021, doi: 10.1109/TII.2020.2990682.
- [3] M. Aghamohamadi, A. Mahmoudi, John K. Ward, M. H. Haque, João P. S. Catalão, "Block Coordinate Decent Robust Bidding Strategy of a Solar Photovoltaic coupled Energy Storage System operating in a Day-ahead Market," **2021 IEEE PES Innovative Smart Grid Technology – Asia**, Brisbane, Australia, 2021.
- [4] M. Aghamohamadi, A. Mahmoudi, John K. Ward, M. Sleep, M. H. Haque, "Recourse-based BCD Robust Integrated Bidding Strategy for Multi-energy Systems under Uncertainties of Load and Energy Prices," **2021 IEEE Energy Conversion Congress and Exposition (ECCE)**, Toronto, Canada, 2021.
- [5] M. Aghamohamadi, A. Mahmoudi, John K. Ward, M. H. Haque, "Review on the State-of-the-art Operation and Planning of Electric Vehicle Charging Stations in Electricity Distribution Systems," **2021 IEEE Energy Conversion Congress and Exposition (ECCE)**, Toronto, Canada, 2021.
- [6] M. Aghamohamadi, C. Chuah, A. Mahmoudi, John K. Ward, M. H. Haque, "A New General Multi-Layout Energy Hub Management Model for Industrial and Commercial Multi-energy Systems with

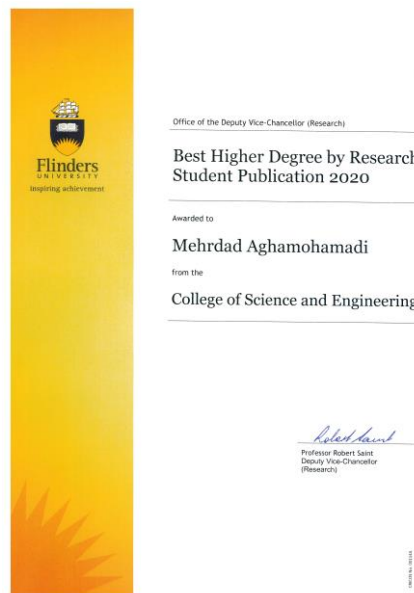
- Complex Configurations," **2021 IEEE Energy Conversion Congress and Exposition (ECCE)**, Toronto, Canada, 2021.
- [7] M. Aghamohamadi, M. H. Haque, A. Mahmoudi, John K. Ward " A Novel Directly-solvable Non-iterative Load Flow Model for Radial Distribution System Studies," **IEEE Power Electronics Drives and Energy System (PEDES)**, Jaipur, Rajasthan, India, 2020.
- [8] M. Aghamohamadi, M. H. Haque, A. Mahmoudi, John K. Ward "Two-stage Robust Management of PEV Parking Lots Coupled with Multi-energy Prosumers under Load and Energy Market Uncertainty," **IEEE Power Electronics Drives and Energy System (PEDES)**, Jaipur, Rajasthan, India, 2020.
- [9] M. Samadi, M. Aghamohamadi, A. Mahmoudi, "Optimal Time Period Clustering of Time-of-use Schemes Based on Elastic Loads' Responsiveness," **International Transactions on Electrical Energy Systems**, Volume 30, April 2020, DOI: <https://doi.org/10.1002/2050-7038.12275>. Online link: <https://onlinelibrary.wiley.com/doi/full/10.1002/2050-7038.12275>
- [10] M. Aghamohamadi, A. Mahmoudi, M. H. Haque, "Robust Allocation of Residential Solar Photovoltaic Systems Paired with Battery Units in South Australia," **2019 IEEE Energy Conversion Congress and Exposition (ECCE)**, Baltimore, USA, 2019. Online link: <https://ieeexplore.ieee.org/abstract/document/8913208>
- [11] M. Aghamohamadi, A. Mahmoudi, "From Bidding Strategy in Smart Grid toward Integrated Bidding Strategy in Smart Multi-energy Systems, an Adaptive Robust Solution Approach," **Energy**, Volume 183, 15 September 2019, Pages 71-91.

Honors and Awards

- "Chris Marlin Postgraduate Publication of the Year" Award 2021, Flinders University



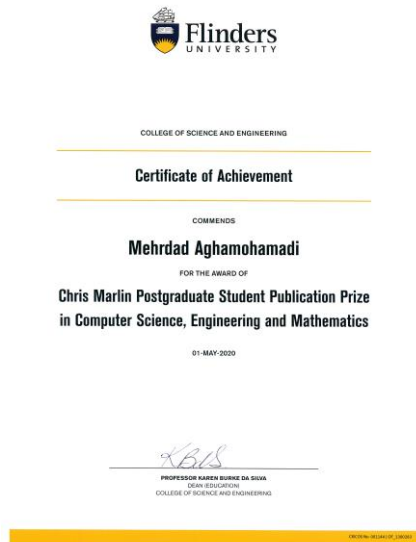
- "CSE Best HDR Student Publication of the Year" Award 2020, Flinders University



- Selected for the "HDR Student in Focus" June 2021 by Flinders university

The screenshot shows a Flinders University article page. At the top, there is a yellow navigation bar with the Flinders University logo and links for Study, Research, Engage, Alumni, Giving, and About. Below the navigation bar, the article title is "PhD Student, Mehrdad Aghamohamadi, conducting research in renewable and sustainable power and energy systems". To the left of the main text, there is a "RELATED POSTS" section with three entries, each featuring a small image and a title. The main text includes a photograph of Mehrdad Aghamohamadi and a short biography of him.

- "Chris Marlin Postgraduate Publication of the Year" Award 2020, Flinders University



- 2021 South Australia representor and winner of Fresh Science (specialist science communication and public relations agency) amongst 178 nominations from around the country.
- Equipment Fund 2020, \$6000 AUD, Flinders University

- CSIRO Top-up Scholarship, \$45,000 AUD, 2019

CSIRO HUMAN RESOURCES
www.csiro.au



HR Services
GPO Box 1700, Canberra ACT 2601, Australia
T 1300 301 509 • ABN 41 687 119 230

STUDENT AGREEMENT - POSTGRADUATE STUDENT

Details

CONTACT DETAILS	
Business Unit: ENERGY	University: The Flinders University of South Australia
Contact: John Ward	Contact: Dr Amin Mahmoudi
Email: JOHN.K.WARD@CSIRO.AU	Email: amin.mahmoudi@flinders.edu.au
AGREEMENT DETAILS	
Student	Mehrdad Aghamohamadi
Student Email	Mehrdad.ghamohamadi@flinders.edu.au
Position	PHD Postgraduate Student
Position Number	50075042
Functional Area	Res. Sci/Eng
Degree	Postgraduate (PHD)
Academic Supervisor (University)	Dr Amin Mahmoudi
Supervisor (CSIRO)	John Ward
Project	Investigating and Analysing the Effects of Electric Vehicles on the Electricity Distribution System Electric vehicles (EVs) are experiencing a considerable sales growth worldwide. The integration of EVs in electricity distribution grid is not simply modelled as a new load. In fact, the uncoordinated charging of EVs may pose noticeable effects on the optimal operation of the upstream grid such as voltage imbalance, frequency deviations, etc. In contrary, if EVs are optimally integrated into the system, they may become useful assets to deal with the aforementioned problems. The main aim of this proposal is to investigate the long-term and short-term effects of EVs' coordinated operation on the electricity distribution system. Moreover, it suggests operational and planning requirements of distribution networks in Australia to provide the capacity for integrating EVs into the network. Since, these vehicles have not been broadly employed in the country, the advantages and disadvantages of integrating EVs into the electricity grid have not been properly evident so far. Accordingly, the ongoing research works on this area are mainly based on some predictions and assumptions associated with EVs' behaviour which is subject to a great deal of uncertainty in practice. Therefore, another attempt of this proposal is to characterize the associated uncertainties when integrating EVs into distribution system. It is suggested to characterize these uncertainties through robust optimization which is a powerful tool compared to other methodologies such as Monte-Carlo and stochastic. Further, a comprehensive case study on

Page 1 of 7

- 3rd Flinders University HDR Conference Poster Presentation Award (2019)
- Finalist of Pitch Competition 2019, Bridgestone World Solar Challenge
- Australian Government Research Training Program Scholarship, \$84,000 AUD

Table of contents

Certificate of Original Authorship	i
Acknowledgments	ii
Abstract	iii
Publications	ix
Honors and Awards	xi
Table of contents	xiv
List of Tables	xvi
List of Figures	xvii
List of Abbreviations	xix
1. Introduction	20
1.1. Problem Description	20
1.2. Research objectives and scope	22
1.3. Dataset	23
1.4. Thesis organization	23
2. Literature Review, Knowledge Gap, Motivations, and Contributions	24
2.1. EDS Management at the Presence of EVs, BESs, and RESs	25
2.2. EDS uncertainty modeling	27
2.3. EVCS Operation and Planning in EDS	32
2.4. Quantitative Evaluation of the Literature	40
2.5. Knowledge Gap and Motivations of this Study	42
2.6. Contributions of this study	43
2.7. Conclusion	46
3. Proposed General and Directly-solvable EDS Power Flow Equations	47
3.1. Introduction	48
3.2. The Proposed Modified EDS Load Flow Equations	51
3.3. Validating the Proposed EDS Power Flow Model	56
3.4. Conclusion	59
4. Proposed General Inverter-Based EDS Energy Management Model at the Presence of RES and BES	60
4.1. Background	63
4.2. Motivations	66
4.3. Contributions	67

4.4. Proposed Directly Solvable EDS Load Flow Model.....	68
4.5. Inverter-based Modeling of Battery Energy Storage System.....	70
4.6. Inverter-based Modeling of Renewable Energy Sources	72
4.7. Proposed EDS Energy Management Model.....	73
4.8. Simulation results.....	79
4.9. Conclusion.....	91
5. Load Modelling of EVs.....	94
5.1. Charger type and EV brands considered in the load model	94
5.2. Scenario No.1 of EV loading (100% fast charging EVs).....	95
5.3. Scenario No.2 of EV loading (100% slow charging EVs).....	96
5.4. Scenario No.3 of EV loading (50% slow charging and 50% EVs).....	96
6. The Proposed BCD Robust Energy Management model to Investigate the Effects of EV Employment under Uncertainties of PV and WT systems.....	98
6.1. Background and Motivation.....	98
6.2. Contributions.....	100
6.3. Two-stage Adaptive Robust Approach	101
6.4. Solution Methodology to Solve the Proposed Robust energy management model	102
6.5. Block Coordinate Descent (BCD) Methodology to Solve the Sub-problem	105
6.6. Numerical Study.....	109
6.7. Conclusion.....	120
7. Conclusion	122
8. Published Studies Employing the Proposed Robust and BCD Robust Optimization Models	124
8.1 Application No. 1	124
8.2 Application No. 2 (references are at the end of the paper).....	174
. ⁹	References
217	

List of Tables

Table 2-1. Approaches in EV integration into EDS energy management.....	27
Table 2-2. Comparison between uncertainty approaches.....	32
Table 3-1. Active and reactive power loss comparison for all scenarios	58
Table 5-1. Considered electric vehicles	95

List of Figures

Fig. 1-1. A sample schematic representation of a sustainable EDS	20
Fig. 2-1. Solar irradiance histogram and its estimated pdf [23]	28
Fig. 2-2. The uncertainty scenarios employed by [29].....	29
Fig. 2-3. Comparison between SP and RO models [29]	30
Fig. 2-4. Categories of the reviewed studies in planning and operation of EVCSs (references in this figure are based on the paper: M. Aghamohamadi, A. Mahmoudi, John K. Ward, M. H. Haque, "Review on the State-of-the-art Operation and Planning of Electric Vehicle Charging Stations in Electricity Distribution Systems," 2021 IEEE Energy Conversion Congress and Exposition (ECCE), Toronto, Canada, 2021.).....	41
Fig. 2-5. Annual (A) and total (B) number of reviewed studies, concerning EVCS operation and planning between 2012-2020	42
Fig. 3-1. Comparison between the conventional and the proposed EDS power flow models	51
Fig. 3-2. Configuration of a simplified 6-bus EDS	51
Fig. 3-3. Considered π configuration for each branch, connecting bus i to bus j	54
Fig. 3-4. IEEE 33-bus system, considered as the case study.....	56
Fig. 3-5. Active (A) and reactive (B) load levels for scenarios 1-4	57
Fig. 3-6. Voltage magnitude comparison for IEEE 33-bus system.....	57
Fig. 3-7. Active power flow comparison for 33-bus system	58
Fig. 3-8. Reactive power flow comparison for 33-bus system.....	58
Fig. 4-1. Dynamic energy balance in BES system.....	71
Fig. 4-2. Representation of the BES and inverter coupling as well as their energy interaction with grid	73
Fig. 4-3. Considered π configuration for each branch of EDS equipped with RES and BES systems.	74
Fig. 4-4. Considered system for numerical simulations (modified IEEE 33 bus system).....	79
Fig. 4-5. Generated power by renewable energy sources in EDS	80
Fig. 4-6. Hourly voltage magnitude for each bus of IEEE 33-bus system for cases 1-3.....	82
Fig. 4-7. Voltage magnitude (24-h basis) for each bus of the system for cases 1-3.....	83
Fig. 4-8. Standard deviation of hourly voltage magnitudes for each bus of the system.....	83

Fig. 4-9. Hourly system power loss during the operating horizon 84

Fig. 4-10. Total system power loss for a 24-h operation..... 84

Fig. 4-11. Effects of inverter-based operation of RESs and BESs on voltage deviation and total power loss..... 86

Fig. 4-12. Inverter-based operation of RESs (active/reactive share of the injected power)..... 87

Fig. 4-13. Inverter-based BES energy level and apparent charging/discharging power as well as active/reactive share of BES power (right) 91

Fig. 5-1. Considered inlet for EVs 94

Fig. 5-2. EV charging load profile for scenario No. 1 of EV loading (100% fast charging EVs) 95

Fig. 5-3. EV charging load profile for scenario No. 2 of EV loading (100% slow charging EVs)..... 96

Fig. 5-4. EV charging load profile for scenario No. 2 of EV loading (50% slow charging and 50% fast charging EVs)..... 97

Fig. 6-1. Outline of the proposed BCD robust methodology 109

Fig. 6-2. Case Study 110

Fig. 6-3. Generated power by PV and WT systems 110

Fig. 6-4. Load of bus 4 and 6 with and without EV charging patterns – Scenario No.1 (100% fast charging EVs)..... 111

Fig. 6-5. Load of bus 4 and 6 with and without EV charging patterns – Scenario No.2 (100% slow charging EVs)..... 111

Fig. 6-6. Load of bus 4 and 6 with and without EV charging patterns – Scenario No.3 (50% slow charging and 50% fast charging EVs)..... 112

Fig. 6-7. Total hourly power loss of EDS for scenario No.1 112

Fig. 6-8. Hourly voltage of each bus of EDS for scenario No.1 113

Fig. 6-9. BES performance in bus 3 for scenario No.1 compared to the base scenario (no EV) 114

Fig. 6-10. Total hourly power loss of EDS for scenario No.2 114

Fig. 6-11. Hourly voltage of each bus of EDS for scenario No.2 115

Fig. 6-12. BES performance in bus 3 for scenario No.2 compared to the base scenario (no EV) 115

Fig. 6-13. Total hourly power loss of EDS for scenario No.3 116

Fig. 6-14. Hourly voltage of each bus of EDS for scenario No.3 116

Fig. 6-15. BES performance in bus 3 for scenario No.3 compared to the base scenario (no EV) 117

Fig. 6-16. Total power loss of the system for each scenario 118

List of Abbreviations

adaptive robust optimization	ARO
battery energy systems	BES
Block Coordinate Descent	BCD
Electric vehicle	EV
Electric vehicle charging station	EVCS
Electricity distribution system	EDS
forward backward sweep-based method	FBS
Genetic Algorithm	GA
internal combustion engine	ICE
Newton–Raphson method	NR
Particle Swarm Optimization	PSO
Renewable energy sources	RES
solar photovoltaic	PV
Vehicle to grid	V2G
wind turbine	WT

1. Introduction

Problem Description

Environmental concerns such as global warming and fossil fuel limitations have been of considerable importance for energy provision sector in 21st century [1]. The transport sector plays one of the main roles in air pollution resulting in road transport electrification, whereby employing electric vehicles (EVs) seems to be a reasonable alternative, compared to combustion vehicles [2]. To supply the upcoming wave of electricity requirements by EVs, further energy alternatives such as renewable energy sources (RESs) should be integrated into electricity distribution system (EDS). In today's energy sector RESs, such as solar photovoltaic (PV) and wind turbine (WT), as well as battery energy systems (BESs) have been remarkably highlighted in practice. A simple schematic representation of a modern EDS with these elements is given as Fig. 1-1 [3]. CS refers to charging station.

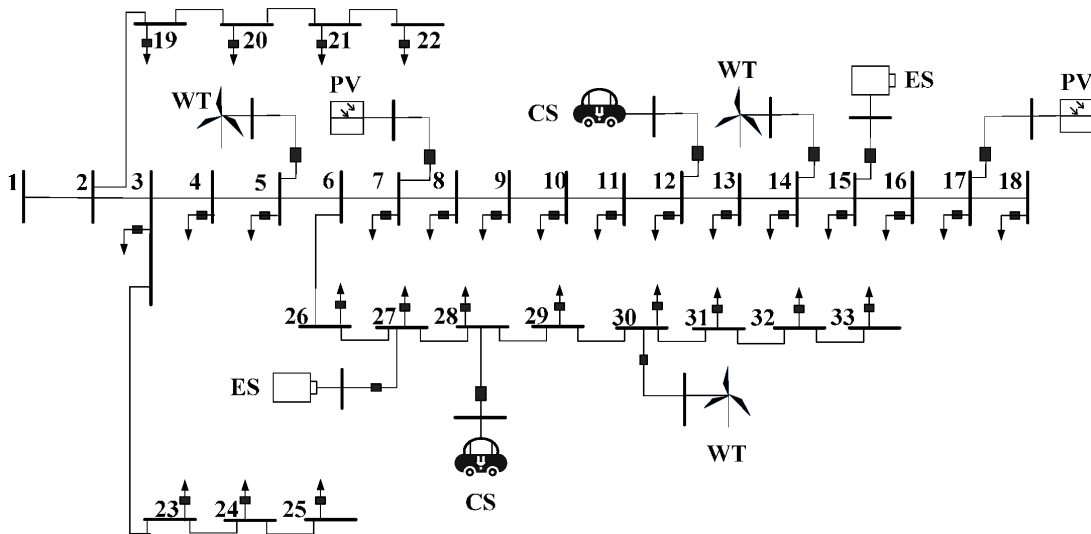


Fig. 1-1. A sample schematic representation of a sustainable EDS

The employment of RESs increments the quality and flexibility of EDS in supplying EVs on one hand, and facilitates meeting the global requirement of air pollution improvement and carbon emission reduction, on the other hand [4]. However, RES generation along with the customers' emerging proactive role has introduced several challenges such as energy imbalance, flickers, reverse power flow, and voltage rise in EDSs [5]. EVs with vehicle-to-grid (V2G) functions can be regarded as ideal assets to level the generation and consumption of electricity throughout the EDS by coordinately integrating into the system [6]. However, EV integration into the EDS must be implemented based on reasonable operational decisions considering system's constraints such as line congestion, voltage deviations, etc.

Although, a proper operation-based energy management model can successfully provide a promising operational status for distribution system operators, the volatile nature of RESs still poses a noticeable effect on the optimal operation of distribution systems in practice. In fact, ignoring the forecast uncertainties associated with RES and EDS's load can result in non-optimal or even infeasible energy management solutions, while, considering these uncertainties along with the arbitrage abilities of V2G technology through EV charging can significantly improve the distribution system efficiency and its energy management [7].

Research Questions

Research questions are added as the required tools to solve the problem.

- 1) A new EDS energy management model is required to model the interactions between RESs, BESs, and EDS in the network as a whole while considering the inverter-based operation of these systems, as in the modern EDS operation, inverters can play a noticeable role in providing reactive power support to the network.

- 2) A new robust optimization model is required to first cope with the associated problems with scenario-based models, and also be applicable when characterizing binary decision variables after uncertainty realizations which is not applicable through conventional dual-based RO models.

Research objectives and scope

This research investigates the optimal energy management of electricity distribution systems at the presence of EVs, by which the overall system power loss, energy cost, and renewable energy curtailments are minimized.

In particular, the aims are:

1. Providing an efficient energy management for electricity distribution system by coordinated integration of RES and BES systems at the presence of EVs. Using the arbitrage ability of BES charging/discharging as well as reactive power controllability of RESs, the system operator (SO) would be able to maintain the distribution system operational constraints such as voltage and frequency tolerance. In fact, the analysis of this thesis is finally conducted to investigate the effects of EV employment of EDS voltage and power loss.

2. Maximizing/Minimizing the integration/curtailment of renewable energy sources (RESs) in electricity distribution system. This would be based on voltage deviations due to the sudden increase in volatile RES generation. The arbitrage ability of BES technology is also used for this purpose.

3. The overall system costs is minimized considering the upstream market energy prices, the arbitrage ability of BES technology, and the energy management model which handles the integration of renewables into electricity distribution system at the presence of EV charging

pattern.

4. Providing immunized solutions against the uncertainties associated with RES generation through a novel robust optimization approach. Unlike previous uncertainty characterizations models, the novel robust model in this research is capable to provide more practical results for system operation.

Dataset

The IEEE 33 bus system is considered as the test systems in the case studies which have been used in numerous studies. Moreover, a realistic 6 bus system in Adelaide, Australia, is used as the final case study under uncertainty. More detailed data set is presented in the body of this thesis.

Thesis organization

The organization of this thesis is as follows:

In Chapter 2, the background of the study is presented. The novel directly solvable EDS power flow model is given in Chapter 3. Chapter 4 is dedicated to the general multi-objective energy management model. The EV load model in EDS energy management model is presented in Chapter 5. The BCD robust model is introduced and discussed in Chapter 6. The thesis is concluded in Chapter 7. Chapter 8 represents further conducted studies at the time of this thesis that relate to the novel BCD robust model.

2.Literature Review, Knowledge Gap, Motivations, and Contributions

This chapter presents the literature review divided into three parts including:

1) Literature review on EDS energy management as a whole at the presence of RESs, BESs, and EVs.

2) Literature review on uncertainty modelling approaches in electricity distribution system, in which probabilistic, stochastic, and robust models are reviewed and the advantages and disadvantages of each are counted.

3) Literature review on EVCS integration into electricity distribution system, in which we review the important undertaken steps in characterizing EVCS to enhance the existing EDS energy management solutions.

Finally, the knowledge gap, forming the main motivations behind this study, are presented.

The contribution of this chapter is presented in the following accepted published research article which was not online at the time of submitting this thesis:

M. Aghamohamadi, A. Mahmoudi, John K. Ward, M. H. Haque, "Review on the State-of-the-art Operation and Planning of Electric Vehicle Charging Stations in Electricity Distribution Systems," 2021 IEEE Energy Conversion Congress and Exposition (ECCE), Toronto, Canada, 2021.

The student has investigated the reviewed studies. Analysis and interpretation of the reviewed papers has been done by him and the co-authors. A draft of the paper was prepared by the student. Revisions and comments were provided by the co-authors so as to contribute to the interpretation.

The literature review is as follows:

2.1. EDS Management at the Presence of EVs, BESs, and RESs

The optimal operation of distribution system at the presence of EVCSs was presented by [8] to enhance the reliability of the distribution system. However, EDS constraints such as voltage/current tolerance weren't considered in the study of [8]. Authors in [9] present a model to mitigate a huge number of EVs' charging patterns in which the EDS constraints are ignored, similar to [8]. This is a disadvantage as the main idea behind coordinated EV charging in EDS is to charge EVs when the system is not under pressure (off-peak hours) and use V2G technology when the system needs support (peak hours) [10]. In [11] a smart charging strategy was proposed for optimal integration of electric vehicles into electricity distribution system through V2G technology. The study of [11] showed that, the small energy trade between a single EV through V2G would not be considerable compared to the EDS energy trade scale. Therefore, the EVs support for distribution system is effective if an EV aggregator or an EVCS operator acts on behalf of EVs. A two layered charging strategy for a parking lot equipped with EV charging points was proposed in [12] considering realistic vehicular mobility and parking patterns. However, the effects of EV charging patterns on EDS were ignored. This becomes vital when EDS is under peak load or configuration-based stress according to which, the reliability constraints of the system may be jeopardized. Authors in [13] investigated the effects of different EV penetration levels on EDS reliability and operational constraints such as voltage deviation limitations and power losses. However, the study of [13] ignored the reactive power throughout the distribution system. In fact, most of the studies presented in the literature have investigated the effects of EV charging patterns on EDS through real power exchange only. In [14], a charging pricing methodology was proposed for EV charging to enhance the voltage profile in EDS, characterizing the EVCS's income and EV owners' response to price signals. However, the

study of [14] ignores the reactive power in its model. This issue also exists in the study of [15] where the real power demand of EVs is controlled through a balanced charging strategy by which both EV owners and system operator can achieve maximum benefits. A two layer energy management model was proposed in [16] to prevent overloading in EDS transformers by controlling EVs real power during charging. It deserves mentioning that, the studies [8, 11-13], similar to studies [14-16], only managed the real power of EVs in their models. However, EVs can also be used to inject/absorb reactive power to/from the grid with the help of their on-board bidirectional battery chargers [17]. Moreover, the inverters in EVCSs can also be employed in providing reactive power and voltage stability for the upstream network.

The correlation between wind energy generation and EV integration was considered through EDS reconfiguration to reduce power losses in [18]. Although RES has been considered in the study of [18], it didn't characterize neither V2G nor BES in the energy management model. A summary of the above literature review, on EV, BES, and RES integration into EDS energy management, is presented by Table 2-1. Accordingly, a comprehensive energy management model is required to model all these elements at the same time while acknowledging the active/reactive power trade in the system, **which forms the first motivation of this thesis.**

Table 2-1. Approaches in EV integration into EDS energy management

Reference No.	EDS constraints	RES integration	BES integration	V2G technology
[6]	✓	✓	✗	✓
[8]	✗	✓	✗	✗
[9]	✗	✗	✗	✓
[11]	✓	✗	✗	✓
[12]	✗	✗	✗	✓
[13]	✓	✗	✗	✓
[14]	✓	✗	✗	✗
[15]	✓	✗	✗	✗
[16]	✓	✗	✗	✓
[17]	✓	✗	✗	✗
[19]	✓	✓	✗	✗
[20]	✓	✗	✗	✗
[18]	✓	✓	✗	✗

2.2. EDS uncertainty modeling

Partial study has focused on characterizing RES forecast uncertainties in distribution systems, so far. In [21], an energy management model was proposed for EDS to reduce prediction error for photovoltaic generation using feature mapping-based kernel function. The study of [21], in fact, did not optimize the energy management model based on uncertainties, as it aims to only reduce errors of RES generation, while these errors may change in practice. In other words, it provided more accuracy in terms of input RES generation prediction and the energy management model was solved as a deterministic problem (no uncertainty characterization was conducted). In [22] and [23], the uncertainties associated with renewable energy sources were modelled by probability density functions formed by Monte Carlo simulation. Such density function for solar

radiation is given by Fig. 2-1 [23].

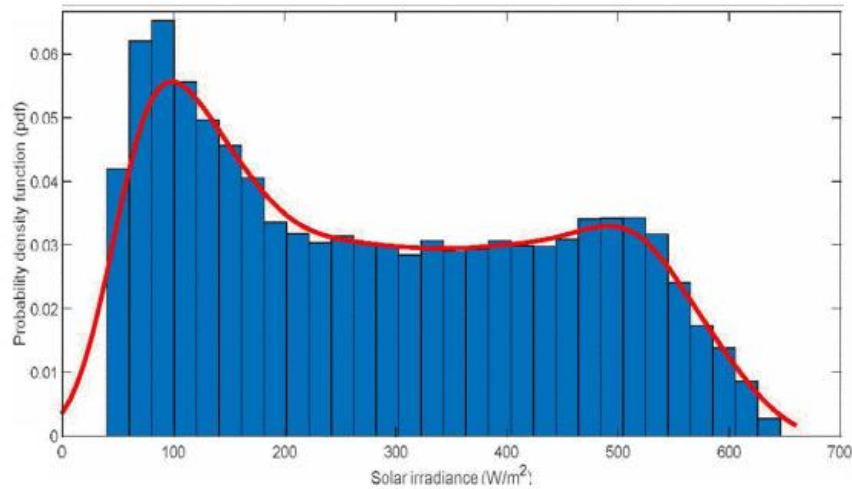


Fig. 2-1. Solar irradiance histogram and its estimated pdf [23]

The scenario-based models of [22, 23] are subject to non-tractability which is due to the high required number of scenarios, especially, when several uncertain parameters are considered and a proper level of feasibility against different realizations of uncertain parameters is required. To obtain more tractable solutions, Stochastic Optimization (SP) was employed in [24] to characterize the uncertainties of renewable energy sources in distribution system. SP was also employed in [25] in a multi-objective economical/environmental operation of distribution system to model the uncertainties of wind generation over time. Similar SP models were also proposed in [26-29]. Despite the advantages of the aforementioned SP models of [24-29], they face the lack of tractability which is due to the required full distributional knowledge of uncertain parameters, which may not be easily available [7]. For example, in [29], the required scenarios for load, electricity price, wind power, and PV power are given in Fig. 2-2 parts A, B, C, and D, respectively, illustrating the huge required input data for scenario-based and stochastic models. Moreover, if the uncertain parameters deviate from the considered scenarios, the performance of

SP cannot be guaranteed against the uncertainties. This issue is also true for probabilistic models in [22, 23].

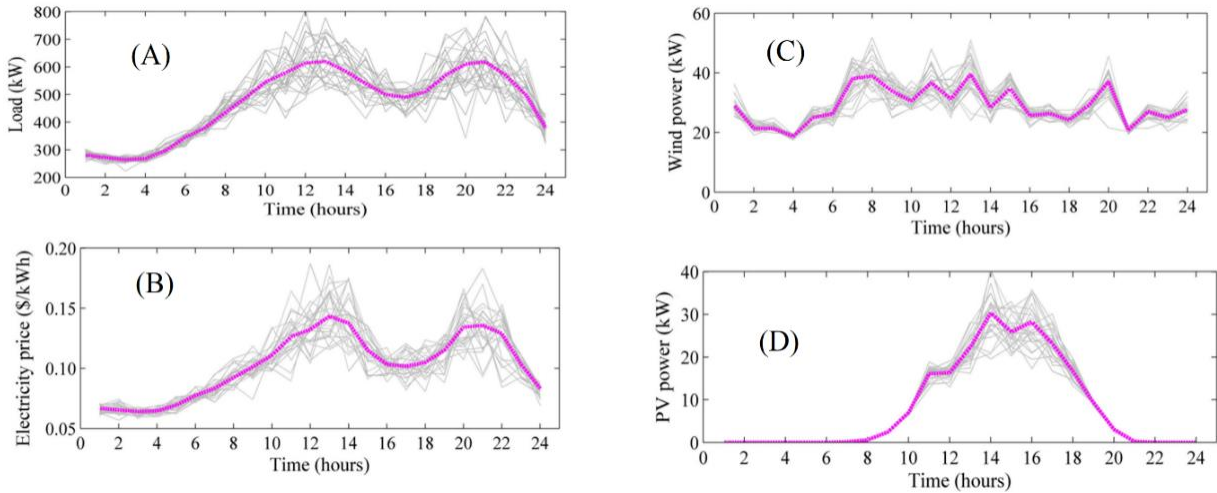


Fig. 2-2. The uncertainty scenarios employed by [29]

To cope with the aforementioned problems in probabilistic and stochastic models, robust optimization (RO) has been recently employed in the energy management of distribution system to characterize the uncertainties of load and renewables. RO considers the worst-case realization of uncertainties instead of modeling them through various scenarios in SP, resulting in a tractable problem with a moderate computational burden. A comparison between scenario-based model and RO is provided in Fig. 2-3 which shows the difference in SP and RO in terms of characterizing the uncertainties of electrical energy [29]. Fig. 2-3A represents both the forecast value and the actual realization in real world. To model the forecast uncertainties scenarios are generated as forecast values which is presented by Fig. 2-3B. However, in RO models, polyhedral bounded intervals are used instead of scenarios i.e., Fig. 2-3C.

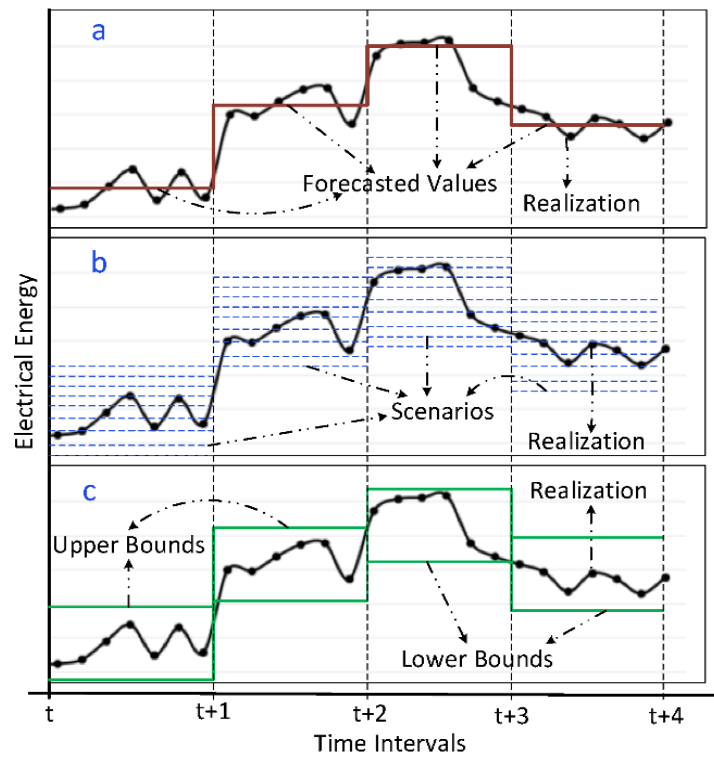


Fig. 2-3. Comparison between SP and RO models [29]

In [30], a robust optimal power flow (OPF) was proposed, characterizing the uncertainty of RESs in the distribution system. In [31] a data-adaptive robust optimization is proposed for economic dispatch of active distribution systems to characterize the uncertainties of RES. However, no BES was considered in the model of [30, 31], while the arbitrage ability of BES can significantly improve the renewables integration into distribution system. The data-adaptive model in [31] is conducted to reduce the conservativeness of RO which is due to the consideration of worst-case realization of uncertain parameters. However, it is subject to an extensive mathematical burden, which is due to the consideration of different uncertainty scenarios in solving the problem, while this can be achieved by examining the robust solutions (after solving the RO model) against trial scenarios. The forecast uncertainties associated with RES were modeled through RO in [32, 33] in which the tri-level min-max-min problem was

solved through the column-and-constraint generation (C&CG) methodology presented by [34], while, duality theory and linearization techniques (such as big-M technique) were used to recast the inner bi-level max-min problem into a single-level max problem. Despite the advantages of [30, 32, 33], they are subject to an extensive mathematical/computational burden which is due to the employment of decomposition methodology, duality theory, and big-M transformation technique when solving the RO problem. Moreover, the use of duality theory limits the application area of RO in terms of characterizing mixed-integer models in the second-stage problem (the inner max-min problem). This is due to the fact that, dual of a mixed-integer model is generally weak, non-tractable and complicated [35]. This issue becomes more important when binary variables such as BES charging/discharging status need to be obtained after uncertainty realizations in the second-stage problem. Due to this limitation, the BES charging/discharging status, which is controlled by binary variables in [32, 33], was modelled in the first-stage problem with no uncertainty characterization, while, BES can optimally contribute to reduce the impact of uncertain production on the system by absorbing/injecting power in cases of surplus/deficit of renewable generation. Therefore, BES charging/discharging status should be adjusted in the second-stage problem in the face of uncertainties rather than the first-stage problem, which is solved prior to uncertainties. **This conclusion forms the second motivation of this study.**

A comparison between the reviewed studies [22] - [33] is given by Table 2-2.

Table 2-2. Comparison between uncertainty approaches

Reference No.	Uncertainty modeling approach			Considered uncertainty source		
	Probabilistic	Stochastic	Robust	load	RES	Price
[22]	✓			✓	✓	✗
[23]	✓			✓	✓	✗
[24]		✓		✓	✓	✗
[25]		✓		✓	✓	✗
[26]		✓		✓	✓	✗
[27]		✓		✓	✓	✗
[28]		✓		✓	✓	✗
[29]		✓		✓	✓	✓
[30]			✓	✗	✓	✗
[31]			✓	✗	✓	✗
[32]			✓	✓	✓	✗
[33]			✓	✗	✓	✗

2.3. EVCS Operation and Planning in EDS

Considering the environmental concerns associated with internal combustion engine (ICE) vehicles in recent years, a significant increase has been observed in transportation electrification. One of the trending approaches in this field is the EV employment which is a green alternative for ICE vehicles and can result in reducing CO₂ emissions, air pollutions, greenhouse gases, etc. Although, EVs are environment friendly, these assets can pose noticeable effects on the planning and operation of EDS. This is because each EV can be considered as three apartment units in terms of electricity consumption, which is a serious issue for EDS given the considerable number of EVs in today's transportation system. In particular, the new escalating electricity demand by

EVs may result in serious EDS technical problems such as supply imbalance, unwanted harmonics, energy shortage, and voltage/frequency deviations. Despite the operational disadvantages associated with non-coordinated charging of EVs, these vehicles can become useful assets to EDS as many recent EVs are equipped with V2G technology which enables the energy trade from EVs to EDS [36]. This provides further operational flexibility and support for EDS if EVs are coordinately integrated. In this context, EV charging stations (EVCS) play a crucial role as they are responsible for the coordinated integration of a considerable number of EVs in EDS operation at a time [37]. EVCSs can level the load curve through peak shaving or valley filling and, accordingly, enhance the stability and performance of the EDS. EVCSs can also provide support for EDS when concerned by coordinating intermittent renewable energies, such as wind farm (WF) and Photovoltaic (PV) systems [38]. Considering the crucial role of EVCSs in EDS, however, inappropriate siting and sizing of EV charging stations could have negative effects on EDS [39]. This is important as EVCSs are not the only elements in EDS as many variables forming RESs, large-scale battery energy storages (BESs) are included in the conducted operation/planning models [40]. Although, there have been partial review studies on EV integration into EDS [41], no study has focused on the planning and operation of EV charging stations in EDS, while, these systems are about to be broadly installed in electricity distribution system in the coming years. Therefore, there is an urgent need for a proper summary on the operation and planning of EVCSs and their associated impacts on EDS to better reflect the pros and cons associated with these assets. The current section reviews the state-of-the-art operation and planning of electric vehicle charging stations as well as their associated impacts on electricity distribution system. The recent studies are introduced considering both qualitative and quantitative aspects. Study areas in operation/planning of EVCSs are introduced in Section 2.

Studies focusing on the operation of EVCSs in EDS include five subsections concerning energy management, market participation, EDS support, renewable energy system (RES) integration, and demand response (DR) programs. Studies focusing on the planning of EVCSs include EVCS planning considering EDS operational constraints, EDS reinforcements, traffic and transportation constraints, coupled traffic-electric network constraints, and RES reinforcements in EDS. In Section 3, pros and cons of the reviewed studies are introduced. A quantitative study is also conducted in Section 4 on the current literature. Finally, highlights, observations, and possible future studies are presented in Conclusion Section.

Electric vehicle charging stations are considered as hot load points in EDS, if working in a high percentage of their capacity [42]. Therefore, operation of EVCSs and their interaction with upstream EDS can become challenging, considering the dramatic increase in EV employment in the last and the coming years. Uncontrolled and unregulated charging of EVs can also result in an unexpected peak load at a specific time, which may exceed the capacity of the distribution grid [43]. Generally, there are two main solutions to meet the required electricity consumption by EVCSs and avoid operational issues such as loss of load, voltage/frequency imbalance in EDS. The first solution is the optimal operation of EVCS's and their interaction with EDS and other elements such as RESs and BESs systems in order to meet the required electricity by EVs while using the capacity of EDS [44]. The second solution is the EDS enforcement which requires an optimal planning to increase the capacity of EDS with different alternatives [45].

Optimal Operation of EVCSs in Distribution System

In the recent years, there has been a considerable focus on optimal operation and integration of EVCSs and each study has investigated these solutions through different perspectives. In the current review, five main important aspects of EVCS operation are presented and discussed as

follows:

Energy management: The rapid increasing demand of EVs has significantly reformed the net electricity consumption pattern in EDS among different sectors, i.e., residential, commercial, industrial, etc. This accordingly changes the power flow profiles and voltage/frequency status in EDS. Some studies have focused on the energy management of EVCSs equipped with RES and/or BES systems to maximize their benefits through optimal interactions with upstream EDS. To more realistically reflect the EVCS electricity demand, [46] presented a mathematical model for EV charging patterns in a rapid EVCS. The study also provided a forecast on EV arrival rates and the EVCS's demand. Despite their extra demand, EVCSs can provide remarkable opportunities for improving EDS energy management and grid support if coordinately operated [47]. In [48] a fuzzy-based control methodology was proposed for coordinated integration of EVs in a EVCS through V2G, while, dynamic load profile was employed to evaluate the effectiveness of the model in peak shaving and valley filling. Authors of [48] extended their work in [49], for real-time support of distribution system considering possible energy dispatch approaches at substation level. In [50] a systematic co-modeling and simulation framework was proposed to investigate the impacts of PEV charging facilities on the electric distribution system and transportation system. Six more references will be added in the full version of the paper.

RES integration: Several studies have investigated the effectiveness of EVCSs in maximizing RES integration in EDS. In [51] a rule-based energy management strategy was proposed for Photovoltaic-assisted EVCSs to participate in upstream network ancillary services. An adaptive EVCS charging energy management model was introduced in [52] for optimal operation and reconfiguration of EDSs with high penetration of PVs. Integration of PV system was also considered in the proposed model of [36] to assist with EV charging patterns regarding

energy prices, V2G interactions, and reserve market dynamics. In recent years, many EVCSs have become equipped with PV systems to assist with EV charging patterns. In [43] an energy management for a solar-powered EVCS was introduced to optimally support the EDS network. Three more references will be added in the full version of the paper.

EDS support: Considering the availability of V2G technology in EVs, EVCSs can play the role of an interface between a group of EVs and EDS to provide support for upstream network. This support can result in voltage/frequency stabilization, power loss minimization, reliability improvement, etc. [53]. A considerable number of studies have been investigating the possible EDS supporting opportunities by optimal operation of EVCSs, considering V2G availability. In [54] an operation managing strategy was proposed to reduce the cost of EV charging while providing technical support for upstream distribution system through V2G aggregators. The study of [43] proposes an efficient energy management approach for residential PV systems to power EVs while employing the V2G technology to mitigate the PV penetration impacts and allow the growth of PV systems in power grids.

Market participation: Several studies have focused on the market participation concepts, such as bidding strategy, relying on the arbitrage ability of EVCS (due to V2G technology). In fact, EVCSs can be considered as prosumers with the ability of absorbing/injecting power from/to the upstream EDS in different time periods to maximize their daily benefit and meet the EV charging patterns at the same time [44]. In [55] the optimal model of an EV route has been proposed based on upstream market pricing, in particular time-of-use (TOU) pricing, to minimize the total distribution costs of the EV route while satisfying operating constraints. A learnable Parthenon-genetic algorithm with integration of expert knowledge about EV charging station and customer selection was developed to solve the model in [55]. An online pricing

scheme for EV charging was proposed in [56] with the application in EVSCs. According to the model. A myopic charging station was considered in the model of [56] illustrating that there exists a pricing mechanism which jointly maximizes the social welfare and the profit of the charging station when the charging station knows the utilities of the users. A price incentive-based charging navigation strategy has been proposed for optimal charging/discharging management of EVs in EVCSs in [57]. The study considered the price variations and the spatial-temporal influence of EVs' charging decision, especially the simultaneous charging requests. Four more studies will be introduced in the final version of the paper.

Demand response: EV load distribution is skewed toward the stations located in the hotspot areas, instigating longer queues and waiting times, particularly during afternoon peak traffic hours. This can result in major challenges such as the increase of peak load and voltage/frequency instability. These cross effects have motivated researchers to conduct a series of studies to exploit the potential of EVCSs in demand response, especially in peak periods. In [58] a new dynamic pricing has been proposed to reduce the overlaps between residential loads and EVCSs load through EV load shifting in peak periods. The study results in dynamic prices to motivate EV owners to select EVCSs with lower prices which levels the distribution system's load. The ability of EVCSs in active participation in demand response provision has been shown in [59]. In the conducted study, an EV queuing model is employed to form the EV parameters associated with charging patterns. The model is then used for smart load control of EVCS to maximize the DR participation. The study of [59] shows a significant potential of EVCSs in DR provision by comparing the results with uncontrolled EV charging. DR participation of EV owners towards time-of-use tariff was considered in the optimal planning of EVCSs in [60]. The proposed model involved distribution system manager (DSM) benefit maximization derived from

the appropriate use of EVCS for charging and discharging vehicle batteries, reliability improvement and supplying network's load demand at peak times. Two more studies will be added to this section in the final version.

Optimal Planning of EVCSs in Distribution System

Regarding the considerable operational effects of EVCSs on EDS, it is important to investigate the expansion planning of these systems [38]. A considerable number of studies have been focusing on optimal sitting and sizing EVCSs in EDS. According to the conducted review, these studies have investigated the planning problem of EVCSs considering the following concerns:

EDS reinforcement: The considerable increase in electric vehicles' employment counts as a load growth for EDS which results in EDS reinforcement. This has motivated several researchers to come up with solutions for joint planning of EDS and EVCSs. In [61] a robust mixed-integer model was proposed for multistage joint expansion planning of EDS and EVCSs, regarding the uncertainties of EDS and EV loads. The construction of substations, EVCSs, lines, and distributed generations (DGs) were determined through each stage of the planning horizon. Authors of [62] also proposed a joint planning of EVCSs and EDS with the objective of minimizing the investment and operation costs while capturing maximum traffic flow in the selected residential area. Similar studies associated with joint planning of EDS and EVCSs are also given by [63, 64].

RES, BES and DG reinforcement: Prominent features of RESs and DGs has been proven as an appropriate alternative for compensating relevant problems of EVCS installation. In [65] simultaneous optimal planning of EVCSs and DGs was presented to address the financial/technical/environmental challenges associated with EV charging patterns. The model was solved for the IEEE 33-bus system through a genetic algorithm, illustrating the effects of

EVCS installation in the presence/absence of DGs on total costs, reliability, loss, voltage profile, and emission. In the study of [66], authors have considered the time-varying nature of DG generation and load consumption (instead of the static values in previous literature) in optimal planning of EVCSs, DGs, and BESs in distribution system. A similar study was conducted in [67] for joint planning of RES, BES, and EVCSs. However, in the model of [67] the necessary charging demand of EVs was modeled based on travel patterns which makes it more realistic than other EV load modeling models. Moreover, scenario generation was employed to simulate the uncertainties associated with RES. To achieve more practical solutions, stochastic programming was employed in [68] to model uncertainties associated with EV charging patterns in the joint planning of EVCSs, RES, and BES.

EDS operation constraints: Considering the dynamic nature of EDS and its sensitivity to load deviation in different load points, it is essential to reasonably locate and install the EVCSs throughout the EDS. Several studies in literature have focused on this problem in which EDS operational constraints such as voltage/frequency deviation as well as EDS reliability constraints are taken into consideration. In [69] an optimal planning model has been proposed for EVCSs considering the constraints of EDS. The study considers the voltage profile improvement as the benchmark, while, a combination of particle swarm optimization algorithm and genetic algorithm was used to solve the planning model. Power loss minimization is another important aspect to be considered in EDS operation and planning of EVCSs. In [38] EVCS planning was conducted considering both voltage profile improvement and power loss minimization as operating constraints, while the objective function was to minimize the total cost associated with EV charging stations to be planned. Two more references will be added to this section in the final version of the paper.

Transportation and traffic constraints: A practical perspective in the planning of EVCSs in distribution system is the consideration of traffic constraints. This is due to the fact that, EV changings are strongly dependent on EV travel patterns and the distribution of population in the area. A EVCS planning model capturing traffic and EV location parameters was proposed in [70] to maximize the EVCS service. The study was conducted on the IEEE 33-bus EDS joint with a 25-node traffic network system. In [71] the traffic demand and battery data as well as the distribution of EVs were modelled by Monte Carlo simulation. The data was then used for optimal siting and sizing stand-alone EVCSs on highway networks.

Coupled traffic-EDS constraints: EVCSs couple future transportation systems and power systems. That is, EV driving and charging behavior will influence the two networks simultaneously. To achieve more realistic and practical EVCS planning solutions, the cross-effects between EDS and traffic network was considered in [72] and [73]. In [74] the EVCS's benefits was maximized through optimal sitting and sizing of the system considering changes in time, location and capacity. The model integrated electricity distribution system constraint, the user constraint and the traffic flow captured constraint. In addition to operational aspects of EDS and traffic network, the expansion of these system was considered in the optimal planning of EVCSs in [75]. In fact, the study of [75] conducted a simultaneous planning model including sites and sizes of new EVCSs, charging spots, traffic network lanes, and EDS lines. A similar study was also presented by [76] employing parking lots as an innovative solutions to achieve sustainable development in terms of EVCS planning.

2.4. Quantitative Evaluation of the Literature

In this section the conducted studies on optimal planning and operation of EVCSs are

analyzed on a quantitative basis. The reviewed studies in Section 3 are illustratively given by Fig. 2-4.

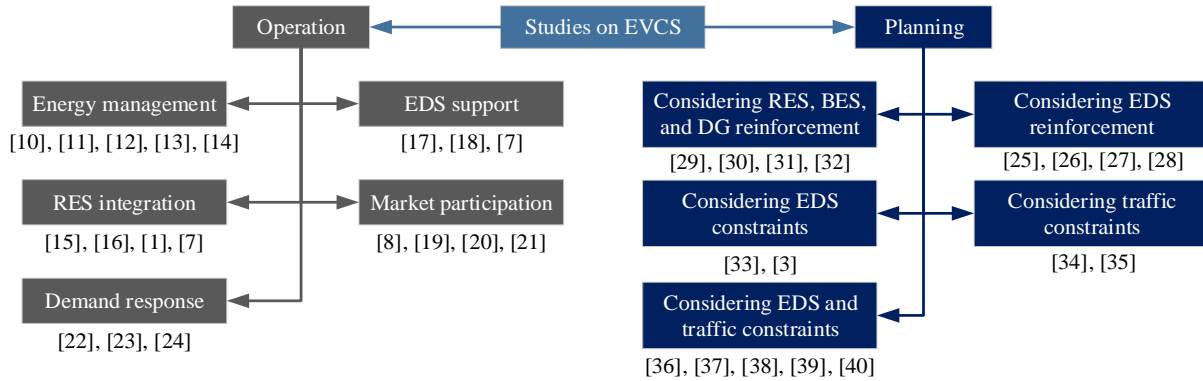


Fig. 2-4. Categories of the reviewed studies in planning and operation of EVCSs (references in this figure are based on the paper: M. Aghamohamadi, A. Mahmoudi, John K. Ward, M. H. Haque, "Review on the State-of-the-art Operation and Planning of Electric Vehicle Charging Stations in Electricity Distribution Systems," 2021 IEEE Energy Conversion Congress and Exposition (ECCE), Toronto, Canada, 2021.)

Fig. 2-5A shows the distribution of the reviewed studies over years starting from 2012, while, Fig. 2-5B shows the total number of the reviewed studies. According to Fig. 2-5A, number of the conducted studies in both operation and planning of EVCSs have significantly increased over years, especially after 2017. This is due to the increasing pattern of EV employment in cities and facing challenges in operation and planning of EVCSs in recent years. As it is seen in Fig. 2-5B, there has been more interest in the operation of EVCS in electricity distribution system, i.e., 33 studies, compared to the planning of these systems, i.e., 25 studies. This is reasonable as the main challenge in recent years has been the integration of EVs into electricity network, while the number of EVs has not been considerable in many countries in the world. However, it is expected to face more EVCS planning studies in future which will be in line with the upcoming wave of EV employment.

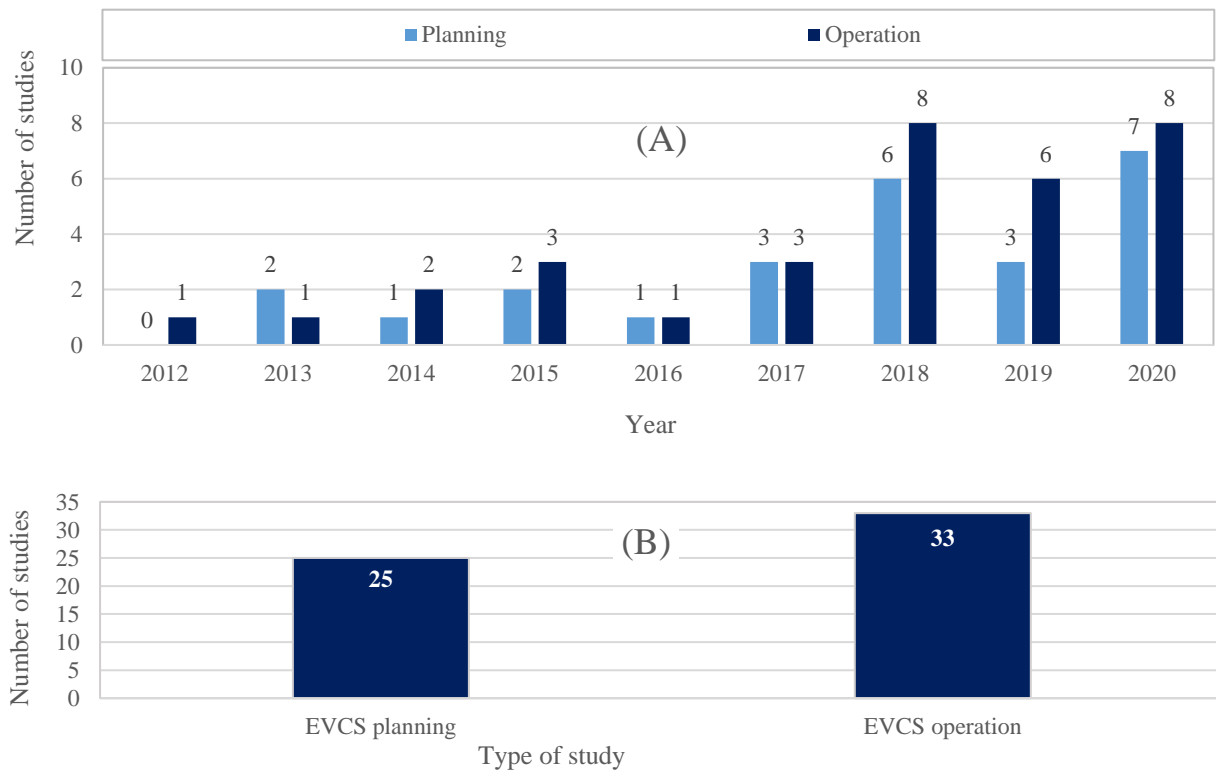


Fig. 2-5. Annual (A) and total (B) number of reviewed studies, concerning EVCS operation and planning between 2012-2020

2.5. Knowledge Gap and Motivations of this Study

According to the conducted review, following knowledge gaps are presented:

- 3) A new EDS energy management model is required to model the interactions between RESs, BESs, and EDS in the network as a whole while considering the inverter-based operation of these systems, as in the modern EDS operation, inverters can play a noticeable role in providing reactive power support to the network.
- 4) A new robust optimization model is required to first cope with the associated problems with scenario-based models, and also be applicable when characterizing binary decision variables after uncertainty realizations which is not applicable through conventional dual-based RO models.

- 5) And finally a proper exploration is required to investigate the effects of EVs on EDS voltage and power losses under the uncertainty of EDS load, to provide more realistic solutions for EDS energy management.

2.6. Contributions of this study

Following contributions are presented in this thesis to achieve the objectives in section 1.2:

Contribution 1: A novel directly solvable set of power flow equations

A new directly solvable power flow problem has been proposed for EDS, introducing a connectivity matrix in line with a new indexing of load flow equations. The new power flow model is developed generally and is capable to be added to any EDS study as the constraints of the model. This means, the power flow calculation does not need to be conducted separately. Therefore, the need of load flow calculation methodologies, such as Newton–Raphson method (NR) and forward backward sweep-based method (FBS), as well as optimization approaches, such as Genetic Algorithm (GA) and Particle Swarm Optimization (PSO), is eliminated as the proposed model characterizes both load flow and energy management constraints in a single and unified model. This provides users the opportunity of solving the problem with commercial optimization packages, i.e., CPLEX, GAMS, etc., in a single shot with no need to develop further optimization approaches involving iterative procedures and load flow calculations. Note that, the employed modified load flow equations in line with the connectivity matrix can be used in any other EDS study, concerning load flow calculation, as the constraints of the model.

Contribution 2: A general multi-objective energy management model for inverter-based integration of RES, and BES system

The proposed directly solvable power flow problem is used to build up a multi-objective

energy management model for RES-BES-equipped distribution systems. The first objective of the model minimizes total EDS power losses, and the second objective minimizes the voltage deviations of each bus over time. These objective functions are optimized being subject to load flow constraints, RES/BES optimal operation, and voltage/current tolerance of EDS. The proposed energy management model enables both active and reactive power controllability of RES and BES systems. New continuous variables are defined for RES and BES representing active and reactive power share of these systems during the operation. Accordingly, BES can absorb active or reactive power in each time slot and inject it back to the network as active or reactive power in another time slot.

Contribution 3: Integration of EV loading into the energy management model and investigating the effects of EV charging on EDS voltage and power loss

Electric vehicle activity is modelled by probability distribution functions. The EV's dynamic energy balance is modelled based on EV connections and the model is merged into the energy management model.

Contribution 4: The new robust optimization model to characterize uncertainties of RESs employing block coordinate decent method

An adaptive robust optimization (ARO) approach is implemented to deal with the uncertainties of load in operating EDS through the proposed energy management model. Uncertain parameters are characterized by bounded intervals in polyhedral uncertainty sets. The ARO model is a tri-level min-max-min problem which is not directly solvable. Therefore, a decomposition methodology is employed to recast the min-max-min ARO problem into two problems including a master problem and a sub-problem. A column-and-constraints (C&C) generation methodology is used to iteratively solve the decomposed problem through primal

cutting planes. Two main decisions are made in ARO, namely "here-and-now" decisions, which are obtained before any uncertainty realizations, and "wait-and-see" decisions, which are obtained after the realization of uncertain parameters. Several binary variables such as BES charging/discharging status must be obtained after uncertainty realizations in the sub-problem to be able to compensate the effects of uncertain load/price as recourse decisions. However, this is not possible by conventional dual-based robust models as considering these binary variables results in a mixed-integer sub-problem and the dual of a mixed-integer model is generally weak, non-tractable and complicated. Therefore, instead of using duality theory in solving the sub-problem, Block Coordinate Descent (BCD) method is used in the proposed model.

In terms of solution methodology, BCD method is used in the robust approach to iteratively solve the inner bi-level max-min sub-problem by means of Taylor series instead of transforming it into a single-level max problem by duality theory in conventional ARO models. BCD technique was originally devised to deal with single-level problems. By extending the application of the BCD technique to solve the two-level max-min sub-problem (resulted from the C&C generation technique), it is possible to avoid duality theory in solving the sub-problem.

Therefore, the associated limitation in considering binary variables in the sub-problem is eliminated. In fact, mixed-integer models (even non-linear models) can be solved in the sub-problem through the proposed BCD robust model. As a result, uncertainty-dependent binary variables such as BES charging/discharging statuses can be obtained after uncertainty realization in the sub-problem as recourse decisions, resulting in more system flexibility in compensating the uncertainty effects of load. Moreover, the linearization of the dualized inner problem is avoided as the Lagrange multipliers are eliminated in this methodology. Thus, the case-sensitivity of the proposed model reduces as it does not reflect dual variables.

2.7. Conclusion

This chapter presented a comprehensive review on the employment of EVs as well as different aspects considered in operation and planning of EVCSs in EDS. Contributions of the thesis were introduced and the aim of the research were developed. The rest of this thesis presents each contribution and the methodology used to achieve it.

In the next chapter a directly solvable power flow model is developed to use in the energy management model.

3. Proposed General and Directly-solvable EDS Power Flow Equations to Solve Power Flow Problem

This chapter presents a new directly solvable and non-iterative load flow model which is developed using a new bus indexing procedure. A connectivity matrix is also introduced to characterize the configuration of EDS and provide a feasible general representation of load flow equations. This enables the proposed modified load flow equations to be mergeable in any type of EDS study as the constraints of the model. Moreover, unlike previous iterative models, it can be solved directly through off-the-shelf optimization packages in a single shot with no need to further iterative optimization procedures such as metaheuristic methods. This results in a moderate mathematical and programming burden.

The contribution of this chapter is presented in the following published research article [77]:

M. Aghamohamadi, M. H. Haque, A. Mahmoudi and J. K. Ward, "A Novel Directly-solvable Non-iterative Load Flow Model for Radial Distribution System Studies," 2020 IEEE International Conference on Power Electronics, Drives and Energy Systems (PEDES), 2020, pp. 1-6, doi: 10.1109/PEDES49360.2020.9379828.

A Novel Directly-solvable Non-iterative Load Flow Model for Radial Distribution System Studies

Publisher: **IEEE**

[Cite This](#)

[PDF](#)

Mehrdad Aghamohamadi ; Mohammed H. Haque ; Amin Mahmoudi ; John K. Ward [All Authors](#)

46
Full
Text Views



The student has developed the conceptualization. He designed the optimization model. Analysis and interpretation of research data has been done by him and the co-authors. A draft of the paper was prepared by the student. Revisions and comments were provided by the co-authors

so as to contribute to the interpretation.

NOMENCLATURE (for Chapter 3)

i/j	Index of bus number
P_{ij}/Q_{ij}	Active/Reactive power flow
L_{ij}/L_{ji}	Indicator for branch existence between buses i and j
$\mathcal{E}^I/\mathcal{E}^J$	Set of indices i/j
$P_{ij}^{loss}/Q_{ij}^{loss}$	Active/Reactive power loss in each branch
P_j^L/Q_j^L	Active/Reactive load at each bus
Q'_{ij}	Reactive power flow through each branch
Q_{ij}^a/Q_{ij}^b	Shunt capacitors' reactive power in π configuration
V_i	Voltage of bus i
r_{ij}/x_{ij}	Resistance/Reactance of each branch
B_{ij}^a/B_{ij}^b	Shunt susceptance at sending/receiving end

3.1. Introduction

The solution of load flow problem is very important for operation, planning, expansion, and management of electricity distribution systems (EDSs). The load flow solution of EDS is usually obtained by various methods, such as Newton-Raphson [78], Gauss-Seidel [79], and forward-backward sweep-based (FBS) methods [80]. In [81], a power flow analysis for droop-based

islanded microgrids was conducted using current injection-based Newton-Raphson (NR) method. An extended fast decoupled NR method was used in [82] for EDS reconfiguration. Although, NR is suitable for transmission system, it may have a poor convergence pattern for some radial EDSs having high R/X ratios of branches [83]. Moreover, the need of partial derivative of equations makes NR a time-consuming method in terms of both mathematical and programming burden. In [84], Gauss-Seidel (GS) method was employed for voltage stability in EDS. It was also used for EDS loadability analysis in [85]. However, GS method is generally complex, and has poor convergence pattern. In fact, computational time of GS method increases as the number of buses/branches increases. This issue becomes even more vital for larger EDSs [84].

To overcome the aforementioned issues, FBS method was employed in [86] to integrate open unified power quality conditioners for EDS loss minimization. However, the model of [86] utilizes particle swarm optimization (PSO) to determine planning solutions as they need to be fixed in the FBS method to determine EDS load flow solutions. In fact, in each iteration of particle swarm optimization in [86], FBS is conducted to determine EDS load flow based on the given planning solutions by PSO. In [87] genetic algorithm (GA) was used to minimize EDS power losses and voltage deviations by optimal integration of distributed generations and electric vehicles, where EDS load flow was conducted in each iteration of GA. Harmony search algorithm (HSA) was used in [88] to optimize the EDS reconfiguration and the placement of distributed generation units in EDS. Some of these models have been also employed for planning and operation of renewables and battery systems [89].

Although, the aforementioned load flow calculation methods are able to do the job, they need to be conjointly combined with other optimization algorithms such as GA, PSO, HSA, to be able

to optimize the required objective function and the related constraints in EDS studies. This is due to the fact that, existing EDS load flow methods only calculate the load flow and bus voltages and they are not mergeable into the main model to maintain the objective function throughout the network. In fact, it's the optimization engine that determines the EDS optimal planning or energy management solutions [90] while these solutions are fixed in the load flow calculation problem.

The combination of metaheuristic optimization algorithms (or any other optimization approach) with EDS load flow calculation brings additional mathematical and programming burden to the model. Moreover, the computation time of the optimization may easily increase for complex models as it involves two procedures, i.e., optimization algorithm and load flow calculation in each iteration of the optimization procedure. Therefore, further load flow models are required with the ability of being directly solvable with no need to iterative and time-consuming procedures, while, being easily mergeable in different EDS operational/planning models to avoid the use of external optimization engines such as GA, PSO, etc.

To do so, a new EDS connectivity matrix in line with a new indexing of load flow equations have been used to develop a modified load flow model which can be solved directly without using iterative methods such as NR and FBS in EDS studies. Moreover, it can be merged into any other EDS study as the constraints of the model, considering the general structure of the proposed model. In fact, the need of optimization approaches, such as GA and PSO, is eliminated as the proposed model characterizes both load flow and the required constraints (depending on the application) in a unified model. This has been illustratively shown by Fig. 3-1. This provides users the opportunity of solving the problem with commercial optimization packages, i.e., CPLEX, GAMS, etc., in a single shot solving process with no need to develop further

optimization approaches involving iterative procedures and load flow calculations. As it is seen in Fig 3-1, in the proposed model, the need of optimization engines is eliminated as a single-shot solvable unified problem is developed for both power flow and optimization. Note that, Capacitor banks and voltage regulators are not included in the power flow model.

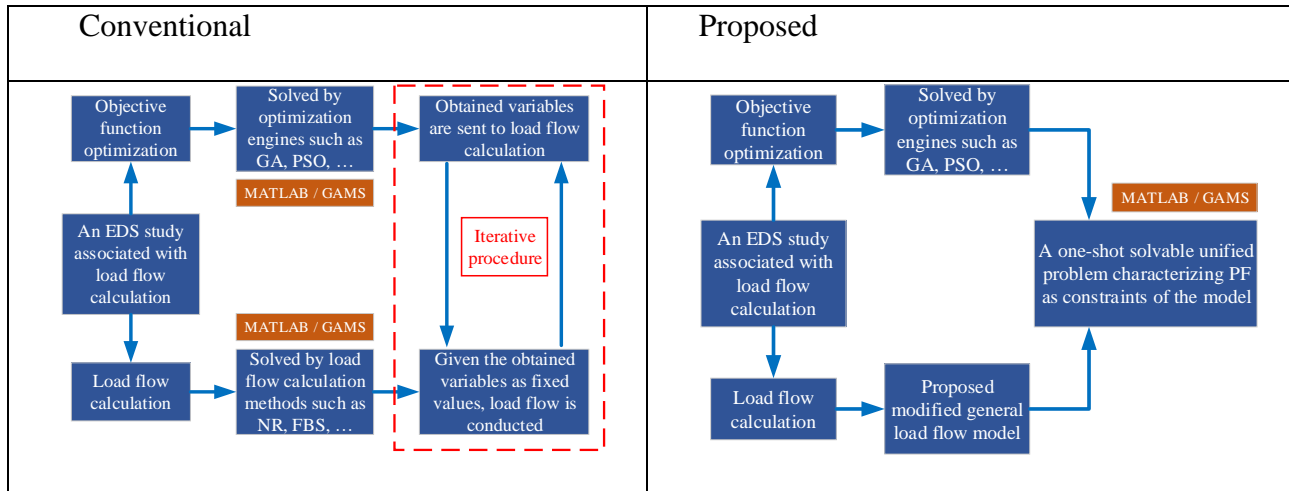


Fig. 3-1. Comparison between the conventional and the proposed EDS power flow models

3.2. The Proposed Modified EDS Load Flow Equations

Fig. 3-2 shows the configuration of a simplified 6-bus distribution system as an example, considering the active power flow only, for the sake of simplicity (no load is considered). This configuration is only employed to numerically introduce the new indexing used in this study.

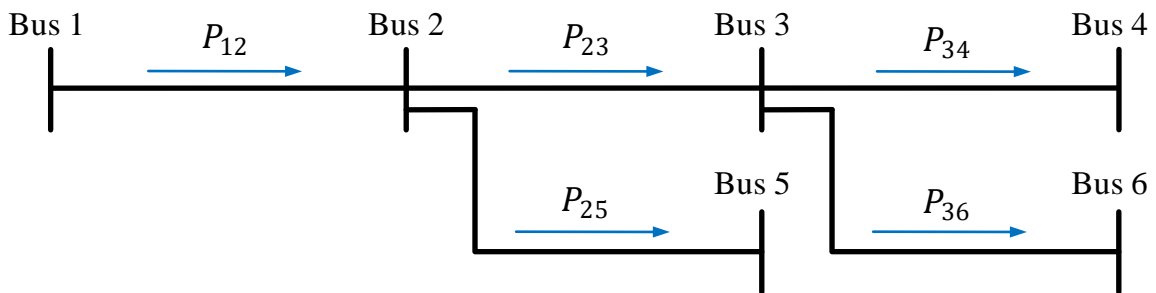


Fig. 3-2. Configuration of a simplified 6-bus EDS

P_{ij} is the power flow through the branch connecting the sending-end bus i to the receiving-end bus j . For the considered system in Fig. 3-2, the relation between actual active power flow is

expressed as (1a)-(1b).

$$P_{12} = P_{23} + P_{25}; \quad (1a)$$

$$P_{23} = P_{34} + P_{36}; \quad (1b)$$

As it is seen in (1a)-(1b), two indexes are needed to generally model the power flow considering both sending and receiving ends. Therefore, it is possible to have different values for i and j in one equation (e.g., $P_{i=1,j=2}$ and $P_{i=2,j=3}$ in (1a)) which is not feasible in a general parametric representation of load flow equations. This is due to the fact that, each bus plays the role of a sending-end and a receiving-end at the same time. In fact, each bus is counted by i if it is a sending-end and is counted by j if it is a receiving-end. To cope with the mentioned infeasibility and avoid ambiguity, alias sets are employed for bus numbering in this study. Alias is an alternate name for a member or a shared member in a set which is used to improve the readability of an outline by descriptive names [91]. Accordingly, power flow equations in (1a)-(1b) can be rewritten as (1c)-(1d), respectively, where the value of j is equal at both sides of the equations.

$$P_{i=1,j=2} = P_{j=2,i=3} + P_{j=2,i=5}; \quad (1c)$$

$$P_{i=2,j=3} = P_{j=3,i=4} + P_{j=3,i=6}; \quad (1d)$$

However, (1c)-(1d) still do not meet the requirements of a general representation to be feasible for all buses and branches of the system which is due to the different values of i in either sides of the equation. In order to cope with this issue, a new connectivity matrix \mathbf{L} is proposed to represent the configuration of the EDS system. Each element of matrix \mathbf{L} , represents the existence of a branch connecting bus i to bus j ($L_{ij} = 1$ if a branch exists and $L_{ij} = 0$ otherwise). Elements of matrix \mathbf{L} alongside alias sets are further employed to develop the new modified load flow

equations. Regarding the fact that, i and j are alias indexes in alias sets Ξ^I and Ξ^J , respectively, the connectivity matrix can be either presented by (1e) or (1f) in the following:

$$\mathbf{L} = \begin{bmatrix} L_{11} & \dots & L_{1j} & \dots & L_{1n} \\ \vdots & \ddots & \vdots & & \vdots \\ L_{i1} & \dots & L_{ij} & \dots & L_{in} \\ \vdots & & \vdots & \ddots & \vdots \\ L_{n1} & \dots & L_{nj} & \dots & L_{nn} \end{bmatrix}; \quad (1e)$$

$$\mathbf{L} = \begin{bmatrix} L_{11} & \dots & L_{1i} & \dots & L_{1n} \\ \vdots & \ddots & \vdots & & \vdots \\ L_{j1} & \dots & L_{ji} & \dots & L_{jn} \\ \vdots & & \vdots & \ddots & \vdots \\ L_{n1} & \dots & L_{ni} & \dots & L_{nn} \end{bmatrix}; \quad (1f)$$

$$\text{where, } 1 \leq i \leq n; \quad , \quad 1 \leq j \leq n; \quad (1g)$$

Therefore, the load flow equations for the 6-bus EDS in Fig. 3-2 can be rewritten as (1h) in the following:

$$\sum_{i \in \Xi^I} (P_{ij} \cdot L_{ij}) = \sum_{i \in \Xi^I} P_{ji} \cdot L_{ji}; \quad \forall j \in \Xi^J; \quad (1h)$$

The values of i and j cannot be the same as there is no branch connecting bus i/j to bus i/j . Therefore, $i \neq j$. Therefore, $P_{i(j+1)}$ is used instead of P_{ij} . Although n can have any other value, but it should not be bigger than 1 because of the existence of sequential bus numbers in a radial system, i.e., $P_{1,2}$, $P_{2,3}$, $P_{3,4}$, etc. Note that, $n = 1$ is still true for other variables. For example, $P_{2,23}$ is defined as $P_{i=2,((j=22)+1)}$. However, if $n = 2$ the problem would be infeasible for $P_{1,2}$ as it is defined as $P_{i=1,((j=0)+2)}$, while, j cannot be zero (note that i and j are alias indices and don't have to be the same). Therefore, the general and feasible parametric representation of load flow equations can be expressed by (1i):

$$\sum_{i \in \Xi^I} (P_{i(j+1)} \cdot L_{i(j+1)}) = \sum_{i \in \Xi^I} P_{(j+1)i} \cdot L_{(j+1)i}; \quad \forall j \in \Xi^J; \quad (1i)$$

This new presentation provides a general structure of the load flow problem that can be extended to any low voltage distribution system. This is due to the fact that, the new indices as well as the new connection matrix formulates any distribution system in a general way.

Fig. 3-3 illustrates the considered well-known π configuration of each branch of distribution system connecting bus i to bus j in the EDS energy management model as per the notations in nomenclature.

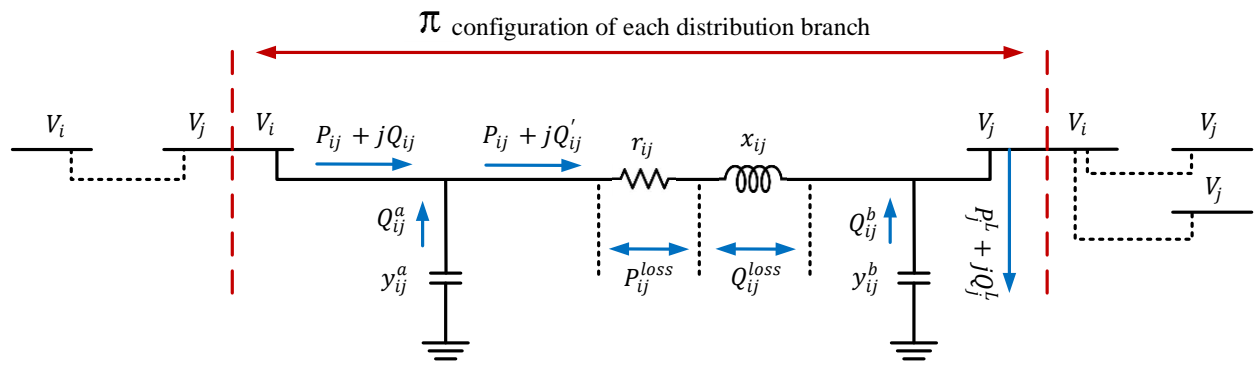


Fig. 3-3. Considered π configuration for each branch, connecting bus i to bus j

A general representation for active and reactive power flow equations as well as bus voltage is given by (2) for a single period of time, derived from the π configuration in Fig. 3-3 and the proposed general representation of power flow equations in (1) (which can be developed for both active and reactive power flows).

$$\sum_{i \in \mathcal{E}^I} (P_{i(j+1)} - P_{i(j+1)}^{loss} - P_{(j+1)}^L) \cdot L_{i(j+1)} = \sum_{i \in \mathcal{E}^I} P_{(j+1)i} \cdot L_{(j+1)i}; \forall j \in \mathcal{E}^J \quad (2a)$$

$$\sum_{i \in \mathcal{E}^I} (Q'_{i(j+1)} - Q_{i(j+1)}^{loss} + Q_{i(j+1)}^b - Q_{(j+1)}^L) \cdot L_{i(j+1)} = \sum_{i \in \mathcal{E}^I} Q_{(j+1)i} \cdot L_{(j+1)i}; \forall j \in \mathcal{E}^J \quad (2b)$$

$$|V_{(j+1)}|^2 = \sum_{i \in \mathcal{E}^I} |V_i|^2 \cdot L_{i(j+1)} + \sum_{i \in \mathcal{E}^I} \frac{r_{i(j+1)}^2 + x_{i(j+1)}^2}{|V_i|^2} \cdot (P_{i(j+1)}^2 + Q'_{i(j+1)}{}^2) - \sum_{i \in \mathcal{E}^I} 2(r_{i(j+1)}P_{i(j+1)} + x_{i(j+1)}Q'_{i(j+1)}); \forall i \in \mathcal{E}^I \quad (2c)$$

where,

$$P_{ij}^{loss} = \frac{r_{ij}}{|V_i|^2} \cdot (P_{ij}^2 + Q'_{ij}{}^2); \forall i \in \mathcal{E}^I, \forall j \in \mathcal{E}^J \quad (2d)$$

$$Q_{ij}^{loss} = \frac{x_{ij}}{|V_i|^2} \cdot (P_{ij}^2 + Q'_{ij}{}^2); \forall i \in \mathcal{E}^I, \forall j \in \mathcal{E}^J \quad (2e)$$

$$Q'_{ij} = Q_{ij} + Q_{ij}^a; \forall i \in \mathcal{E}^I, \forall j \in \mathcal{E}^J \quad (2f)$$

$$Q_{ij}^a = Y_{ij}^a |V_i|^2; \forall i \in \mathcal{E}^I, \forall j \in \mathcal{E}^J \quad (2g)$$

$$Q_{ij}^b = Y_{ij}^b |V_j|^2; \forall i \in \mathcal{E}^I, \forall j \in \mathcal{E}^J \quad (2h)$$

In (2), the active power flow equation is given by (2a) for the branch connecting bus i to bus j , if such a branch exists, i.e., $L_{ij} = 1$. In a similar way, (2b) represents the reactive power flow equation for each branch of EDS system. Voltage of each EDS bus is given by equation (2c) which is the modified version of voltage magnitude equation presented by [92]. Active and reactive power losses for each branch are given by (2d) and (2e), respectively. Equation (2f), represents the reactive power flow encountering shunt reactive losses at the sending end of each branch which is given by (2g), according to the considered π configuration. Equation (2h) also represents the shunt reactive losses at the receiving end of each branch, i.e., Q_{ij}^b . The above presented EDS load flow equations are further employed to build-up the proposed unified EDS energy management model.

3.3. Validating the Proposed EDS Power Flow Model

The proposed modified load flow equations in (2) are employed to calculate EDS load flow for 33-bus systems. The input data of 33-bus system is available in [93]. The single-line diagram of the system is shown in Fig. 3-4.

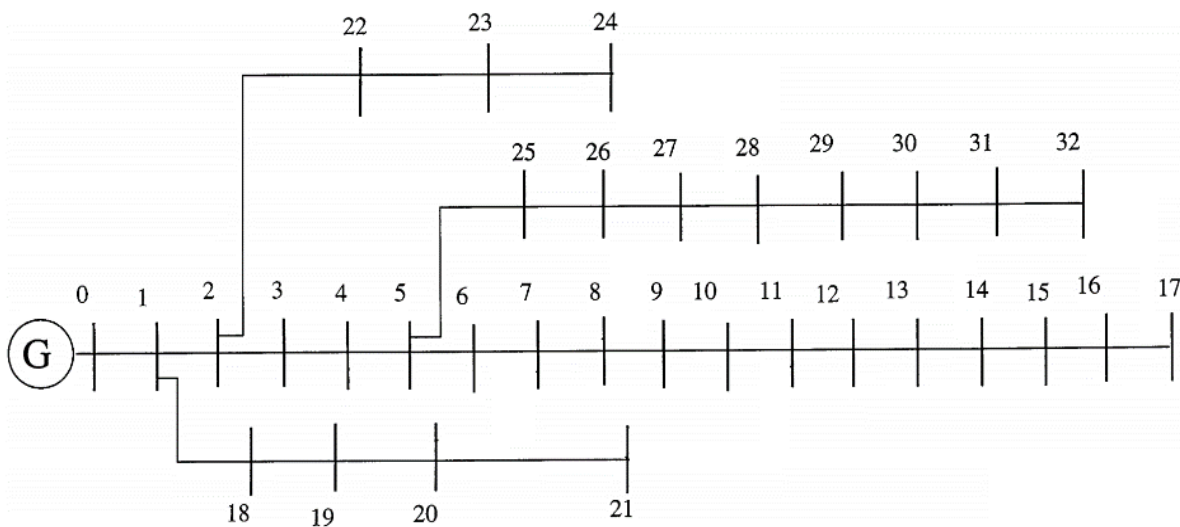


Fig. 3-4. IEEE 33-bus system, considered as the case study

Four scenarios or load levels (50%, 75%, 100%, and 125% of nominal load as scenario 1 to 4, respectively) are considered to evaluate the performance of the proposed model in underload/overload circumstances. These scenarios are considered for comparing the results obtained by the proposed model with that of the FBS load flow method. Fig. 3-5 shows the employed load levels for each bus of the system for scenarios 1, 2, and 4 (scenario 3 is the 100% similar to the IEEE 33-bus data set). Simulations are conducted using GAMS software package. Voltage magnitude at slack bus is 12.66 kV which is considered as the base value, while, the base value for power is 100 kVA. The obtained voltage magnitude of each bus is shown by Fig. 3-6

for scenarios 1-4. As it is seen in Fig. 3-6, the voltage values obtained by the proposed model are the same as that obtained by FBS for all load level scenarios.

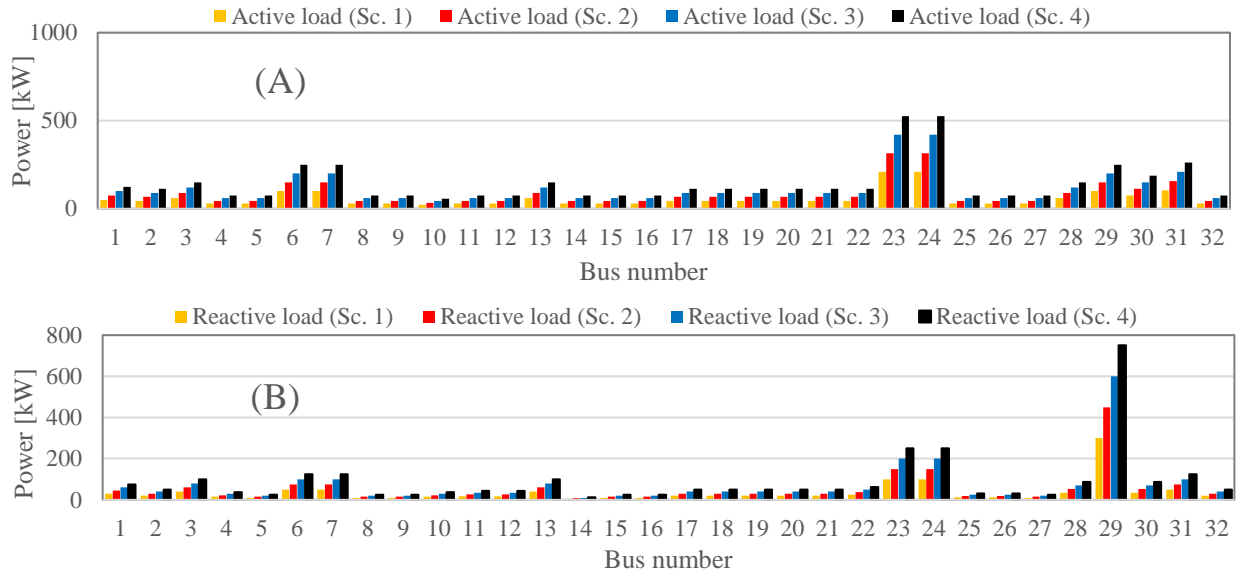


Fig. 3-5. Active (A) and reactive (B) load levels for scenarios 1-4

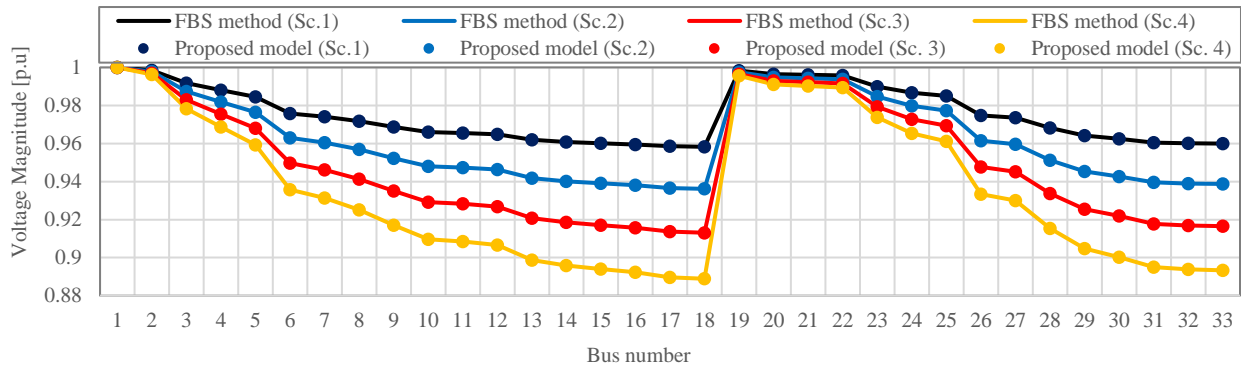


Fig. 3-6. Voltage magnitude comparison for IEEE 33-bus system

In addition to voltage magnitude, the active and reactive power flow through each branch of the system is compared with the FBS model in Fig. 3-7 and Fig. 3-8, respectively. Note that, the power flow solutions are reported for the nominal load level which is scenario 3 in this study. As shown in Fig. 3-7 and Fig. 3-8, the load flow results, obtained by proposed model, are exactly the same as the FBS results for both active and reactive power which validates the optimality of the

obtained solutions by the proposed load flow in this paper.

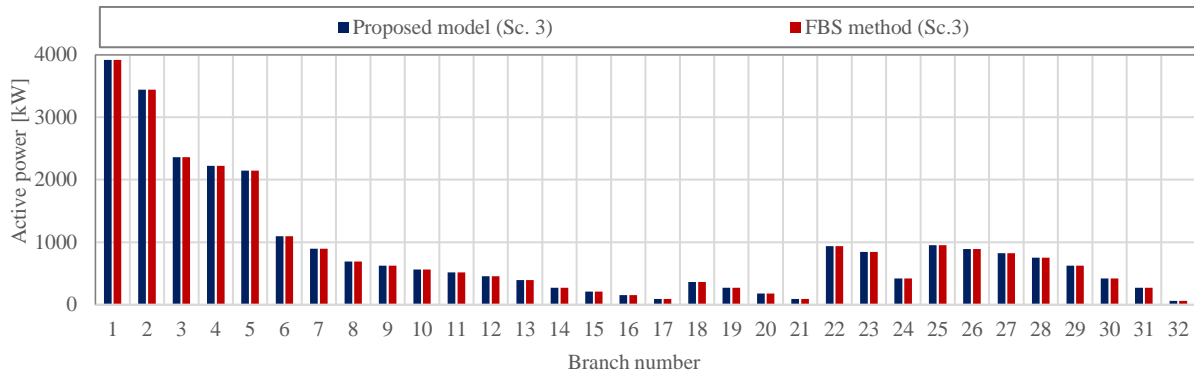


Fig. 3-7. Active power flow comparison for 33-bus system

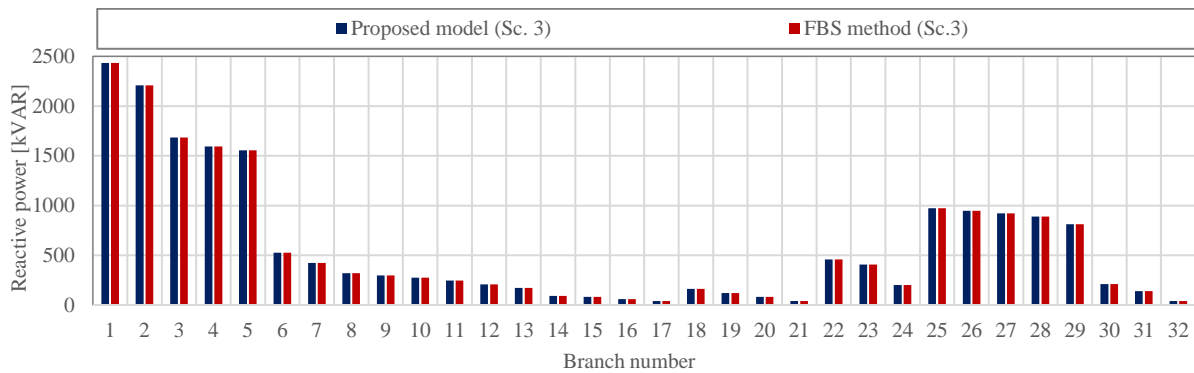


Fig. 3-8. Reactive power flow comparison for 33-bus system

The total power loss in the system obtained by the proposed model are compared with that of the FBS method in Table I for all scenarios. As it is seen in Table I, the obtained values by the FBS method and the proposed model are the same for all scenarios. The similarity of the obtained results was also observed for other load levels in scenarios 1, 2, and 4 in the simulations.

Table 3-1. Active and reactive power loss comparison for all scenarios

Power type [kW]/[kVAR]	Scenario No. 1		Scenario No. 2		Scenario No. 3		Scenario No. 4	
	Active	Reactive	Active	Reactive	Active	Reactive	Active	Reactive
Proposed model	47.07	31.35	109.75	73.13	202.67	135.14	329.85	220.08
FBS method	47.06	31.34	109.75	73.13	202.67	135.14	329.85	220.08

3.4. Conclusion

This chapter presented a directly solvable EDS load flow problem by introducing a new bus indexing model alongside a connectivity matrix to characterize the EDS configuration. The proposed model is directly solvable through off-the-shelf optimization packages in a single shot (it has been directly solved by GAMS software package in this study). Moreover, it is generally developed to be mergeable into any EDS studies involving load flow calculation, i.e., loss minimization, reconfiguration, planning, etc., as the constraints of the model. The ability of the proposed model in being directly solvable with no iterative optimization technique, eliminated the need of iterative optimization methods such as NR, GS, and FBS. The results obtained by the proposed load flow model were compared to those of the FBS method. Comparison of results indicated that the proposed model maintained the same outcome as FBS method, which shows its optimality in achieving expected active/reactive power flow and bus voltages.

In the net chapter, the power flow model in Chapter 3 will be used to develop the energy management model.

4. Proposed General Inverter-Based EDS Energy Management Model at the Presence of RES and BES

This chapter presents a directly solvable multi-objective energy management model for electricity distribution system to minimize total power losses and bus voltage deviations by employing the arbitrage ability of distributed battery energy storage systems and renewable energy sources. The developed power flow equations in Chapter 3 are further employed to characterize the power flow of BES and RES to develop the proposed energy management model. Since the load flow equations are generally developed, they can be merged into the energy management model as the operating constraints. Therefore, the energy management model can also be directly solved in a single shot with off-the-shelf optimization packages and there is no need to conduct iterative algorithms to separately solve the load flow and the optimization problem. Both active/reactive shares of BES and RES are considered as variables of the model to provide active/reactive support for EDS. IEEE 33-bus system is employed to evaluate the effectiveness of the proposed model. The obtained results show significant improvement in both system power losses and voltage deviations which is due to the active and reactive power controllability of RES and BES systems.

NOMENCLATURE (for Chapter 4)

A. Indices

$/j_i$	Index of EDS buses
t	Index of operating time periods

B. Parameters

L_{ij}	Bus connection indicator ($L_{ij} = 1$ if a branch connects bus i to bus j)
n	Total number of buses
P_j^L	Active load at bus j
r_{ij}	Resistance of the branch connecting bus i to bus j
x_{ij}	Series reactance of the branch connecting bus i to bus j
Y_{ij}^a	Shunt admittance at the sending end of the branch connecting bus i to bus j
Y_{ij}^b	Shunt admittance at the receiving end of the branch connecting bus i to bus j
η_j^{chg}	Charging efficiency of battery located at bus j
η_j^{dis}	Discharging efficiency of battery located at bus j
E_j^l	Steady-state energy loss of battery located at bus j
T	Total operation time
V_j^{min}	Minimum allowable voltage magnitude at bus j
V_j^{max}	Maximum allowable voltage magnitude at bus j
I_{ij}^{max}	Maximum allowable current through the branch connecting bus i to bus j
S_{max}^{chg}	Maximum allowable charging apparent power for battery systems
S_{max}^{dis}	Maximum allowable discharging apparent power for battery systems
E_{max}	Maximum allowable energy level for battery systems

C. Variables

P_{ijt}	Active power flow from bus i to bus j in hour t
P_{ijt}^{loss}	Active power loss in the branch connecting bus i to bus j in hour t
Q'_{ijt}	Reactive power flow from bus i to bus j in hour t
Q_{ijt}^{loss}	Reactive power loss on the branch connecting bus i to bus j in hour t

Q_{ijt}^b	Shunt reactive power loss at receiving end of the branch connecting bus i to bus j in hour t
V_{jt}	Voltage magnitude of bus i/j in hour t
Q_{ijt}^a	Shunt reactive power loss at sending end of the branch connecting bus i to bus j in hour t
E_{jt}	Energy level for battery connected to bus j in hour t
S_{jt}^{chg}	Apparent charging power for battery connected to bus j in hour t
S_{jt}^{dis}	Apparent discharging power for battery connected to bus j in hour t
P_{jt}^{chg}	Active charging power for battery connected to bus j in hour t
Q_{jt}^{chg}	Reactive charging power for battery connected to bus j in hour t
P_{jt}^{dis}	Active discharging power for battery connected to bus j in hour t
Q_{jt}^{dis}	Reactive discharging power for battery connected to bus j in hour t
P_{jt}^{PV}	Active power generated by PV connected to bus j in hour t
Q_{jt}^{PV}	Reactive power generated by PV connected to bus j in hour t
P_{jt}^{WF}	Active power generated by WF connected to bus j in hour t
Q_{jt}^{WF}	Reactive power generated by WF connected to bus j in hour t
S_{jt}^{WT}	Total generated apparent power by WF connected to bus j in hour t
S_{jt}^{PV}	Total generated apparent power by PV connected to bus j in hour t
I_{ijt}	Current in the branch connecting bus i to bus j in hour t
β_j	Indicator for battery existence of bus j , i.e., $\beta_j = 1$ if a battery is connected to bus j , $\beta_j = 0$ otherwise
α_{jt}^{chg}	Charging status indicator for battery connected to bus j in hour t

α_{jt}^{dis} Discharging status indicator for battery connected to bus j in hour t

D. Sets

$\mathcal{E}^J \mathcal{E}^I$ Set of EDS buses

\mathcal{E}^T Set of operation time

E. Vectors/Matrices

L Connectivity matrix

4.1. Background

Load flow methodologies become of importance when it comes to topics related to expansion, operation, and management of EDSs. In particular, load flow calculation methodologies are simultaneously employed with other optimization engines such as genetic algorithm (GA) and particle swarm optimization (PSO) to determine the optimal solution of a given objective function and the associated constraints, depending on the application, i.e., EDS loss minimization, voltage control, sizing and siting of BES systems, etc. EDS load flow calculation is usually conducted by methodologies such as Newton-Raphson-based method [78], Gauss-Seidel [79], forward-backward sweep-based methods [80], etc. In [81], a power flow analysis for droop-based islanded microgrids was conducted using current injection-based Newton-Raphson (NR) methodology. NR method was also employed to solve the EDS power flow for calculating maximum loadability in [94]. An extended fast decoupled NR methodology was used in [82] for EDS reconfiguration. Although, NR is suitable for transmission system, it may have a poor convergence ratio for most radial EDSs which is due to their high R/X ratios of branches [83]. Moreover, the need of partial derivative of equations makes NR a time-consuming methodology in terms of both mathematical and computational burden. In [84], Gauss-Seidel methodology was

employed for voltage stability in EDS. It was also used for EDS loadability analysis in [85]. However, Gauss-Seidel methodology is generally complex, and its convergence may be long. In fact, calculation time of Gauss-Seidel method increases almost proportionally with the number of buses/branches. This issue becomes even more vital for larger EDSs [84]. To overcome the aforementioned issues in conventional load flow algorithms, forward/backward sweep (FBS) method was employed in [95] to integrate open unified power quality conditioners for EDS loss minimization. The model of [95] utilizes particle swarm optimization (PSO) to determine planning solutions as they need to be fixed in the FBS methodology to determine EDS load flow. In fact, in each iteration of particle swarm optimization in [95], FBS is conducted to determine EDS load flow based on the given planning solutions for open unified power quality conditioners throughout EDS. In a similar way, particle swarm optimization was used in [96] as the optimization engine to optimally integrate distributed generations into EDS and reduce power losses and voltage deviations. FBS was used in [96] for EDS load flow calculations in each iteration of particle swarm optimization. In [97] genetic algorithm (GA) was used to minimize EDS power losses and voltage deviations by optimal integration of distributed generations and electric vehicles, where FBS was used to calculate EDS load flow. Harmony search algorithm (HSA) was used in [98] to optimize the EDS reconfiguration and the placement of distributed generation units in EDS.

Although, the aforementioned load flow calculation methodologies are able to do the job, they need to be conjointly combined with other optimization algorithms such as GA, PSO, HSA, etc., to be able to optimize the required objective function and the related constraints in EDS studies. This is because, EDS load flow methodologies only calculate the load flow and bus voltages and

they are not able to characterize the optimal operation of BES and RES elements throughout the network. In fact, it's the optimization engine that determines the EDS optimal planning or energy management solutions [95-97] while these solutions are fixed in the load flow calculation problem. The combination of metaheuristic optimization algorithms (or any other optimization approach) with EDS load flow calculation brings additional mathematical and programming burden to the model. Moreover, the computation time of the optimization may easily increase for complex models as it involves two procedures, i.e., optimization algorithm and load flow calculation in each iteration of the optimization.

In addition to the methodological aspects in solving EDS optimization problems, characterizing technical features in modeling EDS elements, such as renewable energy sources (RESs) and battery energy storage (BES) systems, is of high importance in distribution systems. Recently, the role of BES systems has been magnified due to the employment of RES in today's smart grid. BES can compensate the negative effects of RES volatile generation on electricity distribution system's voltage stability and losses. Moreover, it offers distribution systems different and unique applications such as peak shaving [99], loss reduction [100], congestion management [101], and reliability enhancement [102]. In the study of [103] BES was used to improve the RES integration into distribution system using dynamic programming algorithm. However, the reactive power trade of RES and BES wasn't modeled in [103]. An energy management model for radial EDS was proposed by [104] using Vanadium redox flow batteries for load leveling and peak shaving. The study of [104] did not consider the reactive power capability of BES, while in practice, converter elements are coupled with BES systems and can provide reactive power trade for EDS. In a similar way, reactive capability of BES was ignored in

the study of [105] where an energy management model was developed for peak shaving and valley filling. In [106], an EDS energy management model was proposed to flatten network voltage profile and reduce system losses/costs in which no BES reactive power trade was considered, while, voltage profile in EDS is strongly dependent on reactive power flow throughout the network. In the study of [107], a control strategy for distributed BESs was developed to enhance the voltage profile on each bus of the EDS. However, BES reactive power trade was not modeled in [107], while, inverter-based operation of BES systems offers flexibility in absorbing or injecting active and/or reactive power. This practice is also applicable for RES generation employing the available energy conversion technologies in today's distribution systems. In [108], an EDS energy management model was developed to manage intermittent renewable resources through optimal operation of BES systems. Although, BES reactive power was considered in the study of [108], the controllability of RES reactive power was ignored. It deserves mentioning that, both RES and BES systems are equipped with inverter elements being able to control the active and reactive share of the generated power in each time slot of the operation. However, this should be modeled accurately in EDS studies to capture its applicability in practice.

4.2. Motivations

Relying on the literature, the motivations of this study are as follows:

1) In terms of solution methodology, further approaches for conducting EDS studies involving load flow calculations, are required to:

a) directly solve the optimization model and its EDS load flow together in a single shot by off-

the-shelf optimization packages, with no need to additional load flow calculations and iterative optimization approaches such as PSO, GA, and HSA, and

b) be able to perform in different EDS applications, involving load flow calculations, i.e., loss minimization, voltage control, sizing and siting of BES systems, EDS reconfiguration, etc.

2) In terms of RES and BES modeling in distribution systems, further models should be undertaken to enable the reactive controllability of these elements in real world electricity distribution systems, considering the applicability of inverter-based operation, nowadays. In fact, the practical potential of RES and BES cannot be fully exploited if the inverter-based operation of these systems is ignored in EDS studies.

4.3. Contributions

Following contributions are presented to extend the existing body of the work:

1) A new directly solvable power flow problem has been proposed for EDS, introducing a connectivity matrix in line with a new indexing of load flow equations. The modified load flow equations are considered as constraints of the energy management model. Accordingly, the optimal RES and BES operations are obtained based on feasible load flow solutions. Therefore, the need of load flow calculation methodologies, such as NR and FBS, as well as optimization approaches, such as GA and PSO, is eliminated as the proposed model characterizes both load flow and energy management constraints in a single and unified model. This provides users the opportunity of solving the problem with commercial optimization packages, i.e., CPLEX, GAMS, etc., in a single shot with no need to develop further optimization approaches involving iterative procedures and load flow calculations. Note that, the employed modified load flow

equations in line with the connectivity matrix can be used in any other EDS study, concerning load flow calculation, as the constraints of the model.

2) The proposed directly solvable power flow problem is used to build up a multi-objective energy management model for RES-BES-equipped distribution systems. The first objective of the model minimizes total EDS power losses and the second objective minimizes the voltage deviations of each bus over time. These objective functions are optimized being subject to load flow constraints, RES/BES optimal operation, and voltage/current tolerance of EDS. The proposed energy management model enables both active and reactive power controllability of RES and BES systems. RES generation is limited by its apparent power while the active/reactive share of power is reasonably decided through the optimization model. This is also developed for BES systems in both charging and discharging power trades. In fact, BES constraints including dynamic energy balance constraint and end coupling constraint are modeled based on BES apparent power trade, while, the active and reactive share of BES is modeled in EDS load flow constraints. New continuous variables are defined for RES and BES representing active and reactive power share of these systems during the operation. Accordingly, BES can absorb active or reactive power in each time slot and inject it back to the network as active or reactive power in another time slot.

4.4. Proposed Directly Solvable EDS Load Flow Model

A general representation for active and reactive power flow equations as well as bus voltage is given by (2) for a single period of time, derived from the π configuration in Fig. 3-3 and the proposed general representation of power flow equations in (1) in Chapter 3 (which can be developed for both active and reactive power flows).

$$\sum_{i \in \mathcal{E}^I} (P_{i(j+1)} - P_{i(j+1)}^{loss} - P_{(j+1)}^L) \cdot L_{i(j+1)} = \sum_{i \in \mathcal{E}^I} P_{(j+1)i} \cdot L_{(j+1)i}; \forall j \in \mathcal{E}^J \quad (2a)$$

$$\sum_{i \in \mathcal{E}^I} (Q'_{i(j+1)} - Q_{i(j+1)}^{loss} + Q_{i(j+1)}^b - Q_{(j+1)}^L) \cdot L_{i(j+1)} = \sum_{i \in \mathcal{E}^I} Q_{(j+1)i} \cdot L_{(j+1)i}; \forall j \in \mathcal{E}^J \quad (2b)$$

$$|V_{(j+1)}|^2 = \sum_{i \in \mathcal{E}^I} |V_i|^2 \cdot L_{i(j+1)} + \sum_{i \in \mathcal{E}^I} \frac{r_{i(j+1)}^2 + x_{i(j+1)}^2}{|V_i|^2} \cdot (P_{i(j+1)}^2 + Q'_{i(j+1)}^2) - \sum_{i \in \mathcal{E}^I} 2(r_{i(j+1)}P_{i(j+1)} + x_{i(j+1)}Q'_{i(j+1)}); \forall i \in \mathcal{E}^I \quad (2c)$$

where,

$$P_{ij}^{loss} = \frac{r_{ij}}{|V_i|^2} \cdot (P_{ij}^2 + Q'_{ij}^2); \forall i \in \mathcal{E}^I, \forall j \in \mathcal{E}^J \quad (2d)$$

$$Q_{ij}^{loss} = \frac{x_{ij}}{|V_i|^2} \cdot (P_{ij}^2 + Q'_{ij}^2); \forall i \in \mathcal{E}^I, \forall j \in \mathcal{E}^J \quad (2e)$$

$$Q'_{ij} = Q_{ij} + Q_{ij}^a; \forall i \in \mathcal{E}^I, \forall j \in \mathcal{E}^J \quad (2f)$$

$$Q_{ij}^a = Y_{ij}^a |V_i|^2; \forall i \in \mathcal{E}^I, \forall j \in \mathcal{E}^J \quad (2g)$$

$$Q_{ij}^b = Y_{ij}^b |V_j|^2; \forall i \in \mathcal{E}^I, \forall j \in \mathcal{E}^J \quad (2h)$$

In (2), the active power flow equation is given by (2a) for the branch connecting bus i to bus j , if such a branch exists, i.e., $L_{ij} = 1$. In a similar way, (2b) represents the reactive power flow equation for each branch of EDS system. Voltage of each EDS bus is given by equation (2c) which is the modified version of voltage magnitude equation presented by [92]. Active and reactive power losses for each branch are given by (2d) and (2e), respectively. Equation (2f), represents the reactive power flow encountering shunt reactive losses at the sending end of each branch which is given by (2g), according to the considered π configuration. Equation (2h) also

represents the shunt reactive losses at the receiving end of each branch, i.e., Q_{ij}^b . The above presented EDS load flow equations are further employed to build-up the proposed unified EDS energy management model.

4.5. Inverter-based Modeling of Battery Energy Storage System

In this study, BES is used to contribute in the energy management of EDS through optimal charging/discharging cycles. Therefore, detailed insights into BES characteristics is necessary and the need for an appropriate model arises accordingly. In the following discussion, BES is modelled considering its practical limitations such as capacity, charging/discharging rates and efficiencies, standby power losses over time, and both the active and reactive power controllability through its inverter-based operation. Fig. 4-1 is a presentation of the dynamic energy balance of BES during charging/discharging and standby modes. As illustrated by Fig. 4-1, BES absorbs E^{chg} during charging cycle. However, due to charging efficiency, resulting in charging losses, i.e., E_{CL} , the actual stored energy is E^A . The stored energy level drops to E^B , representing the available energy for BES discharging during standby mode, which is due to standby losses of BES, i.e., E_{SL} . Finally, the BES discharged energy, is lower than the available stored energy in BES, which is due to discharging efficiency of BES, resulting in discharging losses, i.e., E_{DL} .

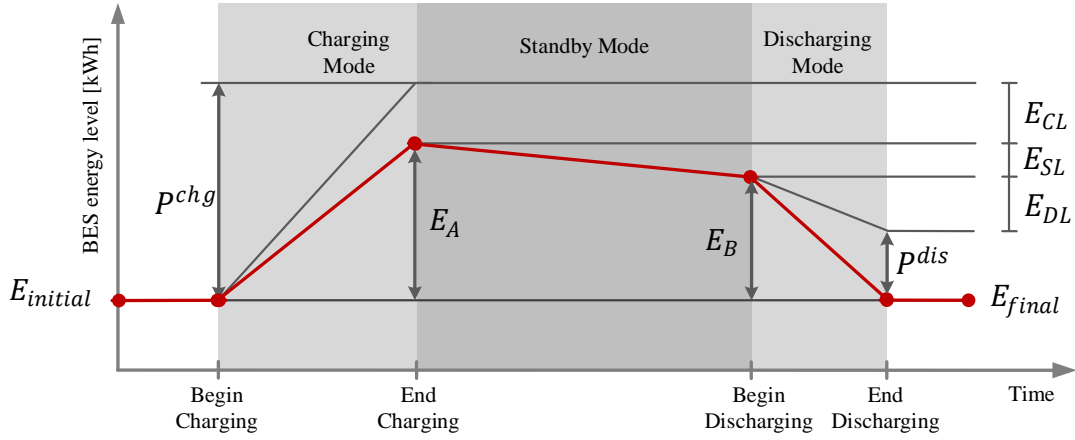


Fig. 4-1. Dynamic energy balance in BES system

Accordingly, the multi-period dynamic energy balance of BES located at bus j is given by (3a), which represents the stored energy level in BES considering the stored energy level in previous time period, i.e., $E_{j(t-1)}$, charging/discharging rates in the current time period, i.e., $P_{jt}^{chg}/P_{jt}^{dis}$, and the standby losses of BES, i.e., E_j^l .

$$E_{jt} = E_{j(t-1)} + \eta_j^{chg} \cdot P_{jt}^{chg} - \frac{1}{\eta_j^{dis}} \cdot P_{jt}^{dis} - E_j^l; \quad \forall j \in \mathcal{E}^J; \forall t \in \mathcal{E}^T \quad (3a)$$

The end-coupling constraint of BES is presented by (3b) making sure that the final and initial energy levels of BES are similar.

$$\sum_{t \in \mathcal{E}^T} \left(\eta_j^{chg} \cdot P_{jt}^{chg} - \frac{1}{\eta_j^{dis}} \cdot P_{jt}^{dis} \right) = E_j^l \cdot T; \quad \forall j \in \mathcal{E}^J \quad (3b)$$

Given the ability of inverters in generating internal reactive power, the share of active and reactive power is controlled in both charging and discharging cycles of BES. In inverter-based operation of BES, the inverter is responsible for absorbing/injecting reactive power from/to the

grid while BES is responsible for absorbing/injecting active power from/to the grid [109]. The BES active power is limited to its maximum allowable range which is dependent on the BES capacity. Since, the charging/discharging active power of inverter is supplied by BES, the internally generated reactive power in inverter is limited to its maximum allowable capacity which is expressed by inverter's apparent power. Therefore, constraints (3c) and (3d) are employed to express the relation between active and reactive power in inverter and BES. Note that, the efficiency of inverter, i.e., $\eta_j^{inv,BES}$, has been considered in (3c)-(3d) when inverting BES active power to AC active power.

$$|S_{jt}^{chg}|^2 = (P_{jt}^{chg} \cdot \eta_j^{inv,BES})^2 \pm Q_{jt}^{inv,BES^2}; \quad \forall j \in \mathcal{E}^J; \forall t \in \mathcal{E}^T \quad (3c)$$

$$|S_{jt}^{dis}|^2 = (P_{jt}^{dis} \cdot \eta_j^{inv,BES})^2 \pm Q_{jt}^{inv,BES^2}; \quad \forall j \in \mathcal{E}^J; \forall t \in \mathcal{E}^T \quad (3d)$$

According to the above BES-inverter model, the limitation of reactive power generation by inverter is completely dynamic in each operational time period, as it is dependent on the inverter capacity on one hand, and the BES charged/discharged active power on the other hand (as the inverted active power uses a portion of inverter's capacity). Therefore, by limiting the inverter's capacity, its reactive power generation is also limited to the allowable range, regarding the value of inverted active power in each time slot.

4.6. Inverter-based Modeling of Renewable Energy Sources

The same as BES inverter-based integration, RESs are modeled by their active power while the inverter is responsible for reactive power absorption/injection from/to the grid. Therefore, the active power produced by RES is directly injected to grid through inverter while the reactive

power is generated by the inverter. The apparent power of RES-inverter pack is given by (4a)/(4b) for PV/WF, while, it has been limited to converter's allowable capacity through (4c)-(4d). Note that, the efficiency of PV/WF inverter, i.e., $\eta_j^{inv,PV}/\eta_j^{inv,WF}$, has been considered in (4a)-(4b) as the PV/WF active power is injected to the grid through inverter.

$$|S_{jt}^{PV}|^2 = (P_{jt}^{PV} \cdot \eta_j^{inv,PV})^2 \pm Q_{jt}^{inv,PV^2}; \quad \forall j \in \mathcal{E}^J; \forall t \in \mathcal{E}^T \quad (4a)$$

$$|S_{jt}^{WF}|^2 = (P_{jt}^{WF} \cdot \eta_j^{inv,WF})^2 \pm Q_{jt}^{inv,WF^2}; \quad \forall j \in \mathcal{E}^J; \forall t \in \mathcal{E}^T \quad (4b)$$

$$S_{jt}^{PV} \leq S_{max}^{inv,PV}; \quad \forall j \in \mathcal{E}^J; \forall t \in \mathcal{E}^T \quad (4c)$$

$$S_{jt}^{WF} \leq S_{max}^{inv,WF}; \quad \forall j \in \mathcal{E}^J; \forall t \in \mathcal{E}^T \quad (4d)$$

The coupling and the energy interaction between BES/RES, inverter, and grid are given by

Fig. 4-2.

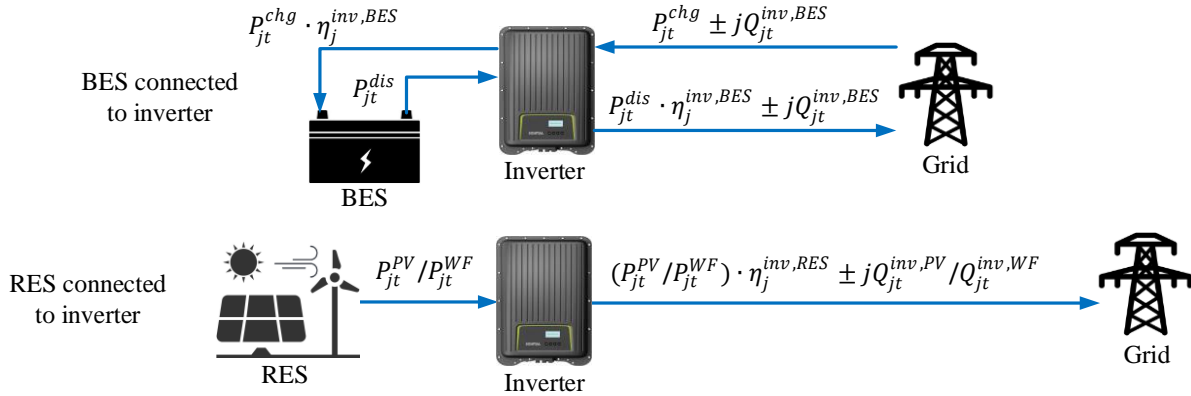


Fig. 4-2. Representation of the BES and inverter coupling as well as their energy interaction with grid

4.7. Proposed EDS Energy Management Model

The considered system configuration for the EDS, equipped with RES and BES systems, is

given by Fig. 4-3, which illustrates the location of these elements at the receiving end of each branch as well as the power flow directions (injection/absorption of power for each element), as per the nomenclature. In the following, each element of the considered EDS configuration in Fig. 4-3 is modelled and discussed.

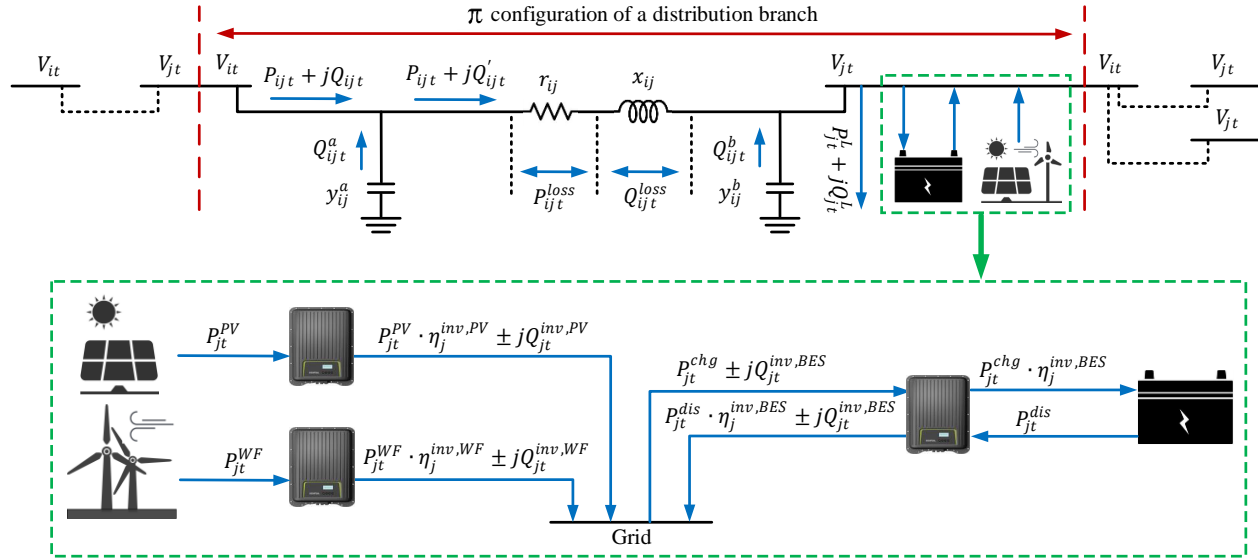


Fig. 4-3. Considered π configuration for each branch of EDS equipped with RES and BES systems

The modified load flow equations in (2) are employed to build-up the proposed EDS energy management model, considering the general configuration of EDS branches in Fig. 4-3. The proposed model is expressed through (5).

Multi-objective function:

$$O. F. = \begin{cases} f_1 = \min \sum_{i \in \mathcal{E}^I} \sum_{j \in \mathcal{E}^J} \sum_{t \in \mathcal{E}^T} P_{ijt}^{loss}; \\ f_2 = \min \sum_{i \in \mathcal{E}^I} \sum_{t \in \mathcal{E}^T} |V_{it} - V_{i(t-1)}|; \end{cases} \quad (5a)$$

s.t.

Power flow constraints including BES and RES active/reactive power:

$$\begin{aligned}
 \sum_{i \in \mathcal{E}^I} & \left(P_{i(j+1)t} - P_{i(j+1)t}^{loss} - P_{(j+1)t}^L + (P_{(j+1)t}^{PV} \cdot \eta_j^{inv,PV}) + (P_{(j+1)t}^{WF} \cdot \eta_j^{inv,WF}) \right. \\
 & \left. - P_{(j+1)t}^{chg} + (P_{(j+1)t}^{dis} \cdot \eta_j^{inv,BES}) \right) \cdot L_{i(j+1)} \\
 & = \sum_{i \in \mathcal{E}^I} P_{(j+1)it} \cdot L_{(j+1)i}; \forall i \in \mathcal{E}^I, \forall j \in \mathcal{E}^J, \forall t \in \mathcal{E}^T
 \end{aligned} \tag{5b}$$

$$\begin{aligned}
 \sum_{i \in \mathcal{E}^I} & \left(Q'_{i(j+1)t} - Q_{i(j+1)t}^{loss} - Q_{(j+1)t}^L + Q_{i(j+1)t}^b \pm (Q_{(j+1)t}^{inv,PV} \cdot \eta_j^{inv,PV}) \right. \\
 & \left. \pm (Q_{(j+1)t}^{inv,WF} \cdot \eta_j^{inv,WF}) \pm Q_{(j+1)t}^{inv,BES} \right) \cdot L_{i(j+1)} \\
 & = \sum_{i \in \mathcal{E}^I} Q_{(j+1)it} \cdot L_{(j+1)i}; \forall i \in \mathcal{E}^I, \forall j \in \mathcal{E}^J, \forall t \in \mathcal{E}^T
 \end{aligned} \tag{5c}$$

$$P_{ijt}^{loss} = \frac{r_{ij}}{|V_{it}|^2} \cdot (P_{ijt}^2 + Q'_{ijt}{}^2); \forall i \in \mathcal{E}^I, \forall j \in \mathcal{E}^J, \forall t \in \mathcal{E}^T \tag{5d}$$

$$Q_{ijt}^{loss} = \frac{x_{ij}}{|V_{it}|^2} \cdot (P_{ijt}^2 + Q'_{ijt}{}^2); \forall i \in \mathcal{E}^I, \forall j \in \mathcal{E}^J, \forall t \in \mathcal{E}^T \tag{5e}$$

$$Q'_{ijt} = Q_{ijt} + Q_{ijt}^a; \forall i \in \mathcal{E}^I, \forall j \in \mathcal{E}^J, \forall t \in \mathcal{E}^T \tag{5f}$$

$$Q_{ijt}^a = Y_{ij}^a |V_{it}|^2; \forall i \in \mathcal{E}^I, \forall j \in \mathcal{E}^J, \forall t \in \mathcal{E}^T \tag{5g}$$

$$Q_{ijt}^b = Y_{ij}^b |V_{jt}|^2; \forall i \in \mathcal{E}^I, \forall j \in \mathcal{E}^J, \forall t \in \mathcal{E}^T \tag{5h}$$

Voltage magnitude:

$$\begin{aligned}
 |V_{(j+1)t}|^2 &= \sum_{i \in \mathcal{E}^I} |V_{it}|^2 \cdot L_{i(j+1)} \\
 &+ \sum_{i \in \mathcal{E}^I} \frac{r_{i(j+1)}^2 + x_{i(j+1)}^2}{|V_{it}|^2} \cdot (P_{i(j+1)t}^2 + Q'_{i(j+1)t}{}^2) \\
 &- \sum_{i \in \mathcal{E}^I} 2(r_{i(j+1)}P_{i(j+1)t} + x_{i(j+1)}Q'_{i(j+1)t}); \quad \forall i \in \mathcal{E}^I, \forall t \in \mathcal{E}^T
 \end{aligned} \tag{5i}$$

$$V_j^{min} \leq |V_{jt}| \leq V_j^{max}; \quad \forall j \in \mathcal{E}^J, \forall t \in \mathcal{E}^T \tag{5j}$$

Current magnitude:

$$|I_{ijt}|^2 = \frac{P_{ijt}^2 + Q_{ijt}^2}{|V_{it}|^2}; \quad \forall i \in \mathcal{E}^I, \forall j \in \mathcal{E}^J, \forall t \in \mathcal{E}^T \tag{5k}$$

$$|I_{ijt}| \leq I_{ij}^{max} \cdot L_{ij}; \quad \forall i \in \mathcal{E}^I, \forall j \in \mathcal{E}^J, \forall t \in \mathcal{E}^T \tag{5l}$$

Battery storage constraints:

$$(3a)-(3d) \tag{5m}$$

$$S_{jt}^{chg} \leq S_{max}^{inv,BES} \cdot \alpha_{jt}^{chg}; \quad \forall j \in \mathcal{E}^J; \forall t \in \mathcal{E}^T \tag{5n}$$

$$S_{jt}^{dis} \leq S_{max}^{inv,BES} \cdot \alpha_{jt}^{dis}; \quad \forall j \in \mathcal{E}^J; \forall t \in \mathcal{E}^T \tag{5o}$$

$$\alpha_{jt}^{chg} + \alpha_{jt}^{dis} \leq 1; \quad \forall j \in \mathcal{E}^J; \forall t \in \mathcal{E}^T \tag{5p}$$

$$E_{jt} \leq E_{max} \cdot \beta_j; \forall j \in \mathcal{E}^J; \forall t \in \mathcal{E}^T \quad (5q)$$

RES constraints:

$$(4a)-(4d) \quad (5r)$$

In the proposed energy management model, (5a) represents the two objectives of the study including loss minimization, expressed by f_1 , and voltage deviation minimization, expressed by f_2 . The multi-objective optimization model is solved employing goal programming approach.

Constraints (5b) and (5c) are the same as power flow equations (2b) and (2c), respectively, but they are different in two ways, including:

1) They represent a multi-period power flow through EDS, rather than a single-period power flow,

2) They include the power generation by PV and WF, i.e., $P_{jt}^{PV} + P_{jt}^{WF} + jQ_{jt}^{RES}$, as well as charging/discharging power of BES, i.e., $P_{(j+1)t}^{chg} + jQ_{jt}^{chg} / P_{jt}^{dis} + jQ_{jt}^{dis}$.

The active and reactive power losses on each branch of the system are given by (5d) and (5e), respectively. Constraints (5f)-(5h) are the same as constraints (2f)-(2h), but in multi-period form. Constraint (5i) is also the multi-period representation of bus voltage magnitude in (2c) which is limited to its allowable operational ranges in (5j). Current magnitude of each branch connecting bus i to bus j , is given by (5k) and is limited to its allowable operational ranges in (5l). Constraints (5m)-(5q) model the BES system in the proposed energy management model. (5m) refers to BES operation equations in (3a)-(3d). Constraint (5n)/(5o) represents the maximum

allowable charging/discharging power of BES installed on bus j . The maximum capacity of BES is also limited to its maximum value by (5p) if a BES is connected to bus j , i.e., $\beta_{jt}^{chg} = 1$. Constraint (5q) makes sure that the BES is operating in one mode at a time, i.e., charging/discharging. The apparent power of PV and WF is also modeled by equations (4a)-(4b) which are encountered by (5r).

The proposed energy management model in (5) determines the optimal EDS energy management solutions including:

- Active/Reactive power flow and current magnitude of each branch of the system,
- Voltage magnitude and its deviations in two consecutive time slots, for the whole operation horizon,
- Active/Reactive power loss on each branch of the system,
- Charging, discharging, and steady state mode of BES systems,
- Reactive power generation by inverters connected to both BES and RES systems,

According to the proposed model, the above variables are determined in a way that the EDS total power loss as well as voltage deviations are minimized. As it is seen from the mathematical presentation in (5), the load flow equations are considered as constraints of the optimization model and the model is solved directly through optimization softwares with no need to iterative load flow calculations and metaheuristic optimization algorithms.

4.8. Simulation results

To evaluate the effectiveness of the proposed model, an IEEE 33-bus system has been considered for case study in this section. The data of the system is available at [93]. Voltage magnitude at slack bus is 12.66 kV which is considered as the base value, while, the base value for power is 100 kVA. The modified system includes five RESs and six BES systems in different locations of the distribution system. The single-line diagram of the system is shown in Fig. 4-4. The capacity of each BES system is 400 kWh. The generated power of RESs throughout the network are given by Fig. 4-5 for the considered 24-hour operation in this study. The standard active/reactive load of IEEE 33-bus system is used to generate a 24-h load pattern based on South Australia's daily energy consumption pattern which has been taken from [110].

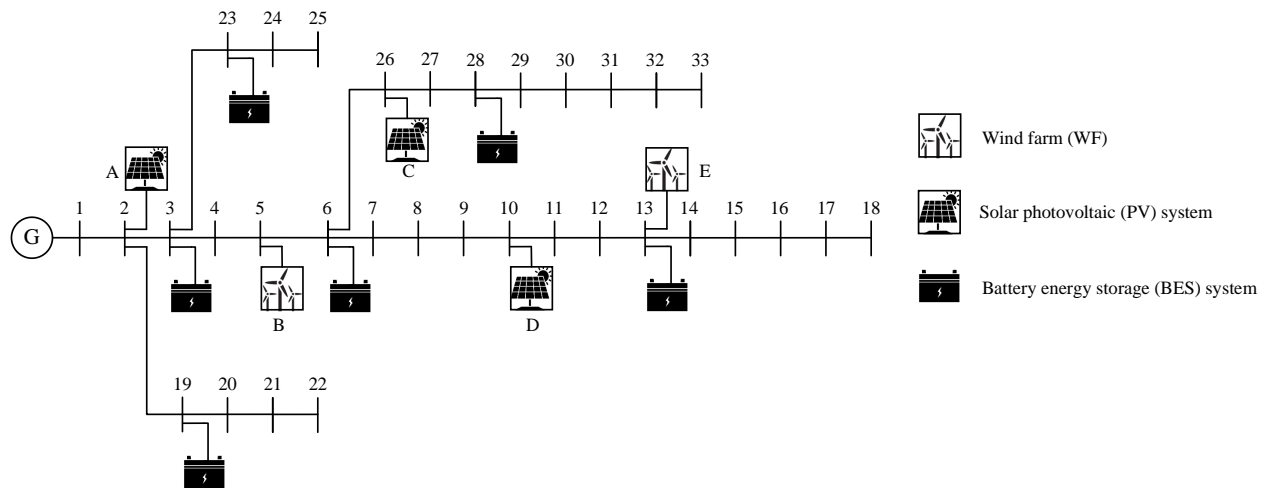


Fig. 4-4. Considered system for numerical simulations (modified IEEE 33 bus system)

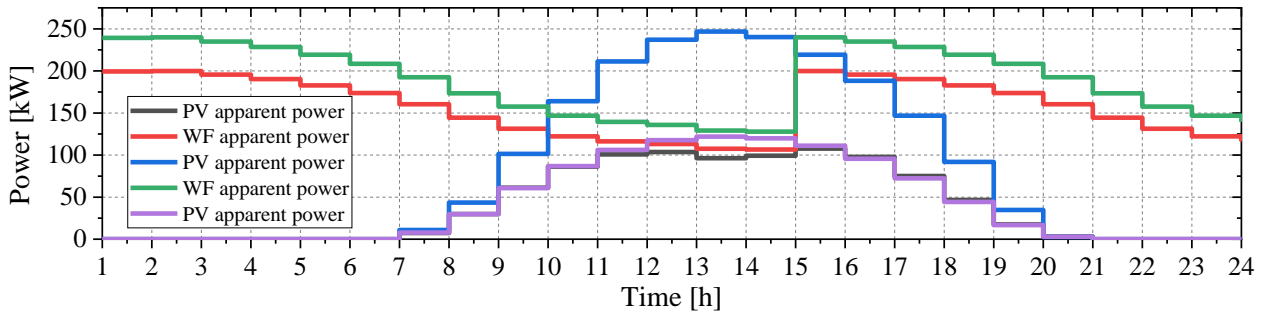


Fig. 4-5. Generated power by renewable energy sources in EDS, Legend from top to bottom referring to renewables in Figure 4-4 as: B, E, A, C, D

The proposed multi-objective energy management model (5) is evaluated under two cases.

Case 1: considers the first objective function, which is EDS loss minimization, i.e., f_1 in (5a).

Case 2: considers both objectives including voltage deviations and loss minimization, i.e., f_1 and f_2 in (5a).

The above cases have been studied through the energy management model, and the obtained results are reported as follows:

The energy management model has been simulated on a 24-h basis. Therefore, there are 24 hourly voltage magnitudes for each bus of the system. Hourly voltage magnitudes have been presented in Fig. 4-6 for both cases 1 and 2. As it is seen, the voltage magnitude of all buses in case 1 follows the IEEE 33-bus voltage pattern with some deviations over time. As expected, these deviations are reduced when case 2 is conducted, i.e., f_2 in (5a) is added to the optimization. This reduction in voltage deviation over time is also highlighted with the reported results in Fig. 4-7 which represents the 25%-75% range of voltage magnitudes for cases 1 and 2.

Each box in Fig. 4-7 represents 24 hourly voltage magnitudes for each bus of the system, while, the median of voltage magnitudes has been presented by red line. As it is seen in Fig. 10, the deviations of hourly voltage magnitude have been reduced over time, i.e., the size of the boxes has decreased.

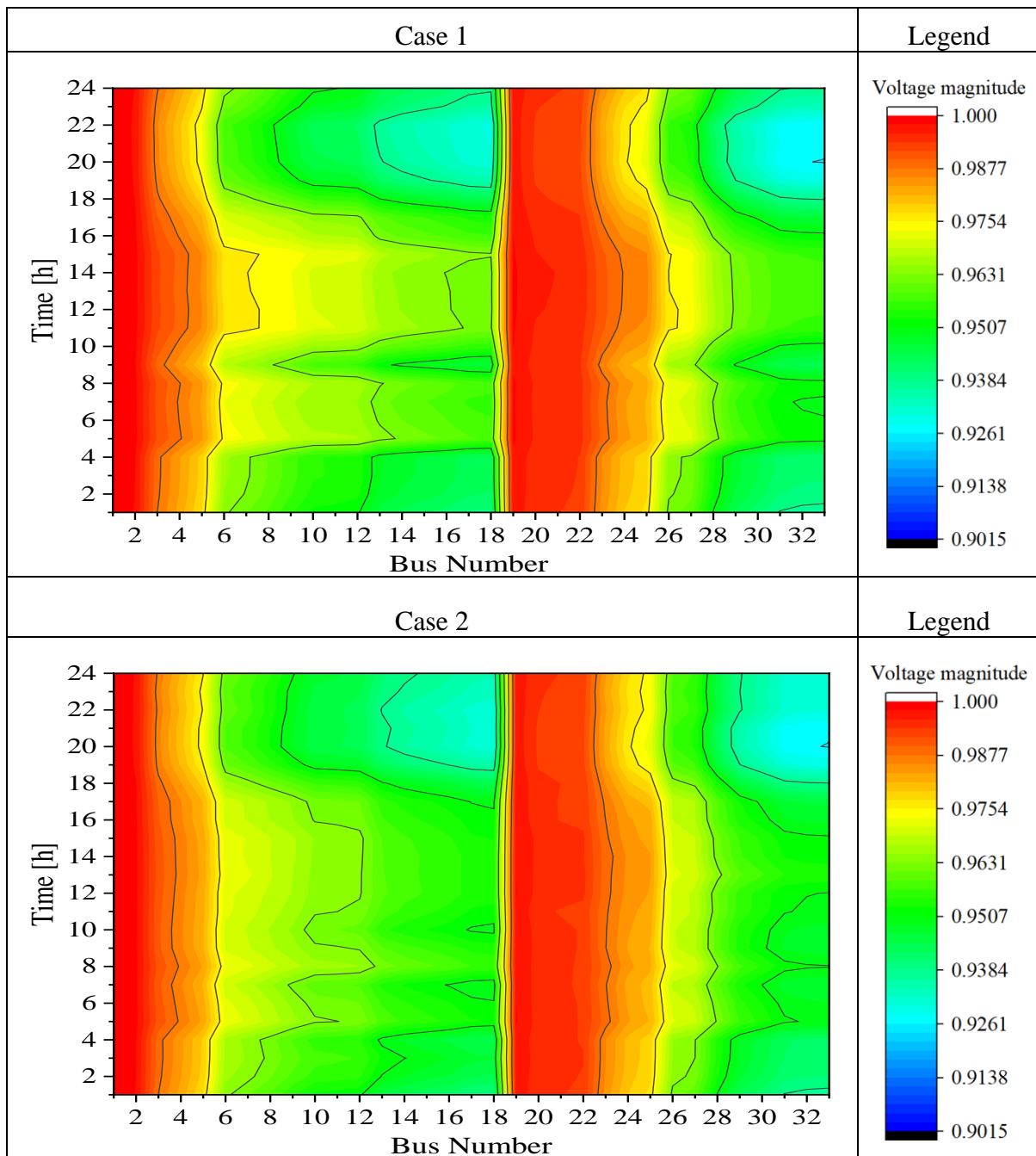


Fig. 4-6. Hourly voltage magnitude for each bus of IEEE 33-bus system for cases 1-2

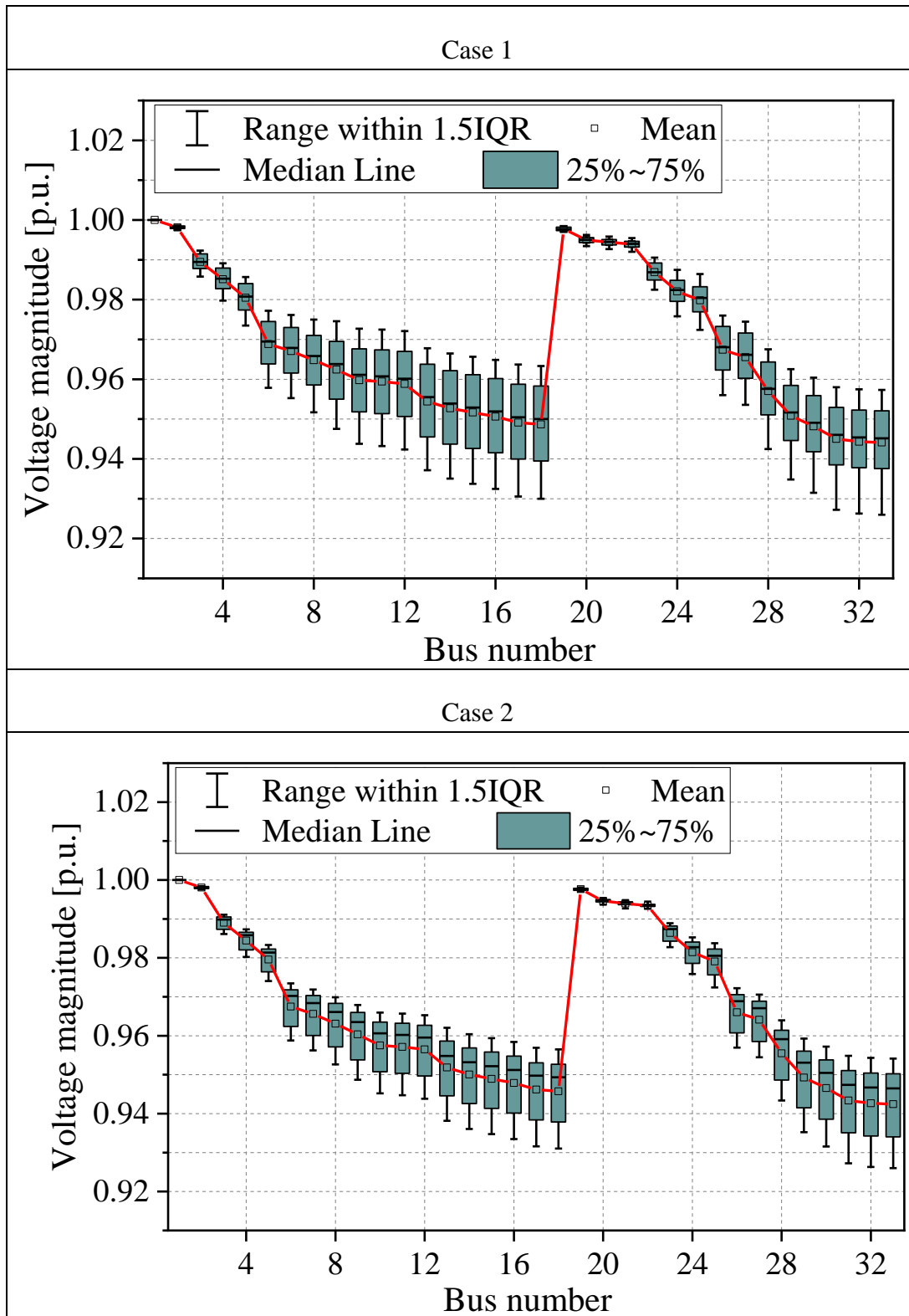


Fig. 4-7. Voltage magnitude (24-h basis) for each bus of the system for cases 1-3

Standard deviations of hourly voltage magnitudes for each bus of the system are also compared in Fig. 4-8 for cases 1 and 2 to demonstrate the contribution of the second objective function, i.e., voltage deviation minimization, in reducing the voltage deviations over time. As it is seen, the standard deviation has considerably reduced on all buses of the system.

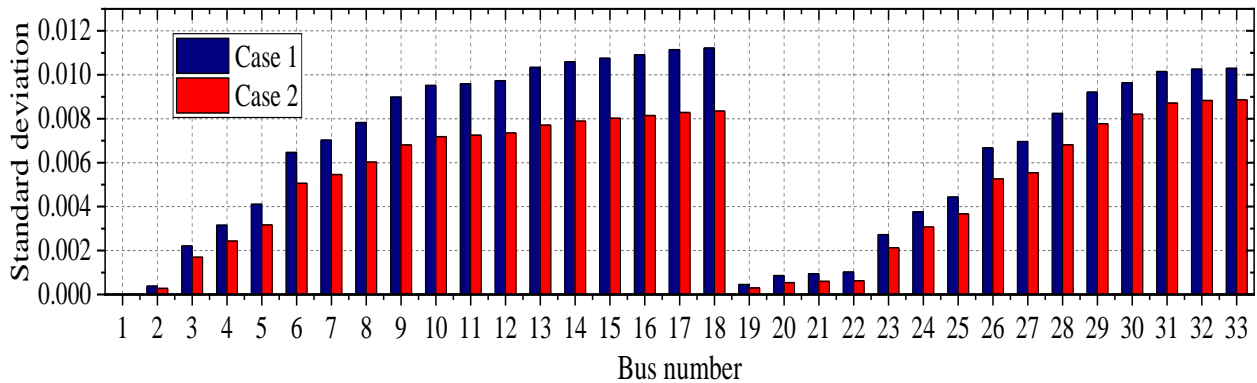


Fig. 4-8. Standard deviation of hourly voltage magnitudes for each bus of the system

The hourly total power loss of EDS as well as the hourly load pattern is given by Fig. 4-9. As it is seen, the EDS total power loss increases as the average load level increases in final hours of the day, i.e., hours 18-24. For the same reason, the total power loss has reduced between hours 5-16. The total EDS daily power loss is obtained as 2098 kW which is also shown by Fig. 4-10.

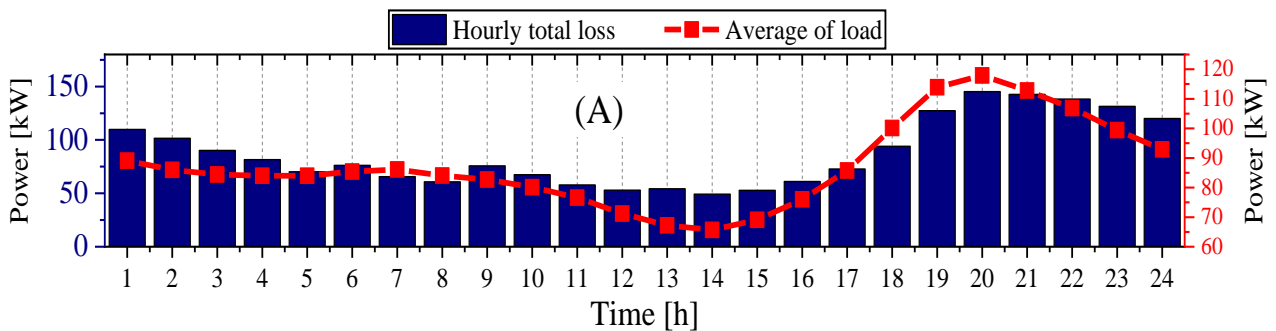


Fig. 4-9. Hourly system power loss during the operating horizon

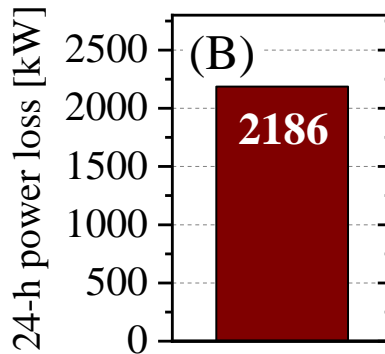


Fig. 4-10. Total system power loss for a 24-h operation

To illustrate the effectiveness of the proposed energy management model in terms of reactive power controllability, EDS is operated with and without this feature and the obtained results are compared. Fig. 4-11 shows the hourly voltage deviations as well as EDS total losses for the operation horizon (24 hours). As it is seen, hourly voltage deviations have reduced as the reactive power controllability is conducted for RES only, BES only and both RES and BES. On the other hand, EDS total power loss has also reduced as the reactive power controllability takes place. This shows that, the inverter-based operation of RES and BES can significantly improve the EDS optimal operation in terms of both voltage regulation and power loss minimization.

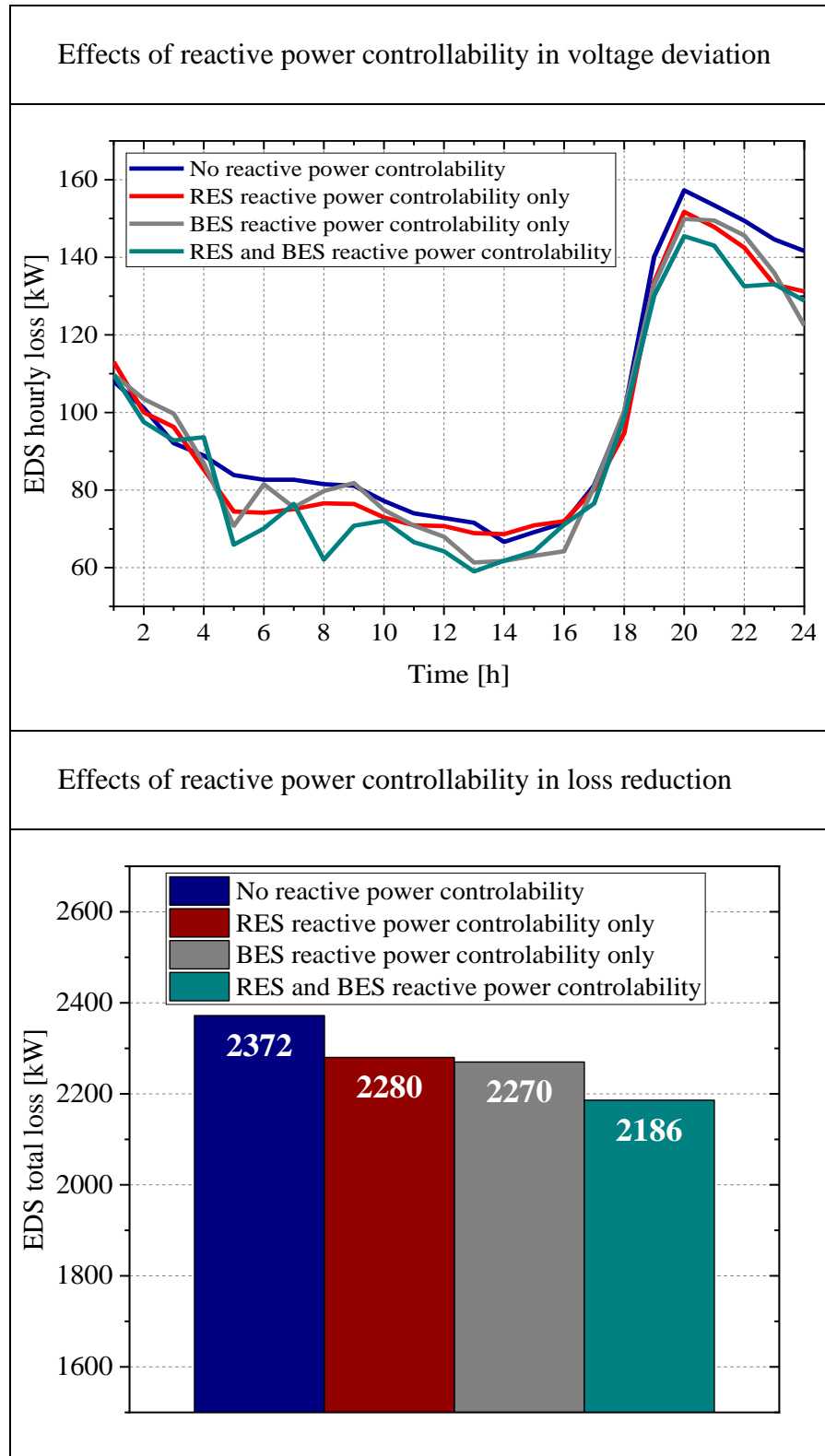
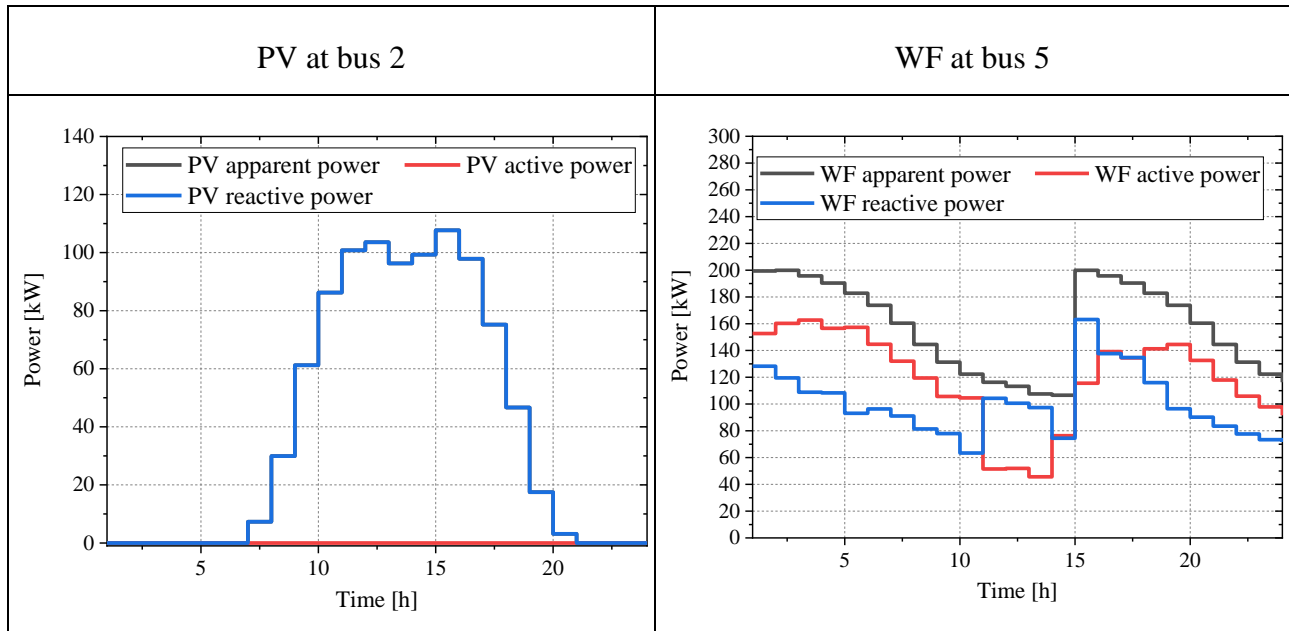


Fig. 4-11. Effects of inverter-based operation of RESs and BESs on voltage deviation and total power loss

According to the inverter-based operation of RESs, it is the active and reactive power of PVs/WFs that contributes in power flow constraints (5b)-(5c), i.e., $P_{(j+1)t}^{WF}$, $P_{(j+1)t}^{PV}$, $Q_{(j+1)t}^{WF}$, $Q_{(j+1)t}^{PV}$, while, these active and reactive shares of RESs are also presented in (4a)-(4b), forming the apparent power of PVs and WFs, i.e., S_{jt}^{PV} , S_{jt}^{WF} . In the following, the optimal decisions on the active/reactive power of RESs has been given by Fig. 14. As it is seen, no active power has been injected to bus 2 the during the whole operation horizon. Most of the injected power to bus 10 is also reactive power. The share of active power, however, is considerably higher than the share of reactive power at buses 5, 13, and 26. These decisions have been optimally made regarding the load level at each bus, value of loss and voltage deviation which have been minimized by the objective function, and the BES charging/discharging power.



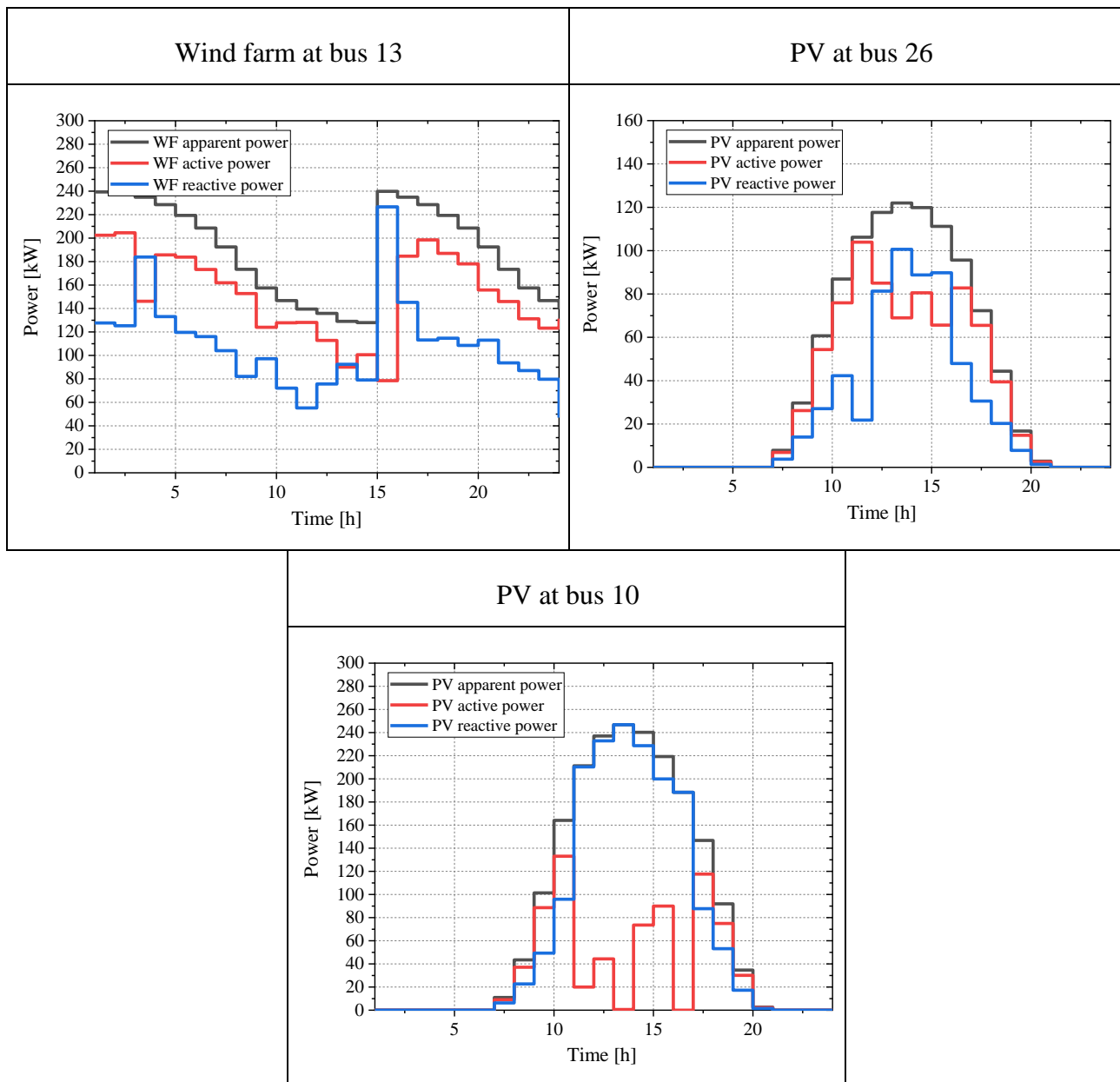
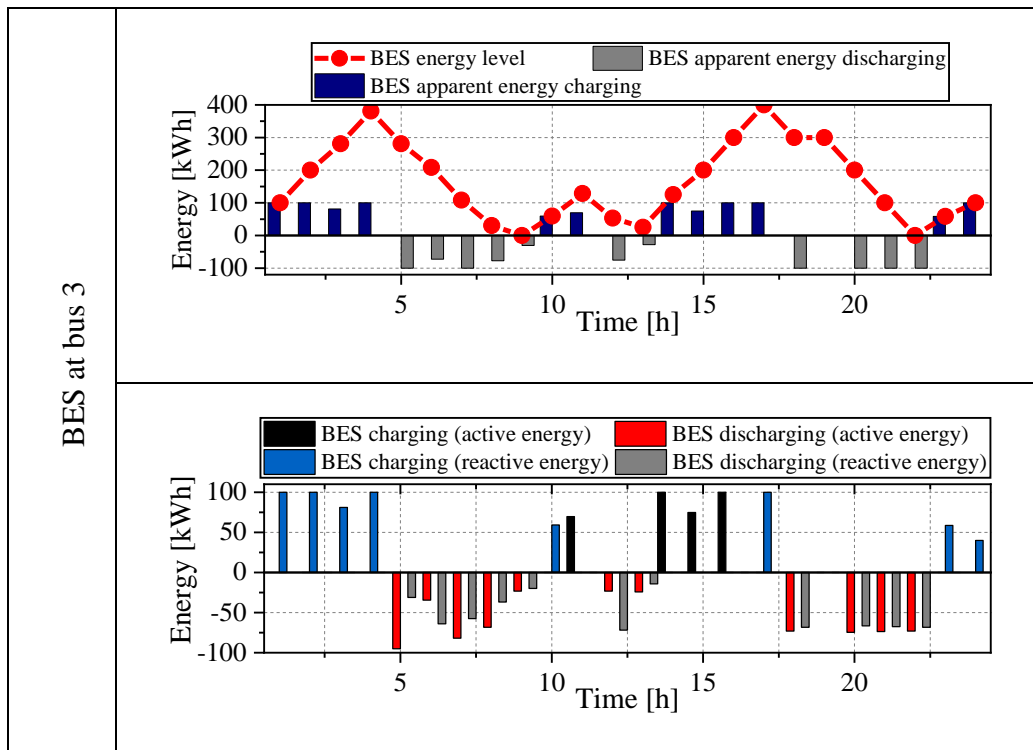


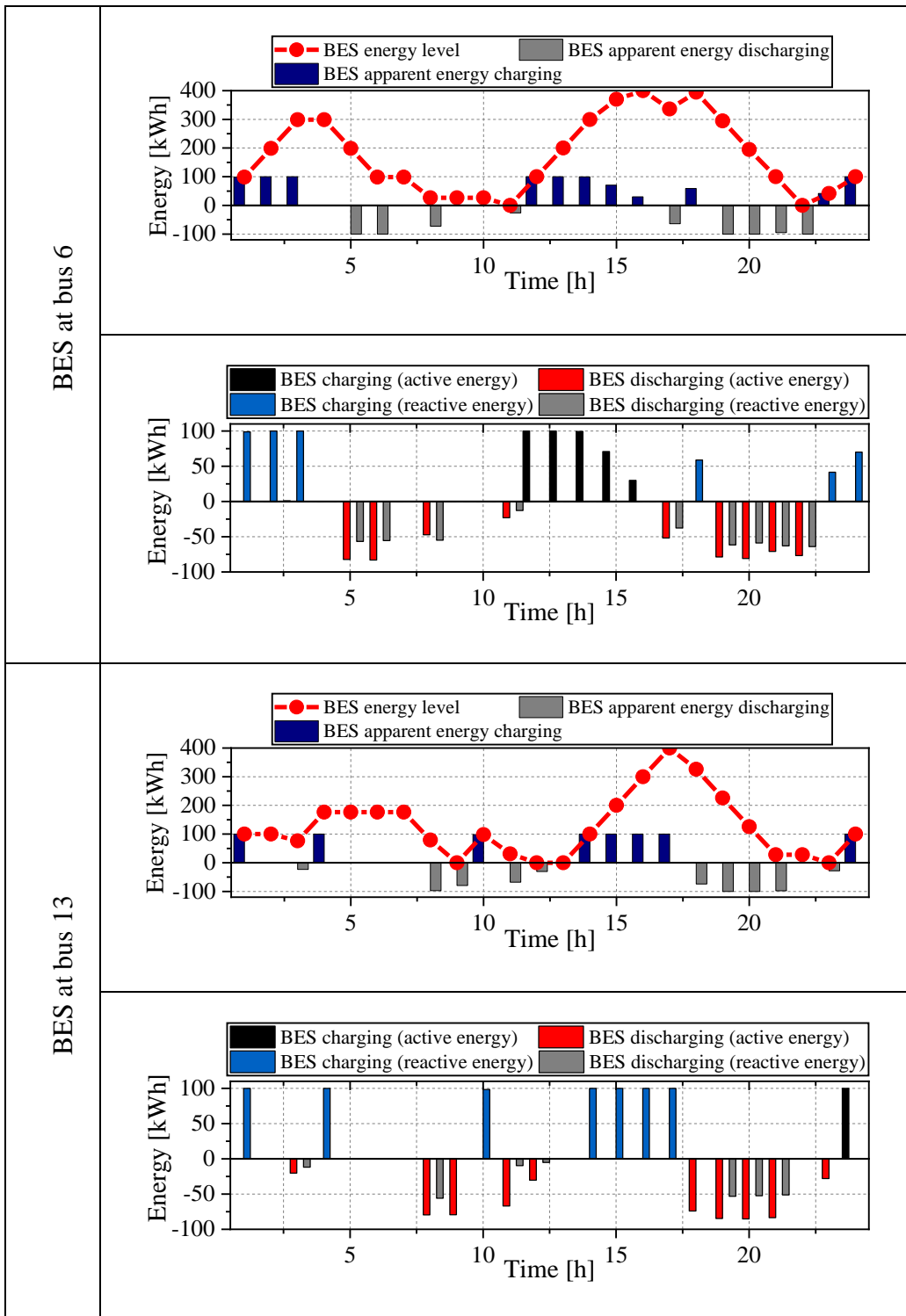
Fig. 4-12. Inverter-based operation of RESs (active/reactive share of the injected power)

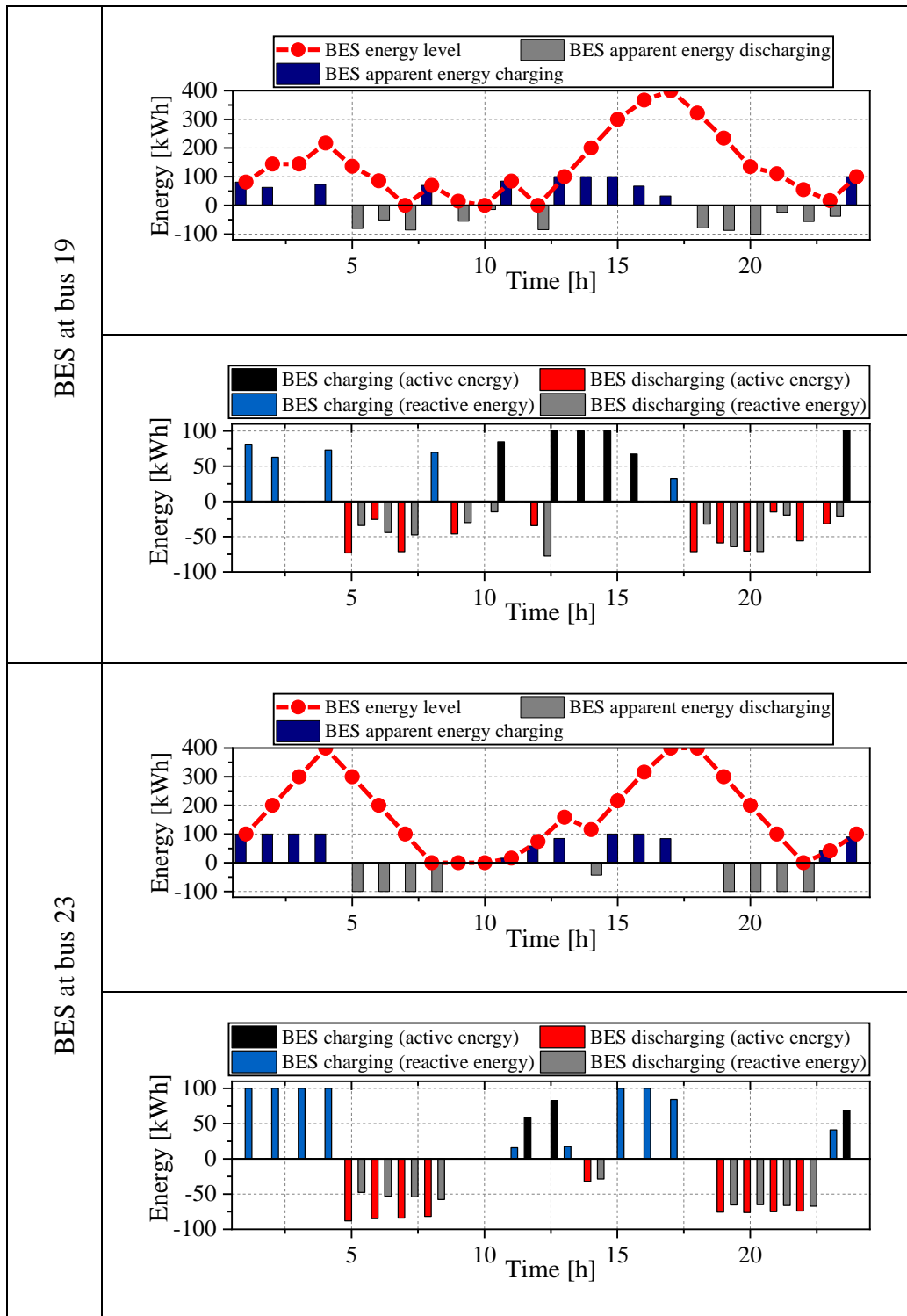
There are six battery storage systems throughout the EDS (see Fig. 4-4). These battery systems are operated according to the inverter-based model (3), according to which the BES can absorb active power in a specific time period and inject it back to the grid as reactive power in another

time period, and vice versa, i.e., $\frac{P_{jt}^{chg}}{Q_{jt}^{chg}}$ is not necessarily equal to $\frac{P_{jt}^{dis}}{Q_{jt}^{dis}}$.

The charging/discharging energy as well as active/reactive support of BESs have been presented by Fig. 4-13. As it is seen at the right-hand side of Fig. 4-13, BESs are mostly charged approximately between hours 1-4 and 13-17. The charging pattern of BESs is mostly due to the surplus of power produced by WFs during under-load hours, while, the stored power by BESs is discharged when RES generation drops, i.e., hours 5-10 and 17-23. Another reason of this discharge is the increase in average load during hours 17-22. The share of active and reactive power of BESs in both charging and discharging modes is given at the right-hand side of Fig. 4-13.







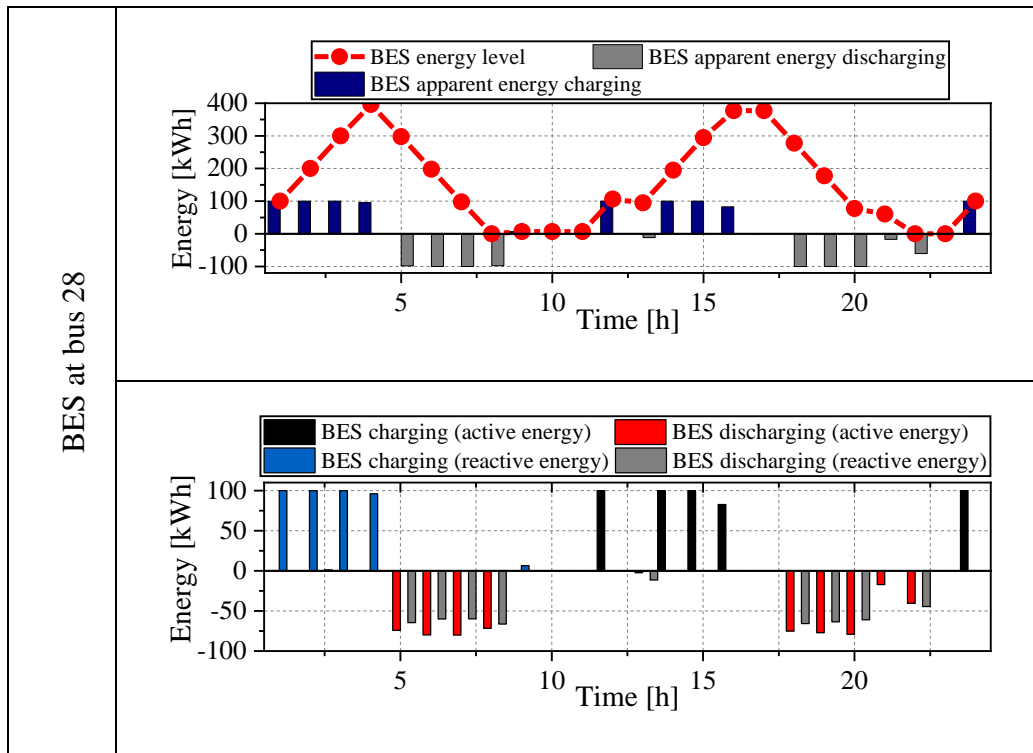


Fig. 4-13. Inverter-based BES energy level and apparent charging/discharging power as well as active/reactive share of BES power (right)

4.9. Conclusion

This chapter presented a new directly solvable energy management model for EDS to minimize total power losses and bus voltage deviations by employing the arbitrage ability of distributed battery energy storage systems and renewable energy sources. Two objectives were considered in the model, including power loss minimization and voltage deviation minimization. A new indexing for EDS buses was introduced which resulted in a general representation of EDS power flow equations. These equations were then introduced as the constraints of the proposed energy management model. Accordingly, the energy management model was able to be solved in a single shot through GAMS solver package with no need to metaheuristic optimization methods. The inverter-based operation (active and reactive power controllability) of RES and BES

elements were also considered in the energy management model to enable a realistic operation of these systems.

A comprehensive case study was conducted using the standard IEEE 33-bus system. The optimality of the proposed power flow model was illustrated by comparing the obtained results with those of the FBS method. The 33-bus system was further equipped by RES and BES elements and the energy management model was conducted for a 24-h operation of the system. According to the obtained numerical results, it was shown that the integration of RES and BES elements can significantly reduce the EDS power loss and voltage deviations over time. This was highlighted by investigating the effects of these elements on the standard deviation of voltage magnitude over the 24-h operation horizon. It was also shown that the inverter-based operation of RESs and BESs can play an important role in reducing system losses and smoothing the voltage magnitudes as these two variables are strongly dependent on both the active and reactive power flow in EDS.

The proposed model in this study can be employed by EDS operators to conduct day-ahead EDS operations and evaluate the effects of inverter-based operation of RESs and BESs on the system characteristics. The ability of the proposed model in being directly solved is another contribution of this study which eliminated the need to iterative load flow calculation methodologies as well as metaheuristic optimization techniques. The proposed inverter-based operation in the energy management model can also be employed to integrate other elements such as electric vehicle charging stations into electricity distribution system.

The energy management model in this chapter, will be used to investigate the effects of EV

charging on distribution system. To do so, an EV model is developed in the next chapter.

5. Load Modelling of EVs

This chapter presents a comprehensive investigation on the effects of EV employment of the optimal operation of EDS. The developed energy management model in Chapter 4 is employed to investigate the effects of EV employment on power loss and voltage deviations of EDS operation at the presence of RES and BES systems. To do so, EV employment is modelled by probability density functions throughout the EDS, considering different probability density functions. Two types of EV charging is considered including fast and average speed charging. Different scenarios are investigated to evaluate the EV load. The obtained load scenarios will be used in Chapter 6 where the directly solvable energy management model is solved under uncertainty through robust optimization. The effects of EV loading will be shown in Chapter 6 as well.

5.1. Charger type and EV brands considered in the load model

Combined Charging System inlet is considered as the charging system for EVs. The Combined Charging System inlet is an industry-standard vehicle connector for convenient charging of Plug-in Hybrid Electric Vehicles (PHEV) and Electric Vehicles. Type 2 inlets and plugs support AC & DC Charging standards of Europe/Australia. This inlet is given by Fig. 5-1.



Fig. 5-1. Considered inlet for EVs

The following vehicles in Table 5-1 are considered for fast and average charging patterns.

Table 5-1. Considered electric vehicles

Vehicle make and model	Vehicle view	Battery Capacity	Charger Type	Driving Range	Charging time	Charging power
Hyundai Kona Electric (slow speed charging)		64kWh	Type s2/CCS	449 km	6 hours	9.4 kW
Nissan LEAF (fast speed charging)		40kWh	Type s2/CCS	243 km	2 hours	17 kW

5.2. Scenario No.1 of EV loading (100% fast charging EVs)

In this scenario 25 fast charging EVs are considered in an individual bus of the distribution system. The distribution of the start of the charging time for these vehicles follows normal distribution. However, the total value of the charging load on the bus is a summation of charging power of EVs over time.

In the following, the EV charging load profile has been given by over 12 operating hours.

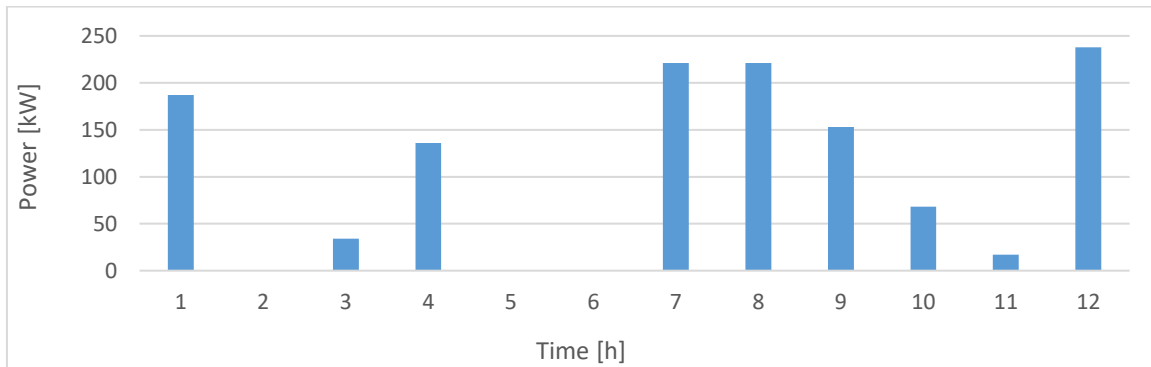


Fig. 5-2. EV charging load profile for scenario No. 1 of EV loading (100% fast charging EVs)

5.3. Scenario No.2 of EV loading (100% slow charging EVs)

In this scenario 25 slow charging EVs are considered in an individual bus of the distribution system. The same as scenario No.1, the distribution of the start of the charging time for these vehicles follows normal distribution. However, the total value of the charging load on the bus is a summation of charging power of EVs over time.

In the following, the EV charging load profile has been given by Fig. 5-3 over 12 operating hours.

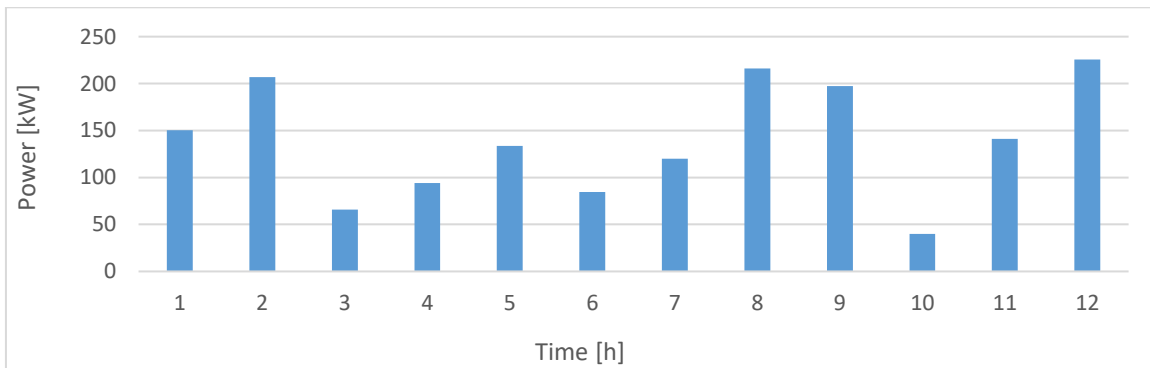


Fig. 5-3. EV charging load profile for scenario No. 2 of EV loading (100% slow charging EVs)

5.4. Scenario No.3 of EV loading (50% slow charging and 50% EVs)

In this scenario 13 slow charging EVs as well as 13 fast charging EVs are considered in an individual bus of the distribution system. The same as scenario No.1 and No.2, the distribution of the start of the charging time for these vehicles follows normal distribution. However, the total value of the charging load on the bus is a summation of charging power of EVs over time.

In the following, the EV charging load profile has been given by over 12 operating hours.

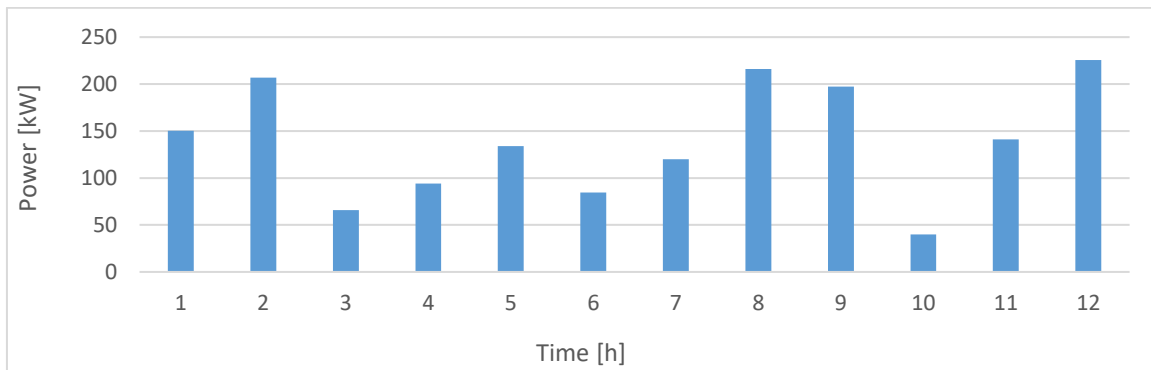


Fig. 5-4. EV charging load profile for scenario No. 2 of EV loading (50% slow charging and 50% fast charging EVs)

Note that, the above EV load models will be considered in the case study in Chapter 6, where the robust optimization approach is conducted to characterize the uncertainties of load in the energy management model which was presented in Chapter 4.

The EV model in this chapter will be used long side the energy management model in chapter 4, to investigate the effects of EV charging on distribution system.

6. The Proposed BCD Robust Energy Management model to Investigate the Effects of EV Employment under Uncertainties of PV and WT systems

This chapter presents a new robust energy management model as an extension to Chapter 4. In Chapter 4, the new inverter-based directly solvable energy management model was introduced for EDS. In this chapter, the associated uncertainties of renewables in EDS are considered into account through robust optimization (RO). A new robust min-max-min optimization problem is developed through a decomposition-based column-and-constraint generation technique. Block-coordinate-descent (BCD) methodology is used to solve the inner max-min problem rather than duality theory in conventional robust models. This enables a recourse-based characterization of integer variables, such as BES charging/discharging status, which was not applicable in previous robust models. A case study has been conducted for an EDS in Adelaide, South Australia including 6 buses. The robust solutions are obtained for different scenarios of EV charging pattern under uncertainty of renewables in EDS. The inverter-based operation of BES and RES systems is also considered in the model.

6.1. Background and Motivation

To cope with the mentioned problems with SP and scenario-based models (as indicated in Chapter 2), robust optimization (RO) has been employed in some recent studies to characterize uncertainties [111]. The advantage of RO is that it models the uncertainties by worst-case realization through bounded intervals, eliminating the need of scenario generation and distributional knowledge of the uncertain parameters [34, 112]. Therefore, the obtained solutions

would be feasible as long as the uncertainty realizations are within the user-defined bounded intervals, which makes it more reliable/practical than scenario-based and SP models in the literature.

However, RO still faces some limitations in modelling uncertainties which is due to the use of duality theory in solving it. In particular, duality theory is used in min-max-min RO problems to transform the inner bi-level max-min problem into a solvable single-level max problem. A Robust bidding strategy was proposed for a wind farm coupled with a storage system in [113]. However, binary variables, indicating buying/selling bids, were eliminated in the model to ease the employment of duality theory. This results in export-only bidding which is not applicable in practice. Duality theory was also employed in [114] to solve a robust model predictive control-based bidding strategy for a wind-storage systems. However, the model of [114] was a single-stage max-min problem only. Binary variables indicating BES charging/discharging status were also eliminated in [115] to make it possible to conduct duality. Moreover, it was not possible to consider both buying and feed-in-tariff for day ahead bids in [115] as no binary variable was used to separate buying/selling status. This becomes important when the feed-in tariff is different than the buying price. To be more realistic, the charging/discharging status of BES was modeled by binary variables in [116]. However, the charging/discharging status of BES was characterized before uncertainty realizations to be able to conduct duality theory with no binary variables involved. Similar to [116], the charging/discharging status of BES was modeled before uncertainty realizations in [117-119].

Note that, the mentioned RO studies in the literature have considered the uncertainties in their models and their solutions have proven to be more efficient than the deterministic approaches.

However, the BES charging/discharging binary variables have been eliminated or modeled in the master problem. As a result, the worst-case realization of uncertainties is determined when these variables are fixed in the sub-problem and therefore, these variables are not affecting the sub-problem's objective function. In other words, these variables are obtained based on the primal cuts, containing the worst-case realization of uncertainties in the master problem and have no accountability in determining the worst-case realization itself. This means that, the sub-problem is solved without considering the cross effects between Operation binary variables and uncertainties. Therefore, the benefit of robust optimization has not been fully exploited.

6.2. Contributions

1) A robust optimization approach is proposed to solve the directly solved energy management model in Chapter 4. To overcome the problems in scenario-based and SP models, a min-max-min adaptive robust optimization is developed to characterize the uncertainties of renewables such as PV and WT generation by polyhedral uncertainty sets instead of scenarios. The problem is solved through a decomposition methodology and a column-and-constraint (C&C) generation technique [34], recasting the tri-level problem into a first-stage min problem and a second-stage max-min problem.

2) The proposed RO model employs Block Coordinate Descent (BCD) method [120], which approximates the worst-case realization of uncertainties by means of Taylor series instead of transforming the inner max-min problem into a single max problem by duality theory. BCD was originally devised to deal with single-level problems. By extending the application of BCD technique to solve the two-level max-min sub-problem (resulted from the C&C generation technique), it is possible to avoid duality theory in solving the sub-problem. Since, dual of a

mixed-integer model is generally weak, non-tractable and complicated [35], the extension of BCD technique instead of duality theory eliminates the limitation in considering binary variables in the max-min sub-problem. As a result, uncertainty-dependent binary variables such as BES charging/discharging statuses can be obtained after uncertainty realization in the sub-problem as recourse decisions, which was not applicable in previous dual-based RO models in the literature. This results in more system flexibility in compensating the uncertainty effects such as PV/WT shortage.

3) Since, no duality is conducted, BES status can be freely modeled with binary indicators. This is the first application of min-max-min robust optimization in which binary variables are modeled in the inner max-min problem. Note that, the proposed model in this study is called "BCD robust", hereafter.

6.3. Two-stage Adaptive Robust Approach

In robust optimization, two main decisions are made including "here-and-now" decisions, which are obtained before any uncertainty realizations, and "wait-and-see" decisions, which are obtained after the realization of uncertain parameters. In this study, all operating variables in EDS, i.e., power loss, voltage, power flow, etc., are considered as "here-and-now" variables which are obtained before uncertainty realizations (as a result of the finalized day ahead operation of the system). Since, the uncertainties associated with PV/WT productions are realized when scheduling BES and RES systems, the BES and RES active power as well as their inverter-based relative power are considered as "wait-and-see" decisions to compensate the effects of uncertainties.

The compact form of the proposed robust model is expressed through a tri-level min-max-min optimization problem as (2).

$$\text{Min}_{\mathbf{X} \in \Xi^I} (\mathbf{A}' \cdot \mathbf{X} + \text{Max}_{\tilde{\mathbf{U}} \in \Xi^{US}} \text{Min}_{\mathbf{Y} \in \Xi^{II}} \mathbf{F}', \mathbf{Y}) \quad (6a)$$

s.t.

$$\Xi^I = \{\mathbf{X} \in \{0, 1\}^{N_x} \mid \mathbf{C}\mathbf{X} \geq \mathbf{D}\} \quad (6b)$$

$$\Xi^{US} = \{\tilde{\mathbf{U}} \in \mathbb{R}^{N_{\tilde{u}}} \mid \tilde{\mathbf{U}} = \bar{\mathbf{U}} + \mathbf{U}^{dev+} - \mathbf{U}^{dev-}\} \quad (6c)$$

$$\Xi^{II} = \{\mathbf{Y} \in \mathbb{R}^{N_y} \mid \mathbf{E}(\mathbf{X}, \mathbf{Y}, \tilde{\mathbf{U}}) \geq 0\} \quad (6d)$$

In (6a), the outer min problem minimizes the objective function over the sizing variables which are obtained as "here-and-now" decisions. The expression $\mathbf{A}' \cdot \mathbf{X}$ represents EDS power flow variables. Therefore, outer min problem is subject to power flow equations in Chapter 4, compactly expressed by (6b). The inner max problem maximizes the remaining term of the objective function (expressed by \mathbf{F}', \mathbf{Y}) over the worst-case realization of uncertain parameters, while the inner min problem minimizes it over the BES/RES operation variables, considered as "wait-and-see" decisions. Therefore, the inner max problem is subject to polyhedral uncertainty sets, expressed by (6c), while, the inner min problem is subject to the BES/RES operation constraints, presented by (6d).

6.4. Solution Methodology to Solve the Proposed Robust energy management model

The tri-level optimization problem in (2a) cannot be solved directly. Therefore, a decomposition methodology, by means of C&C technique [34], is employed to decompose the

tri-level min-max-min problem to a single-level min problem and a bi-level max-min problem. The single-level min problem is called "master problem" and the bi-level max-min problem is called "sub-problem", hereafter. The proposed decomposition methodology is described through the following steps:

Step 1) The master problem is solved to determine "here-and-now" decision variables while being subject to "here-and-now" constraints only. The compact form of master problem is given by (6e)-(6g).

$$\min_{X \in \Xi'} \Lambda_I \equiv \mathbf{A}' \cdot \mathbf{X} + \Psi \quad (6e)$$

s.t.

Here-and-now constraints:

$$\mathbf{CX} \geq \mathbf{D}; \quad \mathbf{X} \in \{0, 1\}^{N_x} \quad (6f)$$

Primal cut constraints:

$$\Psi \geq \mathbf{F}' \cdot \mathbf{Y}; \quad \mathbf{G} \cdot \mathbf{X} + \mathbf{B} \cdot \mathbf{Y}_c + \mathbf{H} \cdot \mathbf{U}^c \geq \mathbf{K}; \quad c \in \Xi^c \quad (6g)$$

In the above problem, (6e) presents the epigraph form of master problem which minimizes the "here-and-now" terms of objective function, which are delivered from the sub-problem in previous iteration of column-and-constraint methodology (if the first iteration, primal cuts are replaced by constraints of the deterministic model). After achieving a solution in master-problem, the obtained "here-and-now" variables, i.e., \mathbf{X} are sent to the sub-problem as fixed values to determine both "wait-and-see" decision variables, and the new worst-case realization of uncertain

parameters including PV/WT generation.

Step 2) Given the obtained here-and-now variables, sub-problem is solved to determine operation decision variables and worst-case realization of uncertain parameters. The vector of the fixed "here-and-now" variables is shown by \mathbf{X}^c in the sub-problem which is given by (6h)-(6j).

$$\text{Max}_{\bar{U} \in \Xi^{US}} \text{Min}_{Y \in \Xi^{II}} \mathbf{F}', \mathbf{Y} \quad (6h)$$

s.t.

Here-and-now constraints:

$$\mathbf{G} \cdot \mathbf{X}^c + \mathbf{B} \cdot \mathbf{Y} + \mathbf{H} \cdot \mathbf{U}^c \geq \mathbf{K}; \quad (6i)$$

Uncertainty set constraints:

$$\mathbf{U}^c = \bar{\mathbf{U}} + \mathbf{U}^{dev+} - \mathbf{U}^{dev-}; \quad \mathbf{U}^c \in \mathbb{R}^{N_U} \quad (6j)$$

The objective function in (6h) minimizes the operating costs over "wait-and-see" variables, while, maximizing it over the worst-case realization of uncertainties. The obtained worst-case realizations are then sent back to master problem as fixed values. In fact, in each iteration of the decomposition methodology a new set of constraints (primal cuts) are added to master-problem.

Step 3) At the next iteration, master problem is solved, given the obtained worst-case realization of uncertain parameters through primal cutting planes in previous iterations, in order to find the new here-and-now decision variables to be sent to the sub-problem. The column-and-constraint methodology iterates between master problem and sub-problem until the convergence

criteria is satisfied (i.e., the value of master problem and sub-problem get sufficiently close).

Since, the inner max-min problem is a bi-level optimization model, it cannot be directly solved. As indicated in the contributions, BCD technique is used to recast the bi-level max-min problem into two single-level problems including a first-stage sub-problem, i.e., the inner min problem, and a second-stage sub-problem, i.e., the inner max problem. Since, duality theory is not used in the proposed robust model, it is possible to determine the binary variables in the sub-problem as "wait-and-see" decisions. Therefore, despite the previous dual-based models, in which BES charging/discharging status was obtained before uncertainty realization as "here-and-now" variables, it is based on the worst-case realization of uncertainties and are treated as recourse decisions ("wait-and-see" decisions) in the BCD model. In the following sub-section, the solving methodology for the sub-problem is described.

6.5. Block Coordinate Descent (BCD) Methodology to Solve the Sub-problem

The sub-problem is solved to determine "wait-and-see" variables at the presence of uncertainties, and 2) the worst-case realization of uncertain parameters, given the fixed values of here-and-now variables obtained by master problem.

Note that the standard application of the BCD method relies on the availability of an analytical expression for the operating cost in terms of middle-level variables. In the absence of such an expression in the max-min sub-problem, at each iteration of the proposed BCD method, the sub-problem for operating/bidding variables is built upon the first-order Taylor series approximation of the operating cost around the uncertainty realizations identified at the previous iteration. Therefore, the max-min sub-problem in (6h) is recast into a first-stage and a second-stage sub-

problem. The first-stage sub-problem is given as (6k)-(6m).

$$\min_{Y \in \Xi^U} \Lambda_{II} \equiv F', Y \quad (6k)$$

PV-WT-BES operation constraints:

$$G \cdot X^c + B \cdot Y + H \cdot U^c \geq K; \quad (6l)$$

Auxiliary constraints:

$$U^c = U^z \quad : \quad \mu \geq 0; \quad (6m)$$

Since, the here-and-now variables are fixed on their obtained values in master problem, the power flow variables are not included in the first-stage sub-problem. Instead, it includes the BES and RES operating constraints. Accordingly, the objective function (6k) minimizes the operating costs over "wait-and-see" variables, while being subject to operating constraints and auxiliary constraints representing the obtained worst-case realization of uncertainties by the second-stage sub-problem in previous iteration of the BCD method , i.e., U^z .

μ is the vector of dual variables representing the sensitivity of objective function (6k) toward uncertain parameters, including PV/WT production at each iteration z of the BCD method. These dual variables are further employed to develop the first-order Taylor series in the second-stage sub-problem only and no duality theory in conducted.

The second-stage sub-problem is built upon the first order Taylor series approximation of the first-stage sub-problem over the uncertain parameters in previous iteration of BCD method, i.e., $z - 1$. Therefore, at iteration z of the BCD method, the second-stage sub-problem is cast as (6n)-

(6o).

$$\max_{\bar{U} \in \Xi^{US}} \Lambda_{III} \equiv \Lambda_{II} + \boldsymbol{\mu} \cdot (\mathbf{U}^z - \mathbf{U}^{z-1}) \quad (6n)$$

Uncertainty set constraints:

$$\mathbf{U}^z = \bar{\mathbf{U}} + \mathbf{U}^{dev+} - \mathbf{U}^{dev-}; \quad \mathbf{U}^z \in \mathbb{R}^{N_{\bar{U}}} \quad (6o)$$

The second-stage sub-problem determines the worst-case realization of uncertain parameters at each iteration z of the BCD method, by which the approximated objective function (6n) is maximized. Constraint (6o) expresses the deviation of uncertain parameters in positive and negative directions. By solving the second-stage sub-problem, the worst-case realization of uncertain parameters is determined to be sent to the first-stage sub-problem. The first-stage sub-problem is solved given the fixed values of worst-case realizations in the second-stage sub-problem.

This procedure continuous until the inner loop converges, i.e., the value of first-stage and second-stage sub-problems become sufficiently close. Therefore, the methodology to solve the min-max-min problem consists of two nested loops as follows:

Outer loop: The master problem communicates with the sub-problem through the outer loop, conducting the C&C methodology,

Inner loop: The iterations between first-stage and second-stage sub-problems are directed through the inner loop by means of BCD method.

Fig. 6-1. Outline of the proposed BCD robust methodology Fig. 6-1 gives the outline of the

proposed methodology and the compact formulation of each problem. In Fig. 6-1, the outer loop is shown by red lines and the inner loop is shown by blue lines.

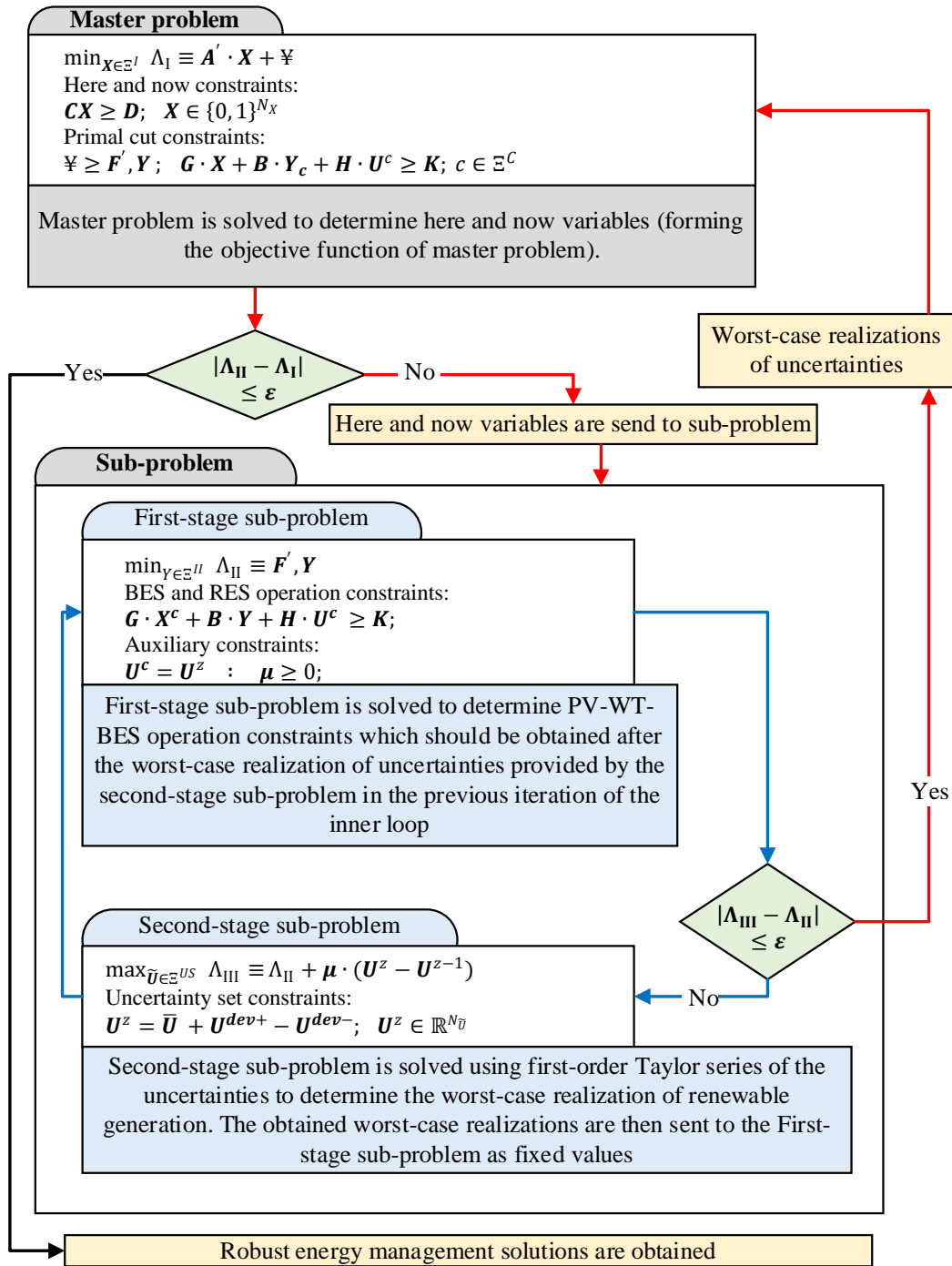


Fig. 6-1. Outline of the proposed BCD robust methodology

6.6. Numerical Study

The simulations in this section are conducted on a 6-bus real world EDS in Adelaide, South Australia. Case study includes a PV and a WT system as well as a BES as indicated by Fig. 6-2. The employed EVs are as indicated in Chapter 5. Voltage magnitude at slack bus is 12.66 kV which is considered as the base value, while, the base value for power is 100 kVA. The obtained load models in Chapter 5 are also used in the simulations in this chapter. The capacity of each BES system is 400 kWh. The generated power of RESs throughout the network are given by Fig. 6-3 for the considered 12-hour operation in this study (as 24 hour operation requires more time to solve, so for the sake of simplicity 12 hour operation is considered). The standard active/reactive load of EDS system is used to generate a 12-h load pattern based on South Australia's daily energy consumption pattern which has been taken from [110]. The uncertainty of PV and WT system has taken into consideration through polyhedral uncertainty sets. The number of uncertain PV and WT generation parameters is 24 including 12 uncertain parameters for each source in a 12-hour operation horizon. The considered deviation range of uncertainties is 10% in negative direction for PV and WT generation to achieve the worst-case realization of uncertainties. The 10% deviation is just an indication of uncertainties. It can be biased based on any other case study.

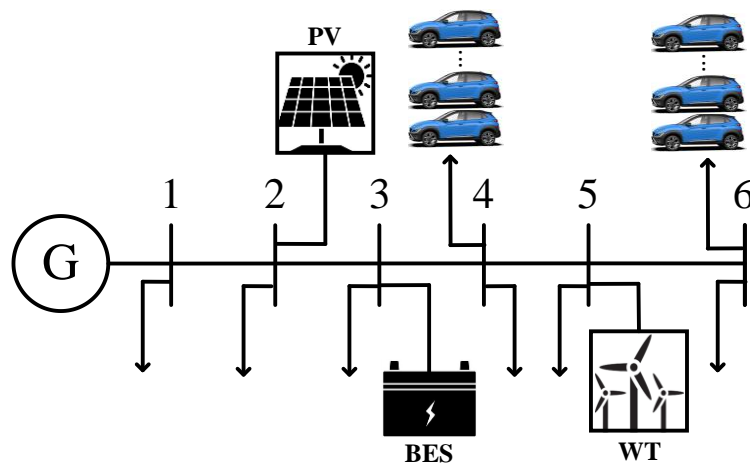


Fig. 6-2. Case Study

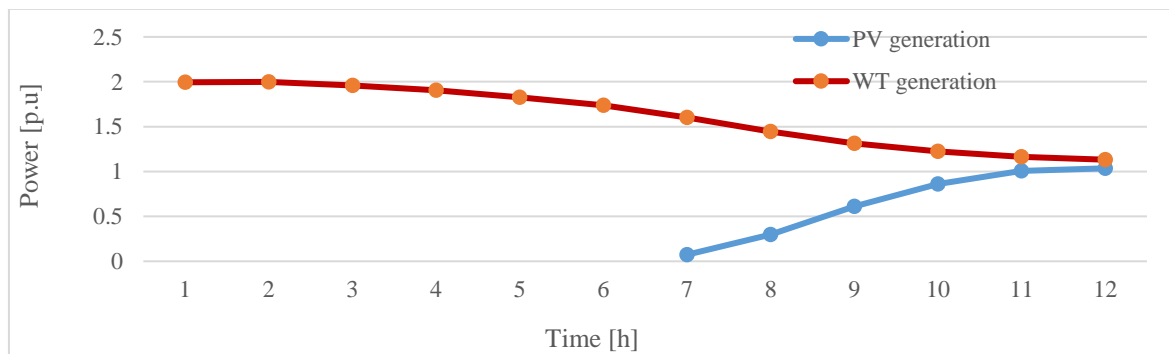


Fig. 6-3. Generated power by PV and WT systems

Load of bus 4 and 6 have been given by Fig. 6-4, Fig. 6-5, and Fig. 6-6 with and without EV charging patterns for scenarios No.1, 2, and 3, respectively (see Chapter 5 for scenarios). As it is seen, the load profile is smoother as the number of slow charging cars increases.

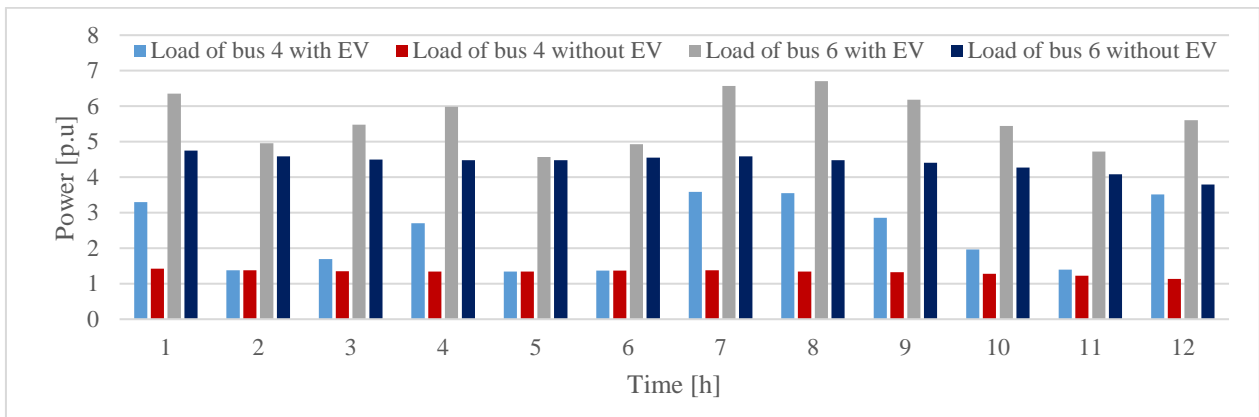


Fig. 6-4. Load of bus 4 and 6 with and without EV charging patterns – Scenario No.1 (100% fast charging EVs)

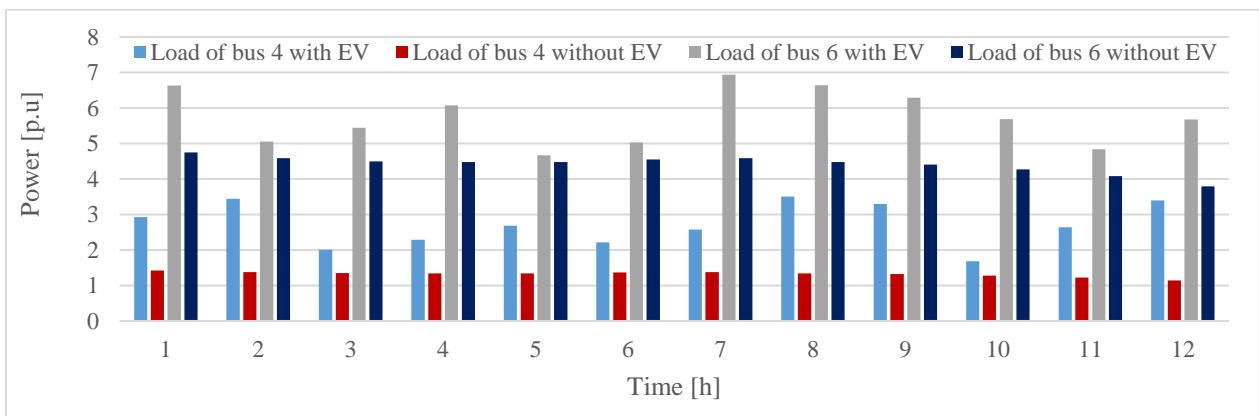


Fig. 6-5. Load of bus 4 and 6 with and without EV charging patterns – Scenario No.2 (100% slow charging EVs)

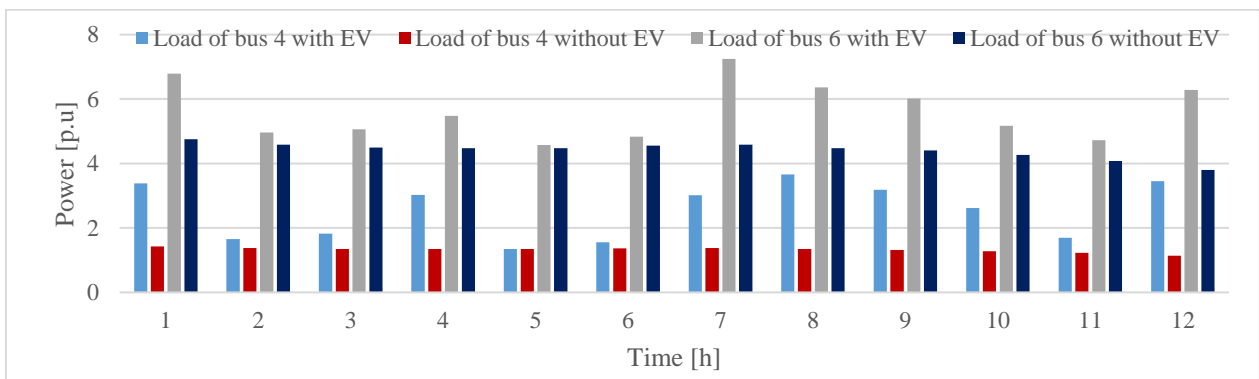


Fig. 6-6. Load of bus 4 and 6 with and without EV charging patterns – Scenario No.3 (50% slow charging and 50% fast charging EVs)

In the following each scenario is considered for simulation which is based on the robust optimization of the energy management model in Chapter 4, considering the EV charging patterns in Chapter 5. However, a basic scenario is also conducted with no EV charging for comparison purposes.

Considering scenario No.1 of EV charging patterns, the total hourly power loss of EDS is obtained as Fig. 6-7.

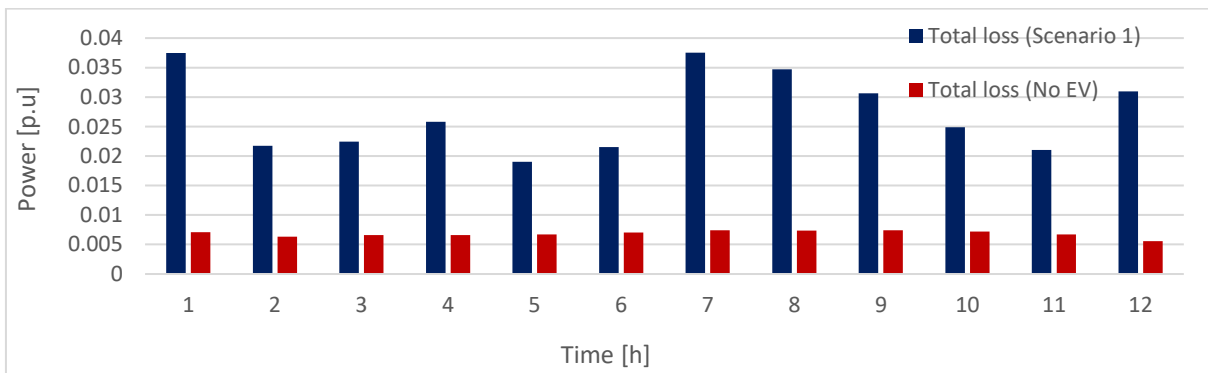


Fig. 6-7. Total hourly power loss of EDS for scenario No.1

As it is seen, the value of power loss has increased dramatically, compared to the “No EV” scenario. This is due to the high increase in line current which has reached the maximum possible line current in some lines. Moreover, the loss of each line follows the square of the current which means small changes in current will result in high loss values on the line.

The value of voltage magnitude for each bus of the system has been given by Fig. 6-8. As it is seen, the first bus has a higher voltage magnitude, and it reduces as we reach the last bus.

However, the overall voltage deviation is not out of the allowable operating rate which is $\pm 5\%$. The deviations of bus 6 of the system is more considerable as it involves bus load and EV charging patterns which makes the voltage of this bus more dynamic compared to other buses.

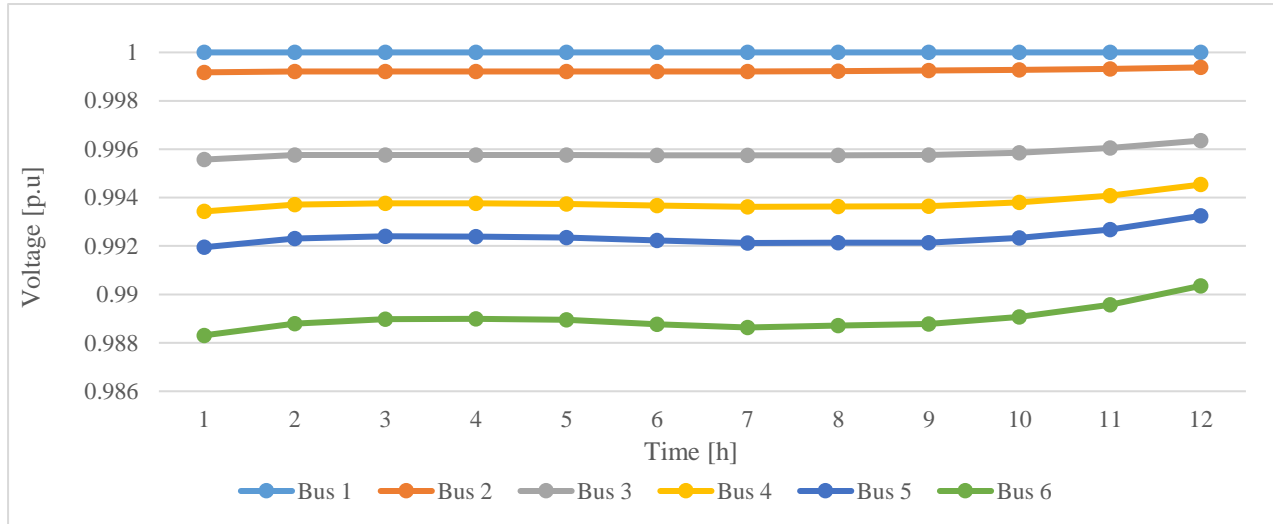


Fig. 6-8. Hourly voltage of each bus of EDS for scenario No.1

The BES optimal operation is given by Fig. 6-9 in which the BES energy level as well as charging/discharging power is compared with the “no EV” scenario. As it is seen, the performance of the battery in terms of discharging rate has changed in hours 6-10 where the EV load increases dramatically (see Fig. 6-4).

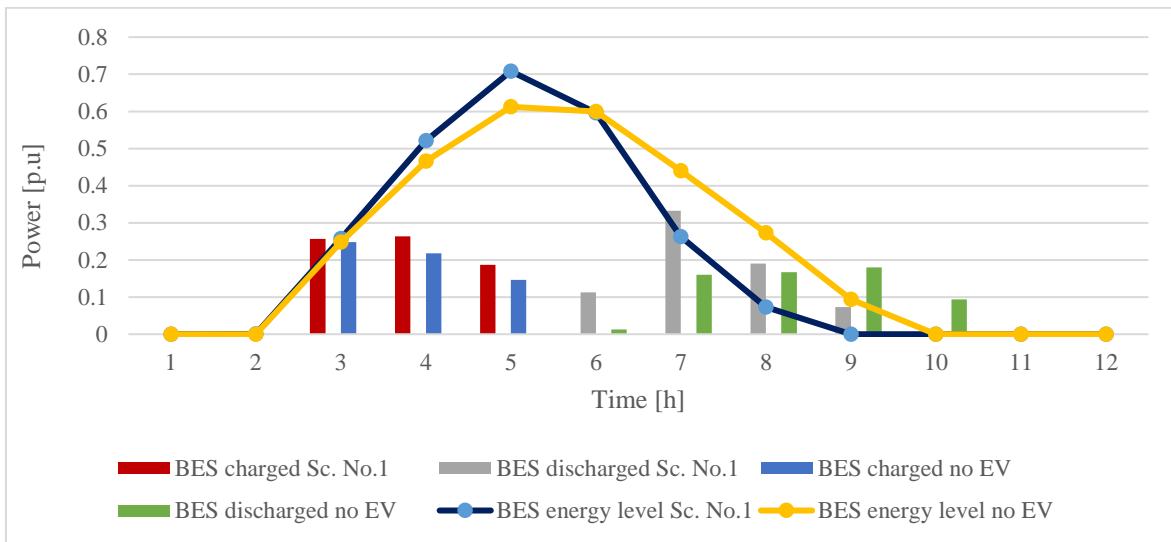


Fig. 6-9. BES performance in bus 3 for scenario No.1 compared to the base scenario (no EV)

The same set of data has been given for scenario No.2 which includes 100% of slow charging EVs. As it is seen in Fig. 6-10, the power loss increased in the same way as scenario No.1. The voltage behavior is also given by Fig. 6-11. As the same as scenario No.1, the voltage has dropped a little at the first hour of the operation horizon and has increased in the last couple of hours in buses 3-6.

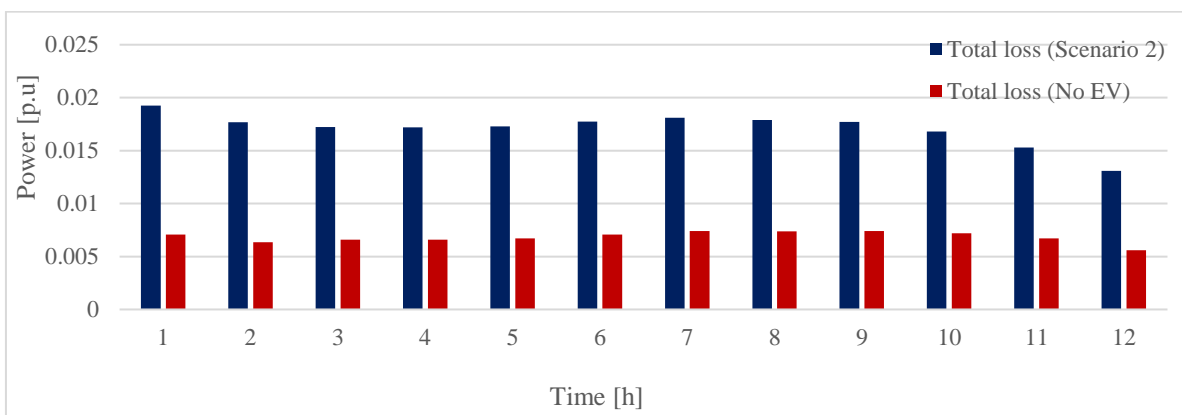


Fig. 6-10. Total hourly power loss of EDS for scenario No.2

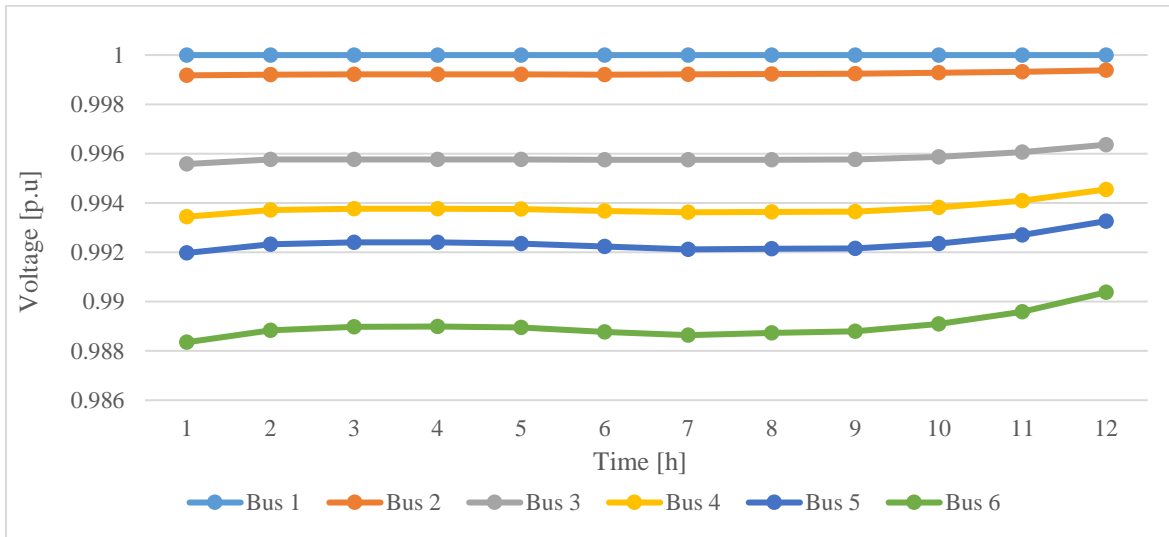


Fig. 6-11. Hourly voltage of each bus of EDS for scenario No.2

The BES operation including the energy level and the charging/discharging power in scenario No.2 has been compared to “no EV” scenario in Fig. 6-12. As it is seen, the arbitrage ability of BES has been used more in this scenario and it has been more charged/discharged in a higher rate. The reason is that there is lower EV load in this scenario in some hours and therefore, the BES can store more energy to discharge in required operating hours.

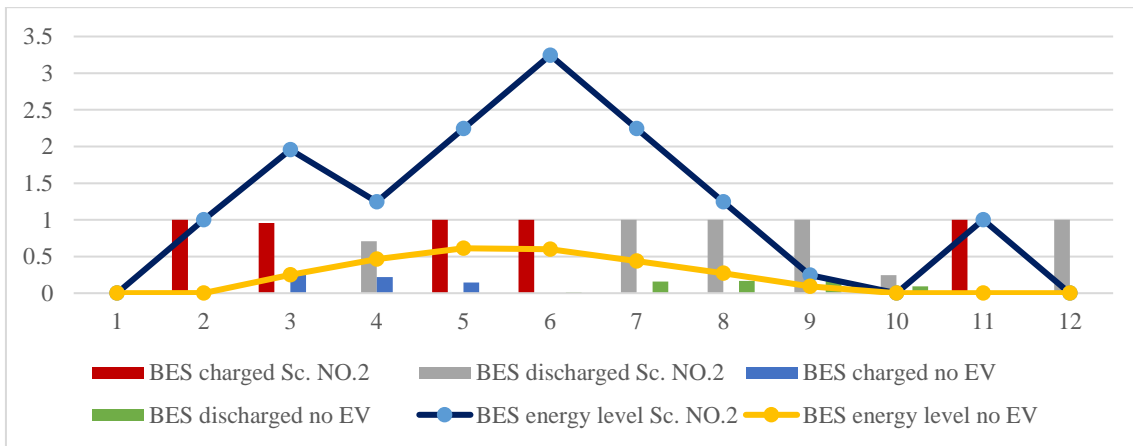


Fig. 6-12. BES performance in bus 3 for scenario No.2 compared to the base scenario (no EV)

The complete set of results has been given by Fig. 6-13, Fig. 6-14, and Fig. 6-15 for scenario

No.3 which includes 50% of fast charging EVs and 50% of slow charging EVs.

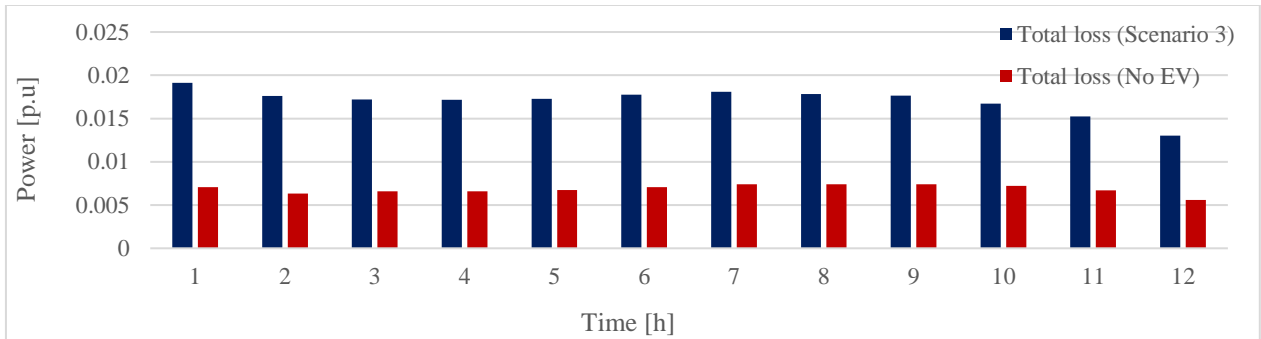


Fig. 6-13. Total hourly power loss of EDS for scenario No.3

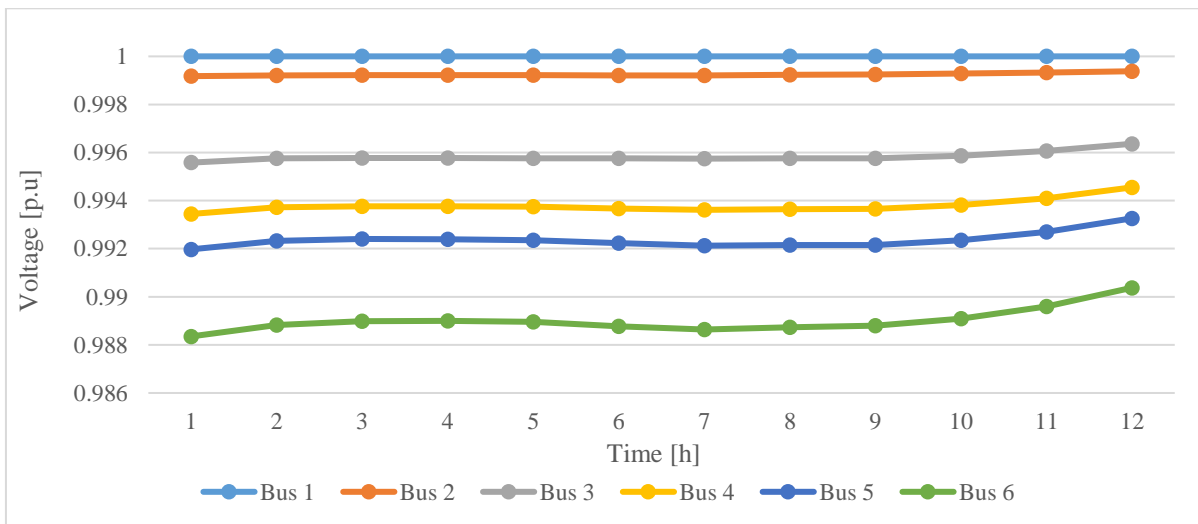


Fig. 6-14. Hourly voltage of each bus of EDS for scenario No.3

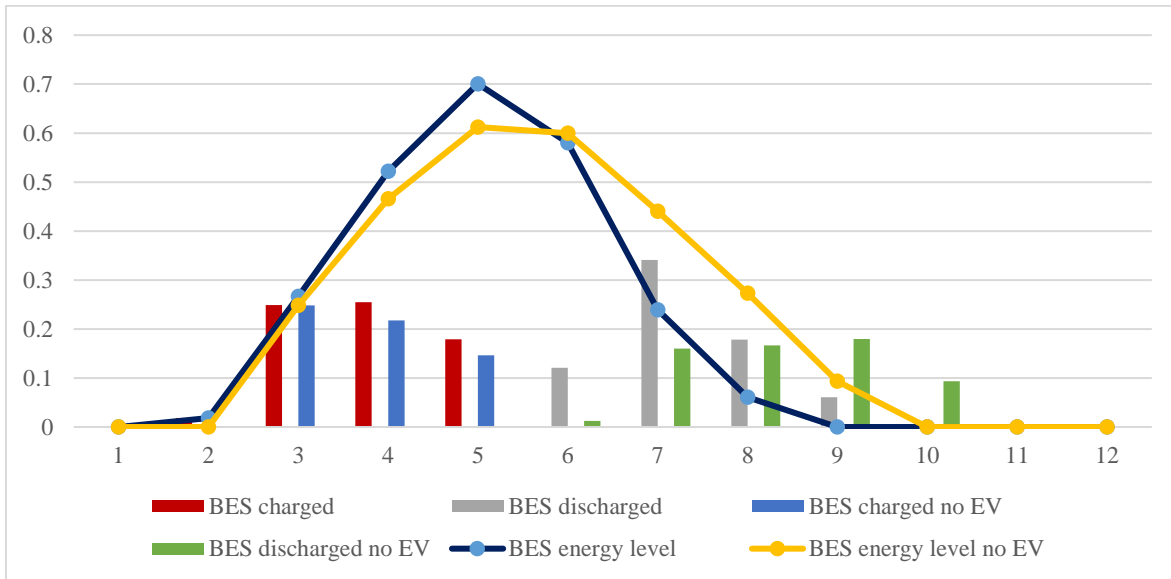


Fig. 6-15. BES performance in bus 3 for scenario No.3 compared to the base scenario (no EV)

The total loss of the system has been given by Fig. 6-16. As it is seen, the increase in fast charging EV employment can significantly increase the EDS power loss as it involves more sudden increasing load patterns over time. This is seen in the total loss of scenario No.1 which has a considerably higher value compared to scenarios NO.2 and 3. This figure shows that the matter of coordinate charging of EVs becomes more vital as the number of fast charging EVs increases.

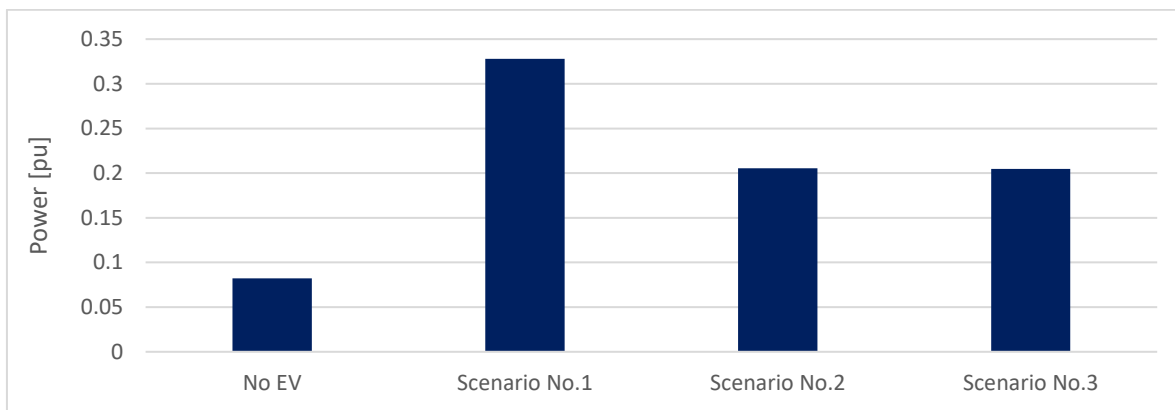


Fig. 6-16. Total power loss of the system for each scenario

As it was shown in Chapter 4, the reactive power controllability of the energy management model was useful for voltage control and reducing the deviations of the voltage over time. However, the value of reactive power injected to the network, through inverters connecting PV and WT to the grid, was limited to the total capacity of inverters according to equation (4) in Chapter 4. Therefore, if reactive power is required, the inverter reasonably curtails a portion of RES generation to enable some capacity for injecting reactive power to the network. However, if more active power is required by the load, such as EV loads, the inverter reasonably injects more reactive power as required by the load. This means at the presence of more reactive power demand, the capacity of inverter becomes less for injecting reactive power. This has been shown by Fig. 6-17 and Fig. 6-18 where the EV demand requires more active power and therefore, the capacity of inverters for injecting reactive power becomes less than the base scenario where inverters have enough capacity to inject more reactive power to network.

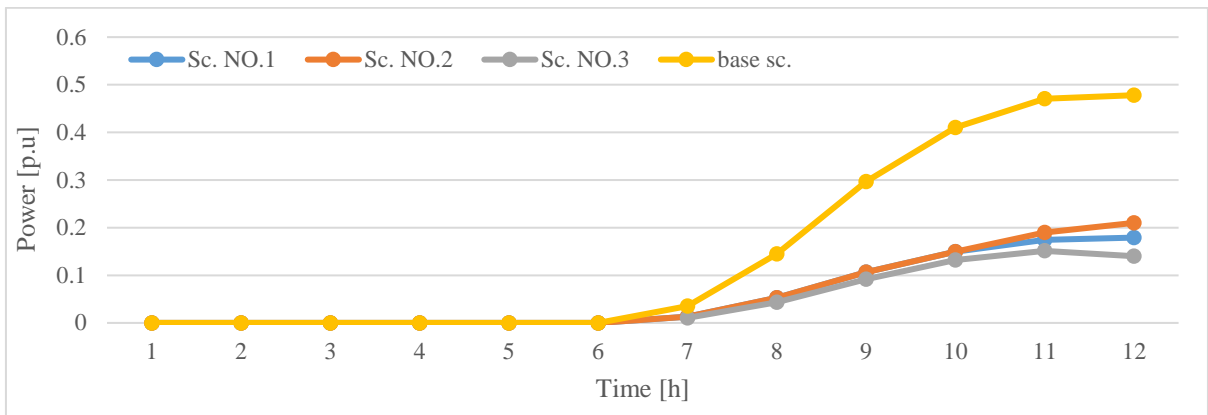


Fig. 6-17. Injected reactive power from PV system

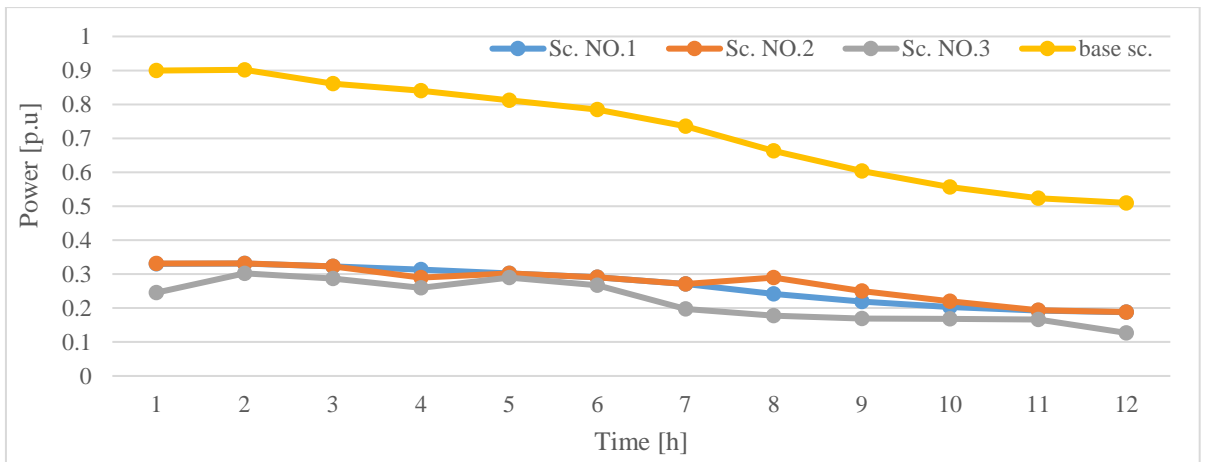


Fig. 6-18. Injected reactive power from WT system

The increase in active power of PV and WT system is shown in Fig. 6-19 and Fig. 6-20. As it is seen, the value of injected active power has reduced in the base scenario to inject more reactive power which is due to the less demand of active power in base scenario (No EV demand in base scenario). However, in all other scenarios all the active power of both PV and WT system has been injected to the network as more active power is required at the presence of EVs.

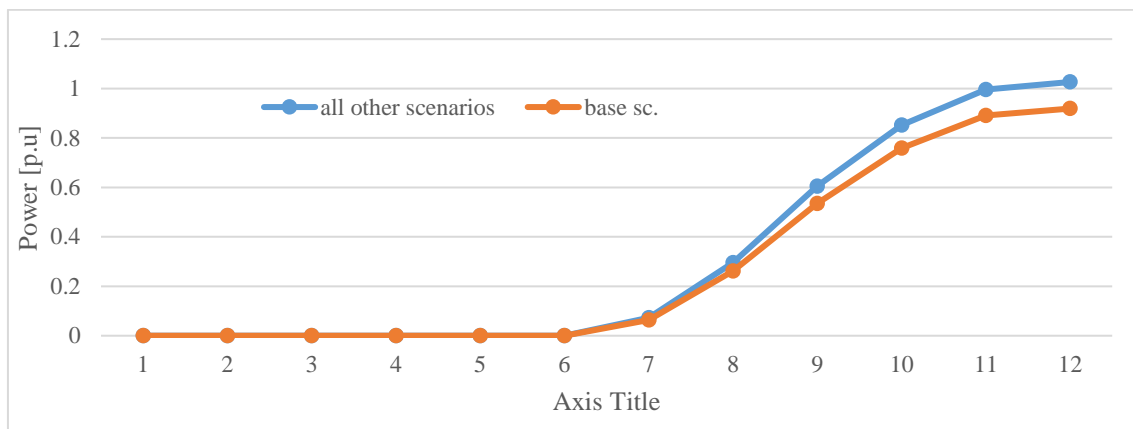


Fig. 6-19. Injected active power of PV to the grid

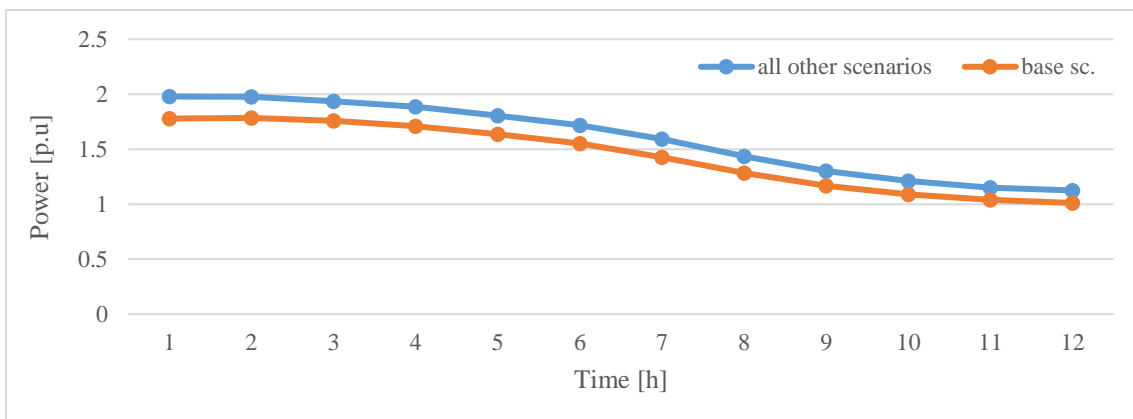


Fig. 6-20. Injected active power of WT to the grid

6.7. Conclusion

This chapter presented an investigation on the effects of EV employment on distribution system. In particular, the energy management of EDS was conducted based on the proposed directly solvable energy management model at the presence of RES, BES, and EVs. As it was shown the power loss of the system increased as the number of fast-charged EVs increases which is because of the higher demand of these vehicles in a shorter period. Moreover, it was observed

that the employment of EVs also affects the reactive power injection by RES and BES inverters. As it was shown in the results, the value of injected active power reduced in the base scenario to inject more reactive power which was due to the lower demand of active power in base scenario (No EV demand in base scenario). However, in all other scenarios, all the active power of both PV and WT system was injected to the network as more active power was required at the presence of EVs.

The observations of this chapter showed that the employment of EVs can significantly affect the EDS total power loss, reactive power controllability, and voltage deviations.

7. Conclusion

The aims and objectives of this thesis was to investigate the effects of EV employment of EDS operation variables such as voltage and power loss. In order to do these following aims were developed and introduced:

- Providing an efficient energy management for electricity distribution system by coordinated integration of RES and BES systems at the presence of EVs.
- Maximizing/Minimizing the integration/curtailment of renewable energy sources (RESs) in electricity distribution system.
- Minimizing the overall system cost.
- Providing immunized solutions against the uncertainties associated with RES generation.

To do so, following contributions were introduced:

- Contribution 1: A novel directly solvable set of power flow equations,
- Contribution 2: A general multi-objective energy management model for inverter-based integration of RES, and BES system,
- Contribution 3: Integration of EV loading into the energy management model and investigating the effects of EV charging on EDS voltage and power loss,
- Contribution 4: A new robust optimization model to characterize uncertainties of RESs employing block coordinate decent method.
- In Chapter 3, the directly solvable power flow model was introduced. The new directly solvable EDS power flow model did not need iterative metaheuristic algorithms to solve the power flow which was the main reason to be able to merge into any type of EDS study concerning power flow. The efficiency of the proposed power flow model was validated

by comparing the obtained results to those of the FBS method.

- In Chapter 4, the energy management model for EDS was developed based on the merged power flow equations from Chapter 3. Moreover, the inverter-based operation of RES and BES systems was enabled in the proposed energy management model to provide more efficient solutions. It was shown that slow charging patterns can result in more smooth EV load patterns and vice versa.
- In Chapter 5, the EV loading patterns were modeled through probability density functions to form a loading profile over 12 operating hours in EDS. This data was then used in Chapter 6 where the BCD robust optimization approach was used to solve the proposed energy management model at the presence of BES, RES, and EVs. Moreover, the uncertainties of RESs were applied in the robust model. By extending the application of BCD technique to solve the two-level max-min sub-problem (resulted from the C&C generation technique), it was possible for the first time to characterize BES charging/discharging status in the inner max-min problem to be obtained after uncertainty realizations, resulting in more practical/realistic solutions. Note that, this feature was not applicable in conventional dual-based robust models in the literature.

According to the observations further studies can be conducted on optimal integration of EVCSs in EDS operation using the proposed energy management model.

8. Published Studies Employing the Proposed Robust and BCD Robust Optimization Models

8.1 Application No. 1

Journals & Magazines > IEEE Transactions on Industry... > Volume: 57 Issue: 4

Adaptive Robust Recourse-Based Bidding Strategy and Capacity Allocation of PV-WT-BES Owning Prosumers Under Uncertainties

Publisher: IEEE

Cite This

PDF

Mehrdad Aghamohamadi  ; Amin Mahmoudi  ; Mohammed H. Haque  [All Authors](#)

187
Full
Text Views



Adaptive Robust Recourse-based Bidding Strategy and Capacity Allocation of PV-WT-BES Owning Prosumers under Uncertainties

Abstract - This paper presents an adaptive robust co-optimization for capacity allocation and bidding strategy of a prosumer equipped with photovoltaic system (PV), wind turbine (WT), and battery energy storage (BES). The uncertainties of load and PV/WT productions are modeled through controllable user-defined polyhedral uncertainty sets. The proposed co-optimization determines the optimal capacity of PV-WT-BES, while, maximizing prosumer's benefit by 1) optimal self-scheduling of PV-WT-BES, and 2) effective interactions with grid through optimal buying/selling bids under uncertainties. In previous min-max-min robust models, it was not possible to characterize bidding strategy binary variables as recourse decisions which was due to

the use of duality theory in solving the inner max-min problem (duality theory is weak and non-tractable in the presence of binary variables). In this study, Block Coordinate Descent (BCD) method is used to solve the inner max-min problem by means of Taylor series instead of transforming it into a single-level max problem by duality theory. As a result, prosumer's bidding status (indicated by binary variables) can be successfully modeled as recourse decisions which makes the obtained solutions more realistic and robust. Linearization of the dualized inner problem is also avoided as Lagrange multipliers are eliminated. A post-event analysis is developed to avoid over/under conservative solutions and to determine the optimal robust settings of the model. A comprehensive case study is conducted for an industrial prosumer. To illustrate the effectiveness of the proposed BCD robust model, its long-term performance is compared with conventional dual-based models in the literature. Results show 10% long-term cost reductions when using the proposed model under uncertainties.

Index Terms— Battery storage system, Block coordinate descent, Capacity optimization, Prosumer, Robust optimization, Renewable energy.

NOMENCLATURE

A. Indices

c	Index of iterations in C&C methodology.
d/t	Index of day/hour.
n	Index of BES replacements.
s	Index of post-event trial scenarios.
z	Index of iterations in BCD methodology.

B. Parameters

A_{max}	Maximum number of PV units.
B_{max}	Maximum number of BES units.
C^{pv}	Price of each PV unit.
C^w	Price of each WT unit.
C_n^{bat}	Price of each BES unit with the capacity of E' .
E^l	BES losses in each scheduling time step.
E^{int}	Initial SOC for each BES unit.
E'_{min}	Minimum allowable energy for each BES unit.
E'	Capacity of each BES unit.
$\bar{L}_{dt}/\tilde{L}_{dt}$	Forecasted/Uncertain load in hour t of day d .
$L_{dt}^{dev\pm}$	Deviations of \tilde{L}_{dt} .
$\hat{L}_{dt}^{dev\pm}$	Maximum value of $L_{dt}^{dev\pm}$.
\check{L}_{dts}	Load in sth post-event trial scenario.
M	Sufficiently large constant.
N_X	Number of start-up variables in vector \mathbf{X} .
$N_{\tilde{U}}$	Number of uncertain parameters in vector $\tilde{\mathbf{U}}$.
N_Y	Number of operation variables in vector \mathbf{Y} .
$\bar{P}_{dt}^v/\tilde{P}_{dt}^v$	Forecasted/Uncertain generation for each PV unit.
\check{P}_{dts}^v	PV generation in sth post-event trial scenario.
$\bar{P}_{dt}^w/\tilde{P}_{dt}^w$	Forecasted/Uncertain generation for each WT unit.
\check{P}_{dts}^w	WT generation in sth post-event trial scenario.
$P_{dt}^{v,dev\pm}/P_{dt}^{w,dev\pm}$	Deviations of $\tilde{P}_{dt}^v/\tilde{P}_{dt}^w$.

$\hat{P}_{dt}^{dev\pm} / \hat{P}_{dt}^{wdev\pm}$	Maximum value of $P_{dt}^{vdev\pm} / P_{dt}^{wdev\pm}$.
$P_{min}^{in} / P_{max}^{in}$	Minimum/Maximum allowable range of P_{dt}^{in} .
$P_{min}^{out} / P_{max}^{out}$	Minimum/Maximum allowable range of P_{dt}^{out} .
$P_{min}^{chg} / P_{max}^{chg}$	Minimum/Maximum allowable range of P_{dt}^{chg} .
$P_{min}^{dis} / P_{max}^{dis}$	Minimum/Maximum allowable range of P_{dt}^{dis} .
Q_n^{bat}	NPV coefficient for BES replacements.
Q^{sys}	NPV coefficient for annual values.
T	Number of scheduling time periods in each day.
W_{max}	Maximum number of WT units.
y	Maintenance cost as a percentage of CAPEX.
π_{dt}	Electricity price in hour t of day d .
$\eta^{cc} / \eta^{inv} / \eta^{con}$	Efficiency of charge controller/inverter/converter.
η^{chg} / η^{dis}	Charging/discharging efficiency of BES.
θ	Feed-in tariff price for electricity export to network.
C. Sets	
Ξ^C	Set of iterations in C&C methodology.
Ξ^D	Set of days.
Ξ^I / Ξ^{II}	Set of "here-and-now"/"wait-and-see" variables.
$\Xi^N / \Xi^T / \Xi^{US}$	Set of BES replacements/operational hours/uncertainties.
D. Variables	
A	Integer variable indicating the number of PV units.
A^c	Fixed value of A in sub-problem at iteration c .
B	Integer variable indicating the number of BESs.

B^c	Fixed value of B in sub-problem at iteration c .
E_{dt}	Battery SOC in hour t of day d .
P_{dt}^{in}	Imported electricity from network in hour t of day d .
P_{dt}^{out}	Exported electricity to network in hour t of day d .
P_{dt}^h	Inverter output power in hour t of day d .
P_{dt}^s	Inverter input power in hour t of day d .
P_{dt}^w	Generated electricity by WT units in hour t of day d .
P_{dt}^v	Generated electricity by PV units in hour t of day d .
P_{dt}^{chg}	BES charging power in hour t of day d .
P_{dt}^{dis}	BES discharging power in hour t of day d .
W	Integer variable indicating the number of WT units.
W^c	Fixed value of W in sub-problem at iteration c .
x_{dt}^{in}/x_{dt}^{out}	Binary variable indicating energy importing/exporting status in hour t of day d .
$x_{dt}^{chg}/x_{dt}^{dis}$	Binary variable indicating charging/discharging status of BES in hour t of day d .
$x_{dt}^{L\pm}$	Indicator for deviation of \tilde{L}_{dt} .
$x_{dt}^{v^{dev\pm}}/x_{dt}^{w^{dev\pm}}$	Indicator for deviations of $\tilde{P}_{dt}^v/\tilde{P}_{dt}^w$.
$\alpha_{dt}^{chg}/\alpha_{dt}^{dis}$	Axillary variables.
Λ_I	Value of master problem.
Λ_{II}	Value of first-stage sub-problem.
Λ_{III}	Value of second-stage sub-problem.
Υ	Auxiliary continuous variable.
Ψ	Uncertainty budget.

E. Vectors/Matrices

A, F	Coefficient matrices of objective function.
$B, C, E, G, H/D, K$	Coefficient/requirement vectors.
\bar{U}	Vector of forecasted value of uncertain parameters.
U^{dev+}/U^{dev-}	Vector of positive/negative deviation of \bar{U} .
\tilde{U}	Vector of uncertain parameters.
X/Y	Vector of sizing/scheduling variables.
X^c/Y_c	X/Y at iteration c of the C&C method.
U^c	Worst-case realization of uncertain parameters in sub-problem to be send to master problem as fixed values.
U^z	Obtained worst-case realization of uncertain parameters in second-stage sub-problem.
μ	Vector of dual variables.

I. INTRODUCTION

A. *problem description*

Renewable energy sources (RESs) are boosting the evolution of energy systems worldwide [121]. The huge share of solar photovoltaic systems (PVs) as well as small-scale wind turbine (WT) employments have introduced some unexpected challenges such as energy imbalance, extra costs, and out-of-bid penalty allocations for RES-based prosumers [122]. To cope, battery energy storage (BES) systems have been employed by prosumers to a) provide more flexibility in market participation, and b) avoid out-of-bid power trades with upstream network [123-125]. Although, the integration of PV, WT and BES (PV-WT-BES) can provide a promising operational status, the arbitrage ability of prosumers cannot be fully exploited if their bidding strategy is scheduled

regardless of uncertainty realizations. This is because, the associated costs/benefits of the system are considered in the long-term planning such as capacity allocation solutions. Therefore, if the short-term schedule is obtained with no uncertainty characterization, the obtained capacity allocation solutions would not be exact and practical and may result in extra costs for both short-term and long-term performance of the system. Therefore, further studies are required to provide realistic solutions for capacity allocation and bidding strategies of PV-WT-BES systems, considering the cross effects between short-term and long-term planning of such a system. In fact, the bidding strategies need to be modeled as recourse decisions after uncertainty realizations to be practical [126]. However, this is not applicable in the current robust optimization approaches as characterizing binary recourse variables (indicating buying/selling bids) is impossible due to the use of duality theory in these approaches. This is because, dual of a mixed-integer model is generally weak, non-tractable and complicated [35]. Accordingly, the optimality of PV-WT-BES sizing solutions becomes questionable as it depends on the benefits associated with bidding strategy [127].

Therefore, further uncertainty modeling approaches are required to model prosumer's bidding strategies as recourse decisions to be obtained after uncertainties, resulting in more practical and realistic operation and capacity allocation solutions.

B. Background

Partial study has focused on characterizing uncertainties with sizing and bidding strategy of PV-WT-BES owning prosumers. Uncertainties of PV/WT generation and load were modeled by typical scenarios in [128]. Monte Carlo simulation was performed in [129] to model RES

uncertainties through scenario generation. Uncertainties of wind production were captured by probability density functions in [130]. However, scenario-based models [128, 129] and the probabilistic model of [130] require a full distributional knowledge of uncertain parameters which may not be easily available in practice [7]. To obtain more reliable solutions, optimal sizing of a PV-battery system was modeled through stochastic programming (SP) in [131]. SP was employed to model the uncertainties of solar radiation, wind, and load in BES sizing approach in [132]. In [133] the bidding strategy of a virtual power plant was conducted under a considerable number of uncertainty realization scenarios for electricity price and electric vehicle behavior through SP. The uncertainty of electricity price was characterized through SP in [134]. Despite the advantages of the aforementioned SP models, they are subject to a high computation time which is due to the huge number of uncertainty scenarios. To cope, a backward scenario reduction method was employed in [135] to decrease the computation time. Although, scenario reduction can accelerate the computation time in SP but it faces the lack of tractability which is due to the required distributional knowledge of uncertain scenarios, especially, when several uncertain parameters are considered and a proper level of feasibility against different uncertainty realizations is required (this may not be practical in practice) [136]. Moreover, if the uncertain parameters deviate from scenarios, performance of SP cannot be guaranteed. This issue is also true for Monte-Carlo and probabilistic methods.

To cope with the mentioned problems, robust optimization (RO) has been employed in some recent studies to characterize uncertainties [111]. The advantage of RO is that RO models the uncertainties by worst-case realization through bounded intervals, eliminating the need of scenario generation and distributional knowledge of the uncertain parameters [34, 112].

Therefore, the obtained solutions would be feasible as long as the uncertainty realizations are within the user-defined bounded intervals, which makes it more reliable/practical than scenario-based and SP models in the literature.

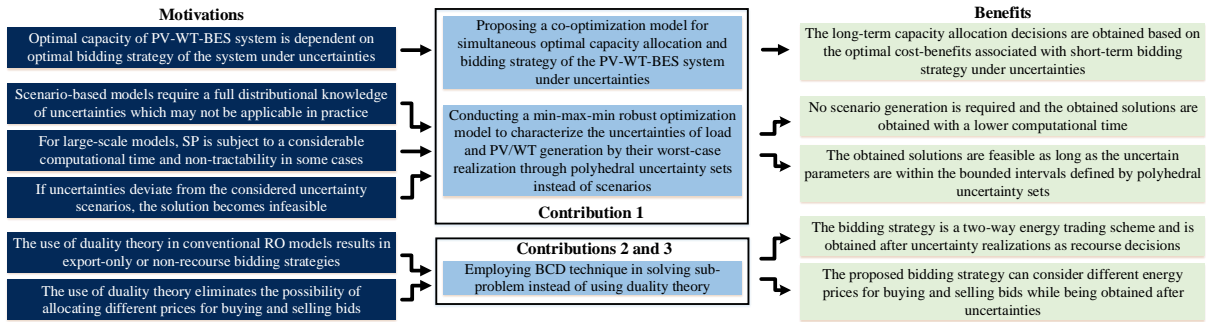


Fig. 1. Motivations, contributions, and benefits of the proposed model.

However, RO still faces some limitations in modelling uncertainties which is due to the use of duality theory in solving it (duality theory is used in min-max-min RO problems to transform the inner bi-level max-min problem into a solvable single-level max problem). A Robust bidding strategy was proposed for a wind farm coupled with a storage system in [113]. However, binary variables, indicating buying/selling bids, were eliminated in the model to ease the employment of duality theory. This results in export-only bidding which is not applicable in practice. Duality theory was also employed in [114] to solve a robust model predictive control-based bidding strategy for a wind-storage systems. However, the model of [114] was a single-stage max-min problem only. Bidding binary variables were also eliminated in [115] to make it possible to conduct duality. Accordingly, it was not possible to consider both buying and feed-in-tariff for day ahead bids in [115] as no binary variable was used to separate buying/selling status. This becomes important when the feed-in tariff is different than the buying price. To be more realistic,

the buying/selling status of bidding strategy was modeled by binary variables in [116]. However, the buying/selling status was characterized before uncertainty realizations to be able to conduct duality theory with no binary variables involved. Similar to [116], the buying/selling status of prosumer was modeled before uncertainty realizations in [117-119].

Note that, the mentioned RO studies in the literature have considered the uncertainties in their models and their solutions have proven to be more efficient than the deterministic approaches. However, the bidding binary variables have been eliminated or modeled in the master problem. As a result, the worst-case realization of uncertainties is determined when these variables are fixed in the sub-problem and therefore, these variables are not affecting the sub-problem's objective function. In other words, these variables are obtained based on the primal cuts, containing the worst-case realization of uncertainties in the master problem and have no accountability in determining the worst-case realization itself. This means that, the sub-problem is solved without considering the cross effects between bidding strategy and uncertainties. Therefore, the benefit of robust optimization has not been fully exploited.

C. Motivations

Ignoring the effects of uncertainties on bidding strategy, (determining buying/selling status before uncertainty realizations but not as recourse decisions to be obtained after uncertainty realization) is not realistic, as in practice, the bidding strategy should be modified when uncertainties of renewables and load arise. This also affects the system sizing solution as it is based on the benefits arisen from bidding strategies (Prosumer's benefit is directly dependent on the optimality of the bidding strategy). Based on the literature therefore, there is a lack of

viability in the existing robust bidding strategies which is due to the following reasons:

1) Probabilistic, Scenario-based, and SP models may become infeasible and non-tractable in complex and large-scale cases.

2) In some RO studies, bidding binary variables were eliminated to enable the application of duality theory. This results in export-only bidding and non-flexible feed-in tariff pricing.

3) Although, bidding binary variables were modeled in some recent RO studies, these variables were characterized before uncertainty realizations so the duality could be conducted with no binary variables involved. Therefore, the bidding solutions were obtained ignoring the uncertainties.

D. Contributions

This paper is a continuation of an earlier work [137] in which duality theory was conducted to solve the inner max-min problem. Regarding the three aforementioned drawbacks of employing duality theory in the previous subsection (C. Motivations), the following contributions are presented in the proposed model:

1) A robust sizing/scheduling co-optimization is proposed for a PV-WT-BES owning prosumer which determines the optimal system capacity while maximizing the prosumer's benefits by optimal scheduling of PV-WT-BES system and effective electricity buying/selling bids. To overcome the problems in scenario-based and SP models, a min-max-min adaptive robust optimization is developed to characterize the uncertainties of prosumer's load and PV/WT generation by polyhedral uncertainty sets instead of scenarios. The problem is solved through a

decomposition methodology and a column-and-constraint (C&C) generation technique [34], recasting the tri-level problem into a first-stage min problem and a second-stage max-min problem. Since the proposed RO model characterizes uncertainties by their worst-case realization, there is no need to scenario generation nor the distributional knowledge of uncertainty scenario. Therefore, the obtained RO solutions are feasible as long as the uncertainties are within bounded intervals of polyhedral uncertainty sets.

TABLE I. Advantages of the proposed model compared to the literature

Reference No.	Uncertainty modelling approach	Consideration of RES/BES	Recourse-based BES operation	Recourse-based bidding	Scheduling strategy	Capacity allocation
[9]	Scenario-based	PV/WT/BES	×	×	×	✓
[10]	Scenario-based	PV/WT/BES	×	×	✓	✓
[11]	Scenario-based	WT/BES	×	×	×	✓
[13]	SP	PV/BES	×	×	✓	✓
[14]	SP	PV/WT/BES	×	×	✓	✓
[15]	SP	PV/BES	×	✓	✓	×
[16]	SP	PV/WT/BES	✓	×	✓	×
[17]	SP	PV/WT/BES	✓	✓	✓	×
[18]	Scenario-based	PV/BES	×	×	✓	×
[19]	Dual-based RO	WT	×	×	✓	×
[20]	Dual-based RO	-	×	×	✓	×
[22]	Dual-based RO	WT/BES	×	×	✓	×
[23]	Dual-based RO	WT/BES	×	×	✓	×
[24]	Dual-based RO	PV/BES	×	×	✓	✓
[25]	Dual-based RO	WT/BES	×	×	✓	×
[26]	Dual-based RO	PV/BES	×	×	✓	×
[27]	Dual-based RO	WT/BES	×	×	✓	×
[28]	Dual-based Affinely RO	PV/BES	×	×	✓	×
Proposed model	BCD robust	PV/WT/BES	✓	✓	✓	✓

2) The proposed RO model employs Block Coordinate Descent (BCD) method [120], which approximates the worst-case realization of uncertainties by means of Taylor series instead of

transforming the inner max-min problem into a single max problem by duality theory. BCD was originally devised to deal with single-level problems. By extending the application of BCD technique to solve the two-level max-min sub-problem (resulted from the C&C generation technique), it is possible to avoid duality theory in solving the sub-problem. Since, dual of a mixed-integer model is generally weak, non-tractable and complicated [35], the extension of BCD technique instead of duality theory eliminates the limitation in considering binary variables in the max-min sub-problem. As a result, uncertainty-dependent binary variables such as buying/selling bids and BES charging/discharging statuses can be obtained after uncertainty realization in the sub-problem as recourse decisions, which was not applicable in previous dual-based RO models in the literature. This results in more system flexibility in compensating the uncertainty effects such as PV/WT shortage or sudden increase in load.

3) Since, no duality is conducted, prosumer's power trading with upstream network can be freely modeled with binary indicators, resulting in a two-way power trading scheme instead of an export-only bidding strategy such as [113]. Followed with the same reason, it can model both buying and selling bids with different buying and feed-in tariff prices. To the best of authors' knowledge, this is the first application of min-max-min robust optimization in which binary variables are modeled in the inner max-min problem. The motivations, contributions, and the associated benefit with each contribution are summarized in Fig. 1. Note that, the proposed model in this study is called "BCD robust", hereafter.

E. Validation

The following validations are conducted in order to demonstrate the effectiveness of the

proposed BCD robust model:

1) The obtained BCD robust solutions are examined against a sufficiently large number of uncertainty realizations through a post-event analysis.

2) Long-term performance of the optimal BCD robust solutions is compared to the solutions obtained based on conventional dual-based robust models such as [116-119] in which bidding strategy decisions are made prior to uncertainties.

F. Significance compared to the literature

The advantages of the proposed BCD robust co-optimization model are compared to the previous models in the literature in Table I. As it is seen, only some SP models, i.e., [15-17], have considered recourse-based bidding and BES operation which is due to the fact that SP does not involve duality in its solving methodology. However, no capacity allocation was considered in these studies. Moreover, SP may become infeasible and non-tractable in complex and large-scale cases (See Section I.A). In particular, the advantages of the proposed BCD robust co-optimization model are as follows:

It considers the correlation between optimal bidding strategy of the system and its capacity allocation, which is more practical than considering these problems individually,

There is no need to scenario generation techniques as robust optimization is used instead of SP which characterizes uncertainties by their worst-case realization,

Due to the employment of BCD technique instead of duality theory in solving the inner max-

min sub-problem, it is possible to model bidding variables as well as BES variables as recourse decisions after uncertainty realization which is more realistic in practice.

Since there is no limitation in modelling recourse-based binary variables in the proposed BCD model, it is also possible to have two-way bidding with different buying/selling prices, while, these variables are obtained as recourse decision which was not possible in conventional dual-based models.

II. DETERMINISTIC PV-WT-BES SIZING/OPERATION MODEL

Fig. 2 represents the configuration of PV-WT-BES system, its interactions with upstream network, and the energy flow through each element, as per the notations in nomenclature. The inverter in Fig. 2 is responsible for synchronizing the injected power to the network. The objective of the deterministic model is to minimize system costs that includes capital expenditures (CAPEX), operational & maintenance expenditures (OPEX), and energy costs. The proposed deterministic model is formulated as (1).

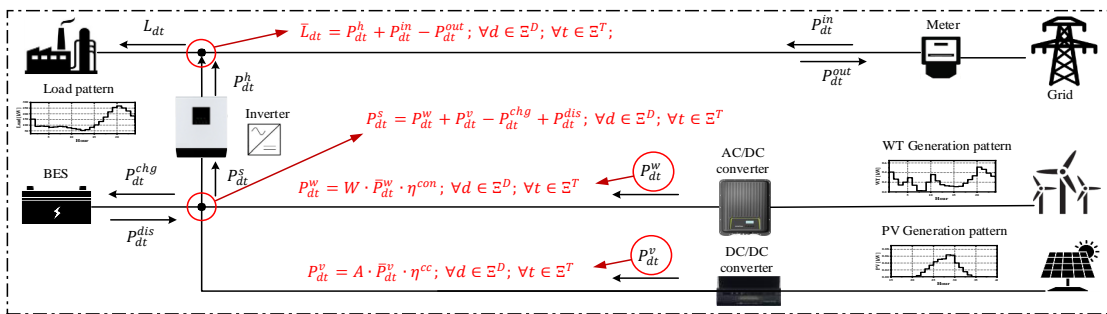


Fig. 2. Considered PV-WT-BES configuration and its energy flow.

$$\begin{aligned} & \text{M1= NPV of System CAPEX} \\ \text{Min } & \overbrace{A \cdot C^{pv} + W \cdot C^w + \sum_{n \in \Xi^N} B \cdot C_n^{bat} \cdot Q_n^{bat}} + \\ & \overbrace{y \cdot Q^{sys} \cdot (A \cdot C^{pv} + W \cdot C^w + B \cdot C_{n=1}^{bat})}^{\text{M2= NPV of maintenance costs}} + \overbrace{Q^{sys} \cdot \sum_{d \in \Xi^D} \sum_{t \in \Xi^T} (P_{dt}^{in} \cdot \pi_{dt} - P_{dt}^{out} \cdot \theta)}^{\text{M3= NPV of energy costs}}; \end{aligned} \quad (1a)$$

s.t.

AC/DC Power flow constraints:

$$\bar{L}_{dt} = P_{dt}^h + P_{dt}^{in} - P_{dt}^{out}; \forall d \in \Xi^D; \forall t \in \Xi^T; \quad (1b)$$

$$P_{dt}^h = P_{dt}^s \cdot \eta^{inv}; \forall d \in \Xi^D; \forall t \in \Xi^T \quad (1c)$$

$$P_{dt}^s = P_{dt}^w + P_{dt}^v - P_{dt}^{chg} + P_{dt}^{dis}; \forall d \in \Xi^D; \forall t \in \Xi^T \quad (1d)$$

PV/WT generation constraints:

$$P_{dt}^v = A \cdot \bar{P}_{dt}^v \cdot \eta^{cc}; \forall d \in \Xi^D; \forall t \in \Xi^T \quad (1e)$$

$$P_{dt}^w = W \cdot \bar{P}_{dt}^w \cdot \eta^{con}; \forall d \in \Xi^D; \forall t \in \Xi^T \quad (1f)$$

BES operational constraints:

$$E_{dt} = E_{d(t-1)} + \left(P_{dt}^{chg} \cdot \eta^{chg} - P_{dt}^{dis} \cdot \frac{1}{\eta^{dis}} \right) \cdot \Delta t \quad (1g)$$

$$-E^l \cdot B; \forall d \in \Xi^D; \forall t \in \Xi^T$$

$$\sum_{t \in \Xi^T} \left(P_{dt}^{chg} \cdot \eta^{chg} - P_{dt}^{dis} \cdot \frac{1}{\eta^{dis}} \right) = E^l \cdot B \cdot T; \forall d \in \Xi^D \quad (1h)$$

$$E_{d(t=0)} = E^{int} \cdot B; \forall d \in \Xi^D \quad (1i)$$

$$P_{min}^{chg} \cdot \alpha_{dt}^{chg} \leq P_{dt}^{chg} \leq P_{max}^{chg} \cdot \alpha_{dt}^{chg}; \forall d \in \Xi^D; \forall t \in \Xi^T \quad (1j)$$

$$P_{min}^{dis} \cdot \alpha_{dt}^{dis} \leq P_{dt}^{dis} \leq P_{max}^{dis} \cdot \alpha_{dt}^{dis}; \forall d \in \Xi^D; \forall t \in \Xi^T \quad (1k)$$

$$-M \cdot x_{dt}^{chg} \leq \alpha_{dt}^{chg} \leq M \cdot x_{dt}^{chg}; \forall d \in \Xi^D; \forall t \in \Xi^T \quad (1l)$$

$$B - M \cdot (1 - x_{dt}^{chg}) \leq \alpha_{dt}^{chg} \leq B + M \cdot (1 - x_{dt}^{chg}); \quad (1m)$$

$$\forall d \in \Xi^D; \forall t \in \Xi^T$$

$$-M \cdot x_{dt}^{dis} \leq \alpha_{dt}^{dis} \leq M \cdot x_{dt}^{dis}; \forall d \in \Xi^D; \forall t \in \Xi^T \quad (1n)$$

$$B - M \cdot (1 - x_{dt}^{dis}) \leq \alpha_{dt}^{dis} \leq B + M \cdot (1 - x_{dt}^{dis}); \quad (1o)$$

$$\forall d \in \Xi^D; \forall t \in \Xi^T$$

$$E'_{min} \cdot B \leq E_{dt} \leq B \cdot E'; \forall d \in \Xi^D; \forall t \in \Xi^T \quad (1p)$$

$$x_{dt}^{chg} + x_{dt}^{dis} \leq 1; \forall d \in \Xi^D; \forall t \in \Xi^T \quad (1q)$$

Upstream network interaction constraints:

$$P_{min}^{in} \cdot x_{dt}^{in} \leq P_{dt}^{in} \leq P_{max}^{in} \cdot x_{dt}^{in}; \forall d \in \Xi^D; \forall t \in \Xi^T \quad (1r)$$

$$P_{min}^{out} \cdot x_{dt}^{out} \leq P_{dt}^{out} \leq P_{max}^{out} \cdot x_{dt}^{out}; \forall d \in \Xi^D; \forall t \in \Xi^T \quad (1s)$$

$$x_{dt}^{in} + x_{dt}^{out} \leq 1; \forall d \in \Xi^D; \forall t \in \Xi^T \quad (1t)$$

Allowable sizing limitation constraints:

$$A \leq A_{max}; \quad (1u)$$

$$B \leq B_{max}; \quad (1v)$$

$$W \leq W_{max}; \quad (1w)$$

The objective function (1a) involves three terms M1, M2 and M3. Term M1 minimizes the net present value (NPV) of CAPEX which includes the cost of PV-WT-BES installation and replacement during the planning horizon. The inverter cost has been considered as a part of BES cost, while, the charge controller and converter costs are considered as a part of PV and WT costs, respectively.

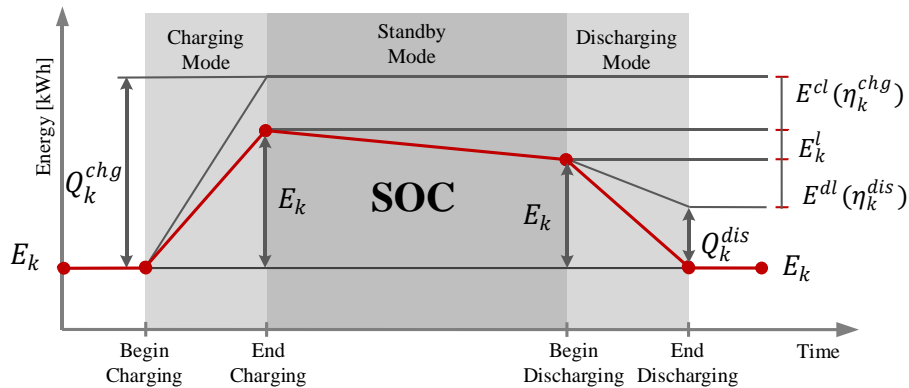


Fig. 3. Dynamic changes of state-of-charge (SOC) of BES

The NPV of annual OPEX, includes maintenance costs, i.e., M2, and energy cost, i.e., M3. M2 represents a pre-determined percentage of PV-WT-BES installation cost, excluding

replacement costs, while the annual energy costs including electricity buying/selling bids are optimized through M3. In fact, M3 maximizes the annual benefits of PV-WT-BES through its interactions with grid.

The objective function is subject to constraints (1b)-(1w). The power flow through the PV-WT-BES system is expressed by constraints (1b)-(1f) (see Fig. 2). Accordingly, constraint (1b) represents the AC power flow between inverter, load, and upstream grid. The power flow through the inverter is modeled by (1c). The DC power flow between inverter, BES charging/discharging, and PV-WT system is also given by constraint (1d). Note that the assumed configuration for PV panels is parallel. Therefore, the total generated power is calculated by (1e), regarding the number of installed PV panels (i.e., A) with the capacity of \bar{P}_{dt}^v . Constraint (1f) presents the available power outputs for WT, considering the number of installed units (i.e., W) with the capacity of \bar{P}_{dt}^w . Constraints (1b), (1d) and (1e)-(1f) are shown in Fig. 2 along with the related junction points.

The dynamic behavior of BES and its SOC has been illustrated in Fig. 3. As it is shown, the charging and discharging status are subject to loss of energy, i.e., E^{cl} and E^{dl} , respectively, which is due to the storage efficiency in charging/discharging mode. Moreover, each storage is subject to steady-state mode losses. Accordingly, the dynamic energy balance for storage k representing battery state-of-charge (SOC) is expressed by (1g). At the final operational time period, BES must have the same SOC as the first time period which is known as end-coupling constraint and is expressed by (1h). Note that, Δt in (1g) is 1 hour. Constraint (1i) indicates the initial SOC of battery at the first operating period of each daily operation horizon which is

provided at the last operation period of the previous day. The BES charging and discharging rates are limited to the allowable ranges by constraints (1j) and (1k), respectively. Note that constraints (1j) and (1k) represent the allowable charging and discharging rate of the entire battery bank. Therefore, the number of BESs in the battery bank must be multiplied with the binary variables x_{dt}^{chg} and x_{dt}^{dis} to represent the maximum/minimum allowable ranges for the battery bank (P_{max}^{chg} , P_{min}^{chg} , P_{max}^{dis} , P_{min}^{dis} account for each individual BES). To avoid non-linearity (products of $x_{dt}^{chg}/x_{dt}^{dis}$ and B) big-M linearization technique is used to develop a linear model. Accordingly, auxiliary constraints (1l)-(1o) illustrate the linear relationship between BES charging/discharging rate and two other decisive variables including sizing variable B , as the available BES capacity, and binary variables x_{dt}^{chg} and x_{dt}^{dis} , indicating charging/discharging status of BES. Constraint (1p) limits the BES SOC to its minimum/maximum values with regard to the number of installed BESs (i.e., B) with the capacity of E' . The BES can either be charged, discharged, or out of operation at a time, regarding constraint (1q). Constraint (1r)/(1s) represents the allowable range of power trade through buying/selling bids by means of binary variables x_{dt}^{in}/x_{dt}^{out} . Constraint (1t) ensures that the prosumer can either buy or sell electricity at each operation time-step. If $x_{dt}^{in} + x_{dt}^{out} = 0$ means no energy trading is happened. Finally, the number of installed PV panels, WTs, and BESs are limited to their allowable ranges by constraints (1u)-(1w).

III. BCD ROBUST PV-WT-BES SIZING/SCHEDULING MODEL

As seen from the proposed deterministic model, the uncertainties associated with prosumer's load and PV/WT generation are ignored as they are substituted by their forecasts i.e., \bar{L}_{dt} , and $\bar{P}_{dt}^v/\bar{P}_{dt}^w$, in the deterministic model (1), respectively. Therefore, the obtained solutions from

solving this deterministic model would not be feasible if the uncertain parameters deviate from their forecasts. To have a reliable sizing/scheduling, these uncertainties have been characterized through a BCD robust model in this section.

In robust optimization, two main decisions are made including "here-and-now" decisions, which are obtained before any uncertainty realizations, and "wait-and-see" decisions, which are obtained after the realization of uncertain parameters. In this study, sizing variables including the number of PV panels, WTs, and BES units i.e., A , B , and W , respectively, are considered as "here-and-now" decisions which are obtained before uncertainty realizations. Since, the uncertainties associated with load demand and PV/WT productions are realized when scheduling PV-WT-BES system (after installation), the operation variables (i.e., all variables excluding sizing variables A , B , and W) are considered as "wait-and-see" decisions.

The compact form of the proposed BCD robust model is expressed through a tri-level min-max-min optimization problem as (2).

$$\text{Min}_{\mathbf{X} \in \Xi^I} (\mathbf{A}' \cdot \mathbf{X} + \text{Max}_{\tilde{\mathbf{U}} \in \Xi^{US}} \text{Min}_{\mathbf{Y} \in \Xi^{II}} \mathbf{F}', \mathbf{Y}) \quad (2a)$$

s.t.

$$\Xi^I = \{\mathbf{X} \in \{\mathbf{0}, \mathbf{1}\}^{N_x} \mid \mathbf{C}\mathbf{X} \geq \mathbf{D}\} \quad (2b)$$

$$\Xi^{US} = \{\tilde{\mathbf{U}} \in \mathbb{R}^{N_{\tilde{U}}} \mid \tilde{\mathbf{U}} = \bar{\mathbf{U}} + \mathbf{U}^{dev+} - \mathbf{U}^{dev-}\} \quad (2c)$$

$$\Xi^{II} = \{\mathbf{Y} \in \mathbb{R}^{N_Y} \mid \mathbf{E}(\mathbf{X}, \mathbf{Y}, \tilde{\mathbf{U}}) \geq 0\} \quad (2d)$$

In (2a), the outer min problem minimizes the objective function over the sizing variables

which are obtained as "here-and-now" decisions. The expression $A' \cdot X$ represents terms M1 and M2 of the objective function (1a) containing sizing decision variables. Therefore, outer min problem is subject to sizing constraints (1u)-(1w), compactly expressed by (2b). The inner max problem maximizes the remaining term of the objective function (i.e., term M3 expressed by F', Y) over the worst-case realization of uncertain parameters, while the inner min problem minimizes it over the operation variables, considered as "wait-and-see" decisions. Therefore, the inner max problem is subject to polyhedral uncertainty sets, expressed by (2c), while, the inner min problem is subject to the operation constraints, presented by (2d). In fact, (2d) represents the set of constraints (1b)-(1t).

A. Solution Methodology to Solve the Proposed Robust PV-WT-BES Sizing/Bidding Problem

The tri-level optimization problem in (2a) cannot be solved directly. Therefore, a decomposition methodology, by means of C&C technique [34], is employed to decompose the tri-level min-max-min problem to a single-level min problem and a bi-level max-min problem. The single-level min problem is called "master problem" and the bi-level max-min problem is called "sub-problem", hereafter. The proposed decomposition methodology is described through the following steps:

Step 1) The master problem is solved to determine "here-and-now" decision variables including PV, WT, and BES sizing solutions while being subject to sizing constraints only. Therefore, the objective function (3a) includes the terms M1, and M2 of the deterministic objective function (1a). Therefore, the objective function (3a) includes the terms M1, and M2 of

the deterministic objective function (1a). It is also subject to constraints (1u)-(1w) including sizing variables. The compact form of master problem is given by (3).

$$\min_{\mathbf{X} \in \mathbb{E}^I} \Lambda_I \equiv \mathbf{A}' \cdot \mathbf{X} + \mathbb{Y} \quad (3a)$$

s.t.

Sizing constraints:

$$\mathbf{C}\mathbf{X} \geq \mathbf{D}; \quad \mathbf{X} \in \{0, 1\}^{N_x} \quad (3b)$$

Primal cut constraints:

$$\mathbb{Y} \geq \mathbf{F}', \mathbf{Y}; \quad \mathbf{G} \cdot \mathbf{X} + \mathbf{B} \cdot \mathbf{Y}_c + \mathbf{H} \cdot \mathbf{U}^c \geq \mathbf{K}; \quad c \in \mathbb{E}^C \quad (3c)$$

In the above problem, (3a) presents the epigraph form of master problem which minimizes the "here-and-now" terms of objective function, i.e., \mathbb{Y} , while, being subject to sizing constraints in (3b) and primal cuts in (3c) which are delivered from the sub-problem in previous iteration of column-and-constraint methodology (if the first iteration, primal cuts are replaced by constraints of the deterministic model). After achieving a solution in master-problem, the obtained "here-and-now" variables, i.e., \mathbf{X} (representing A , B and W), are sent to the sub-problem as fixed values to determine both "wait-and-see" decision variables, i.e., PV-WT-BES scheduling/bidding variables, and the new worst-case realization of uncertain parameters.

Step 2) Given the obtained sizing decision variables, sub-problem is solved to determine operation decision variables (including system scheduling and prosumer's bidding strategy) and worst-case realization of uncertain parameters. The vector of the fixed "here-and-now" variables

is shown by X^c in the sub-problem which is given by (4).

$$\text{Max}_{\bar{U} \in \Xi^{US}} \text{Min}_{Y \in \Xi^{II}} F', Y \quad (4a)$$

s.t.

PV-WT-BES operation constraints:

$$G \cdot X^c + B \cdot Y + H \cdot U^c \geq K; \quad (4b)$$

Uncertainty set constraints:

$$U^c = \bar{U} + U^{dev+} - U^{dev-}; \quad U^c \in \mathbb{R}^{N_U} \quad (4c)$$

The objective function in (4a) minimizes the operating costs over "wait-and-see" variables, while, maximizing it over the worst-case realization of uncertainties. The obtained worst-case realizations are then sent back to master problem as fixed values. In fact, in each iteration of the decomposition methodology a new set of constraints (primal cuts) are added to master-problem.

Step 3) At the next iteration, master problem is solved, given the obtained worst-case realization of uncertain parameters through primal cutting planes in previous iterations, in order to find the new sizing decision variables to be sent to the sub-problem. The column-and-constraint methodology iterates between master problem and sub-problem until the convergence criteria is satisfied (i.e., the value of master problem and sub-problem get sufficiently close).

Since, the inner max-min problem is a bi-level optimization model, it cannot be directly solved. As indicated in the contributions, BCD technique is used to recast the bi-level max-min

problem into two single-level problems including a first-stage sub-problem, i.e., the inner min problem, and a second-stage sub-problem, i.e., the inner max problem. Since, duality theory is not used in the proposed robust model, it is possible to determine the bidding binary variables in the sub-problem as "wait-and-see" decisions. Therefore, despite the previous dual-based models, in which bidding strategy was obtained before uncertainty realization as "here-and-now" variables, the obtained bidding strategy solutions of the proposed BCD robust model are based on the worst-case realization of uncertainties and are treated as recourse decisions ("wait-and-see" decisions). In the following sub-section, the solving methodology for the sub-problem is described.

B. Block Coordinate Descent (BCD) Methodology to solve the sub-problem

The sub-problem is solved to determine 1) the optimal PV-WT-BES operation variables as "wait-and-see" decisions at the presence of uncertainties, and 2) the worst-case realization of uncertain parameters, given the fixed values of sizing variables obtained by master problem. In the conducted BCD methodology, the first-stage sub-problem is responsible for determining "wait-and-see" decision variables, while the second-stage sub-problem determines the worst-case realization of uncertain parameters.

Note that the standard application of the BCD method relies on the availability of an analytical expression for the operating cost in terms of middle-level variables. In the absence of such an expression in the max-min sub-problem, at each iteration of the proposed BCD method, the sub-problem for operating/bidding variables is built upon the first-order Taylor series approximation of the operating cost around the uncertainty realizations identified at the previous iteration.

Therefore, the max-min sub-problem in (4) is recast into a first-stage and a second-stage sub-problem. The first-stage sub-problem is given as (5).

$$\min_{Y \in \Xi''} \Lambda_{II} \equiv F', Y \quad (5a)$$

PV-WT-BES operation constraints:

$$G \cdot X^c + B \cdot Y + H \cdot U^c \geq K; \quad (5b)$$

Auxiliary constraints:

$$U^c = U^z : \mu \geq 0; \quad (5c)$$

Since, the sizing variables are fixed on their obtained values by master problem, the terms M1, and M2 of the deterministic objective function (1a), as well as the sizing constraints (1u)-(1w) are not included in the first-stage sub-problem. Instead, it includes the term M3 in (1a) and the associated operation constraints (1b)-(1t). Accordingly, the objective function (5a) minimizes the operating costs over "wait-and-see" variables, while being subject to operating constraints in (5b) and auxiliary constraints representing the obtained worst-case realization of uncertainties by the second-stage sub-problem in previous iteration of the BCD method , i.e., U^z .

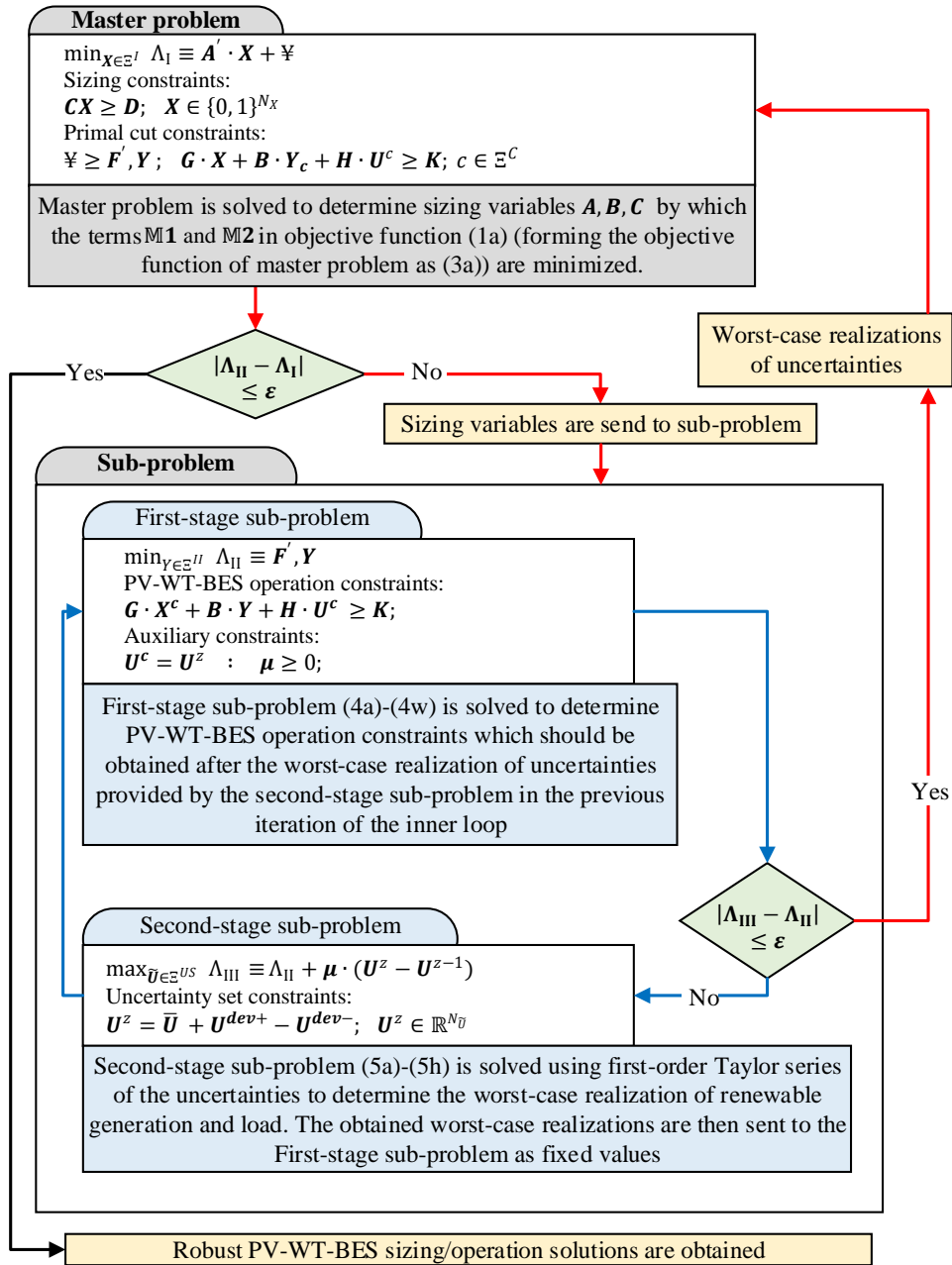


Fig. 4. Outline of the proposed BCD robust methodology.

μ is the vector of dual variables representing the sensitivity of objective function (5a) toward uncertain parameters, including load demand and PV/WT production at each iteration z of the BCD method. These dual variables are further employed to develop the first-order Taylor series

in the second-stage sub-problem only and no duality theory is conducted.

The second-stage sub-problem is built upon the first order Taylor series approximation of the first-stage sub-problem over the uncertain parameters in previous iteration of BCD method, i.e., $z - 1$. Therefore, at iteration z of the BCD method, the second-stage sub-problem is cast as (6).

$$\max_{\bar{U} \in \Xi^{US}} \Lambda_{III} \equiv \Lambda_{II} + \boldsymbol{\mu} \cdot (\mathbf{U}^z - \mathbf{U}^{z-1}) \quad (6a)$$

Uncertainty set constraints:

$$\mathbf{U}^z = \bar{\mathbf{U}} + \mathbf{U}^{dev+} - \mathbf{U}^{dev-}; \quad \mathbf{U}^z \in \mathbb{R}^{N_{\bar{U}}} \quad (6b)$$

The second-stage sub-problem determines the worst-case realization of uncertain parameters at each iteration z of the BCD method, by which the approximated objective function (6a) is maximized. Constraint (6b) expresses the deviation of uncertain parameters in positive and negative directions. By solving the second-stage sub-problem, the worst-case realization of uncertain parameters is determined to be sent to the first-stage sub-problem. The first-stage sub-problem is solved given the fixed values of worst-case realizations in the second-stage sub-problem.

This procedure continuous until the inner loop converges, i.e., the value of first-stage and second-stage sub-problems become sufficiently close. Therefore, the methodology to solve the min-max-min problem consists of two nested loops as follows:

Outer loop: The master problem communicates with the sub-problem through the outer loop, conducting the C&C methodology,

Inner loop: The iterations between first-stage and second-stage sub-problems are directed through the inner loop by means of BCD method.

Fig. 4 gives the outline of the proposed methodology and the compact formulation of each problem. In Fig. 4, the outer loop is shown by red lines and the inner loop is shown by blue lines.

IV. Extended Form of Master Problem and Sub-problem

A. Master Problem

The epigraph form of the master problem including primal cutting planes given by sub-problem, can be written as (8).

$$\begin{aligned} \text{Min } \Lambda_I \equiv & (A \cdot C^{pv} + W \cdot C^w + \sum_{n \in \Xi^N} B \cdot C_n^{bat} \cdot Q_n^{bat}) + y \cdot Q^{sys} \cdot (A \cdot C^{pv} + W \cdot \\ & C^w + B \cdot C_{n=1}^{bat}) + \Upsilon \end{aligned} \quad (8a)$$

s.t.

$$A \leq A_{max}; \quad (8b)$$

$$B \leq B_{max}; \quad (8c)$$

$$W \leq W_{max}; \quad (8d)$$

$$\Upsilon \geq Q^{sys} \cdot \sum_{d \in \Xi^D} \sum_{t \in \Xi^T} (P_{dtc}^{in} \cdot \pi_{dt} - P_{dtc}^{out} \cdot \theta); \quad \forall c \in \Xi^C \quad (8e)$$

$$\tilde{L}_{dt}^c = P_{dtc}^h + P_{dtc}^{in} - P_{dtc}^{out}; \quad \forall d \in \Xi^D; \quad \forall t \in \Xi^T; \quad \forall c \in \Xi^C \quad (8f)$$

$$P_{d_{tc}}^h = P_{d_{tc}}^s \cdot \eta^{inv} - P_{d_{tc}}^{dmp}; \forall d \in \Xi^D; \forall t \in \Xi^T; \forall c \in \Xi^C \quad (8g)$$

$$P_{d_{tc}}^s = P_{d_{tc}}^w + P_{d_{tc}}^v - P_{d_{tc}}^{chg} + P_{d_{tc}}^{dis}; \forall d \in \Xi^D; \forall t \in \Xi^T; \forall c \in \Xi^C \quad (8h)$$

$$P_{d_{tc}}^v = A \cdot \tilde{P}_{d_{tc}}^{v^c} \cdot \eta^{cc}; \forall d \in \Xi^D; \forall t \in \Xi^T; \forall c \in \Xi^C \quad (8i)$$

$$P_{d_{tc}}^w = W \cdot \tilde{P}_{d_{tc}}^{w^c} \cdot \eta^{con}; \forall d \in \Xi^D; \forall t \in \Xi^T; \forall c \in \Xi^C \quad (8j)$$

$$E_{d_{tc}} = E_{d(t-1)c} + \left(P_{d_{tc}}^{chg} \cdot \eta^{chg} - P_{d_{tc}}^{dis} \cdot \frac{1}{\eta^{dis}} \right) \cdot \Delta t - E^l \cdot B; \forall d \in \Xi^D; \forall t \in \Xi^T; \forall c \in \Xi^C \quad (8k)$$

$$\sum_{t \in \Xi^T} \left(P_{d_{tc}}^{chg} \cdot \eta^{chg} - P_{d_{tc}}^{dis} \cdot \frac{1}{\eta^{dis}} \right) = E^l \cdot B \cdot T; \forall d \in \Xi^D; \forall c \in \Xi^C \quad (8l)$$

$$E_{d(t=0)c} = E^{int}; \forall d \in \Xi^D; \forall c \in \Xi^C \quad (8m)$$

$$P_{min}^{chg} \cdot \alpha_{d_{tc}}^{chg} \leq P_{d_{tc}}^{chg} \leq P_{max}^{chg} \cdot \alpha_{d_{tc}}^{chg}; \forall d \in \Xi^D; \forall t \in \Xi^T; \forall c \in \Xi^C \quad (8n)$$

$$P_{min}^{dis} \cdot \alpha_{d_{tc}}^{dis} \leq P_{d_{tc}}^{dis} \leq P_{max}^{dis} \cdot \alpha_{d_{tc}}^{dis}; \forall d \in \Xi^D; \forall t \in \Xi^T; \forall c \in \Xi^C \quad (8o)$$

$$-M \cdot x_{d_{tc}}^{chg} \leq \alpha_{d_{tc}}^{chg} \leq M \cdot x_{d_{tc}}^{chg}; \forall d \in \Xi^D; \forall t \in \Xi^T; \forall c \in \Xi^C \quad (8p)$$

$$B - M \cdot (1 - x_{d_{tc}}^{chg}) \leq \alpha_{d_{tc}}^{chg} \leq B + M \cdot (1 - x_{d_{tc}}^{chg}); \quad (8q)$$

$$\forall d \in \Xi^D; \forall t \in \Xi^T; \forall c \in \Xi^C$$

$$-M \cdot x_{d_{tc}}^{dis} \leq \alpha_{d_{tc}}^{dis} \leq M \cdot x_{d_{tc}}^{dis}; \forall d \in \Xi^D; \forall t \in \Xi^T; \forall c \in \Xi^C \quad (8r)$$

$$B - M \cdot (1 - x_{d_{tc}}^{dis}) \leq \alpha_{d_{tc}}^{dis} \leq B + M \cdot (1 - x_{d_{tc}}^{dis}); \quad (8s)$$

$$\forall d \in \Xi^D; \forall t \in \Xi^T; \forall c \in \Xi^C$$

$$E'_{min} \cdot B \leq E_{d_{tc}} \leq B \cdot E'; \forall d \in \Xi^D; \forall t \in \Xi^T; \forall c \in \Xi^C \quad (8t)$$

$$x_{d_{tc}}^{chg} + x_{d_{tc}}^{dis} \leq 1; \forall d \in \Xi^D; \forall t \in \Xi^T \quad (8u)$$

$$P_{min}^{in} \cdot x_{d_{tc}}^{in} \leq P_{d_{tc}}^{in} \leq P_{max}^{in} \cdot x_{d_{tc}}^{in}; \forall d \in \Xi^D; \forall t \in \Xi^T; \forall c \in \Xi^C \quad (8v)$$

$$P_{min}^{out} \cdot x_{d_{tc}}^{out} \leq P_{d_{tc}}^{out} \leq P_{max}^{out} \cdot x_{d_{tc}}^{out}; \forall d \in \Xi^D; \forall t \in \Xi^T; \forall c \in \Xi^C \quad (8w)$$

$$x_{d_{tc}}^{in} + x_{d_{tc}}^{out} \leq 1; \forall d \in \Xi^D; \forall t \in \Xi^T; \forall c \in \Xi^C \quad (8x)$$

The objective function (8a) minimizes the NPV of CAPEX and maintenance costs by determining the optimal PV-WT-BES sizing solutions as "here-and-now" decision variables i.e., A, B, W . The limitations of sizing variables are given by (8b)-(8d). Constraints (8e)-(8x) represent the primal cuts submitted from the sub-problem. The subscript (c) and the superscript (c) in (8), indicate the associated "wait-and-see" variables and the fixed values of the uncertain parameters at iteration c of the C&C methodology, respectively. Constraints (8f)-(8x) are equivalent to constraints (1b)-(1t). However, the forecast values of uncertain parameters in (1) (i.e., $\bar{L}_{dt}, \bar{P}_{dt}^v, \bar{P}_{dt}^w$) are replaced with the obtained worst-case realizations from the sub-problem at iteration c ($\tilde{L}_{dt}^c, \tilde{P}_{dt}^{v^c}, \tilde{P}_{dt}^{w^c}$).

B. Sub-problem

In the following, both first and second-stage sub-problems are presented and discussed.

1) First-stage Sub-problem

The first-stage sub-problem is given by (9).

$$\text{Min } \Lambda_{II} \equiv Q^{sys} \cdot \sum_{d \in \Xi^D} \sum_{t \in \Xi^T} (P_{dt}^{in} \cdot \pi_{dt} - P_{dt}^{out} \cdot \theta) \quad (9a)$$

s.t.

$$\tilde{L}_{dt} = P_{dt}^h + P_{dt}^{in} - P_{dt}^{out}; \forall d \in \Xi^D; \forall t \in \Xi^T; \quad (9b)$$

$$P_{dt}^h = P_{dt}^s \cdot \eta^{inv} - P_{dt}^{dmp}; \forall d \in \Xi^D; \forall t \in \Xi^T; \quad (9c)$$

$$P_{dt}^s = P_{dt}^w + P_{dt}^v - P_{dt}^{chg} + P_{dt}^{dis}; \forall d \in \Xi^D; \forall t \in \Xi^T \quad (9d)$$

$$P_{dt}^v = A^c \cdot \tilde{P}_{dt}^v \cdot \eta^{cc}; \forall d \in \Xi^D; \forall t \in \Xi^T \quad (9e)$$

$$P_{dt}^w = W^c \cdot \tilde{P}_{dt}^w \cdot \eta^{con}; \forall d \in \Xi^D; \forall t \in \Xi^T \quad (9f)$$

$$E_{dt} = E_{d(t-1)} + \left(P_{dt}^{chg} \cdot \eta^{chg} - P_{dt}^{dis} \cdot \frac{1}{\eta^{dis}} \right) \cdot \Delta t - E^l \cdot B^c; \forall d \in \Xi^D; \forall t \in \Xi^T \quad (9g)$$

$$\sum_{t \in \Xi^T} \left(P_{dt}^{chg} \cdot \eta^{chg} - P_{dt}^{dis} \cdot \frac{1}{\eta^{dis}} \right) = E^l \cdot B^c \cdot T; \forall d \in \Xi^D \quad (9h)$$

$$E_{d(t=0)} = E^{int}; \forall d \in \Xi^D \quad (9i)$$

$$P_{min}^{chg} \cdot \alpha_{dt}^{chg} \leq P_{dt}^{chg} \leq P_{max}^{chg} \cdot \alpha_{dt}^{chg}; \forall d \in \Xi^D; \forall t \in \Xi^T \quad (9j)$$

$$P_{min}^{dis} \cdot \alpha_{dt}^{dis} \leq P_{dt}^{dis} \leq P_{max}^{dis} \cdot \alpha_{dt}^{dis}; \forall d \in \Xi^D; \forall t \in \Xi^T \quad (9k)$$

$$-\mathbb{M} \cdot x_{dt}^{chg} \leq \alpha_{dt}^{chg} \leq \mathbb{M} \cdot x_{dt}^{chg}; \forall d \in \Xi^D; \forall t \in \Xi^T \quad (9l)$$

$$B^c - \mathbb{M} \cdot (1 - x_{dt}^{chg}) \leq \alpha_{dt}^{chg} \leq B^c + \mathbb{M} \cdot (1 - x_{dt}^{chg}); \quad (9m)$$

$$\forall d \in \Xi^D; \forall t \in \Xi^T$$

$$-\mathbb{M} \cdot x_{dt}^{dis} \leq \alpha_{dt}^{dis} \leq \mathbb{M} \cdot x_{dt}^{dis}; \forall d \in \Xi^D; \forall t \in \Xi^T \quad (9n)$$

$$B^c - \mathbb{M} \cdot (1 - x_{dt}^{dis}) \leq \alpha_{dt}^{dis} \leq B^c + \mathbb{M} \cdot (1 - x_{dt}^{dis}); \quad (9o)$$

$$\forall d \in \Xi^D; \forall t \in \Xi^T$$

$$E'_{min} \cdot B^c \leq E_{dt} \leq B^c \cdot E'; \forall d \in \Xi^D; \forall t \in \Xi^T \quad (9p)$$

$$x_{dt}^{chg} + x_{dt}^{dis} \leq 1; \forall d \in \Xi^D; \forall t \in \Xi^T \quad (9q)$$

$$P_{min}^{in} \cdot x_{dt}^{in} \leq P_{dt}^{in} \leq P_{max}^{in} \cdot x_{dt}^{in}; \forall d \in \Xi^D; \forall t \in \Xi^T \quad (9r)$$

$$P_{min}^{out} \cdot x_{dt}^{out} \leq P_{dt}^{out} \leq P_{max}^{out} \cdot x_{dt}^{out}; \forall d \in \Xi^D; \forall t \in \Xi^T \quad (9s)$$

$$x_{dt}^{in} + x_{dt}^{out} \leq 1; \forall d \in \Xi^D; \forall t \in \Xi^T \quad (9t)$$

$$\tilde{L}_{dt} = \tilde{L}_{dt}^{(z)} : \mathfrak{f}_{dt}; \forall d \in \Xi^D; \forall t \in \Xi^T \quad (9u)$$

$$\tilde{P}_{dt}^v = \tilde{P}_{dt}^{v(z)} : \mathfrak{k}_{dt}; \forall d \in \Xi^D; \forall t \in \Xi^T \quad (9v)$$

$$\tilde{P}_{dt}^w = \tilde{P}_{dt}^{w(z)} : \mathfrak{y}_{dt}; \forall d \in \Xi^D; \forall t \in \Xi^T \quad (9w)$$

The objective function (9a) determines the optimal annual energy costs including

buying/selling bids as "wait-and-see" decisions. Constraints (9b)-(9t) are similar to those of the deterministic model but different in two ways, including 1) sizing variables, i.e., A , B , and W , are fixed on the obtained "here-and-now" solutions by master problem at iteration c of the C&C methodology, i.e., A^c , B^c , and W^c , and 2) the forecast values of uncertain parameters, i.e., \bar{L}_{dt} , \bar{P}_{dt}^v , and \bar{P}_{dt}^w , are fixed on the worst-case realization of uncertain parameters obtained by the second-stage sub-problem at iteration z of the BCD method, i.e., $\tilde{L}_{dt}^{(z)}$, $\tilde{P}_{dt}^{v(z)}$, and $\tilde{P}_{dt}^{w(z)}$, by constraints (9u)-(9w).

Dual variables f_{dt} , k_{dt} , and y_{dt} , in (9u)-(9w) represent the sensitivity of objective function (9a) toward uncertain parameters, including load demand and PV/WT production at each iteration z of the BCD method.

2) Second-stage Sub-problem

The second-stage sub-problem is cast as (10).

$$\begin{aligned} \text{Max } \Lambda_{\text{III}}^{(z)} \equiv & \Lambda_{\text{II}}^{(z)} + \sum_{d \in \Xi^D} \sum_{t \in \Xi^T} f_{dt} \left(\tilde{L}_{dt}^{(z)} - \tilde{L}_{dt}^{(z-1)} \right) + \sum_{d \in \Xi^D} \sum_{t \in \Xi^T} k_{dt} \left(\tilde{P}_{dt}^{v(z)} - \right. \\ & \left. \tilde{P}_{dt}^{v(z-1)} \right) + \sum_{d \in \Xi^D} \sum_{t \in \Xi^T} y_{dt} \left(\tilde{P}_{dt}^{w(z)} - \tilde{P}_{dt}^{w(z-1)} \right) \end{aligned} \quad (10a)$$

s.t.

$$\tilde{L}_{dt}^{(z)} = \bar{L}_{dt} + L_{dt}^{dev+}; \forall d \in \Xi^D; \forall t \in \Xi^T \quad (10b)$$

$$\tilde{L}_{dt}^{(z)} = \bar{L}_{dt} - L_{dt}^{dev-}; \forall d \in \Xi^D; \forall t \in \Xi^T \quad (10c)$$

$$\tilde{P}_{dt}^{v(z)} = \bar{P}_{dt}^v + P_{dt}^{v^{dev+}}; \forall d \in \Xi^D; \forall t \in \Xi^T \quad (10d)$$

$$\tilde{P}_{dt}^{v(z)} = \bar{P}_{dt}^v - P_{dt}^{v^{dev-}}; \forall d \in \Xi^D; \forall t \in \Xi^T \quad (10e)$$

$$\tilde{P}_{dt}^{w(z)} = \bar{P}_{dt}^w + P_{dt}^{w^{dev+}}; \forall d \in \Xi^D; \forall t \in \Xi^T \quad (10f)$$

$$\tilde{P}_{dt}^{w(z)} = \bar{P}_{dt}^w - P_{dt}^{w^{dev-}}; \forall d \in \Xi^D; \forall t \in \Xi^T \quad (10g)$$

$$0 \leq L_{dt}^{dev+} \leq \hat{L}_{dt}^{dev+} \cdot x_{dt}^{L+}; \forall d \in \Xi^D; \forall t \in \Xi^T \quad (10h)$$

$$0 \leq L_{dt}^{dev-} \leq \hat{L}_{dt}^{dev-} \cdot x_{dt}^{L-}; \forall d \in \Xi^D; \forall t \in \Xi^T \quad (10i)$$

$$0 \leq P_{dt}^{v^{dev+}} \leq \hat{P}_{dt}^{v^{dev+}} \cdot x_{dt}^{v^{dev+}}; \forall d \in \Xi^D; \forall t \in \Xi^T \quad (10j)$$

$$0 \leq P_{dt}^{v^{dev-}} \leq \hat{P}_{dt}^{v^{dev-}} \cdot x_{dt}^{v^{dev-}}; \forall d \in \Xi^D; \forall t \in \Xi^T \quad (10k)$$

$$0 \leq P_{dt}^{w^{dev+}} \leq \hat{P}_{dt}^{w^{dev+}} \cdot x_{dt}^{w^{dev+}}; \forall d \in \Xi^D; \forall t \in \Xi^T \quad (10l)$$

$$0 \leq P_{dt}^{w^{dev-}} \leq \hat{P}_{dt}^{w^{dev-}} \cdot x_{dt}^{w^{dev-}}; \forall d \in \Xi^D; \forall t \in \Xi^T \quad (10m)$$

$$x_{dt}^{L+} + x_{dt}^{L-} \leq 1; ; \forall d \in \Xi^D; \forall t \in \Xi^T \quad (10n)$$

$$x_{dt}^{v^{dev+}} + x_{dt}^{v^{dev-}} \leq 1; ; \forall d \in \Xi^D; \forall t \in \Xi^T \quad (10o)$$

$$x_{dt}^{w^{dev+}} + x_{dt}^{w^{dev-}} \leq 1; ; \forall d \in \Xi^D; \forall t \in \Xi^T \quad (10p)$$

$$\sum_{t \in \Xi^T} (x_{dt}^{L+} + x_{dt}^{L-} + x_{dt}^{v^{dev+}} + x_{dt}^{v^{dev-}} + x_{dt}^{w^{dev+}} + x_{dt}^{w^{dev-}}) \leq \Psi; \forall d \in \Xi^D \quad (10q)$$

The objective function (10a) maximizes the operating cost under the worst-case realization of uncertainties. Constraints (10b)-(10g), express the deviations of uncertain load and PV/WT generation in positive and negative directions, respectively. The deviations of uncertain parameters are limited to their allowable ranges through constraints (10h)-(10m). Constraints (10n)-(10p) make sure that the uncertain parameters only deviate in positive or negative directions. The total number of hourly deviations for all uncertain parameters is limited to the user-defined uncertainty budget Ψ in constraint (10q). $\Psi = 0$ represents a deterministic model as no uncertain parameter is allowed to deviate. However, as the value of Ψ increases, the robustness of the solution increases. Accordingly, the highest value of Ψ leads to the most robust solution against the uncertain parameters.

V. Numerical Study

A. Data Set

Studies of this paper are conducted over a 20-year planning horizon, indicating PV/WT lifetime, while the BES/inverter lifetime is estimated for 10 years [138]. The forecasted load data has been obtained from [139] and scaled for an industrial prosumer, illustrated by Fig. 5A. The forecasted PV generation for a PV panel with 1kW capacity on north facing 30° tilted using solar insolation and ambient temperature at Port Augusta, South Australia, is given by Fig. 5B [140]. Note that, the considered configuration of PV array is parallel. This is because a) parallel configuration of PV panels makes the maximum power point (MPP) tracking more efficient, exact, and cheaper, and b) it has a more reliable performance under certain shading conditions [141] (the use of either the conventional series configuration or the parallel configuration is

highly dependent on both the application type and the climatic conditions). The WT generation is also given by Fig. 5C for a WT with the capacity of 1kW at Port Augusta, South Australia [140]. The WT generation is also given by Fig. 5C for a WT with the capacity of 1kW at Port Augusta, South Australia [140]. The wind turbine is considered as dynamic speed. The cost of BES is \$800/kWh [138], while, the cost of PV and WT is \$1,300/kW and \$2,800/kW, respectively [142]. These costs are based on Australian Dollars. The maximum power range for PV/WT, BES capacity, BES charging/discharging rate, and import/export bids are given by Table II. Note that the steady-state energy losses of each BES has been considered as %3 of the BES capacity. Moreover, the characteristics of all BESs are the same. The electricity buying price is considered as TOU tariff with 41.53 ¢/kWh for hours 07-20 and 27.01 ¢/kWh for other hours, while, the feed-in tariff is 14 ¢/kWh in all times [143]. These prices are considered through smart metering of buying/selling bids. Since the operation is conducted for 24 hours and in each hour there are three uncertainty sources (accounting for hourly load, hourly PV generation, and hourly WT generation), 72 uncertain parameters exist in the 24-h operation horizon, i.e., $3 \times 24 = 72$. Some of the uncertain PV generation parameters are already zero during night hours. Four cases with different uncertainty budgets (i.e., Ψ) are considered in this study. These cases include Case 1, Case 2, Case 3, and Case 4. Each case is subject to 5%, 10%, 15%, and 20% deviation of uncertain parameters, respectively. These cases also become more conservative against uncertainties by increasing the values of Ψ . The simulations were conducted using CPLEX [110].

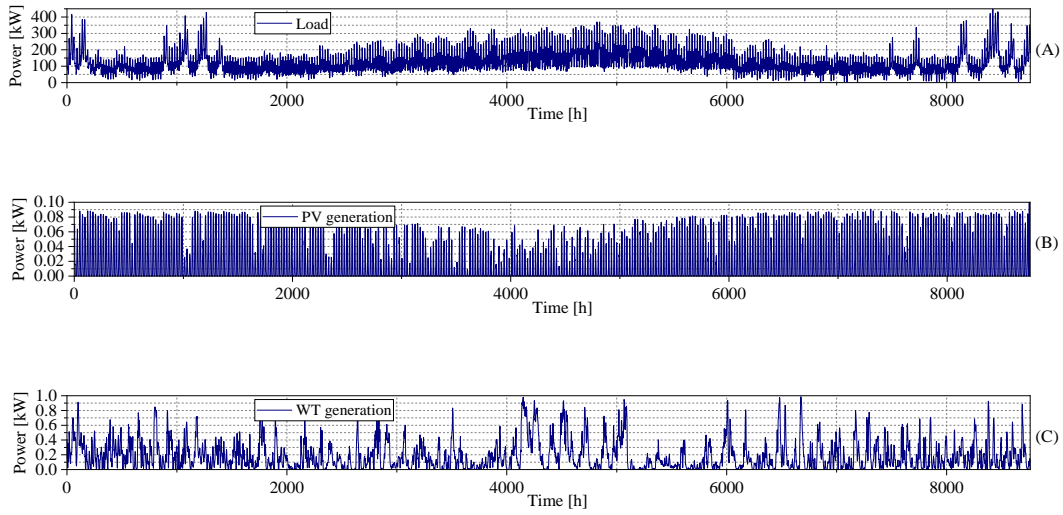


Fig. 5. The considered load, PV generation, and WT generation data.

TABLE II. Power ranges of the Studied PV-WT-BES system (Fig. 2)

Parameter	Range [kW/h]	Parameter	Range [kW]
PV capacity	$0 \leq P_{dt}^v \leq 500$	BES discharging rate	40% of E'
WT capacity	$0 \leq P_{dt}^w \leq 500$	Imported power	$0 \leq P_{dt}^{in} \leq 400$
BES capacity	$0 \leq E_{dt} \leq 500$	Exported power	$0 \leq P_{dt}^{out} \leq 50$
BES Charging rate	40% of E'	-	-

B. Robust Solutions

Tables III and IV show the obtained optimal values of objective function and capacity of PV/WT/BES for each case toward different uncertainty budgets, respectively. According to the reported results in Tables III and IV, it is pointed out that:

TABLE III. Total NPV of PV-WT-BES installation/operation costs (20 years)

Ψ	Total installation/operation cost [\$] over 20 years			
	Case 1	Case 2	Case 3	Case 4
0	4,032,492	4,032,492	4,032,492	4,032,492
24	4,298,258	4,586,364	4,891,449	5,240,414
48	4,350,143	4,685,701	5,041,602	5,489,975
72	4,365,654	4,722,127	5,104,865	5,548,492

TABLE IV. PV-WT-BES capacities for Cases 1-4 with 24-step size of Ψ (units are based on kW)

Ψ	Case 1			Case 2			Case 3			Case 4		
	PV	WT	BES									
0	332	366	402	332	366	402	332	366	402	332	366	402
24	328	397	482	284	424	500	223	452	500	218	454	500
48	354	402	431	377	443	466	390	486	480	324	500	354
72	362	400	412	399	439	433	435	481	441	408	500	322

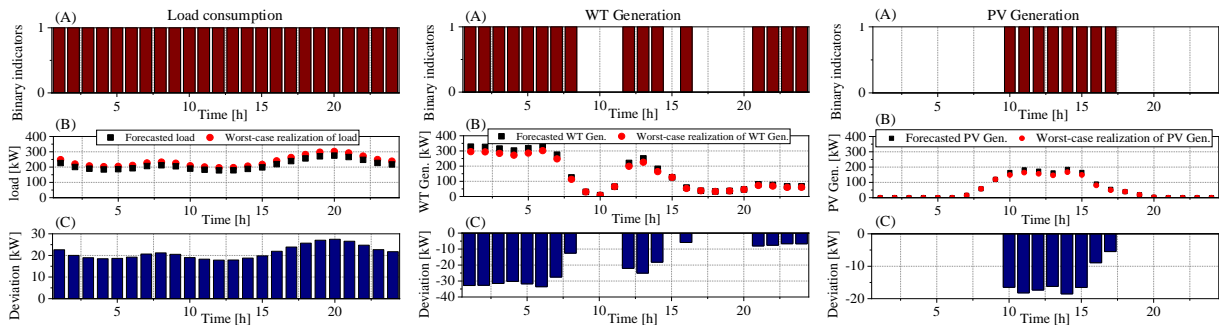


Fig. 6. Deviation indicators, deviation ranges, and worst-case realizations of uncertain parameters (for $\Psi = 48$ and 10% deviation based on post-event analysis).

1) Since no uncertainty has been realized in for $\Psi = 0$, it represents a deterministic sizing/scheduling model with no uncertainty realization, regardless of the associated deviation ranges in each case. The deterministic results are shaded in Tables III and IV.

2) The value of objective function increases as the robustness level (both the uncertainty budget Ψ and deviation range) increases, reflecting higher values of load and lower values of PV/WT generation.

3) The capacity of PV, WT, and BES does not follow a decreasing/increasing pattern as the robustness level increases. This is because, the optimality of objective function depends on both investment cost and the prosumer's operation costs. Therefore, in some cases, it is more beneficial to reduce the system capacity as the robustness level increases.

C. Post-event Analysis

The obtained RO solutions become more immunized against uncertainties as the robustness level increases. This feature is called "robustness worth" which means that the prosumer will face minimum extra costs if uncertainties arise.

However, this immunization comes at a higher expense which is called "robustness cost" (see Table III). Therefore, selecting a very high robustness level leads to over-conservative solutions resulting in unnecessary robustness cost and impractical robustness worth, and vice versa. To provide an optimal balance between robustness worth and cost, and to avoid over/under

conservative RO solutions, a post-event analysis has been conducted in this study. According to this analysis, the obtained RO solutions for each robustness level (uncertainty budget Ψ and deviation range) are examined against a sufficiently large number of uncertainty realizations, leading to unavoidable electricity shortage/surplus. The energy shortage, i.e., specified as load shedding, and the energy surplus, i.e., specified as PV/WT curtailment, have been modeled by additional free variables in the post-event analysis, while the obtained robust solutions are fixed. Therefore, the mixed-integer linear model in (1) becomes a linear model, only characterizing load shedding and PV/WT curtailment. The mathematical model of post-event analysis is given as (7). Note that, only constraints associated with load shedding and PV/WT curtailment are considered in post-event model and other constraints are eliminated as they are fixed on the obtained robust solutions (they are constants and have no effect on the post-event value). The subscript (s) in (7), indicates the associated variables in each trial scenario.

$$PE = \sum_{s \in \Xi^S} \sum_{d \in \Xi^D} \sum_{t \in \Xi^T} \left(\frac{|Y_{dts}^{sh}| + |Y_{dts}^{cu}|}{\text{Total number of trial scenarios}} \right) \quad (7a)$$

where;

$$\check{L}_{dts} = P_{dt}^h + P_{dt}^{in} - P_{dt}^{out} + Y_{dts}^{sh}; \forall d \in \Xi^D; \forall t \in \Xi^T; \forall s \in \Xi^S; \quad (7b)$$

$$P_{dt}^s = P_{dt}^w + P_{dt}^v - P_{dt}^{chg} + P_{dt}^{dis} + Y_{dts}^{cu}; \forall d \in \Xi^D; \forall t \in \Xi^T; \forall s \in \Xi^S \quad (7c)$$

$$P_{dt}^v = A \cdot \check{P}_{dts}^v \cdot \eta^{cc}; \forall d \in \Xi^D; \forall t \in \Xi^T; \forall s \in \Xi^S \quad (7d)$$

$$P_{dt}^w = W \cdot \check{P}_{dts}^w \cdot \eta^{con}; \forall d \in \Xi^D; \forall t \in \Xi^T; \forall s \in \Xi^S \quad (7e)$$

$$\forall Y_{dts}^{sh}, \forall Y_{dts}^{cu} \in \mathbb{R} \quad (7f)$$

The post-event value is obtained by (7a) in which the summation of the absolute value of load shed and PV/WT curtailment, i.e., Y_{dts}^{sh} , and Y_{dts}^{cu} , respectively, for each trial scenario is normalized over the total number of trial scenarios. Since, the considered uncertainties include load and PV/WT generation, only the energy flow constraints (1b) and (1d) as well as PV/WT generation constraints (1e) and (1f) are considered in the post-event model. These constraints are rewritten as (7b)-(7e) in which the load shedding variable Y_{dts}^{sh} and the PV/WT curtailment variable Y_{dts}^{cu} are employed to provide feasibility. The type of these variables is indicated in (7f). Problem (7) is solved for different robust setting as presented by Table III and the robust setting resulting in the lowest post-event cost is considered as the optimal robust setting for the model.

After solving the post-event model, these settings are obtained as $\Psi = 48$ with 10% deviation of uncertain parameters. Fig. 6 provides information on the exact deviation indicators, i.e., $x_{dt}^{L\pm}$, $x_{dt}^{v^{dev\pm}}$, and $x_{dt}^{w^{dev\pm}}$, worst-case realizations, i.e., $\tilde{L}_{dt}^{(z)}$, $\tilde{P}_{dt}^{v^{(z)}}$, and $\tilde{P}_{dt}^{w^{(z)}}$, and deviation range of uncertain parameters, i.e., $L_{dt}^{dev\pm}$, $P_{dt}^{v^{dev\pm}}$, and $P_{dt}^{w^{dev\pm}}$, regarding the optimal robust settings obtained by post-event analysis. As it is seen in Fig. 6, row (A), the summation of all binary indicators, is 48. The inner max problem has allocated each one of these 48 indicators to selected parameters to deliver a worst-case event (24 for load, 16 for WT generation, and 8 for PV generation). The 10% deviation range results in the worst-case realization of the selected parameters which is given by row (B) in Fig. 6. The value of deviation is also illustrated by row (C) in Fig. 6 for each uncertain parameter. As it is seen, the worst-case load has increased after uncertainty realization, while, both PV and WT generations have reduced.

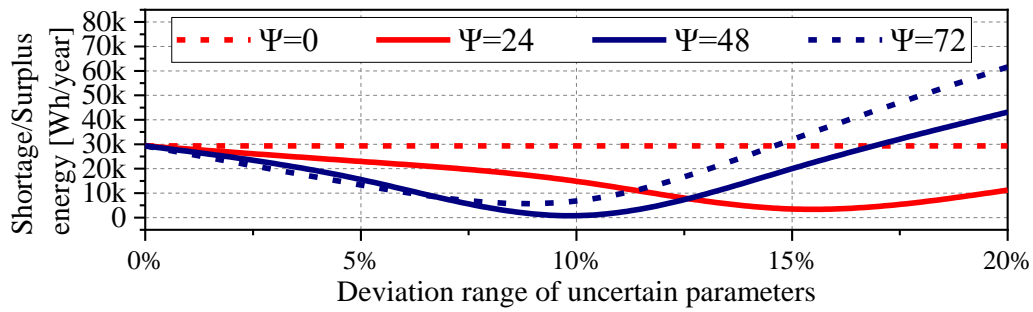


Fig. 7. Results of the conducted post-event analysis (for $\Psi = 48$ and 10% deviation based on post-event analysis).

The numerical results of the post-event analysis are given in Fig. 7 which indicates that the lowest value of electricity shortage/surplus has occurred for $\Psi = 48$ and 10% deviation.

Economical and Operational Solutions under the Obtained Optimal Robust Settings

The prosumer's cash-flow over the 20-year planning horizon is given by Fig. 8. The installation cost accounts for 377/443 kW of PV/WT capacity and 466 kWh of BES capacity. The BES itself is replaced each 10 years. The whole system is subject to annual maintenance and operation costs which are obtained as \$70,815 and \$197,294 in the first year, respectively. The total NPV cost of prosumer for a 20-year horizon with and without PV-WT-BES system is compared in Fig. 9 for both deterministic model (Fig. 9A) and the BCD robust model (Fig. 9B). The prosumer's total NPV cost before the PV-WT-BES installation is \$7,679,709 which only accounts for electricity importing cost as the prosumer has no capacity in exporting electricity. However, this value has reduced after installing PV-WT-BES by \$2,994,008 in Fig. 9A where no uncertainty has been considered. This reduction in NPV cost of the system is due to the system's ability in supplying load and providing upstream network interactions through buying/selling

bids. Note that, the NPV cost of the system has also been reduced by \$2,994,008 when considering uncertainties which is shown in Fig. 9A. However, the NPV cost is higher than the deterministic model which is due to the consideration of worst-case realization of uncertainties (as mentioned in the post-event analysis, conservativeness comes at a higher costs). The annual payments/payoffs of prosumer are also given in Fig. 9B. As it is seen, the annual payment has considerably reduced from \$834,522 to \$124,560 for the deterministic model and \$133,861 for the BCD robust solutions. As expected, no payoff would be obtained before installation of PV-WT-BES system, while, after installation, the annual payoff reaches \$709,962 for deterministic solution and \$700,661 for the BCD robust solution.

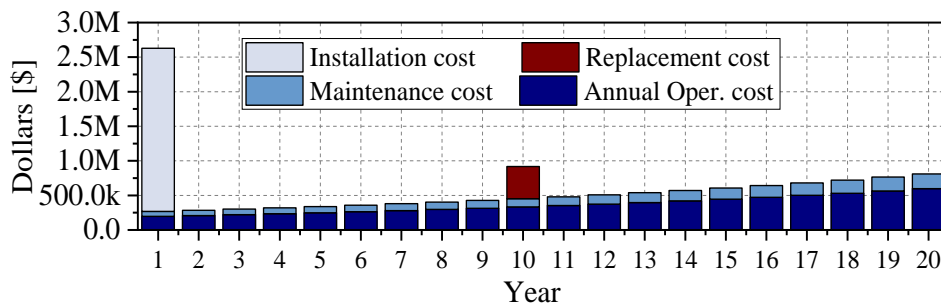


Fig. 8. Cash flow for the PV-WT-BES installation/operation (for $\Psi = 48$ and 10% deviation based on post-event analysis).

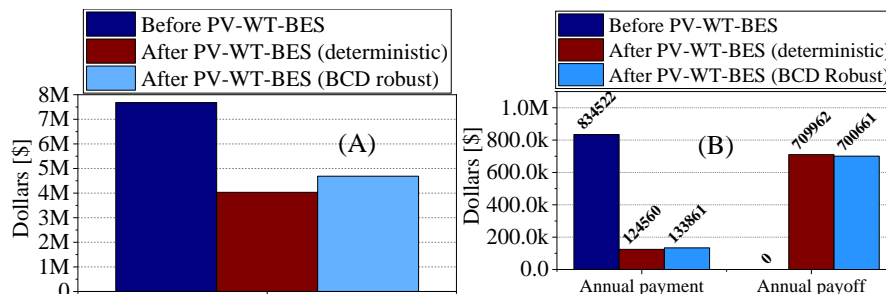


Fig. 9. Total NPV cost in 20-years (A) and Annual payment/payoff (B) (for $\Psi = 48$ and 10% deviation based on

post-event analysis).

The operational decisions, including import and export electricity, PV/WT generation, and hourly load demand are presented by Fig. 10 for a random day. The maximum generated power by PV/WT has been shown by blue and red lines in Fig. 10. These operational decisions are obtained based on the energy availability and upstream network TOU price signals in each hour. As seen in Fig. 10, the value of imported electricity is zero or very low between hours 7-20 which are the high-priced hours under TOU rate. Instead, the produced energy by PV/WT is consumed by prosumer during these hours. Also, BES is charged by the produced PV/WT to be discharged during night. As expected, the imported electricity is approximately zero in hours 19-20 where the BES has extensively discharged in these hours to contribute in the optimal operation of the system. These operational decisions are made based on M3 in (1a), and constraints (1b)-(1t).

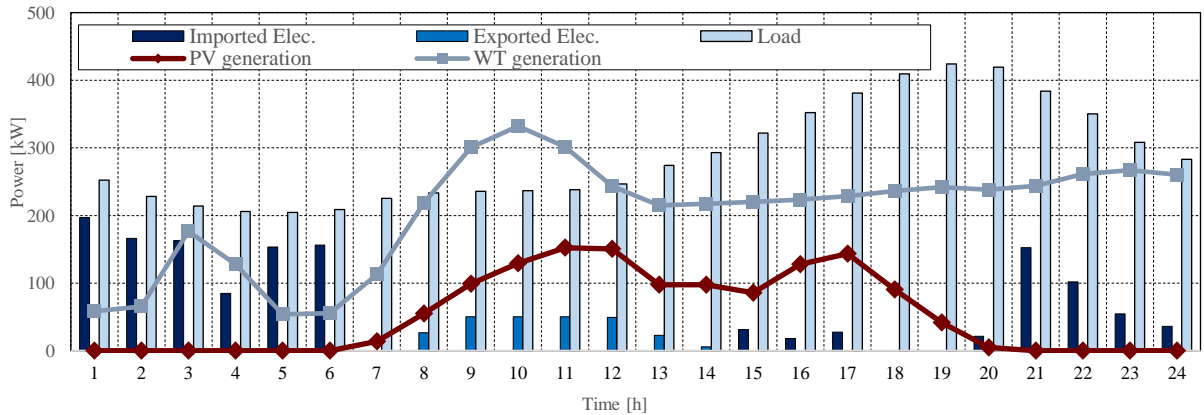


Fig. 10. Hourly operational decisions for a random day (for $\Psi = 48$ and 10% deviation).

The hourly SOC of battery, i.e., SOC, and its charging/discharging rates for a random day are given by Fig. 11 to illustrate the optimal 24-h scheduling solutions obtained from the proposed BCD robust model.

As mentioned in the introduction section, binary variables indicating buying/selling bids as well as BES charging/discharging status have been obtained in the sub-problem after the uncertainty realizations. These binary variables are given in Fig. 12 and Fig. 13.

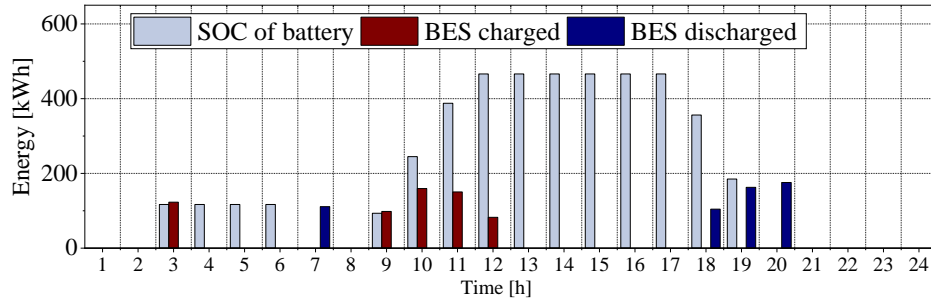


Fig. 11. State-of-charge (SOC) and charging/discharging rates for a random day (for $\Psi = 48$ and 10% deviation based on post-event analysis).

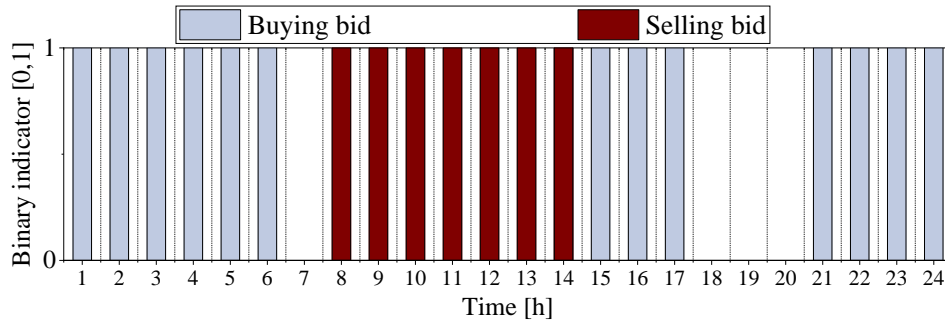


Fig. 12. Binary variables indicating prosumer's buying/selling bids

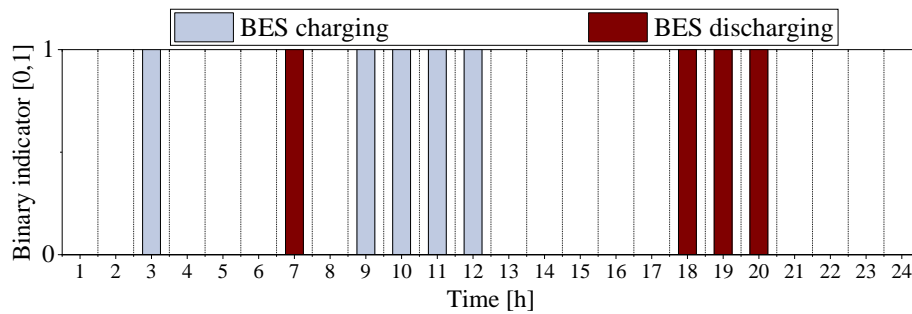


Fig. 13. Binary variables indicating BES charging/discharging status

The energy balance between PV-WT-BES system, load, and grid is given in Fig. 14 by Sankey diagram for both the deterministic and BCD robust models. As it is seen in Fig. 14, the value of load has increased by 10% which is based on the obtained worst-case realization in Fig. 6B for load consumption. Although, the capacity of the PV/WT system has increased in BCD robust model the increase in generated power by PV/WT is not as much as the capacity growth. This is due to the consideration of uncertainties in the robust model. For example, WT capacity has increased by 17.3%, while the generated power by WT has only increased by 9.97%. The same behavior is observed for PV system where its capacity has increased by 11.9%, while the generated power has only increased by 5.8%. This is due to the negative deviations of PV/WT generation when uncertainties are considered. These deviations, indicating the worst-case realization of uncertain PV/WT generation, have been illustrated by black dots in Fig. 6B for both PV and WT generation.

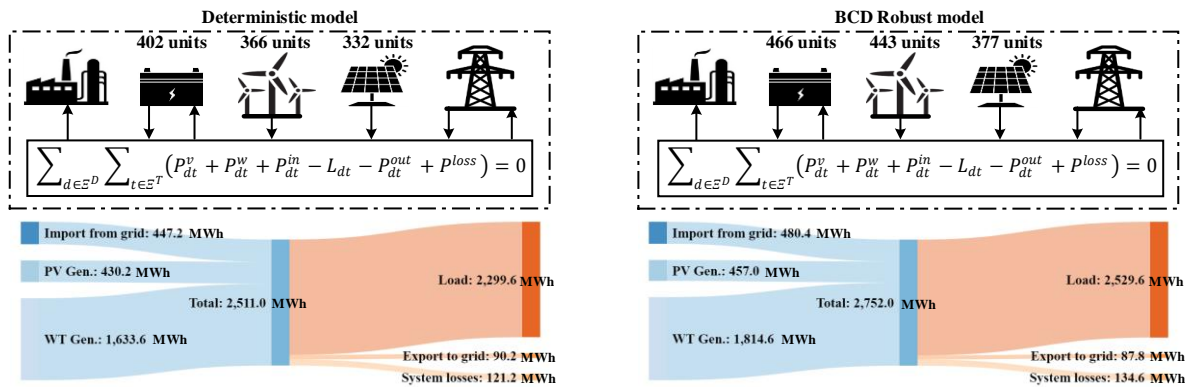


Fig. 14. Energy balance between PV-WT-BES system elements

D. Validation of the Obtained BCD Robust Results

To validate the effectiveness of the proposed model, the obtained BCD robust solutions are

compared to the obtained results of conventional dual-based robust models such as [116-119] in which the bidding strategy decisions are made prior to uncertainties (to ease the employment of duality theory). Fig. 15 shows the results of this comparison for optimal robust settings $\Psi = 48$ and 10% deviation of uncertainties. As it is seen, the value of objective function has reduced by \$553,115 which is due to the ignorance of uncertainties in the conventional dual-based robust model (ignoring uncertainties results in lower conservative bidding strategy). However, the results of the post-event analysis show that the long-term performance of the BCD robust model is subject to a lower amount of post-event cost when facing different uncertainty realizations. In particular, the post-event cost has been reduced by 10% when employing the proposed BCD robust model which shows its long-term effectiveness in comparison to conventional dual-based robust models.

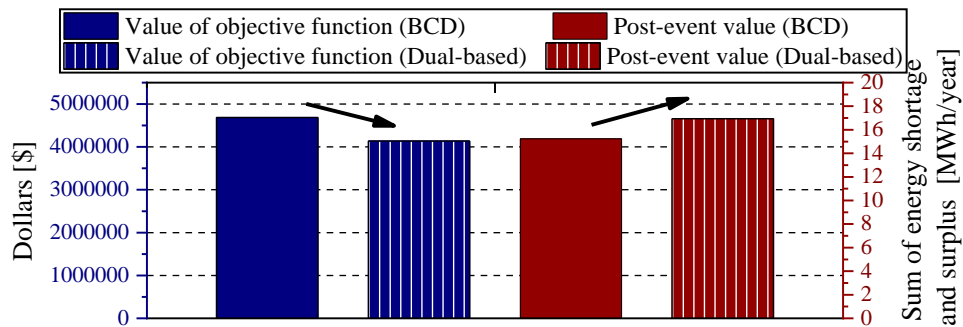


Fig. 15. Comparison results between the proposed BCD robust model and the conventional dual-based robust models in the literature

VI. Conclusion

This paper presented a BCD robust co-optimization model for simultaneous capacity allocation and bidding strategy of a PV-WT-BES owning prosumer, considering uncertainties of

prosumer's load and PV/WT generations. The proposed model was solved using column-and-constraint methodology through primal cutting planes. In terms of methodology, BCD method was conducted to solve the inner max-min problem instead of using duality theory. The conducted robust co-optimization as well as its solution methodology resulted in the following benefits:

Since sizing solutions can affect the benefits associated with daily operation/bidding strategy of the system, considering the uncertainty-dependent bidding strategy in the capacity allocation, results in optimal benefits for both long-term (capacity-related) and short-term (operation-related) perspectives.

By extending the application of BCD technique to solve the two-level max-min sub-problem (resulted from the C&C generation technique), it was possible for the first time to characterize prosumer's buying/selling bids in the inner max-min problem to be obtained after uncertainty realizations, resulting in more practical/realistic solutions. Note that, this feature was not applicable in conventional dual-based robust models in the literature.

Followed by point 2, it was also possible to consider different pricing schemes for buying bids and feed-in tariffs as each were modelled by different binary variables.

Results for different robust settings were reported, illustrating the effects of uncertain parameters on the value of objective function and the optimal capacity, illustrating the effects of different conservativeness levels on the solutions.

To avoid over/under conservative solutions, the optimal robust settings were determined

through the conducted post-event analysis, i.e., $\Psi = 48$ and 10% deviation on uncertain parameters, by which the minimum electricity shortage/surplus is achieved in the long-term performance.

Based on the optimal robust settings, the value of objective function over a 20-year horizon was \$4,685,701 and the capacities of PV, WT, and BES were obtained as 377, 443, and 466, respectively.

Moreover, the BCD robust solutions were compared to the solutions obtained from solving the conventional dual-based robust models such as [116-119]. For this comparison, dual-based RO model was developed and solved for the case study by authors. This comparison illustrated that the proposed model is subject to 10% reduction of post-event cost at the presence of uncertainties which indicates more robustness against the uncertainties in practice.

This study can assist commercial/industrial prosumers by providing practical and financially optimal sizing and bidding solutions when designing PV-WT-BES systems.

8.2 Application No. 2 (references are at the end of the paper)

Journals & Magazines > IEEE Transactions on Industri... > Volume: 17 Issue: 2 

Two-Stage Robust Sizing and Operation Co-Optimization for Residential PV–Battery Systems Considering the Uncertainty of PV Generation and Load

Publisher: IEEE

[Cite This](#)

[PDF](#)

Mehrdad Aghamohamadi  ; Amin Mahmoudi  ; Mohammed H. Haque  [All Authors](#)

11
Paper
Citations

751
Full
Text Views



Two-stage Robust Sizing and Operation Co-optimization for Residential PV-battery Systems Considering the Uncertainty of PV Generation and Load

This study presents a two-stage adaptive robust optimization (ARO) for optimal sizing and operation of residential solar-photovoltaic (PV) systems coupled with battery units. Uncertainties of PV generation and load are modeled by user-defined bounded intervals through polyhedral uncertainty sets. The proposed model determines the optimal size of PV-battery system while minimizing operating costs under the worst-case realization of uncertainties. ARO model is proposed as a tri-level min-max-min optimization problem. The outer min problem characterizes sizing variables as "here-and-now" decisions to be obtained prior to uncertainty realization. The inner max-min problem, however, determines the operation variables in place of "wait-and-see" decisions to be obtained after uncertainty realization. An iterative decomposition methodology is developed by means of column-and-constraint technique to recast the tri-level problem into a single-level master problem (the outer min problem) and a bi-level sub-problem (the inner max-min problem). Duality theory and Big-M linearization technique are used to transform the bi-level sub-problem into a solvable single-level max problem. The immunization of the model against uncertainties is justified by testing the obtained solutions against 36500 trial uncertainty

scenarios in a post-event analysis. The proposed post-event analysis also determines the optimum robustness level of the ARO model to avoid over/under conservative solutions.

Index Terms— PV-battery system, Renewable energy, Residential energy system, Robust optimization, Solar photovoltaic.

NOMENCLATURE

A. Indices

c	Index of iterations
d	Index of day
n	Index of battery replacements
t	Index of hour

B. Parameters

A_{max}	Maximum allowable number of PV panels
B_{max}	Maximum allowable number of batteries
C^{pv}	Price of PV panel with power generation \bar{P}_{dt}
C_n^b	Price of battery with the capacity of E'
E'	Capacity of battery
E'_{min}	Minimum energy level of battery
E^{int}	Initial energy level of battery in hour $t = 0$
E^l	Stand-by losses of battery
LT^{pv}	Lifetime of PV panels
LT_n^b	Lifetime of battery
\bar{L}_{dt}	Forecast electric load in hour t of day d
L_{dt}^{dev+}	Deviation of \bar{L}_{dt} in positive direction
y	Percentage of maintenance cost
M1, M2	Sufficiently large constants
N_X	Number of sizing variables in vector X

$N_{\tilde{U}}$	Number of uncertain parameters in vector \tilde{U}
N_Y	Number of operation variables in vector Y
\bar{P}_{dt}	Forecasted power generation by each PV unit
P_{dt}^{dev-}	Deviation of \bar{P}_{dt} in negative direction
P_{max}^h/P_{min}^h	Maximum/minimum capacity of inverter unit
P_{max}^n/P_{min}^n	Maximum/Minimum allowable power trade
$P_{max}^{ch}/P_{min}^{ch}$	Maximum/minimum charging rate for battery
Q_n^b	NPV coefficient for battery replacements
Q^{pv}	NPV coefficient for annual operation costs
T	Number of scheduling time periods in each day
$T1, \dots, T17$	Dualized terms of sub-problem objective function
η^{inv}/η^b	Efficiency of inverter/battery
Ψ^u	Uncertainty budget
Ψ^l/Ψ^p	Number of uncertain hourly loads/ PV generation
Ψ	Auxiliary continuous variable
π_{dt}	Price of electricity in hour t of day d
C. Sets	
\mathbb{E}^D	Set of days
\mathbb{E}^I	Set of sizing (here-and-now) decision variables
\mathbb{E}^{II}	Set of operation (wait-and-see) decision variables
\mathbb{E}^N	Set of battery replacements during PV panels' lifetime
\mathbb{E}^R	Set of dual variables
\mathbb{E}^T	Set of hours at each day of the scheduling horizon
\mathbb{E}^{UL}	Polyhedral load uncertainty set
\mathbb{E}^{UP}	Polyhedral PV generation uncertainty set
\mathbb{E}^{US}	Set of uncertain parameters
D. Variables	
A	Number of PV panels with power generation \bar{P}_{dt}
B	Number of batteries with the capacity of E'

E_{dt}	Total installed battery capacity in hour t of day d
\tilde{L}_{dt}	Uncertain load in hour t of day d
P_{dt}^n	Purchased electricity from grid in hour t of day d
P_{dt}^{dmp}	Dumped power in hour t of day d
P_{dt}^{ch}	Charging rate for each battery in hour t of day d
P_{dt}^v	Total PV generation in hour t of day d
P_{dt}^s	Inverter input in hour t of day d
P_{dt}^h	Inverter output in hour t of day d
\tilde{P}_{dt}	Uncertain generation of PV unit in hour t of day d
W_{dt}^+, W_{dt}^-	Auxiliary binary variables
$\lambda_{dt}^+, \lambda_{dt}^-$	Auxiliary dual variables
Λ_I/Λ_{II}	Objective function value of master/sub-problem

E. Vectors and matrices

\mathbf{A}, \mathbf{F}	Coefficient matrices of objective function
$\mathbf{C}, \mathbf{E}/\mathbf{D}$	Coefficient/requirement vector
$\bar{\mathbf{U}}$	Forecast of uncertain parameters
$\tilde{\mathbf{U}}$	Uncertain value of $\bar{\mathbf{U}}$
$\mathbf{U}^{dev+}/\mathbf{U}^{dev-}$	Positive/negative deviation of $\bar{\mathbf{U}}$
\mathbf{X}, \mathbf{Y}	Vector of sizing/operation variables

I. INTRODUCTION

A. Problem Description

Solar photovoltaics (PVs) are boosting the evolution of energy systems worldwide. Government of South Australia reports 880 MW installed PV through small-scale residential systems by 2018 [1]. The application of PVs in both residential and industrial sectors has

introduced several technical problems such as supply imbalance, reverse power flow, and voltage/frequency deviations. To cope, batteries are becoming of interest for PV owners/merchants to a) improve the integration of PVs into grid, and b) provide arbitrage abilities for a more efficient energy management and market participation [2].

The economic benefit of a PV-battery system is directly dependent on its optimal operation and interaction with upstream network, considering the value of load, PV generations and network prices in each hour. Although, the integration of PV and batteries can provide a promising operational status, unexpected uncertainties associated with PV generation and load can significantly affect their optimal operation, resulting in additional costs. In fact, ignoring the operational uncertainties can change the optimal long-term benefits considered in the cost-benefit analysis when designing PV-battery systems which leads to over/under design solutions. Moreover, the obtained solutions of deterministic studies such as [3-5] might be non-optimal or even infeasible when the uncertain parameters deviate from their forecast values [6]. Therefore, an accurate modeling of these uncertainties can lead to lower/higher operational costs/benefits for PV-battery owners, on one hand, and avoid over/under design solutions for such system, on the other hand.

B. Background and Motivation

Partial study has characterized the associated uncertainties with sizing of PVs and battery units. In [7], the sizing problems were conducted based on scenario generation to model the deviations of input data. In the sizing model presented in [8], Monte Carlo simulation was conducted to generate scenarios for renewables uncertainties. Monte Carlo simulation was also

performed in the battery sizing problem in [9] to model the uncertainties of PV generation. K-means clustering method was used in [10] to simulate the uncertain PV generations. Uncertainties were also modeled through probability density functions in [11-12]. The main drawback of the mentioned studies [7-12] is the lack of tractability due to the huge number of required scenarios, especially, when several uncertain parameters are considered, and a proper level of feasibility is required against different realizations of uncertain parameters. To obtain more reliable solutions, stochastic programming (SP) was performed in optimal sizing of a PV-battery system and a PV-diesel-storage system in [13] and [14], respectively. Followed by [15] SP was employed to model the uncertainties of solar radiation in optimal facility sizing of a microgrid. The application of SP was extended for optimal battery sizing in an isolated microgrid, using probabilistic scenarios in [16]. The study of [17] also characterized the uncertainties associated with battery capacity sizing through stochastic programming. Despite the advantages of the SP models in literature, i.e., [13-17], they face the lack of tractability which is due to the required full distributional knowledge of uncertain parameters in stochastic programming, which may not be easily available in practice [6]. Moreover, if the uncertain parameters deviate from the simulated scenarios, the performance of SP cannot be guaranteed against the uncertainty realizations. This issue is also true for the scenario-based models in [7-12].

To cope with these limitations, robust optimization (RO), as a tractable and practical methodology, was employed in different application areas. The uncertainties in RO are characterized by bounded intervals within polyhedral uncertainty sets. Therefore, it eliminates the need of scenario generation as it does not depend on distributional knowledge of the uncertain parameters [18-20]. As a result, the obtained solutions would be feasible as long as the

uncertainty realizations are within the bounded intervals, which makes it more reliable and tractable than SP and scenario-based models in the literature. So far, no study has been conducted to appropriately characterize the uncertainties associated with PV-battery sizing/operation problem through robust optimization technique.

C. Contributions

Following contributions are presented in this paper to extend the existing body of work:

1) In this paper, both deterministic and adaptive robust optimization (ARO) models for sizing and operation of PV-battery systems are proposed to a) cope with the aforementioned issues associated with scenario-based models, and b) obtain reliable and tractable solutions for PV-battery sizing/operation under different realizations of uncertain parameters. The proposed model is generally developed to be applicable in other sectors such as industrial, commercial, etc.

2) Uncertainties associated with PV generation and load are considered in the ARO model. The proposed model characterizes the sizing/operation variables in place of "here-and-now"/"wait-and-see" decisions, which are independent/dependent on uncertainty realizations. The robustness of PV-battery sizing/operation solution is measured via uncertainty budgets formed by polyhedral uncertainty sets which limit the number of uncertain parameters pertaining to PV generation and load. The proposed ARO sizing-operation model is a tri-level min-max-min optimization problem, which is not solvable by off-the-shelf optimization packages. Therefore, a decomposition methodology is developed to recast the tri-level min-max-min problem into a single-level min problem and a bi-level max-min problem. The single-level min problem characterizes the sizing variables as "wait-and-see" decisions, while, the PV-battery operational

variables are determined by the bi-level max-min problem as "here-and-now" decisions. The compact formulation of column-and-constraint technique in [21], is extended and adapted to iteratively solve the decomposition methodology with primal cuts. Moreover, duality theory as well as Big-M transformation technique are applied to recast the bi-level max-min problem into a solvable single-level linear max problem.

3) Since, robust optimization determines the optimal solution based on the worst-case realization of uncertain parameters, it may result in over conservative solutions. To avoid this, a post-event analysis is developed to justify the immunization of the obtained results against uncertainties and determine the optimal robust settings of the proposed PV-battery sizing/operation model.

The Motivations and Contributions of this study are illustratively given by Fig. 1.

II. DETERMINISTIC PV-BATTERY SIZING/OPERATION MODEL

In this section, a deterministic sizing/operation optimization model is presented for a PV-battery system.

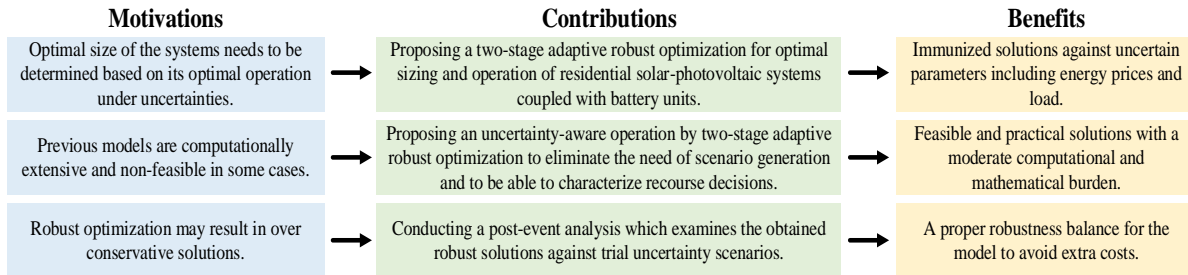


Fig. 1: Motivations, contributions, and benefits of the conducted study

Fig. 2 illustrates the considered configuration of the system and the power flow through each element, as per the notations in nomenclature.

The objective function of the proposed PV-battery sizing/operation model (i.e., $O.F.$) minimizes the investment costs, maintenance costs, and PV-battery system operating costs. The proposed deterministic model is formulated as (1). In (1a), S1 models the PV-battery installation cost including the capital expenditures and the net present value (NPV) of battery replacements. Inverter investment/replacement cost has been also considered in this term as a constant. The NPV of system maintenance cost is modeled by S2, which indicates a pre-identified percentage of installation cost of PV-battery. S3 is the power trade cost between PV-battery system and grid.

$$O.F. \equiv \min \overbrace{A \cdot C^{pv} + \sum_{n \in \Xi^N} B \cdot C_n^b \cdot Q_n^b}^{S1} + \overbrace{y \cdot Q^{pv} \cdot (A \cdot C^{pv} + B \cdot C_{n=1}^b)}^{S2} + \overbrace{Q^{pv} \cdot \sum_{d \in \Xi^D} \sum_{t \in \Xi^T} (P_{dt}^n \cdot \pi_{dt})}^{S3} \quad (1a)$$

Power flow constraints:

$$\bar{L}_{dt} = P_{dt}^h + P_{dt}^n; \forall d \in \Xi^D; \forall t \in \Xi^T \quad (1b)$$

$$P_{dt}^s = P_{dt}^v - P_{dt}^{ch} \cdot \eta^b; \forall d \in \Xi^D; \forall t \in \Xi^T \quad (1c)$$

$$P_{dt}^h = P_{dt}^s \cdot \eta^{inv} - P_{dt}^{dmp}; \forall d \in \Xi^D; \forall t \in \Xi^T \quad (1d)$$

Operational constraints:

$$P_{dt}^v = A \cdot \bar{P}_{dt}; \forall d \in \Xi^D; \forall t \in \Xi^T \quad (1e)$$

$$E_{dt} = E_{d(t-1)} + P_{dt}^{ch} \cdot \eta^b - E^l \cdot B; \forall d \in \Xi^D; \forall t \in \Xi^T \quad (1f)$$

$$\sum_{t \in \Xi^T} P_{dt}^{ch} = E^l \cdot B \cdot T; \forall d \in \Xi^D \quad (1g)$$

$$E_{d(t=0)} = E^{int} \cdot B; \forall d \in \Xi^D \quad (1h)$$

Allowable limitations:

$$P_{min}^h \leq P_{dt}^h \leq P_{max}^h; \forall d \in \Xi^D; \forall t \in \Xi^T \quad (1i)$$

$$P_{min}^n \leq P_{dt}^n \leq P_{max}^n; \forall d \in \Xi^D; \forall t \in \Xi^T \quad (1j)$$

$$-P_{max}^n \leq P_{dt}^n \leq -P_{min}^n; \forall d \in \Xi^D; \forall t \in \Xi^T \quad (1k)$$

$$P_{min}^{ch} \cdot B \leq P_{dt}^{ch} \leq P_{max}^{ch} \cdot B; \forall d \in \Xi^D; \forall t \in \Xi^T \quad (1l)$$

$$-P_{max}^{ch} \cdot B \leq P_{dt}^{ch} \leq -P_{min}^{ch} \cdot B; \forall d \in \Xi^D; \forall t \in \Xi^T \quad (1m)$$

$$E'_{min} \cdot B \leq E_{dt} \leq E' \cdot B; \forall d \in \Xi^D; \forall t \in \Xi^T \quad (1n)$$

$$A \leq A_{max}; \quad (1o)$$

$$B \leq B_{max}; \quad (1p)$$

Note that, $\forall P_{dt}^n, \forall P_{dt}^{ch} \in \mathbb{R}$. Therefore, positive values of P_{dt}^n represent electricity buying from the network, while the negative values illustrate electricity sold to the network. In a similar way, P_{dt}^{ch} represents both battery charging and discharging rates by positive and negative values, respectively. Constraints (1b)-(1c) give the power equality expressions on each junction of PV-

battery system (see Fig. 2). In fact, (1b) shows the power flow between load, network, and inverter output at the AC side of the system (after inverter), while, (1c) illustrates the power flow between PV, battery, and inverter at the DC side of the system (before inverter). The power conversion through the inverter is presented by (1d).

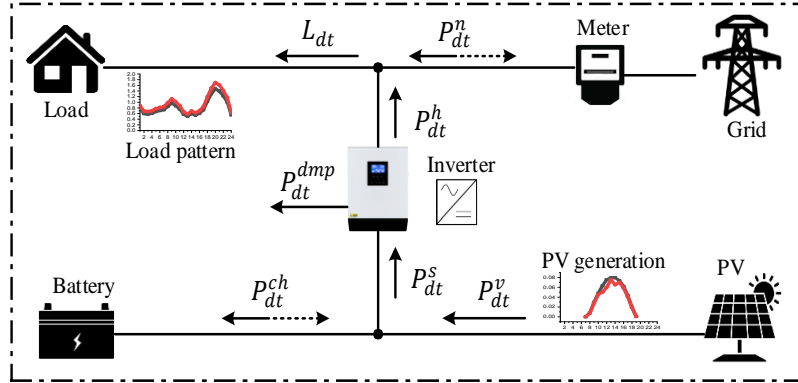


Fig. 2: Residential PV-battery system configuration and its power flow

Constraint (1e) presents the available PV generations for the total number of installed PV panels (i.e., A) with the capacity of \bar{P}_{dt} . The dynamic energy balance of battery is specified by (1f). The end-coupling constraint is given by (1g), making sure that the total charging energy is equal to the total discharging energy in battery, during the operation horizon. Therefore, the initial and final battery levels are equal, providing enough battery level for the next 24-h operation horizon. Constraint (1h) indicates the initial energy level of battery at the first time period of the next 24-hour operation, which is provided at the previous 24-hour operation of the system. Constraint (1i) limits the inverter capacity. The grid power trade and the battery charging rate are limited to their allowable ranges in constraints (1j)-(1m). Constraint (1n) limits the battery energy level with regard to the total number of installed batteries (i.e., B) with the capacity of E' . The number of PV panels and battery units are limited to their allowable ranges

through (1o)-(1p), respectively. Note that, the values of A_{max} and B_{max} are controlled by user and are dependent on the available space for PV and battery installation, respectively. In the proposed deterministic model, the uncertainties associated with PV generation and load are ignored as they are substituted by their forecasts i.e., \bar{P}_{dt} and \bar{L}_{dt} in (1), respectively. Therefore, the obtained solutions of the proposed deterministic model would not be optimal if the uncertain parameters deviate from their forecasts.

III. ADAPTIVE ROBUST PV-BATTERY SIZING/OPERATION

A. Uncertainty Set Realization

In this study, the uncertainties associated with PV generation and load are characterized through bounded intervals within polyhedral uncertainty sets as presented by (2).

$$\Xi^{UL} = \{\tilde{L}_{dt} = \bar{L}_{dt} + L_{dt}^{dev+}; \forall d \in \Xi^D; \forall t \in \Xi^T\} \quad (2a)$$

$$\Xi^{UP} = \{\tilde{P}_{dt} = \bar{P}_{dt} - P_{dt}^{dev-}; \forall d \in \Xi^D; \forall t \in \Xi^T\} \quad (2b)$$

$$0 \leq L_{dt}^{dev+} \leq \hat{L}_{dt}^{dev+}; \forall d \in \Xi^D; \forall t \in \Xi^T \quad (2c)$$

$$0 \leq P_{dt}^{dev-} \leq \hat{P}_{dt}^{dev-}; \forall d \in \Xi^D; \forall t \in \Xi^T \quad (2d)$$

$$\sum_{t \in \Xi^T} \sum_{d \in \Omega^d} \left| \frac{L_{dt}^{dev+}}{\hat{L}_{dt}^{dev+}} \right| \leq \Psi^l \quad (2e)$$

$$\sum_{t \in \Xi^T} \sum_{d \in \Omega^d} \left| \frac{P_{dt}^{dev-}}{\hat{P}_{dt}^{dev-}} \right| \leq \Psi^p \quad (2f)$$

$$\Psi^u = \Psi^l + \Psi^p \quad (2g)$$

The uncertain parameters \tilde{L}_{dt} and \tilde{P}_{dt} in (2), can deviate from their forecast values \bar{L}_{dt} and \bar{P}_{dt} in both positive and negative directions. However, the worst-case of load uncertainty happens in positive deviations and the worst-case of PV generation uncertainty happens in negative directions (reduction/increase in load/PV is a beneficial uncertainty, not a worst-case). Therefore, the negative deviations of load, and the positive deviations of PV generation are disregarded in the uncertainty set realizations (2a)-(2b). These deviations are limited to their user-defined allowable ranges through constraints (2c)-(2d). The parameters \hat{L}_{dt}^{dev+} and \hat{P}_{dt}^{dev-} are the maximum allowable values of bounded intervals, representing the deviation range of uncertain parameters. The number of uncertain parameters pertaining to PV generation and load are determined by uncertainty budgets Ψ^l , and Ψ^p in (2e) and (2f), respectively, while Ψ^u in (2g) represents the overall uncertainty budget. Since, robust optimization determines the solution based on the worst-case realization of uncertain parameters, it selects the maximum allowable value of deviation for each uncertain parameter. In fact, in the optimization we have $L_{dt}^{dev+} = \hat{L}_{dt}^{dev+}$ and $P_{dt}^{dev-} = \hat{P}_{dt}^{dev-}$. Therefore, in (2e) and (2f) we have $\frac{L_{dt}^{dev+}}{\hat{L}_{dt}^{dev+}} = 1$ and $\frac{P_{dt}^{dev-}}{\hat{P}_{dt}^{dev-}} = 1$. The highest value for Ψ^u is equal to the total number of uncertain parameters. In this circumstances, all uncertain parameters can deviate from their forecast values. Although, the value of Ψ^u is determined by the user, in this paper we have developed a post-event analysis in Section V which provides user the optimum value of Ψ^u , \hat{L}_{dt}^{dev+} , and \hat{P}_{dt}^{dev-} .

B. Proposed Adaptive Robust Model

In robust optimization, two main decisions are made including "here-and-now" decisions, which are obtained before any uncertainty realizations, and "wait-and-see" decisions, which are obtained after the realization of uncertain parameters. In this study, the PV-battery sizing variables including the number of PV panels and battery units (i.e., A and B , respectively) are considered as "here-and-now" decisions. This is because, the PV-battery system would be installed before any uncertainty realizations associated with load, and PV generation during system operation. However, uncertainties become of importance when operating PV-battery system (after installation). Therefore, these operation variables are considered as "wait-and-see" decisions and are obtained under uncertainty realizations.

The compact form of the proposed adaptive robust model is expressed through a tri-level min-max-min optimization problem as (3).

$$\min_{\mathbf{X} \in \Xi^I} (\mathbf{A}' \cdot \mathbf{X} + \max_{\tilde{\mathbf{U}} \in \Xi^{US}} \min_{\mathbf{Y} \in \Xi^{II}} \mathbf{F}', \mathbf{Y}) \quad (3a)$$

s.t.

$$\Xi^I = \{\mathbf{X} \in \{\mathbf{0}, \mathbf{1}, \mathbf{2}, \mathbf{3}, \dots\}^{N_X} \mid \mathbf{C}\mathbf{X} \geq \mathbf{D}\} \quad (3b)$$

$$\Xi^{US} = \{\tilde{\mathbf{U}} \in \mathbb{R}^{N_U} \mid \tilde{\mathbf{U}} = \bar{\mathbf{U}} + \mathbf{U}^{dev+} - \mathbf{U}^{dev-}\} \quad (3c)$$

$$\Xi^{II} = \{\mathbf{Y} \in \mathbb{R}^{N_Y} \mid \mathbf{E}(\mathbf{X}, \mathbf{Y}, \tilde{\mathbf{U}}) \geq 0\} \quad (3d)$$

In (3a), the outer min problem minimizes the objective function over the sizing variables. Accordingly, the outer min problem would be subject to the associated sizing constraints, presented by (3b). The inner max problem maximizes the objective function \mathbf{F}', \mathbf{Y} over the worst-

case realization of uncertain parameters, while the inner min problem minimizes it over the operation variables.

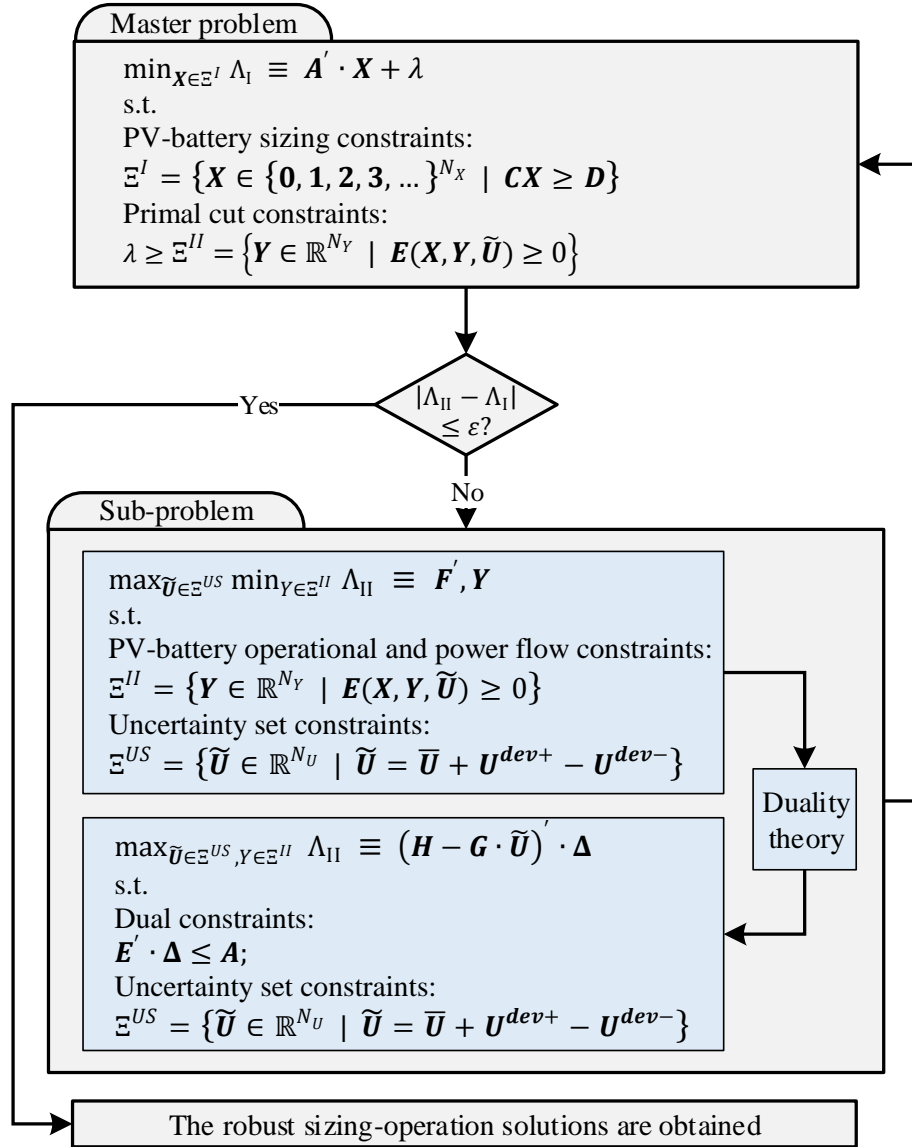


Fig. 3: Outline of the conducted methodology

Accordingly, the inner max problem is subject to polyhedral uncertainty sets in (3c) while, the inner min problem is subject to the operation constraints as (3d). The tri-level optimization

problem in (3) cannot be solved by off-the-shelf optimization packages. Therefore, a decomposition methodology is employed to decompose the tri-level min-max-min problem into a single-level min problem and a bi-level max-min problem by means of column-and-constraint technique [21]. The single-level min problem is called "master problem" and the bi-level max-min problem is called "sub-problem", hereafter. The decomposition methodology is shown by Fig. 3 and discussed through the following steps:

Step 1) The master problem is solved to obtain PV-battery sizing decisions. The obtained results are then sent to the sub-problem as fixed values.

Step 2) Given the obtained sizing decision variables, sub-problem is solved to determine both operation decision variables and the worst-case realization of uncertain parameters. These results are sent to the master problem as primal cuts.

Step 3) At the next iteration master problem is solved, given the obtained worst-case realization of uncertain parameters through primal cutting planes. In this step, the new sizing decision variables are obtained and sent to the sub-problem.

The above methodology iterates between master problem and sub-problem until the convergence criteria is satisfied (i.e., the values of master problem and sub-problem become sufficiently close).

IV. EXTENDED FORM OF MASTER AND SUB-PROBLEM

A. Master Problem

Master problem is solved to determine "here-and-now" decision variables including PV-battery sizing solutions, while being subject to sizing constraints only. Therefore, the objective function of the master problem includes the terms \$S1\$, and \$S2\$ of the deterministic objective function (1a) (as the only terms that are dependent on sizing variables, determining "here-and-now" decisions) and is subject to constraints (1o)-(1p) (as the only dependent constraints on sizing variables). The operational constraints (i.e., (1b)-(1n)) are also added to the master problem through primal cutting planes provided by the sub-problem in each iteration of the decomposition methodology using column-and-constraint technique. The epigraph form of the master problem is presented as (4).

$$\min_{A, B \in \Xi^I, P_{dtc}^n, P_{dtc}^{dmp}, P_{dtc}^h, P_{dtc}^s, P_{dtc}^v, P_{dtc}^{ch}, E_{dtc} \in \Xi^{II}} \Lambda_I \equiv \overbrace{(A \cdot C^{pv} + \sum_{n \in \Xi^N} B \cdot C_n^b \cdot Q_n^b)}^{S1} + \quad (4a)$$

$$\overbrace{y \cdot Q^{pv} \cdot (A \cdot C^{pv} + B \cdot C_{n=1}^b)}^{S2} + \text{¥}$$

s.t.

$$A \leq A_{max}; \quad (4b)$$

$$B \leq B_{max}; \quad (4c)$$

$$\text{¥} \geq Q^{pv} \cdot \sum_{d \in \Xi^D} \sum_{t \in \Xi^T} (P_{dtc}^n \cdot \pi_{dt}); \quad \forall c \in \Xi^C \quad (4d)$$

$$\tilde{L}_{dt}^c = P_{dtc}^h + P_{dtc}^n; \quad \forall d \in \Xi^D; \quad \forall t \in \Xi^T; \quad \forall c \in \Xi^C \quad (4e)$$

$$P_{dtc}^s = P_{dtc}^v + P_{dtc}^{ch} \cdot \eta^b; \quad \forall d \in \Xi^D; \quad \forall t \in \Xi^T; \quad \forall c \in \Xi^C \quad (4f)$$

$$P_{d_{tc}}^h = P_{d_{tc}}^s \cdot \eta^{inv} - P_{d_{tc}}^{dmp}; \forall d \in \Xi^D; \forall t \in \Xi^T \quad (4g)$$

$$P_{d_{tc}}^v = A \cdot \tilde{P}_{d_{tc}}^c; \forall d \in \Xi^D; \forall t \in \Xi^T; \forall c \in \Xi^C \quad (4h)$$

$$E_{d_{tc}} = E_{d_{(t-1)c}} + P_{d_{tc}}^{ch} \cdot \eta^b - E^l \cdot B; \forall d \in \Xi^D; \forall t \in \Xi^T; \forall c \in \Xi^C \quad (4i)$$

$$\sum_{t \in \Xi^T} P_{d_{tc}}^{ch} = E^l \cdot B \cdot T; \forall d \in \Xi^D; \forall c \in \Xi^C \quad (4j)$$

$$E_{d_{(t=0)}} = E^{int} \cdot B; \forall d \in \Xi^D; \forall c \in \Xi^C \quad (4k)$$

$$P_{min}^h \leq P_{d_{tc}}^h \leq P_{max}^h; \forall d \in \Xi^D; \forall t \in \Xi^T; \forall c \in \Xi^C \quad (4l)$$

$$P_{min}^n \leq P_{d_{tc}}^n \leq P_{max}^n; \forall d \in \Xi^D; \forall t \in \Xi^T; \forall c \in \Xi^C \quad (4m)$$

$$-P_{max}^n \leq P_{d_{tc}}^n \leq -P_{min}^n; \forall d \in \Xi^D; \forall t \in \Xi^T; \forall c \in \Xi^C \quad (4n)$$

$$P_{min}^{ch} \cdot B \leq P_{d_{tc}}^{ch} \leq P_{max}^{ch} \cdot B; \forall d \in \Xi^D; \forall t \in \Xi^T; \forall c \in \Xi^C \quad (4o)$$

$$-P_{max}^{ch} \cdot B \leq P_{d_{tc}}^{ch} \leq -P_{min}^{ch} \cdot B; \forall d \in \Xi^D; \forall t \in \Xi^T \quad (4p)$$

$$E'_{min} \cdot B \leq E_{d_{tc}} \leq E' \cdot B; \forall d \in \Xi^D; \forall t \in \Xi^T; \forall c \in \Xi^C \quad (4q)$$

In (4a), the NPV of investment/maintenance cost, i.e., \$S1 and \$S2 in (1a), is minimized over the optimal PV and battery sizing solutions as "here-and-now" decisions. The limitations of sizing variables, which were previously presented by (1o)-(1p), are given by (4b)-(4c). Constraints (4d)-(4q) represent the primal cuts submitted from the sub-problem. The subscript (c) and the superscript (c) in (4), indicate the associated "wait-and-see" variables and the fixed values of the uncertain parameters at iteration c of the column-and-constraint methodology, respectively.

Constraints (4e)-(4q) are the same as constraints (1b)-(1n) but, the forecast values of uncertain parameters (i.e., \bar{L}_{dt} in (1b) and \bar{P}_{dt} in (1e)) are replaced with the obtained worst-case realizations from the sub-problem at iteration c (i.e., \tilde{L}_{dt}^c in (4e) and \tilde{P}_{dt}^c in (4h)). In other words, at each iteration of column-and-constraint methodology, a set of primal cuts including the new obtained worst-case uncertainty realizations, are added to Master problem. The obtained PV and battery sizing variables in master problem (i.e., A and B) are then sent to the sub-problem as fixed values to determine both "wait-and-see" decision variables and the new worst-case realization of uncertain parameters.

B. Sub-problem

The sub-problem is solved to determine the worst-case realization of uncertain parameters based on the given fixed values of sizing solutions obtained by the master problem. Since, the sizing variables in sub-problem are fixed on their obtained values in master problem, the terms §1, and §2 of the deterministic objective function (1a) as well as the sizing constraints (1o)-(1p) are not included in the sub-problem. This is because, they have no impact on the sub-problem optimality as they are constant terms. Therefore, the sub-problem includes the term §3 of the deterministic objective function (1a), and the associated operation constraints (1b)-(1n) only. The sub-problem is given by (5).

$$\max_{\tilde{L}_{dt}, \tilde{P}_{dt}, \epsilon \in \Xi^{US}} \min_{P_{dt}^n, P_{dt}^{dmp}, P_{dt}^c, P_{dt}^s, P_{dt}^v, P_{dt}^{ch}, E_{dt} \in \Xi^{II}} \Lambda_{II} \equiv \overbrace{Q^{pv} \cdot \sum_{d \in \Xi^D} \sum_{t \in \Xi^T} (P_{dt}^n \cdot \pi_{dt})}^{\text{§3}} \quad (5a)$$

s.t.

$$\tilde{L}_{dt} = P_{dt}^h + P_{dt}^n; \forall d \in \Xi^D; \forall t \in \Xi^T : i_{dt} \in \mathbb{R} \quad (5b)$$

$$P_{dt}^s = P_{dt}^v + P_{dt}^{ch} \cdot \eta^b; \forall d \in \Xi^D; \forall t \in \Xi^T : j_{dt} \in \mathbb{R} \quad (5c)$$

$$P_{dt}^h = P_{dt}^s \cdot \eta^{inv} - P_{dt}^{dmp}; \forall d \in \Xi^D; \forall t \in \Xi^T : h_{dt} \in \mathbb{R} \quad (5d)$$

$$P_{dt}^v = A^c \cdot \tilde{P}_{dt}; \forall d \in \Xi^D; \forall t \in \Xi^T : b_{dt} \in \mathbb{R} \quad (5e)$$

$$E_{dt} = E_{d(t-1)} + P_{dt}^{ch} \cdot \eta^b - E^l \cdot B^c; \forall d \in \Xi^D; \forall t \in \Xi^T : f_{dt} \in \mathbb{R} \quad (5f)$$

$$\sum_{t \in \Xi^T} P_{dt}^{ch} = E^l \cdot B^c \cdot T; \forall d \in \Xi^D : n_d \in \mathbb{R} \quad (5g)$$

$$E_{d(t=0)} = E^{int} \cdot B^c; \forall d \in \Xi^D : g_{dt} \in \mathbb{R} \quad (5h)$$

$$P_{min}^h \leq P_{dt}^h \leq P_{max}^h; \forall d \in \Xi^D; \forall t \in \Xi^T : k_{dt}^{lo} \geq 0 : k_{dt}^{up} \geq 0 \quad (5i)$$

$$P_{min}^n \leq P_{dt}^n \leq P_{max}^n; \forall d \in \Xi^D; \forall t \in \Xi^T : \mathcal{L}_{dt}^{lo} \geq 0 : \mathcal{L}_{dt}^{up} \geq 0 \quad (5j)$$

$$-P_{max}^n \leq P_{dt}^n \leq -P_{min}^n; \forall d \in \Xi^D; \forall t \in \Xi^T : p_{dt}^{up} \geq 0 \quad (5k)$$

$$: p_{dt}^{lo} \geq 0$$

$$P_{min}^{ch} \cdot B^c \leq P_{dt}^{ch} \leq P_{max}^{ch} \cdot B^c; \forall d \in \Xi^D; \forall t \in \Xi^T : m_{dt}^{lo} \geq 0 : m_{dt}^{up} \geq 0 \quad (5l)$$

$$-P_{max}^{ch} \cdot B^c \leq P_{dt}^{ch} \leq -P_{min}^{ch} \cdot B^c; \forall d \in \Xi^D; \forall t \in \Xi^T : q_{dt}^{up} \geq 0 : q_{dt}^{lo} \geq 0 \quad (5m)$$

$$E'_{min} \cdot B^c \leq E_{dt} \leq E' \cdot B^c; \forall d \in \Xi^D; \forall t \in \Xi^T : \ell_{dt}^{lo} \geq 0 : \ell_{dt}^{up} \geq 0 \quad (5n)$$

$$(2a)-(2g) \tag{5o}$$

In (5a) the optimal grid integration of PV-battery system is determined through the objective function (5a) which includes the term S3 of the objective function (1a). The constraints (5b)-(5n) are similar to those of the deterministic model (1) but different in two ways including:

1) The sizing decision variables (i.e., A in (1e) and B in (1f)-(1h) and (1l)-(1n)) are fixed on the obtained "here-and-now" solutions by master problem at iteration c of the column-and-constraint methodology (i.e., A^c in (5e) and B^c in (5f)-(5h) and (5l)-(5n)).

2) The forecast values (i.e., \bar{L}_{dt} in (1b) and \bar{P}_{dt} in (1e)) are replaced by the uncertain values (i.e., \tilde{L}_{dt} in (4e) and \tilde{P}_{dt} in (4h)) to be obtained in place of the worst-case realizations. The new introduced variables in (5) (i.e., $\Xi^R = \{i_{dt}, h_{dt}, j_{dt}, b_{dt}, f_{dt}, n_{dt}, g_{dt}, k_{dt}^{lo}, k_{dt}^{up}, L_{dt}^{lo}, L_{dt}^{up}, p_{dt}^{up}, p_{dt}^{lo}, m_{dt}^{lo}, m_{dt}^{up}, q_{dt}^{up}, q_{dt}^{lo}, \ell_{dt}^{lo}, \ell_{dt}^{up}\}$), are the dual variables pertaining to constraints (5b)-(5n) which would be further used to develop the dual problem. Constraint (5o) also refers to the uncertainty sets presented by (2). Since, the proposed model in (5) is a bi-level max-min problem, it cannot be solved by off-the-shelf optimization packages. Therefore, duality theory is applied to recast the max-min problem into a single max problem. Accordingly, the sub-problem can be written as (6) which presents the dual form of (5).

$$\begin{aligned} \max_{\tilde{L}_{jt}, \tilde{C}_{it} \in \Xi^{US}, i_{dt}, \dots, \ell_{dt}^{up} \in \Xi^R} \Lambda_{II} \equiv & \overbrace{\sum_{d \in \Xi^D} \sum_{t \in \Xi^T} i_{dt} \cdot \tilde{L}_{dt}}^{T1} + \overbrace{\sum_{d \in \Xi^D} \sum_{t \in \Xi^T} b_{dt} \cdot \tilde{P}_{dt} \cdot A^c}^{T2} + \\ & \overbrace{\sum_{d \in \Xi^D} \sum_{t \in \Xi^T} f_{dt} \cdot E^l \cdot B^c}^{T3} + \overbrace{\sum_{d \in \Xi^D} n_d \cdot E^l \cdot B^c \cdot T}^{T4} + \overbrace{\sum_{d \in \Xi^D} \sum_{t \in \Xi^T} g_{dt} \cdot E^{int} \cdot B^c}^{T5} - \end{aligned} \tag{6a}$$

$$\begin{aligned}
& \overbrace{\sum_{d \in \Xi^D} \sum_{t \in \Xi^T} h_{dt}^{lo} \cdot P_{min}^h}^{T6} + \overbrace{\sum_{d \in \Xi^D} \sum_{t \in \Xi^T} h_{dt}^{up} \cdot P_{max}^h}^{T7} - \overbrace{\sum_{d \in \Xi^D} \sum_{t \in \Xi^T} \mathcal{L}_{dt}^{lo} \cdot P_{min}^n}^{T8} + \\
& \overbrace{\sum_{d \in \Xi^D} \sum_{t \in \Xi^T} \mathcal{L}_{dt}^{up} \cdot P_{max}^n}^{T9} + \overbrace{\sum_{d \in \Xi^D} \sum_{t \in \Xi^T} \mathcal{P}_{dt}^{up} \cdot P_{max}^n}^{T10} - \overbrace{\sum_{d \in \Xi^D} \sum_{t \in \Xi^T} \mathcal{P}_{dt}^{lo} \cdot P_{min}^n}^{T11} - \\
& \overbrace{\sum_{d \in \Xi^D} \sum_{t \in \Xi^T} m_{dt}^{lo} \cdot P_{min}^{ch} \cdot B^c}^{T12} + \overbrace{\sum_{d \in \Xi^D} \sum_{t \in \Xi^T} m_{dt}^{up} \cdot P_{max}^{ch} \cdot B^c}^{T13} - \\
& \overbrace{\sum_{d \in \Xi^D} \sum_{t \in \Xi^T} q_{dt}^{up} \cdot P_{max}^{ch} \cdot B^c}^{T14} + \overbrace{\sum_{d \in \Xi^D} \sum_{t \in \Xi^T} q_{dt}^{lo} \cdot P_{min}^{ch} \cdot B^c}^{T15} - \\
& \overbrace{\sum_{d \in \Xi^D} \sum_{t \in \Xi^T} \ell_{dt}^{lo} \cdot E'_{min} \cdot B^c}^{T16} + \overbrace{\sum_{d \in \Xi^D} \sum_{t \in \Xi^T} \ell_{dt}^{up} \cdot B^c \cdot E'}^{T17}
\end{aligned}$$

s.t.

$$i_{dt} + \mathcal{L}_{dt}^{lo} + \mathcal{L}_{dt}^{up} + \mathcal{P}_{dt}^{up} + \mathcal{P}_{dt}^{lo} \leq Q^{pv} \cdot \pi_{dt}; \forall d \in \Xi^D; \forall t \in \Xi^T \quad (6b)$$

$$i_{dt} - h_{dt} + h_{dt}^{lo} + h_{dt}^{up} \leq 0; \forall d \in \Xi^D; \forall t \in \Xi^T \quad (6c)$$

$$\eta^{inv} \cdot h_{dt} - j_{dt} \leq 0; \forall d \in \Xi^D; \forall t \in \Xi^T \quad (6d)$$

$$j_{dt} + b_{dt} \leq 0; \forall d \in \Xi^D; \forall t \in \Xi^T \quad (6e)$$

$$\eta^b \cdot j_{dt} + \eta^b \cdot b_{dt} + n_d + m_{dt}^{lo} + m_{dt}^{up} + q_{dt}^{up} + q_{dt}^{lo} \leq 0; \forall d \in \Xi^D; \forall t \in \Xi^T \quad (6f)$$

$$f_{d(t-1)} - f_{dt} + g_{d(t=0)} + \ell_{dt}^{lo} + \ell_{dt}^{up} \leq 0; \forall d \in \Xi^D; \forall t \in \Xi^T \quad (6g)$$

$$(2a)-(2g) \quad (6h)$$

Since, in duality theory the objective function of the dual problem is formed with constraints of the main problem (5), (6a) represents the objective function of the dual problem pertaining to

dual variables introduced among constraints (5b)-(5n). The associated dual constraints, pertaining to primal variables in (5), are presented by (6b)-(6g). These constraints are obtained based on duality theory. The constant value at the right-hand side of each dual constraint pertains to the coefficient of each variable in the objective function of the principal problem (5). Constraint (6h) represents the polyhedral uncertainty sets and the uncertainty budget for PV generation and load.

As seen from the dual problem, the products of $i_{dt} \cdot \tilde{L}_{dt}$ in T1, and $\ell_{dt} \cdot \tilde{P}_{dt}$ in T2 make the sub-problem bilinear. Since, (6a) maximizes the objective function over the uncertain parameters, the solution of the sub-problem is on the extreme points of the polyhedral uncertainty sets. Therefore, auxiliary binary variables along with Big-M transformation technique are employed to 1) search the corners of polyhedrons, and 2) linearize the sub-problem by replacing the products of $i_{dt} \cdot \tilde{L}_{dt}$, and $\ell_{dt} \cdot \tilde{P}_{dt}$ by linear terms as follows:

$$\tilde{L}_{dt} = \bar{L}_{dt} + \hat{L}_{dt}^{dev+} \cdot W_{dt}^+; \forall d \in \Xi^D; \forall t \in \Xi^T \quad (7a)$$

$$\tilde{P}_{dt} = \bar{P}_{dt} - \hat{P}_{dt}^{dev-} \cdot W_{dt}^-; \forall d \in \Xi^D; \forall t \in \Xi^T \quad (7b)$$

where,

$$\sum_{t \in \Xi^T} \sum_{d \in \Omega^d} (W_{dt}^+ + W_{dt}^-) \leq \Psi^u \quad (7c)$$

$$\forall W_{dt}^+, \forall W_{dt}^- \in \{0,1\} \quad (7d)$$

In fact, (7a) and (7b) represent (2a) and (2b), respectively, considering $L_{dt}^{dev+} = \hat{L}_{dt}^{dev+}$ and $P_{dt}^{dev-} = \hat{P}_{dt}^{dev-}$. Therefore, the uncertainty budget Ψ^u would be determined by (7c). Accordingly, the terms T1, and T2 can be represented as (8) in which \tilde{L}_{dt} and \tilde{P}_{dt} are replaced

with $\bar{L}_{dt} + \hat{L}_{dt}^{dev+} \cdot W_{dt}^+$ and $\bar{P}_{dt} - \hat{P}_{dt}^{dev-} \cdot W_{dt}^-$, respectively.

$$T1 = \sum_{d \in \Xi^D} \sum_{t \in \Xi^T} (\bar{L}_{dt} \cdot i_{dt} + \hat{L}_{dt}^{dev+} \cdot W_{dt}^+ \cdot i_{dt}); \quad (8a)$$

$$T2 = \sum_{d \in \Xi^D} \sum_{t \in \Xi^T} (\bar{P}_{dt} \cdot \varrho_{dt} \cdot A^c - \hat{P}_{dt}^{dev-} \cdot W_{dt}^- \cdot \varrho_{dt} \cdot A^c); \quad (8b)$$

As seen in (8), the right-hand side of T1 and T2 includes the products of $W_{dt}^+ \cdot i_{dt}$, and $W_{dt}^- \cdot \varrho_{dt}$, respectively. According to Big-M transformation technique, these nonlinearities are recast into linear terms as follows:

$$T1 = \sum_{d \in \Xi^D} \sum_{t \in \Xi^T} (\bar{L}_{dt} \cdot i_{dt} + \hat{L}_{dt}^{dev+} \cdot \lambda_{dt}^+); \quad (9a)$$

$$T2 = \sum_{d \in \Xi^D} \sum_{t \in \Xi^T} (\bar{P}_{dt} \cdot \varrho_{dt} \cdot A^c - \hat{P}_{dt}^{dev-} \cdot \lambda_{dt}^- \cdot A^c); \quad (9b)$$

where,

$$-\mathbb{M}1 \cdot W_{dt}^+ \leq \lambda_{dt}^+ \leq \mathbb{M}1 \cdot W_{dt}^+; \quad \forall d \in \Xi^D; \forall t \in \Xi^T \quad (9c)$$

$$i_{dt} - \mathbb{M}1 \cdot (1 - W_{dt}^+) \leq \lambda_{dt}^+ \leq i_{dt} + \mathbb{M}1 \cdot (1 - W_{dt}^+); \quad \forall d \in \Xi^D; \forall t \in \Xi^T \quad (9d)$$

$$-\mathbb{M}2 \cdot W_{dt}^- \leq \lambda_{dt}^- \leq \mathbb{M}2 \cdot W_{dt}^-; \quad \forall d \in \Xi^D; \forall t \in \Xi^T \quad (9e)$$

$$\varrho_{dt} - \mathbb{M}2 \cdot (1 - W_{dt}^-) \leq \lambda_{dt}^- \leq \varrho_{dt} + \mathbb{M}2 \cdot (1 - W_{dt}^-); \quad \forall d \in \Xi^D; \forall t \in \Xi^T \quad (9f)$$

$$\mathbb{M}1 \geq |i_{dt}|, \mathbb{M}2 \geq |\varrho_{dt}|; \quad \forall d \in \Xi^D; \forall t \in \Xi^T \quad (9g)$$

According to (9), the terms T1, and T2 in (9a)-(9b), function as the same as (8). Therefore, the sub-problem can be finally written as follows:

$$\max_{\tilde{L}_{jt}, \tilde{C}_{it} \in \Xi^{US}, i_{dt}, \dots, l_{dt}^{up} \in \Xi^R} \Lambda_{II} \equiv T1 + T2 + \dots + T17 \quad (10a)$$

s.t.

$$(7a)-(7d), (8), \text{ and } (9); \quad (10b)$$

The sub-problem (10) is solved to obtain the worst-case realization of uncertain PV generation and load while minimizing the objective function over PV-battery operational variables as "wait-and-see" decisions. The obtained solutions are sent to the master problem as primal cuts in which the uncertain parameters are fixed on their worst-case realization.

C. Algorithm

The proposed iterative approach is presented as Table I.

TABLE I. The proposed algorithm to solve the decomposition methodology

1) Initialization:
i) Set the iteration counter c to 1.
ii) Set the forecasted parameters \bar{L}_{dt} , and \bar{P}_{dt} as the worst-case realization of uncertain parameters in master problem.
iii) Set the value of sub-problem (i.e., Λ_{II}) to $+\infty$.
2) Solution of master problem
Solve the master problem (4) to obtain the value of master problem (i.e., Λ_I) and the sizing variables A and B .
3) Solution of sub-problem
Solve the sub-problem (10) for the given sizing variables obtained by master problem (i.e., A^c , and B^c) to obtain the worst-case realization of uncertain parameters (i.e., \tilde{L}_{dt} , and \tilde{P}_{dt}) as

well as the value of sub-problem Λ_{II} .

4) Parameters update

i) Update the iteration counter $c \rightarrow c + 1$.

ii) Update the worst-case realization of uncertain parameters to \tilde{L}_{dt}^c , and \tilde{P}_{dt}^c , obtained by the sub-problem at previous iteration.

5) Solution of master problem with primal cuts

Solve the master problem (4) to obtain sizing variables A and B as well as the value of master problem Λ_I for the given worst-case realization of uncertain parameters through primal cutting planes.

6) Convergence check

If the convergence criteria is satisfied (i.e., $(\Lambda_{II} - \Lambda_I)/\Lambda_{II} \leq \varepsilon$), the algorithm is terminated; otherwise, go to step 3.

V. RESULTS AND DISCUSSION

A. Data Set

Studies of this paper are conducted over a 24-year planning horizon as PV lifetime. The inverter/battery lifetime is 8 years. Since, the battery lifetime is in relation with the way of its operation, 8-year lifetime is considered based on 20% of total battery capacity as allowable charging/discharging rate in each hour [22]. The annual forecasted load data has been obtained from [23] and scaled for a household, illustrated by Fig. 4A. The annual forecasted PV generation for a PV panel with 100-Watt capacity (on North facing 30° tilted PV array solar insolation in Port Augusta, South Australia) is given by Fig. 4B [24]. The cost of battery is \$700/kWh and the cost of PV is \$1500/kW [22]. These costs are based on Australian Dollar. The electricity price for

both buying and selling electricity is based on time-of-use (TOU) tariff with 27.90 and 42.90 ¢/kWh for off-peak (hours 21-07) and peak (hours 08-20), respectively [25]. 48 uncertain parameters, considering both PV generation and load, are counted in each 24-h daily operation of PV-battery system (some of these parameters are zero due to no PV generation during nights). In Table II, four cases with different uncertainty budgets (i.e., Ψ^u) and deviation ranges are considered. These cases become more conservative against uncertainties by increasing the values of Ψ^u and deviation range of uncertain parameters. Since, no uncertainty has been realized in Case No. 1 (see Table II), it represents a deterministic model with no uncertainty realization. The simulations have been conducted on a laptop computer with 8 GB RAM and a core-i5 processor using CPLEX [26].

B. Numerical Results

Table III shows the obtained objective function values, sizing solutions of PV and battery, investment/maintenance/operation costs, cost of electricity (CoE), number of primal cuts, and the computational burden for each case. Based on the obtained results, it can be pointed out that:

1) The value of objective function increases as the robustness level (uncertainty budget Ψ^u and deviation range) increases, reflecting higher values of household load and lower values of PV generation.

2) The capacity of PV-battery system does not follow a decreasing/increasing pattern as the robustness level increases. This is because, the optimality of objective function depends on both investment cost and the operation cost of PV-battery system. Therefore, in some cases (i.e., Case No. 3), it is more beneficial to reduce the PV-battery system capacity as the robustness level

increases.

3) As the uncertainty budget and deviation range of uncertain parameters change, the feasible solution region of both master problem and sub-problem change accordingly. Therefore, the results of each case are obtained after different numbers of primal cuts and computation times.

4) In cases No. 1 and 2, the energy trade cost has a negative value which is due to the greater PV-battery system capacities in these cases, resulting in higher benefits of exported electricity. In contrary, as the capacity of PV-battery system reduces in cases No. 3 and 4, the operation cost increases accordingly.

The required cash flow for each case is presented by Fig. 5. As it is seen, the value of investment/maintenance/replacement cost depends on the capacity of PV-battery system which reaches its maximum value in Case No. 2 where the maximum PV-battery capacity is allocated.

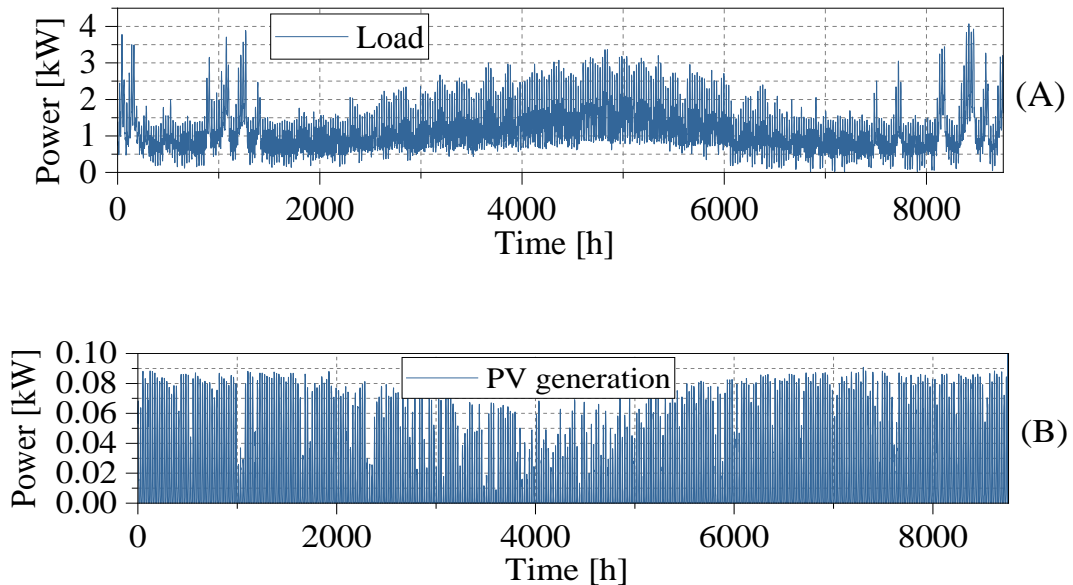


Fig. 4: Load and PV generation data

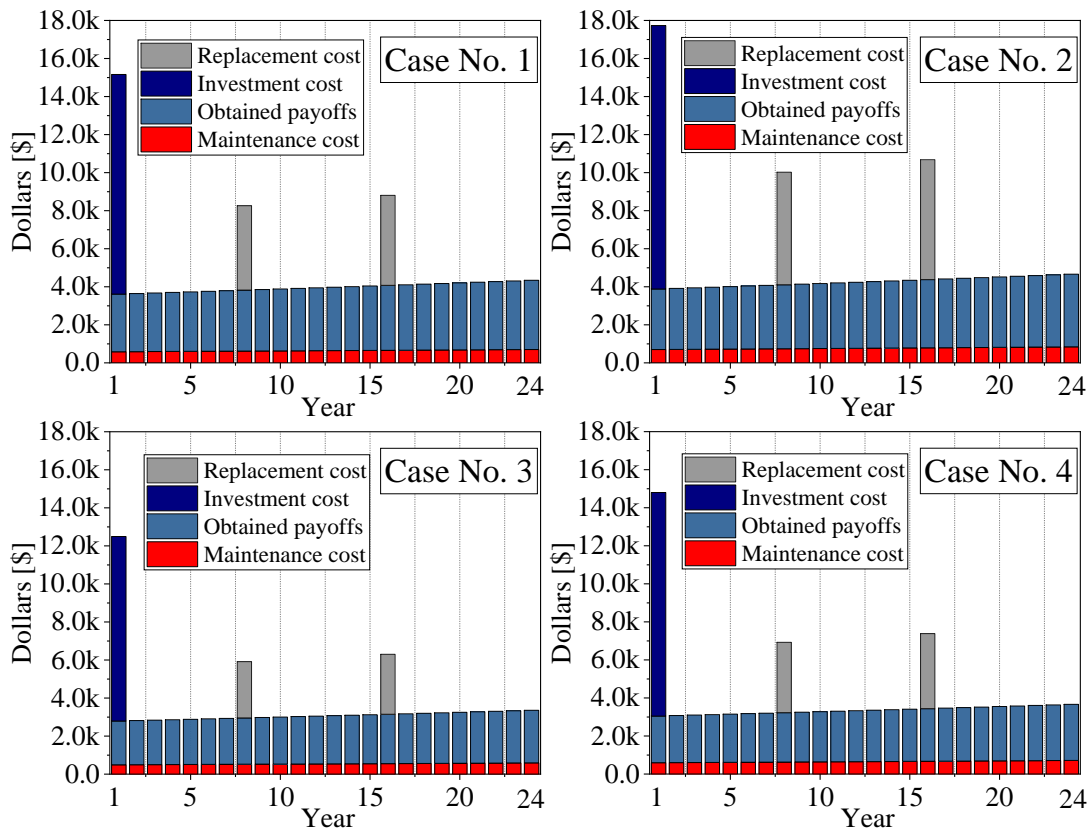


Fig. 5: System cash flow during the planning horizon for Case No. 1-4

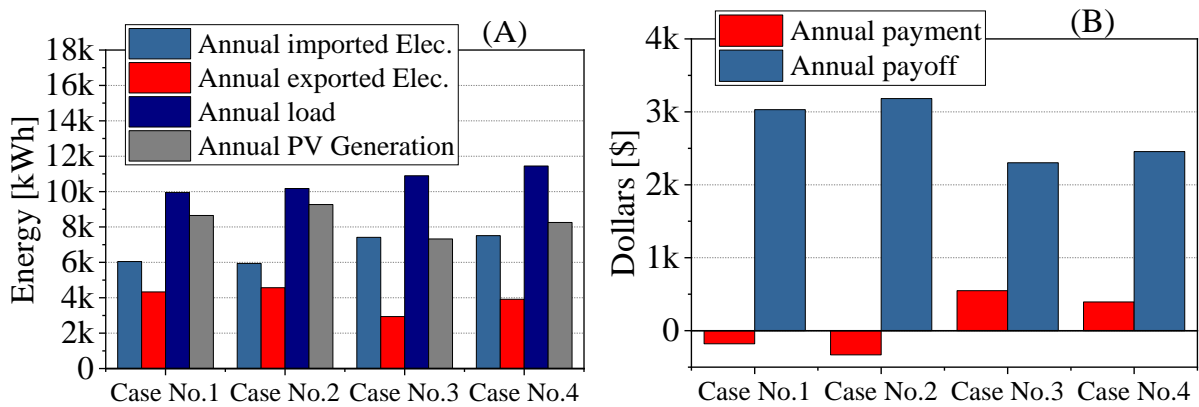


Fig. 6: Annual energy flow and annual payments/payoffs

TABLE II. Under study cases

Cases	No. 1	No. 2	No. 3	No. 4
Ψ^u	0	16	32	48
Deviation	0%	5%	10%	15%

TABLE III. Obtained PV-battery sizing/operation results for each case

Cases	No. 1	No. 2	No. 3	No. 4
Value of objective function	15028	16702	20107	21498
PV capacity [kW]	4.9	5.5	4.6	5.5
Battery Capacity [kWh]	6	8	4	5
Investment cost [\$]	11550	13850	9700	11750
Annual maintenance cost [\$]	577.5	692.5	485.0	587.5
Annual energy trade cost [\$]	-179.7	-331.7	548.1	394.3
CoE [\$/kWh]	0.143	0.156	0.175	0.178
Number of primal cuts	2	4	4	3
Computation time (s)	164	373	296	252

In Case No. 3, however, the value of these costs become lower than the other cases. This is because of the lower PV/battery capacity in this case (see Table III).

Fig. 6A gives the annual imported/exported electricity as well as the annual PV generation and load for each case. It is seen that these values are dependent on system capacity. This is because, the higher/lower capacities of PV-battery system provide more/less ability in terms of exporting electricity to the grid. The annual load has been also increased from Case No. 1 to 4 as the

robustness level has increased in these cases. However, the PV generation is not following such a trend as it is correspondingly dependent on the obtained PV sizing solutions as described in Table III.

The obtained payments/payoffs are given by Fig. 6B for each case. As it is seen, in higher capacities of PV and battery i.e., cases No. 1 and 2, the annual payment is negative which is due to the higher benefits of exported electricity. Although, the value of exported electricity is lower than the imported electricity in these cases (see Fig. 6A), the electricity is mainly imported/exported in low/high price hours which is due to the storage ability in providing arbitrage between these hours. In cases No. 3 and 4, however, payments are positive. This means the benefits of exported electricity are lower than the payments which is due to the lower system capacity in these cases.

The optimal operational solutions, including grid interactions (import/export from/to the grid), PV generation, household load, and battery level have been illustrated by Fig. 7. These results are specified for two working sample days including 180th day, as a cloudy day sample, and 290th day, as a sunny day sample. Note that, these variables are obtained as wait-and-see decision variables which are determined considering the worst-case realization of uncertain parameters. As it is seen in Fig. 7, most of the consumed electricity by load is imported from the grid in day 180 (in all cases), which is due to the lower values of PV generation in this cloudy day. In contrary, the produced electricity by PV has a higher value in day 290 and is mostly exported to the grid or stored by battery during daylight hours (in all cases). Since, peak load periods are after the daylight hours, the battery contributes in optimal system operation by providing arbitrage between these time periods. These results have been obtained considering the worst-case

realization of PV generation and load.

To highlight the optimality of the obtained robust solutions in cases No. 2-4, the deterministic PV-battery sizing solution of Case No. 1 (a deterministic case with no uncertainty characterization) has been examined with the uncertainties in cases No. 2-4. In this examination, the sizing variables are fixed on the obtained deterministic sizing solutions in Case No. 1 ($A = 4.9$ kW and $B = 6$ kWh). According to the obtained results in Fig. 8A, the value of annual imported/exported electricity has increased/decreased due to the PV generation and load uncertainties in cases No. 2-4. This is because, the employed deterministic sizing decisions in case No. 1 are obtained with no uncertainty consideration.

Although, the load and the capacity of PV are fixed in cases 2-4, the load/PV generation increases/reduces from Case No. 2 to Case No. 4. This is due to the uncertainty realization in these cases which becomes more robust (see Table II). Fig. 8B shows the increase of the objective function value in cases No. 2-4. CoE has also increased in each case compared to the obtained values in Table III. Therefore, the obtained operational results of cases No. 2-4 are not optimal when applying the deterministic sizing solutions of Case No. 1.

C. Post-event Analysis

According to the obtained results, the higher values of robustness level lead to more immunized PV-battery sizing/operation solutions which is considered as "robustness worth".

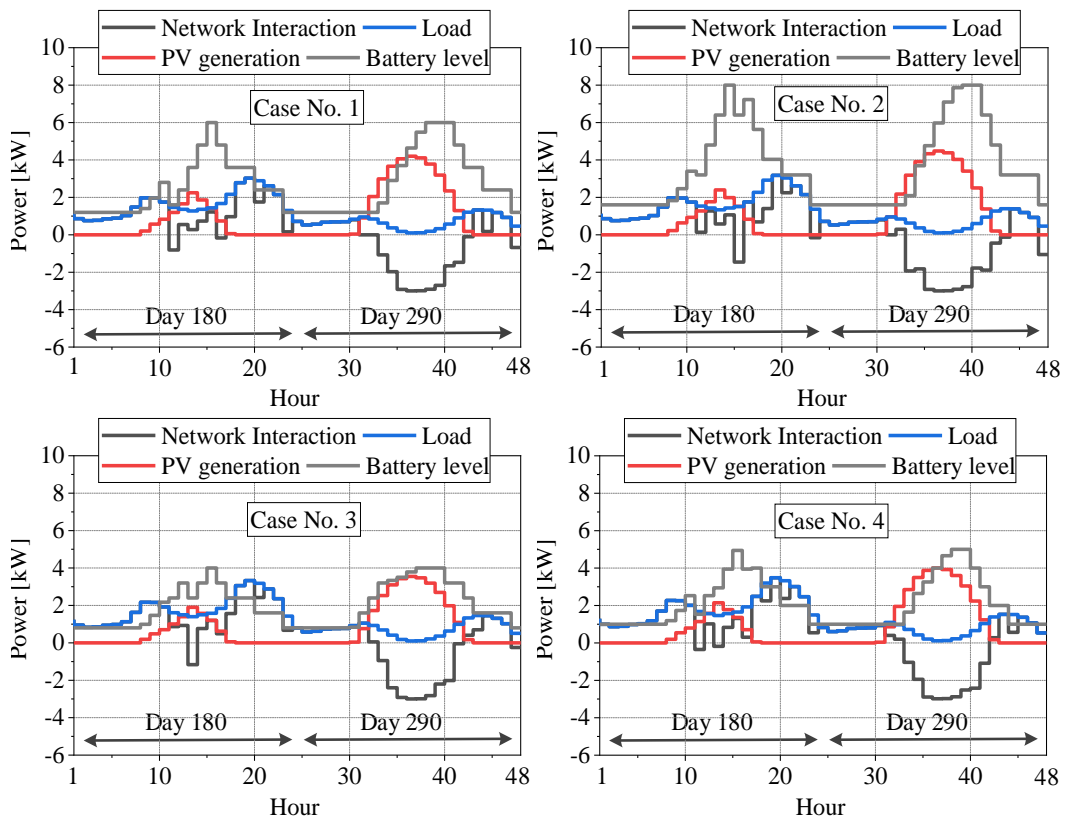


Fig. 7: Optimal system operation for days 180 and 290

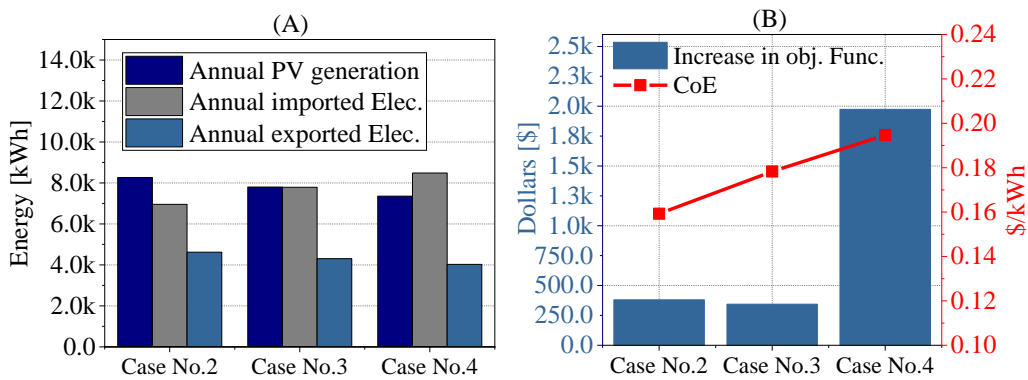


Fig. 8: Operational results of cases No. 2-4 using the capacity of case No. 1

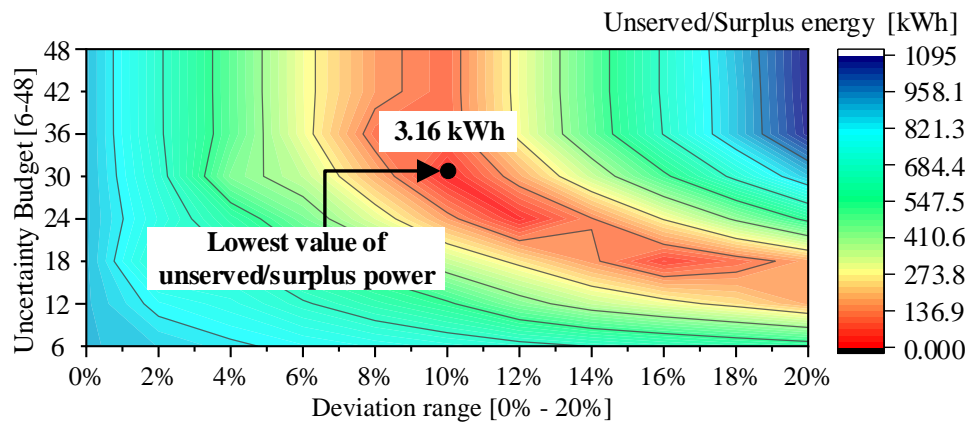


Fig. 9: Post-event analysis results for different robustness levels

However, it causes higher costs in both sizing and operational aspects, as shown in Table III in which the value of objective function increases as the robustness level rises. This imposed cost is considered as "robustness cost". To provide an optimal balance between the robustness worth and robustness cost, and to evaluate the long-run effectiveness of the proposed ARO model, a post-event analysis has been conducted in this study. The aim of this analysis is to determine the optimal robust settings to avoid over/under design solutions. In this analysis, the sizing and operation solutions are fixed on the obtained values from solving the proposed ARO model for different robustness levels. These solutions are examined against 36500 uncertainty realizations of PV generation and load. A new variable models the required unserved/surplus power to stabilize the system when facing uncertainties in lower/higher robustness levels. The unserved/surplus power, pertaining to each robustness level, is then aggregated and scaled over the total number of uncertainty realizations. The robustness level leading to the lowest value of unserved/surplus power is selected as the optimum settings of the ARO model. The obtained results of the conducted post-event analysis are given by Fig. 9. As it is seen, the lowest value of

unserved/surplus power is 3.16 kW which occurs when 30 number of uncertain parameters deviate as 10% of their forecast values. Therefore, allocating these values as robustness level, results in the most effective and reliable sizing/operation solution. Moreover, in lower/higher values of robustness level the model is under/over conservative against the uncertainties, which results in higher values of unserved/surplus power accordingly (i.e., bottom left and top right of Fig. 9).

D. Sensitivity Analysis

In this section, a sensitivity analysis has been conducted to determine the annual cost-of-electricity for different values of PV and battery prices. In this analysis, the price of PV varies from 1000 \$/kW to 1700 \$/kW (for a fixed battery price i.e., 700\$/kWh), while, the battery price varies from 300 \$/kWh to 1100 \$/kWh (for a fixed PV price i.e., 1500\$/kW). The current price of PV and battery has been pointed out in Fig. 10.

Note that, the price of PV and battery are expected to decrease in future which has been also pointed out at Fig. 10. Based on the results, given by Fig. 10, CoE is highly sensitive to PV and battery price as expected. It has an increasing pattern as battery price increases in Fig. 10A. However, after 900 \$/kWh as battery price, no battery is allocated as it is more beneficial to not to have a battery with that price. The value of CoE is also increasing as the PV price increases in Fig. 10B. Moreover, the battery capacity changes with PV price deviations. Therefore, in lower capacities of PV, it is not beneficial to have a high battery capacity. In a similar way, PV capacity depends on battery price changes as seen in Fig. 10A. This shows the cross effects between PV and battery prices and the allocated capacities for each element which is due to the operational

dependencies between these elements.

E. Comparison with Previous Uncertainty Modelling Methods:

In the following, the proposed model of this paper is qualitatively compared to stochastic models and single-stage robust models in the literature to highlight the advantages of the employed two-stage robust model in this study:

F. Comparison with Stochastic Programming Models:

Stochastic models and scenario-based models such as Monte Carlo simulation, use scenario generation techniques to simulate different possible deviations of uncertain parameters. Although, scenario-based approaches are more efficient than deterministic models, in which no uncertainty is considered, they are subject to a great number of scenarios to be considered in calculations, which may not be applicable in practice. Moreover, if an uncertain parameter deviates from the considered scenarios, the solution of the model would not be feasible. To remedy, the number of considered scenarios can be increased to have a more realistic presentation of the uncertainties. However, this may also result in a higher computation time and non-tractability in some cases, especially when several uncertain parameters need to be considered.

On the contrary, the two-stage robust technique in this paper models the uncertainties through bounded intervals by means of polyhedral uncertainty sets instead of scenarios. In fact, it considers the extreme points of uncertainty sets as the worst-case realization of uncertainties. This approach provides user a more moderate computational burden which is due to the fact that,

it once calculates the solution based on the extreme points, instead of calculating numerous scenarios. Therefore, the robust solutions are feasible as long as the uncertainties are within the bounded intervals.

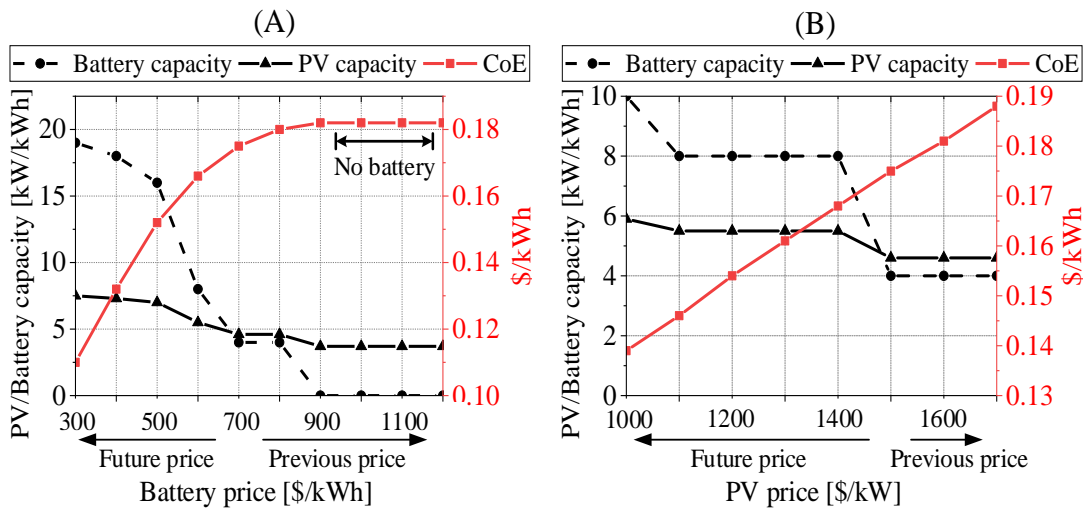


Fig. 10: Sensitivity analysis results

Moreover, the need of full distributional knowledge of uncertain parameters is eliminated as no scenario generation is required.

G. Comparison with single-stage robust optimization models:

In planning models, some variables are not dependent on uncertainties. For example, the sizing solutions in planning models are independent of uncertainties while the operational variables are strongly dependent on uncertainties. This is due to the fact, the planning decisions are made prior to uncertainties (known as "here-and-now" variables), while, the system operational decisions are made at the presence of uncertainties (known as "wait-and-see" variables).

A single-stage robust model cannot model both "here-and-now" and "wait-and-see" variables as it is formulated as a max-min mathematical framework. More specifically, the outer max problem maximizes the objective function over the uncertain parameters, while, the inner min problem minimizes it over the decision variables (with no uncertainty related consideration of variables). Therefore, as long as all the variables are considered in the inner min problem as "here-and-now" decisions, no "wait-and-see" decision can be made prior to uncertainties in single-stage robust models.

In two-stage min-max-min robust models, such as the presented model in this study, there is an additional outer min problem which characterizes "here-and-now" decisions by determining the optimal value of uncertainty non-dependent variables (planning variables in this study). Therefore, as a qualitative comparison, it is noted that the proposed two-stage min-max-min robust solution approach is capable to characterize both "here-and-now" and "wait-and-see" decision variables, while, a single-stage max-min robust model can only characterize "wait-and-see" decision variables. To conclude, it is quite clear that the proposed sizing and operation co-optimization model in this paper cannot be solved through a single-stage max-min robust model as it involves "here-and-now" decisions including sizing variables.

VI. CONCLUSION

This paper proposed an adaptive robust approach to optimal sizing and operation of residential PV-battery systems under uncertain PV generation and load. The objective was to determine the optimal and robust capacity of a residential PV-battery system while maximizing its payoffs by operating PV-battery system in a least-cost manner. The column-and-constraint technique was

employed to solve the proposed model through a decomposition methodology, recasting the tri-level min-max-min problem into a single-level master problem and a bi-level sub-problem. Duality theory and Big-M transformation technique were applied to solve the sub-problem. Optimal sizing/operation solutions were obtained for four cases with different uncertainty budget and deviation range of uncertain parameters. According to numerical results, both the sizing and the operation solutions of PV-battery system became more conservative as the robustness level increased. Since, non-accurate values of robustness level may lead to non-optimal solutions, a post-event analysis was developed against different realizations of uncertain parameters to avoid over/under conservative solutions. The optimal robustness level was found as 30 for uncertainty budget with 10% deviation of uncertain parameters. These robust settings, therefore, lead to the lowest value of additional costs if the uncertainties arise, resulting in higher benefits for PV-battery owner. The ARO model in this study assists renewable energy owners/merchants to appropriately design their PV-battery systems considering the volatile nature of PV generation and their load.

VII. References

- [1] Australian PV Institute, Mapping Australian Photovoltaic installations, <https://pv-map.apvi.org.au/historical#4/-26.67/134.12>
- [2] N. Beniwal, I. Hussain and B. Singh, "Vector-Based Synchronization Method for Grid Integration of Solar PV-Battery System," in *IEEE Transactions on Industrial Informatics*, vol. 15, no. 9, pp. 4923-4933, Sept. 2019.
- [3] K. Chaudhari, A. Ukil, K. N. Kumar, U. Manandhar and S. K. Kollimalla, "Hybrid Optimization for Economic Deployment of ESS in PV-Integrated EV Charging Stations," in *IEEE Transactions on Industrial Informatics*, vol. 14, no. 1, pp. 106-116, Jan. 2018.
- [4] A. Saez-de-Ibarra, A. Milo, H. Gaztañaga, V. Debusschere, S. Bacha, "Co-Optimization of Storage System Sizing and Control Strategy for Intelligent Photovoltaic Power Plants Market Integration," in *IEEE Transactions on Sustainable Energy*, vol. 7, no. 4, pp. 1749-1761, Oct. 2016.
- [5] S. A. Pourmousavi Kani, P. Wild and T. K. Saha, "Improving Predictability of Renewable Generation through Optimal Battery Sizing," in *IEEE Transactions on Sustainable Energy*. doi: 10.1109/TSTE.2018.2883424
- [6] A. J. Conejo, M. Carrion, J. M. Morales, "Decision Making Under Uncertainty in Electricity Markets," Springer, New York, USA, 2010.

- [7] M. Alhaider and L. Fan, "Planning Energy Storage and Photovoltaic Panels for Demand Response With Heating Ventilation and Air Conditioning Systems," in *IEEE Transactions on Industrial Informatics*, vol. 14, no. 11, pp. 5029-5037, Nov. 2018.
- [8] A. Maleki, M. G. Khajeh, M. Ameri, "Optimal sizing of a grid independent hybrid renewable energy system incorporating resource uncertainty, and load uncertainty," in *International Journal of Electrical Power & Energy Systems*, vol. 83, pp. 514-524, Dec. 2016.
- [9] X. Yang, H. He, J. Li and Y. Zhang, "Toward Optimal Risk-Averse Configuration for HESS with CGANs-Based PV Scenario Generation," in *IEEE Transactions on Systems, Man, and Cybernetics: Systems*.
- [10] L. Zhou, Y. Zhang, X. Lin, C. Li, Z. Cai, P. Yang, "Optimal Sizing of PV and BESS for a Smart Household Considering Different Price Mechanisms," in *IEEE Access*, vol. 6, pp. 41050-41059, 2018.
- [11] H. Bludszweit, J. A. Dominguez-Navarro, "A Probabilistic Method for Energy Storage Sizing Based on Wind Power Forecast Uncertainty," in *IEEE Transactions on Power Systems*, vol. 26, no. 3, pp. 1651-1658, Aug. 2011.
- [12] M. S. Islam, N. Mithulananthan, K. Y. Lee, "Suitability of PV and Battery Storage in EV Charging at Business Premises," in *IEEE Transactions on Power Systems*, vol. 33, no. 4, pp. 4382-4396, July 2018.
- [13] R. Hemmati, H. Saboori, "Stochastic optimal battery storage sizing and scheduling in home energy management systems equipped with solar photovoltaic panels," *Energy and Buildings*, Vol. 152, pp. 290-300, 2017.

- [14] A. Dolatabadi, B. Mohammadi-Ivatloo, "Stochastic Risk-Constrained Optimal Sizing for Hybrid Power System of Merchant Marine Vessels," in *IEEE Transactions on Industrial Informatics*, vol. 14, no. 12, pp. 5509-5517, Dec. 2018.
- [15] T. Schittekatte, M. Stadler, G. Cardoso, S. Mashayekh and N. Sankar, "The Impact of Short-Term Stochastic Variability in Solar Irradiance on Optimal Microgrid Design," in *IEEE Transactions on Smart Grid*, vol. 9, no. 3, pp. 1647-1656, May 2018.
- [16] H. Alharbi, K. Bhattacharya, "Stochastic Optimal Planning of Battery Energy Storage Systems for Isolated Microgrids," in *IEEE Transactions on Sustainable Energy*, vol. 9, no. 1, pp. 211-227, Jan. 2018.
- [17] A. Jalali, M. Aldeen, "Risk-Based Stochastic Allocation of ESS to Ensure Voltage Stability Margin for Distribution Systems," in *IEEE Transactions on Power Systems*, vol. 34, no. 2, pp. 1264-1277, March 2019.
- [18] FX. Liu, L. Ma, X. Kong and K. Y. Lee, "Robust Model Predictive Iterative Learning Control for Iteration-Varying-Reference Batch Processes," in *IEEE Transactions on Systems, Man, and Cybernetics: Systems*, Early Access, pp. 1-13, August 2019.
- [19] Y. Liu et al., "Distributed Robust Energy Management of a Multi-microgrid System in the Real-Time Energy Market," in *IEEE Transactions on Sustainable Energy*, vol. 10, no. 1, pp. 396-406, Jan. 2019.
- [20] M. Aghamohamadi, A. Mahmoudi, "From Bidding Strategy in Smart Grid Toward Integrated Bidding Strategy in Smart Multi-energy Systems, an Adaptive Robust Solution Approach," in *Energy*, vol. 183, pp. 75-91, 2019.
- [21] B. Zeng, L. Zhao, "Solving Two-Stage Robust Optimization Problems Using a Column-and-Constraint Generation Method," *Operation Research*, vol. 41, pp. 457-461, 2013.

- [22] Wholesale Solar, www.wholesalesolar.com. Accessed: June 2019.
- [23] Australian Energy Market Operator (AEMO), <https://www.aemo.com.au>. Accessed: September 2019.
- [24] M. Combe, A. Mahmoudi, M. H. Haque and R. Khezri, "Cost-effective sizing of an AC mini-grid hybrid power system for a remote area in South Australia," in *IET Generation, Transmission & Distribution*, vol. 13, no. 2, pp. 277-287, 22 1 2019.
- [25] AGL Energy, www.agl.com.au. Accessed: September 2019.
- [26] CPLEX software package, available online on: www.ibm.com/analytics/cplex-optimizer.

9. References

- [1] B. Bertok and A. Bartos, "Renewable energy storage and distribution scheduling for microgrids by exploiting recent developments in process network synthesis," *Journal of Cleaner Production*, vol. 244, p. 118520, 2020.
- [2] R. R. Kumar and K. Alok, "Adoption of electric vehicle: A literature review and prospects for sustainability," *Journal of Cleaner Production*, vol. 253, p. 119911, 2020/04/20/ 2020.
- [3] L. Luo and W. W. Gu, Y.; Chen, C., "An Affine Arithmetic-Based Power Flow Algorithm Considering the Regional Control of Unscheduled Power Fluctuation," *Energies* vol. 10, p. 1794
2017.
- [4] K. M. Muttaqi, M. R. Islam, and D. Sutanto, "Future Power Distribution Grids: Integration of Renewable Energy, Energy Storage, Electric Vehicles, Superconductor, and Magnetic Bus," *IEEE Transactions on Applied Superconductivity*, vol. 29, no. 2, pp. 1-5, 2019, doi: 10.1109/TASC.2019.2895528.
- [5] G. Masson and M. Brunisholz, "IEA PVPS trends 2015 in photovoltaic applications," IEA Int. Energy Agency, Paris, France, Tech. Rep. IEA-PVPS T1-27, 2015.
- [6] L. Luo, Z. Wu, W. Gu, H. Huang, S. Gao, and J. Han, "Coordinated allocation of distributed generation resources and electric vehicle charging stations in distribution systems with vehicle-to-grid interaction," *Energy*, vol. 192, p. 116631, 2020/02/01/ 2020.
- [7] A. J. Conejo, M. Carrión, and J. M. Morales, *Decision Making Under Uncertainty in Electricity Markets*. New York, USA: Springer, 2010.
- [8] S. Davidov and M. Pantoš, "Optimization model for charging infrastructure planning with electric power system reliability check," *Energy*, vol. 166, pp. 886-894, 2019/01/01/ 2019.
- [9] M. Honarmand, A. Zakariazadeh, and S. Jadid, "Optimal scheduling of electric vehicles in an intelligent parking lot considering vehicle-to-grid concept and battery condition," *Energy*, vol. 65, pp. 572-579, 2014/02/01/ 2014.
- [10] S. Tabatabaee, S. S. Mortazavi, and T. Niknam, "Stochastic scheduling of local distribution systems considering high penetration of plug-in electric vehicles and renewable energy sources," *Energy*, vol. 121, pp. 480-490, 2017/02/15/ 2017.
- [11] R. Mehta, D. Srinivasan, A. M. Khambadkone, J. Yang, and A. Trivedi, "Smart Charging Strategies for Optimal Integration of Plug-In Electric Vehicles Within Existing Distribution System Infrastructure," *IEEE Transactions on Smart Grid*, vol. 9, no. 1, pp. 299-312, 2018, doi: 10.1109/TSG.2016.2550559.
- [12] M. Ş. Kuran, A. C. Viana, L. Iannone, D. Kofman, G. Mermoud, and J. P. Vasseur, "A Smart Parking Lot Management System for Scheduling the Recharging of Electric Vehicles," *IEEE Transactions on Smart Grid*, vol. 6, no. 6, pp. 2942-2953, 2015, doi: 10.1109/TSG.2015.2403287.
- [13] S. Rezaee, E. Farjah, and B. Khorramdel, "Probabilistic Analysis of Plug-In Electric Vehicles Impact on Electrical Grid Through Homes and Parking Lots," *IEEE Transactions on Sustainable Energy*, vol. 4, no. 4, pp. 1024-1033, 2013.
- [14] X. Dong *et al.*, "A charging pricing strategy of electric vehicle fast charging stations for the voltage control of electricity distribution networks," *Applied Energy*, vol. 225, pp.

- 857-868, 2018/09/01/ 2018.
- [15] S.-K. Moon and J.-O. Kim, "Balanced charging strategies for electric vehicles on power systems," *Applied Energy*, vol. 189, pp. 44-54, 2017/03/01/ 2017.
- [16] B. Yagcitekin and M. Uzunoglu, "A double-layer smart charging strategy of electric vehicles taking routing and charge scheduling into account," *Applied Energy*, vol. 167, pp. 407-419, 2016/04/01/ 2016.
- [17] R. Mehta, P. Verma, D. Srinivasan, and J. Yang, "Double-layered intelligent energy management for optimal integration of plug-in electric vehicles into distribution systems," *Applied Energy*, vol. 233-234, pp. 146-155, 2019/01/01/ 2019.
- [18] A. Kavousi-Fard, T. Niknam, and M. Fotuhi-Firuzabad, "Stochastic Reconfiguration and Optimal Coordination of V2G Plug-in Electric Vehicles Considering Correlated Wind Power Generation," *IEEE Transactions on Sustainable Energy*, vol. 6, no. 3, pp. 822-830, 2015, doi: 10.1109/TSTE.2015.2409814.
- [19] G. Sun *et al.*, "Distribution Network Reconfiguration Based on SOCP Considering the Access of Photovoltaic Electric Vehicle Charging Tower," in *2018 China International Conference on Electricity Distribution (CICED)*, 17-19 Sept. 2018 2018, pp. 2047-2050, doi: 10.1109/CICED.2018.8592600.
- [20] L. Zhechao, W. Shaorong, S. Jazebi, F. d. León, and J. Wang, "Assessing the effect of system reconfiguration to enhance the capacity of electric-vehicle charging stations in radial distribution systems," in *2016 IEEE Power and Energy Society General Meeting (PESGM)*, 17-21 July 2016 2016, pp. 1-5, doi: 10.1109/PESGM.2016.7741921.
- [21] P. Satapathy, S. Dhar, and P. K. Dash, "Performance validation of battery management system under prediction error for photovoltaic based distribution system," *IET Renewable Power Generation*, vol. 12, no. 6, pp. 702-717, 2018, doi: 10.1049/iet-rpg.2017.0286.
- [22] G. Carpinelli, P. Caramia, and P. Varilone, "Multi-linear Monte Carlo simulation method for probabilistic load flow of distribution systems with wind and photovoltaic generation systems," *Renewable Energy*, vol. 76, pp. 283-295, 2015/04/01/ 2015, doi: <https://doi.org/10.1016/j.renene.2014.11.028>.
- [23] G. E. Constante-Flores and M. Illindala, "Data-driven probabilistic power flow analysis for a distribution system with Renewable Energy sources using Monte Carlo Simulation," in *2017 IEEE/IAS 53rd Industrial and Commercial Power Systems Technical Conference (I&CPS)*, 6-11 May 2017 2017, pp. 1-8, doi: 10.1109/ICPS.2017.7945118.
- [24] A. Samimi, M. Nikzad, and P. Siano, "Scenario-based stochastic framework for coupled active and reactive power market in smart distribution systems with demand response programs," *Renewable Energy*, vol. 109, pp. 22-40, 2017/08/01/ 2017, doi: <https://doi.org/10.1016/j.renene.2017.03.010>.
- [25] A. Zakariazadeh, S. Jadid, and P. Siano, "Economic-environmental energy and reserve scheduling of smart distribution systems: A multiobjective mathematical programming approach," *Energy Conversion and Management*, vol. 78, pp. 151-164, 2014/02/01/ 2014, doi: <https://doi.org/10.1016/j.enconman.2013.10.051>.
- [26] A. Akrami, M. Doostizadeh, and F. Aminifar, "Optimal Reconfiguration of Distribution Network Using μ PMU Measurements: A Data-Driven Stochastic Robust Optimization," *IEEE Transactions on Smart Grid*, vol. 11, no. 1, pp. 420-428, 2020, doi: 10.1109/TSG.2019.2923740.
- [27] T. Huiling, W. Jiekang, W. Fan, C. Lingmin, L. Zhijun, and Y. Haoran, "An Optimization

- Framework for Collaborative Control of Power Loss and Voltage in Distribution Systems With DGs and EVs Using Stochastic Fuzzy Chance Constrained Programming," *IEEE Access*, vol. 8, pp. 49013-49027, 2020.
- [28] Y. Jiang, C. Wan, C. Chen, M. Shahidehpour, and Y. Song, "A Hybrid Stochastic-Interval Operation Strategy for Multi-Energy Microgrids," *IEEE Transactions on Smart Grid*, vol. 11, no. 1, pp. 440-456, 2020, doi: 10.1109/TSG.2019.2923984.
- [29] M. Vahedipour-Dahraie, H. Rashidizadeh-Kermani, A. Anvari-Moghaddam, and J. M. Guerrero, "Stochastic Risk-Constrained Scheduling of Renewable-Powered Autonomous Microgrids With Demand Response Actions: Reliability and Economic Implications," *IEEE Transactions on Industry Applications*, vol. 56, no. 2, pp. 1882-1895, 2020, doi: 10.1109/TIA.2019.2959549.
- [30] M. Lubin, Y. Dvorkin, and S. Backhaus, "A Robust Approach to Chance Constrained Optimal Power Flow With Renewable Generation," *IEEE Transactions on Power Systems*, vol. 31, no. 5, pp. 3840-3849, 2016, doi: 10.1109/TPWRS.2015.2499753.
- [31] Y. Zhang, X. Ai, J. Wen, J. Fang, and H. He, "Data-Adaptive Robust Optimization Method for the Economic Dispatch of Active Distribution Networks," *IEEE Transactions on Smart Grid*, vol. 10, no. 4, pp. 3791-3800, 2019, doi: 10.1109/TSG.2018.2834952.
- [32] H. Gao, J. Liu, and L. Wang, "Robust Coordinated Optimization of Active and Reactive Power in Active Distribution Systems," *IEEE Transactions on Smart Grid*, vol. 9, no. 5, pp. 4436-4447, 2018, doi: 10.1109/TSG.2017.2657782.
- [33] T. Soares, R. J. Bessa, P. Pinson, and H. Morais, "Active Distribution Grid Management Based on Robust AC Optimal Power Flow," *IEEE Transactions on Smart Grid*, vol. 9, no. 6, pp. 6229-6241, 2018, doi: 10.1109/TSG.2017.2707065.
- [34] B. Zeng and L. Zhao, "Solving two-stage robust optimization problems using a column-and-constraint generation method," *Operations Research Letters*, vol. 41, no. 5, pp. 457-461, 2013/09/01/ 2013.
- [35] M. Guzelsoy and T. K. Ralphs, "Duality for Mixed-Integer Linear Programs," *International Journal of Operations Research*, vol. 4, no. 3, pp. 118-137, 2007.
- [36] G. R. C. Mouli, M. Kefayati, R. Baldick, and P. Bauer, "Integrated PV Charging of EV Fleet Based on Energy Prices, V2G, and Offer of Reserves," *IEEE Transactions on Smart Grid*, vol. 10, no. 2, pp. 1313-1325, 2019, doi: 10.1109/TSG.2017.2763683.
- [37] Y. Song, Y. Zheng, and D. J. Hill, "Optimal Scheduling for EV Charging Stations in Distribution Networks: A Convexified Model," *IEEE Transactions on Power Systems*, vol. 32, no. 2, pp. 1574-1575, 2017, doi: 10.1109/TPWRS.2016.2568746.
- [38] Z. Liu, F. Wen, and G. Ledwich, "Optimal Planning of Electric-Vehicle Charging Stations in Distribution Systems," *IEEE Transactions on Power Delivery*, vol. 28, no. 1, pp. 102-110, 2013, doi: 10.1109/TPWRD.2012.2223489.
- [39] J. Zhu, Y. Li, J. Yang, X. Li, S. Zeng, and Y. Chen, "Planning of electric vehicle charging station based on queuing theory," *The Journal of Engineering*, vol. 2017, no. 13, pp. 1867-1871, 2017, doi: 10.1049/joe.2017.0655.
- [40] M. Jha, F. Blaabjerg, M. A. Khan, V. S. Bharath Kurukuru, and A. Haque, "Intelligent Control of Converter for Electric Vehicles Charging Station," *Energies*, vol. 12, no. 12, p. 2334, 2019. [Online]. Available: <https://www.mdpi.com/1996-1073/12/12/2334>.
- [41] Z. Ding, F. Teng, P. Sarikprueck, and Z. Hu, "Technical Review on Advanced Approaches for Electric Vehicle Charging Demand Management, Part II: Applications in

- Transportation System Coordination and Infrastructure Planning," *IEEE Transactions on Industry Applications*, vol. 56, no. 5, pp. 5695-5703, 2020, doi: 10.1109/TIA.2020.2993760.
- [42] D. Tang and P. Wang, "Probabilistic Modeling of Nodal Charging Demand Based on Spatial-Temporal Dynamics of Moving Electric Vehicles," *IEEE Transactions on Smart Grid*, vol. 7, no. 2, pp. 627-636, 2016, doi: 10.1109/TSG.2015.2437415.
- [43] V. T. Tran, M. R. Islam, K. M. Muttaqi, and D. Sutanto, "An Efficient Energy Management Approach for a Solar-Powered EV Battery Charging Facility to Support Distribution Grids," *IEEE Transactions on Industry Applications*, vol. 55, no. 6, pp. 6517-6526, 2019, doi: 10.1109/TIA.2019.2940923.
- [44] P. H. Divshali and C. Evens, "Stochastic bidding strategy for electrical vehicle charging stations to participate in frequency containment reserves markets," *IET Generation, Transmission & Distribution*, vol. 14, no. 13, pp. 2566-2572, 2020, doi: 10.1049/iet-gtd.2019.0906.
- [45] H. Yang *et al.*, "Operational Planning of Electric Vehicles for Balancing Wind Power and Load Fluctuations in a Microgrid," *IEEE Transactions on Sustainable Energy*, vol. 8, no. 2, pp. 592-604, 2017, doi: 10.1109/TSST.2016.2613941.
- [46] S. Bae and A. Kwasinski, "Spatial and Temporal Model of Electric Vehicle Charging Demand," *IEEE Transactions on Smart Grid*, vol. 3, no. 1, pp. 394-403, 2012, doi: 10.1109/TSG.2011.2159278.
- [47] Y. Zheng, Y. Song, D. J. Hill, and K. Meng, "Online Distributed MPC-Based Optimal Scheduling for EV Charging Stations in Distribution Systems," *IEEE Transactions on Industrial Informatics*, vol. 15, no. 2, pp. 638-649, 2019, doi: 10.1109/TII.2018.2812755.
- [48] M. Singh, P. Kumar, and I. Kar, "A Multi Charging Station for Electric Vehicles and Its Utilization for Load Management and the Grid Support," *IEEE Transactions on Smart Grid*, vol. 4, no. 2, pp. 1026-1037, 2013, doi: 10.1109/TSG.2013.2238562.
- [49] M. Singh, K. Thirugnanam, P. Kumar, and I. Kar, "Real-Time Coordination of Electric Vehicles to Support the Grid at the Distribution Substation Level," *IEEE Systems Journal*, vol. 9, no. 3, pp. 1000-1010, 2015, doi: 10.1109/JSYST.2013.2280821.
- [50] J. Xiong, K. Zhang, Y. Guo, and W. Su, "Investigate the Impacts of PEV Charging Facilities on Integrated Electric Distribution System and Electrified Transportation System," *IEEE Transactions on Transportation Electrification*, vol. 1, no. 2, pp. 178-187, 2015, doi: 10.1109/TTE.2015.2443798.
- [51] Q. Chen, N. Liu, C. Hu, L. Wang, and J. Zhang, "Autonomous Energy Management Strategy for Solid-State Transformer to Integrate PV-Assisted EV Charging Station Participating in Ancillary Service," *IEEE Transactions on Industrial Informatics*, vol. 13, no. 1, pp. 258-269, 2017, doi: 10.1109/TII.2016.2626302.
- [52] M. Rahmani-Andebili and M. Fotuhi-Firuzabad, "An Adaptive Approach for PEVs Charging Management and Reconfiguration of Electrical Distribution System Penetrated by Renewables," *IEEE Transactions on Industrial Informatics*, vol. 14, no. 5, pp. 2001-2010, 2018, doi: 10.1109/TII.2017.2761336.
- [53] G. Ma, M. Ghasemi, and X. Song, "Integrated Powertrain Energy Management and Vehicle Coordination for Multiple Connected Hybrid Electric Vehicles," *IEEE Transactions on Vehicular Technology*, vol. 67, no. 4, pp. 2893-2899, 2018, doi: 10.1109/TVT.2017.2780268.

- [54] S. Amamra and J. Marco, "Vehicle-to-Grid Aggregator to Support Power Grid and Reduce Electric Vehicle Charging Cost," *IEEE Access*, vol. 7, pp. 178528-178538, 2019, doi: 10.1109/ACCESS.2019.2958664.
- [55] H. Yang, S. Yang, Y. Xu, E. Cao, M. Lai, and Z. Dong, "Electric Vehicle Route Optimization Considering Time-of-Use Electricity Price by Learnable Partheno-Genetic Algorithm," *IEEE Transactions on Smart Grid*, vol. 6, no. 2, pp. 657-666, 2015, doi: 10.1109/TSG.2014.2382684.
- [56] A. Ghosh and V. Aggarwal, "Control of Charging of Electric Vehicles Through Menu-Based Pricing," *IEEE Transactions on Smart Grid*, vol. 9, no. 6, pp. 5918-5929, 2018, doi: 10.1109/TSG.2017.2698830.
- [57] X. Li *et al.*, "Price Incentive-Based Charging Navigation Strategy for Electric Vehicles," *IEEE Transactions on Industry Applications*, vol. 56, no. 5, pp. 5762-5774, 2020, doi: 10.1109/TIA.2020.2981275.
- [58] Z. Moghaddam, I. Ahmad, D. Habibi, and M. A. S. Masoum, "A Coordinated Dynamic Pricing Model for Electric Vehicle Charging Stations," *IEEE Transactions on Transportation Electrification*, vol. 5, no. 1, pp. 226-238, 2019, doi: 10.1109/TTE.2019.2897087.
- [59] O. Hafez and K. Bhattacharya, "Integrating EV Charging Stations as Smart Loads for Demand Response Provisions in Distribution Systems," *IEEE Transactions on Smart Grid*, vol. 9, no. 2, pp. 1096-1106, 2018, doi: 10.1109/TSG.2016.2576902.
- [60] S. Shojaabadi, S. Abapour, M. Abapour, and A. Nahavandi, "Optimal planning of plug-in hybrid electric vehicle charging station in distribution network considering demand response programs and uncertainties," *IET Generation, Transmission & Distribution*, vol. 10, no. 13, pp. 3330-3340, 2016, doi: 10.1049/iet-gtd.2016.0312.
- [61] N. B. Arias, A. Tabares, J. F. Franco, M. Lavorato, and R. Romero, "Robust Joint Expansion Planning of Electrical Distribution Systems and EV Charging Stations," *IEEE Transactions on Sustainable Energy*, vol. 9, no. 2, pp. 884-894, 2018, doi: 10.1109/TSTE.2017.2764080.
- [62] S. Wang, Z. Y. Dong, F. Luo, K. Meng, and Y. Zhang, "Stochastic Collaborative Planning of Electric Vehicle Charging Stations and Power Distribution System," *IEEE Transactions on Industrial Informatics*, vol. 14, no. 1, pp. 321-331, 2018, doi: 10.1109/TII.2017.2662711.
- [63] J. Andrade, L. F. Ochoa, and W. Freitas, "Regional-scale allocation of fast charging stations: travel times and distribution system reinforcements," *IET Generation, Transmission & Distribution*, vol. 14, no. 19, pp. 4225-4233, 2020, doi: 10.1049/iet-gtd.2019.1786.
- [64] A. Ehsan and Q. Yang, "Active Distribution System Reinforcement Planning With EV Charging Stations—Part I: Uncertainty Modeling and Problem Formulation," *IEEE Transactions on Sustainable Energy*, vol. 11, no. 2, pp. 970-978, 2020, doi: 10.1109/TSTE.2019.2915338.
- [65] S. Pazouki, A. Mohsenzadeh, S. Ardalan, and M. Haghifam, "Simultaneous Planning of PEV Charging Stations and DGs Considering Financial, Technical, and Environmental Effects," *Canadian Journal of Electrical and Computer Engineering*, vol. 38, no. 3, pp. 238-245, 2015, doi: 10.1109/CJECE.2015.2436811.
- [66] O. Erdiñç, A. Taşçikaraoğlu, N. G. Paterakis, D. İ, M. C. Sinim, and J. P. S. Catalão,

- "Comprehensive Optimization Model for Sizing and Siting of DG Units, EV Charging Stations, and Energy Storage Systems," *IEEE Transactions on Smart Grid*, vol. 9, no. 4, pp. 3871-3882, 2018, doi: 10.1109/TSG.2017.2777738.
- [67] P. M. d. Quevedo, G. Muñoz-Delgado, and J. Contreras, "Impact of Electric Vehicles on the Expansion Planning of Distribution Systems Considering Renewable Energy, Storage, and Charging Stations," *IEEE Transactions on Smart Grid*, vol. 10, no. 1, pp. 794-804, 2019, doi: 10.1109/TSG.2017.2752303.
- [68] D. Yan and C. Ma, "Stochastic planning of electric vehicle charging station integrated with photovoltaic and battery systems," *IET Generation, Transmission & Distribution*, vol. 14, no. 19, pp. 4217-4224, 2020, doi: 10.1049/iet-gtd.2019.1737.
- [69] A. Awasthi, K. Venkitesamy, S. Padmanaban, R. Selvamuthukumar, F. Blaabjerg, and A. K. Singh, "Optimal planning of electric vehicle charging station at the distribution system using hybrid optimization algorithm," *Energy*, vol. 133, pp. 70-78, 2017/08/15/2017, doi: <https://doi.org/10.1016/j.energy.2017.05.094>.
- [70] G. Wang, Z. Xu, F. Wen, and K. P. Wong, "Traffic-Constrained Multiobjective Planning of Electric-Vehicle Charging Stations," *IEEE Transactions on Power Delivery*, vol. 28, no. 4, pp. 2363-2372, 2013, doi: 10.1109/TPWRD.2013.2269142.
- [71] R. Xie, W. Wei, M. E. Khodayar, J. Wang, and S. Mei, "Planning Fully Renewable Powered Charging Stations on Highways: A Data-Driven Robust Optimization Approach," *IEEE Transactions on Transportation Electrification*, vol. 4, no. 3, pp. 817-830, 2018, doi: 10.1109/TTE.2018.2849222.
- [72] G. Battapothula, C. Yammani, and S. Maheswarapu, "Multi-objective simultaneous optimal planning of electrical vehicle fast charging stations and DGs in distribution system," *Journal of Modern Power Systems and Clean Energy*, vol. 7, no. 4, pp. 923-934, 2019, doi: 10.1007/s40565-018-0493-2.
- [73] H. Zhang, S. J. Moura, Z. Hu, and Y. Song, "PEV Fast-Charging Station Siting and Sizing on Coupled Transportation and Power Networks," *IEEE Transactions on Smart Grid*, vol. 9, no. 4, pp. 2595-2605, 2018, doi: 10.1109/TSG.2016.2614939.
- [74] X. Huang, J. Chen, H. Yang, Y. Cao, W. Guan, and B. Huang, "Economic planning approach for electric vehicle charging stations integrating traffic and power grid constraints," *IET Generation, Transmission & Distribution*, vol. 12, no. 17, pp. 3925-3934, 2018, doi: 10.1049/iet-gtd.2018.5456.
- [75] X. Wang, M. Shahidehpour, C. Jiang, and Z. Li, "Coordinated Planning Strategy for Electric Vehicle Charging Stations and Coupled Traffic-Electric Networks," *IEEE Transactions on Power Systems*, vol. 34, no. 1, pp. 268-279, 2019, doi: 10.1109/TPWRS.2018.2867176.
- [76] M. Moradijoz, J. Heidari, M. P. Moghaddam, and M. R. Haghifam, "Electric vehicle parking lots as a capacity expansion option in distribution systems: a mixed-integer linear programming-based model," *IET Electrical Systems in Transportation*, vol. 10, no. 1, pp. 13-22, 2020, doi: 10.1049/iet-est.2018.5062.
- [77] M. Aghamohamadi, M. H. Haque, A. Mahmoudi, and J. K. Ward, "A Novel Directly-solvable Non-iterative Load Flow Model for Radial Distribution System Studies," in *2020 IEEE International Conference on Power Electronics, Drives and Energy Systems (PEDES)*, 16-19 Dec. 2020 2020, pp. 1-6, doi: 10.1109/PEDES49360.2020.9379828.
- [78] H. L. Nguyen, "Newton-Raphson method in complex form [power system load flow

- analysis]," *IEEE Transactions on Power Systems*, vol. 12, no. 3, pp. 1355-1359, 1997, doi: 10.1109/59.630481.
- [79] G. Huang and W. Ongsakul, "Managing the bottlenecks in parallel Gauss-Seidel type algorithms for power flow analysis," *IEEE Transactions on Power Systems*, vol. 9, no. 2, pp. 677-684, 1994, doi: 10.1109/59.317675.
- [80] G. W. Chang, S. Y. Chu, and H. L. Wang, "An Improved Backward/Forward Sweep Load Flow Algorithm for Radial Distribution Systems," *IEEE Transactions on Power Systems*, vol. 22, no. 2, pp. 882-884, 2007, doi: 10.1109/TPWRS.2007.894848.
- [81] A. Kumar, B. K. Jha, D. Singh, and R. K. Misra, "Current injection-based Newton–Raphson power-flow algorithm for droop-based islanded microgrids," *IET Generation, Transmission & Distribution*, vol. 13, no. 23, pp. 5271-5283, 2019, doi: 10.1049/iet-gtd.2019.0575.
- [82] A. G. Fonseca, O. L. Tortelli, and E. M. Lourenço, "Extended fast decoupled power flow for reconfiguration networks in distribution systems," *IET Generation, Transmission & Distribution*, vol. 12, no. 22, pp. 6033-6040, 2018, doi: 10.1049/iet-gtd.2018.5886.
- [83] A. Mahmoudi and S. H. Hosseinian, "Direct solution of distribution system load flow using forward/backward sweep," in *2011 19th Iranian Conference on Electrical Engineering*, 17-19 May 2011 2011, pp. 1-1.
- [84] D. T. K. Viet, K. Agbossou, and M. L. Doumbia, "Voltage unbalance treatment for distribution network with massively connected distributed generators," in *2010 IEEE International Conference on Industrial Technology*, 14-17 March 2010 2010, pp. 994-999, doi: 10.1109/ICIT.2010.5472547.
- [85] T. F. Toledo and V. M. A. León, "Computational Algorithm for the Analysis of Loadability in Distribution Systems," in *2018 IEEE 38th Central America and Panama Convention (CONCAPAN XXXVIII)*, 7-9 Nov. 2018 2018, pp. 1-6, doi: 10.1109/CONCAPAN.2018.8596388.
- [86] S. Lakshmi and S. Ganguly, "Energy loss minimization with open unified power quality conditioner placement in radial distribution networks using particle swarm optimization," in *2017 7th International Conference on Power Systems (ICPS)*, 21-23 Dec. 2017 2017, pp. 55-60, doi: 10.1109/ICPES.2017.8387268.
- [87] M. Moradijuz and M. P. Moghaddam, "Optimum allocation of parking lots in distribution systems for loss reduction," in *2012 IEEE Power and Energy Society General Meeting*, 22-26 July 2012 2012, pp. 1-5, doi: 10.1109/PESGM.2012.6345291.
- [88] R. S. Rao, K. Ravindra, K. Satish, and S. V. L. Narasimham, "Power Loss Minimization in Distribution System Using Network Reconfiguration in the Presence of Distributed Generation," *IEEE Transactions on Power Systems*, vol. 28, no. 1, pp. 317-325, 2013, doi: 10.1109/TPWRS.2012.2197227.
- [89] M. Aghamohamadi, A. Mahmoudi, and M. H. Haque, "Robust Allocation of Residential Solar Photovoltaic Systems Paired with Battery Units in South Australia," in *2019 IEEE Energy Conversion Congress and Exposition (ECCE)*, 29 Sept.-3 Oct. 2019 2019, pp. 6673-6679.
- [90] M. Aghamohamadi, A. Mahmoudi, and M. Haque, "Twostage Robust Sizing and Operation Co-optimization for Residential PV-battery Systems Considering the Uncertainty of PV Generation and Load," *IEEE Transactions on Industrial Informatics*, pp. 1-1, 2020, doi: 10.1109/TII.2020.2990682.

- [91] J. W. P. Hirschfeld and X. Hubaut, "Sets of even type in PG(3, 4), alias the binary (85, 24) projective geometry code," *Journal of Combinatorial Theory, Series A*, vol. 29, no. 1, pp. 101-112, 1980/07/01/ 1980, doi: [https://doi.org/10.1016/0097-3165\(80\)90051-5](https://doi.org/10.1016/0097-3165(80)90051-5).
- [92] D. Das, D. P. Kothari, and A. Kalam, "Simple and efficient method for load flow solution of radial distribution networks," *International Journal of Electrical Power & Energy Systems*, vol. 17, no. 5, pp. 335-346, 1995/10/01/ 1995, doi: [https://doi.org/10.1016/0142-0615\(95\)00050-0](https://doi.org/10.1016/0142-0615(95)00050-0).
- [93] M. E. Baran and F. F. Wu, "Network reconfiguration in distribution systems for loss reduction and load balancing," *IEEE Transactions on Power Delivery*, vol. 4, no. 2, pp. 1401-1407, 1989, doi: 10.1109/61.25627.
- [94] M. Ali, A. Dymarsky, and K. Turitsyn, "Transversality enforced Newton–Raphson algorithm for fast calculation of maximum loadability," *IET Generation, Transmission & Distribution*, vol. 12, no. 8, pp. 1729-1737, 2018, doi: 10.1049/iet-gtd.2017.1273.
- [95] S. Lakshmi and S. Ganguly, "Energy loss minimization with open unified power quality conditioner placement in radial distribution networks using particle swarm optimization," in *2017 7th International Conference on Power Systems (ICPS)*, 21-23 Dec. 2017 2017, pp. 55-60, doi: 10.1109/ICPES.2017.8387268.
- [96] S. K. Injeti and V. K. Thunuguntla, "Optimal integration of DGs into radial distribution network in the presence of plug-in electric vehicles to minimize daily active power losses and to improve the voltage profile of the system using bio-inspired optimization algorithms," *Protection and Control of Modern Power Systems*, vol. 5, no. 1, p. 3, 2020/01/15 2020, doi: 10.1186/s41601-019-0149-x.
- [97] M. Moradijoz and M. P. Moghaddam, "Optimum allocation of parking lots in distribution systems for loss reduction," in *2012 IEEE Power and Energy Society General Meeting*, 22-26 July 2012 2012, pp. 1-5, doi: 10.1109/PESGM.2012.6345291.
- [98] R. S. Rao, K. Ravindra, K. Satish, and S. V. L. Narasimham, "Power Loss Minimization in Distribution System Using Network Reconfiguration in the Presence of Distributed Generation," *IEEE Transactions on Power Systems*, vol. 28, no. 1, pp. 317-325, 2013, doi: 10.1109/TPWRS.2012.2197227.
- [99] A. J. Pimm, T. T. Cockerill, and P. G. Taylor, "The potential for peak shaving on low voltage distribution networks using electricity storage," *Journal of Energy Storage*, vol. 16, pp. 231-242, 2018/04/01/ 2018, doi: <https://doi.org/10.1016/j.est.2018.02.002>.
- [100] H. Saboori and H. Abdi, "Application of a grid scale energy storage system to reduce distribution network losses," in *18th Electric Power Distribution Conference*, 30 April-1 May 2013 2013, pp. 1-5, doi: 10.1109/EPDC.2013.6565963.
- [101] R. Hemmati, H. Saboori, and M. A. Jirdehi, "Stochastic planning and scheduling of energy storage systems for congestion management in electric power systems including renewable energy resources," *Energy*, vol. 133, pp. 380-387, 2017/08/15/ 2017, doi: <https://doi.org/10.1016/j.energy.2017.05.167>.
- [102] A. S. A. Awad, T. H. M. E.-. Fouly, and M. M. A. Salama, "Optimal ESS Allocation and Load Shedding for Improving Distribution System Reliability," *IEEE Transactions on Smart Grid*, vol. 5, no. 5, pp. 2339-2349, 2014, doi: 10.1109/TSG.2014.2316197.
- [103] S. Grillo, M. Marinelli, S. Massucco, and F. Silvestro, "Optimal Management Strategy of a Battery-Based Storage System to Improve Renewable Energy Integration in Distribution Networks," *IEEE Transactions on Smart Grid*, vol. 3, no. 2, pp. 950-958, 2012, doi:

- 10.1109/TSG.2012.2189984.
- [104] M. Hosseina and S. M. T. Bathaee, "Optimal scheduling for distribution network with redox flow battery storage," *Energy Conversion and Management*, vol. 121, pp. 145-151, 2016/08/01/ 2016, doi: <https://doi.org/10.1016/j.enconman.2016.05.001>.
- [105] C. J. Bennett, R. A. Stewart, and J. W. Lu, "Development of a three-phase battery energy storage scheduling and operation system for low voltage distribution networks," *Applied Energy*, vol. 146, pp. 122-134, 2015/05/15/ 2015, doi: <https://doi.org/10.1016/j.apenergy.2015.02.012>.
- [106] M. Cresta, F. M. Gatta, A. Geri, M. Maccioni, A. Mantineo, and M. Paulucci, "Optimal operation of a low-voltage distribution network with renewable distributed generation by NaS battery and demand response strategy: a case study in a trial site," *IET Renewable Power Generation*, vol. 9, no. 6, pp. 549-556, 2015, doi: 10.1049/iet-rpg.2014.0441.
- [107] M. Zeraati, M. E. H. Golshan, and J. M. Guerrero, "Distributed Control of Battery Energy Storage Systems for Voltage Regulation in Distribution Networks With High PV Penetration," *IEEE Transactions on Smart Grid*, vol. 9, no. 4, pp. 3582-3593, 2018, doi: 10.1109/TSG.2016.2636217.
- [108] E. Reihani, S. Sepasi, L. R. Roose, and M. Matsuura, "Energy management at the distribution grid using a Battery Energy Storage System (BESS)," *International Journal of Electrical Power & Energy Systems*, vol. 77, pp. 337-344, 2016/05/01/ 2016, doi: <https://doi.org/10.1016/j.ijepes.2015.11.035>.
- [109] N. G. Hingorani and L. Gyugyi, *Understanding FACTS: Concepts and Technology of Flexible AC Transmission Systems*. Wiley, 2000.
- [110] CPLEX software package [Online] Available: www.ibm.com/analytics/cplex-optimizer
- [111] P. Du, B. Li, Q. Zeng, D. Zhai, D. Zhou, and L. Ran, "Distributionally Robust Two-Stage Energy Management for Hybrid Energy Powered Cellular Networks," *IEEE Transactions on Vehicular Technology*, pp. 1-1, 2020, doi: 10.1109/TVT.2020.3013877.
- [112] M. Aghamohamadi and A. Mahmoudi, "From bidding strategy in smart grid toward integrated bidding strategy in smart multi-energy systems, an adaptive robust solution approach," *Energy*, vol. 183, pp. 75-91, 2019/09/15/ 2019.
- [113] A. A. Thatte, L. Xie, D. E. Viassolo, and S. Singh, "Risk Measure Based Robust Bidding Strategy for Arbitrage Using a Wind Farm and Energy Storage," *IEEE Transactions on Smart Grid*, vol. 4, no. 4, pp. 2191-2199, 2013, doi: 10.1109/TSG.2013.2271283.
- [114] Y. Xie, W. Guo, Q. Wu, and K. Wang, "Robust MPC-based bidding strategy for wind storage systems in real-time energy and regulation markets," *International Journal of Electrical Power & Energy Systems*, vol. 124, p. 106361, 2021/01/01/ 2021, doi: <https://doi.org/10.1016/j.ijepes.2020.106361>.
- [115] M. Aghamohamadi, A. Mahmoudi, and M. Haque, "Two-stage Robust Sizing and Operation Co-optimization for Residential PV-battery Systems Considering the Uncertainty of PV Generation and Load," *IEEE Transactions on Industrial Informatics*, pp. 1-1, 2020, doi: 10.1109/TII.2020.2990682.
- [116] M. Rahimiyan and L. Baringo, "Strategic Bidding for a Virtual Power Plant in the Day-Ahead and Real-Time Markets: A Price-Taker Robust Optimization Approach," *IEEE Transactions on Power Systems*, vol. 31, no. 4, pp. 2676-2687, 2016, doi: 10.1109/TPWRS.2015.2483781.
- [117] A. Attarha, N. Amjady, and S. Dehghan, "Affinely Adjustable Robust Bidding Strategy

- for a Solar Plant Paired With a Battery Storage," *IEEE Transactions on Smart Grid*, vol. 10, no. 3, pp. 2629-2640, 2019, doi: 10.1109/TSG.2018.2806403.
- [118] A. Attarha, N. Amjady, S. Dehghan, and B. Vatani, "Adaptive Robust Self-Scheduling for a Wind Producer With Compressed Air Energy Storage," *IEEE Transactions on Sustainable Energy*, vol. 9, no. 4, pp. 1659-1671, 2018, doi: 10.1109/TSTE.2018.2806444.
- [119] A. Attarha, P. Scott, and S. Thiébaux, "Affinely Adjustable Robust ADMM for Residential DER Coordination in Distribution Networks," *IEEE Transactions on Smart Grid*, vol. 11, no. 2, pp. 1620-1629, 2020, doi: 10.1109/TSG.2019.2941235.
- [120] A. J. Conejo, E. Castillo, R. M'inguez, and R. Garc'ia-Bertrand, *Decomposition Techniques in Mathematical Programming. Engineering and Science Applications*. New York, NY, USA: Springer, 2006.
- [121] R. Singh and R. C. Bansal, "Optimization of an Autonomous Hybrid Renewable Energy System Using Reformed Electric System Cascade Analysis," *IEEE Transactions on Industrial Informatics*, vol. 15, no. 1, pp. 399-409, 2019, doi: 10.1109/TII.2018.2867626.
- [122] J. Ren, J. Hu, R. Deng, D. Zhang, Y. Zhang, and X. Shen, "Joint Load Scheduling and Voltage Regulation in the Distribution System With Renewable Generators," *IEEE Transactions on Industrial Informatics*, vol. 14, no. 4, pp. 1564-1574, 2018, doi: 10.1109/TII.2017.2782725.
- [123] R. Khezri, A. Mahmoudi, and M. H. H. Haque, "Optimal Capacity of Solar PV and Battery Storage for Australian Grid-Connected Households," *IEEE Transactions on Industry Applications*, pp. 1-1, 2020, doi: 10.1109/TIA.2020.2998668.
- [124] S. Majumder, S. A. Khaparde, A. P. Agalgaonkar, P. Ciufo, S. Perera, and S. V. Kulkarni, "DFT-Based Sizing of Battery Storage Devices to Determine Day-Ahead Minimum Variability Injection Dispatch With Renewable Energy Resources," *IEEE Transactions on Smart Grid*, vol. 10, no. 1, pp. 626-638, 2019.
- [125] S. K. Tiwari, B. Singh, and P. K. Goel, "Design and Control of Autonomous Wind-Solar System With DFIG Feeding 3-Phase 4-Wire Loads," *IEEE Transactions on Industry Applications*, vol. 54, no. 2, pp. 1119-1127, 2018, doi: 10.1109/TIA.2017.2780168.
- [126] B. Ke, T. Ku, Y. Ke, C. Chuang, and H. Chen, "Sizing the Battery Energy Storage System on a University Campus With Prediction of Load and Photovoltaic Generation," *IEEE Transactions on Industry Applications*, vol. 52, no. 2, pp. 1136-1147, 2016, doi: 10.1109/TIA.2015.2483583.
- [127] A. Dolatabadi and B. Mohammadi-Ivatloo, "Stochastic Risk-Constrained Optimal Sizing for Hybrid Power System of Merchant Marine Vessels," *IEEE Transactions on Industrial Informatics*, vol. 14, no. 12, pp. 5509-5517, 2018.
- [128] D. Yang, C. Jiang, G. Cai, and N. Huang, "Optimal sizing of a wind/solar/battery/diesel hybrid microgrid based on typical scenarios considering meteorological variability," *IET Renewable Power Generation*, vol. 13, no. 9, pp. 1446-1455, 2019.
- [129] B. Naghibi, M. A. S. Masoum, and S. Deilami, "Effects of V2H Integration on Optimal Sizing of Renewable Resources in Smart Home Based on Monte Carlo Simulations," *IEEE Power and Energy Technology Systems Journal*, vol. 5, no. 3, pp. 73-84, 2018.
- [130] H. Bludszweit and J. A. Dominguez-Navarro, "A Probabilistic Method for Energy Storage Sizing Based on Wind Power Forecast Uncertainty," *IEEE Transactions on Power Systems*, vol. 26, no. 3, pp. 1651-1658, 2011.

- [131] J. Cervantes and F. Choobineh, "Optimal sizing of a nonutility-scale solar power system and its battery storage," *Applied Energy*, vol. 216, pp. 105-115, 2018/04/15/ 2018.
- [132] H. Alharbi and K. Bhattacharya, "Stochastic Optimal Planning of Battery Energy Storage Systems for Isolated Microgrids," *IEEE Transactions on Sustainable Energy*, vol. 9, no. 1, pp. 211-227, 2018.
- [133] Z. Wang, J. Gao, R. Zhao, J. Wang, and G. Li, "Optimal bidding strategy for virtual power plants considering the feasible region of vehicle-to-grid," *Energy Conversion and Economics*, vol. n/a, no. n/a, doi: <https://doi.org/10.1049/enc2.12018>.
- [134] D. Krishnamurthy, C. Uckun, Z. Zhou, P. R. Thimmapuram, and A. Botterud, "Energy Storage Arbitrage Under Day-Ahead and Real-Time Price Uncertainty," *IEEE Transactions on Power Systems*, vol. 33, no. 1, pp. 84-93, 2018, doi: 10.1109/TPWRS.2017.2685347.
- [135] L. Shi, Y. Luo, and G. Y. Tu, "Bidding strategy of microgrid with consideration of uncertainty for participating in power market," *International Journal of Electrical Power & Energy Systems*, vol. 59, pp. 1-13, 2014/07/01/ 2014, doi: <https://doi.org/10.1016/j.ijepes.2014.01.033>.
- [136] G. Mohy-ud-din, D. H. Vu, K. M. Muttaqi, and D. Sutanto, "An Integrated Energy Management Approach for the Economic Operation of Industrial Microgrids Under Uncertainty of Renewable Energy," *IEEE Transactions on Industry Applications*, vol. 56, no. 2, pp. 1062-1073, 2020, doi: 10.1109/TIA.2020.2964635.
- [137] M. Aghamohamadi, A. Mahmoudi, and M. H. Haque, "Robust Allocation of Residential Solar Photovoltaic Systems Paired with Battery Units in South Australia," in *2019 IEEE Energy Conversion Congress and Exposition (ECCE)*, 29 Sept.-3 Oct. 2019 2019, pp. 6673-6679, doi: 10.1109/ECCE.2019.8913208.
- [138] Tesla Co. [Online] Available: https://www.tesla.com/en_AU
- [139] Australian Energy Market Operator (AEMO) [Online] Available: <https://www.aemo.com.au>
- [140] Renewables ninja [Online] Available: www.renewables.ninja
- [141] M. M. Alabbass, "Parallel-connected solar arrays," Master's degree, Missouri University, 2013.
- [142] Commodore independent energy systems [Online] Available: <https://www.commodoreaustralia.com.au/product-category/wind-turbines/>
- [143] AGL Energy [Online] Available: www.agl.com.au